
Adhesive and signaling properties of Dsg2 in intestinal epithelial barrier regulation

Hanna Ungewiß

München 2018



**Adhesive and signaling properties of Dsg2 in
intestinal epithelial barrier regulation**

Dissertation
an der Fakultät für Biologie
der Ludwig-Maximilians-Universität

vorgelegt von

Hanna Ungewiß

München 2018

Dissertation eingereicht am: 31.07.2018

Mündliche Prüfung am: 11.01.2019

Erstgutachter: Prof. Dr. Heinrich Leonhardt

Zweitgutachter: Prof. Dr. Anja Horn-Bochtler

Table of content

Table of content	I
Summary	III
1 Introduction	1
1.1 Function and structure of the human intestinal epithelial barrier	1
1.2 Intestinal epithelial intercellular junctions	4
1.2.1 Tight junctions	5
1.2.2 Adherens junctions	5
1.2.3 Desmosomes	6
1.2.4 Gap junctions	8
1.3 Regulation of the intestinal barrier and intercellular adhesion	9
1.3.1 Regulation of intercellular adhesion via specific expression and turnover of adhesion molecules	9
1.3.2 Regulation of intercellular adhesion via the extracellular domain of transmembrane adhesion proteins	10
1.3.3 Regulation of intercellular adhesion via the cytoplasmic tail of adhesion proteins	13
1.3.4 Regulation of intercellular adhesion via receptor tyrosine kinase signaling	14
1.3.5 Desmosomes as signaling hubs	16
1.3.6 p38MAPK signaling pathway	18
1.3.7 EGFR signaling pathway	21
1.3.8 Glial cell-derived neurotrophic factor	23
1.4 Inflammatory bowel disease	25
1.5 Aim of this study	26
2 Results	29
2.1 Desmoglein 2 regulates the intestinal epithelial barrier via p38 mitogen-activated protein kinase	29
2.2 Dsg2 via Src-mediated transactivation shapes EGFR signaling towards cell adhesion	51
2.3 Desmoglein 2, but not Desmocollin 2, protects intestinal epithelia from injury	79
2.4 Glial cell-line derived neurotrophic factor (GDNF) regulates intestinal barrier function in inflammatory bowel diseases by stabilization of desmoglein 2	135
3 Discussion	189
3.1 Cultured enterocytes as suitable model for the human intestinal epithelium	189
3.2 Dsg2 as cell surface receptor for signal transduction of environmental stimuli	191
3.2.1 Direct interaction of Dsg2 and EGFR via their extracellular domains regulates cell adhesion and proliferation	192
3.2.2 Indirect activation of Dsg2 signaling function through environmental stimuli	195
3.3 Tissue dependent function of desmogleins	199
3.4 Differential biological functions of Dsg2 and Dsc2	201

4	Annex	205
4.1	References	205
4.2	Abbreviations	233
4.3	Contributions	237
4.4	Statuary declaration and statement	239
4.5	Curriculum vitae	241
4.6	Acknowledgements	243

Summary

The human gastrointestinal tract is covered by a simple epithelium that operates as a selective permeable barrier and allows the uptake of essential nutrients while simultaneously preventing the entry of macromolecules and pathogens from the gut lumen. Several types of intercellular junctions tightly connect the epithelial cells and thus establish a functional barrier. While tight junctions (TJ) as well as adherens junctions (AJ) have been studied extensively, less information is available for desmosomes. For a long time, desmosomes were considered to provide primarily the mechanical strength to intercellular cohesion. However, growing evidence suggest a role in regulating signaling cascades. Desmosomal cadherins constitute the adhesive core of desmosomes with extracellular domains (ED) binding to adjacent cadherins and a cytoplasmic tail that anchors the junctional complex to the intermediate filament cytoskeleton. In the human intestine, only two desmosomal cadherins are present, desmoglein 2 (Dsg2) and desmocollin 2 (Dsc2), of which Dsg2 has been reported to be crucial for barrier function and to play a critical role in the pathogenesis of inflammatory bowel disease (IBD).

The main objective of this study was to investigate the adhesive and signaling functions of Dsg2 in human intestinal cells. At first, I characterized cultured enterocytes regarding their ability to establish a functional barrier that is suitable as model for the intestinal epithelium. Here, cultured cells showed mature barrier properties with fully formed apical junctional complexes and characteristic microvilli on the cell surface similar as observed in human tissue. Furthermore, I identified that Dsg2 is present additionally outside of desmosomes on the surface of polarized enterocytes. To characterize Dsg2 binding properties, I established atomic force microscopy (AFM) on living enterocytes, which was then used to investigate the effect of several signaling mediators on Dsg2 binding. An antibody targeting the ED of Dsg2 was able to inhibit binding events in AFM measurements and activated p38MAPK but did not influence cell cohesion under same conditions. To elucidate the signaling properties of Dsg2 more in detail, I compared WT and Dsg2-deficient enterocytes and found a deregulated p38MAPK signaling pathway. Using transepithelial resistance (TER) measurements, I further showed that the interrelationship of p38MAPK and Dsg2 regulates barrier properties.

Moreover, I identified EGFR as direct interaction partner of Dsg2 and that this interaction inhibits the proliferative function of EGFR. In Dsg2-deficient cells, EGFR is absent at cell-cell borders and proliferation is increased. Co-localization of Dsg2 and EGFR was also observed in human tissue samples, indicating that this newly discovered mechanism is universal. Further, I characterized the heterophilic binding and demonstrated that EGFR mediators inhibit the interaction. In addition, EGFR mediators impaired barrier establishment and reduced cell adhesion, suggesting that the Dsg2-EGFR complex regulates barrier properties of intestinal epithelial cells.

Since impaired barrier function and in particular Dsg2 function is implicated in the pathogenesis of Crohn's disease (CD), I participated in studies investigating the mechanisms leading to loss of barrier function in IBD. Here, I analyzed human tissue samples from CD patients and showed changes in desmosome ultrastructure.

Furthermore, comparison of Dsg2 and Dsc2 deficient cells revealed a differential biological relevance of these cadherins. More specifically, Dsg2 had a more profound impact on barrier properties than Dsc2. In addition, I investigated the effect of the neurotrophic factor GDNF on Dsg2 binding, because GDNF has been reported to have a protective function in IBD patients. Here, using AFM, I showed that GDNF increases the binding properties of Dsg2 at cell borders and protects Dsg2 from cytokine-induced reduction at cell borders.

1 Introduction

1.1 Function and structure of the human intestinal epithelial barrier

The human gastrointestinal tract has amazing skills. Consisting of the oesophagus, stomach, small and large intestine, it is designed to fulfill a variety of functions such as storage as well as propulsive transport of food, digestion, absorption of nutrients and elimination of solid food waste. At the same time, it forms an important interface between the body interior and external environment that contains trillions of microorganisms that live in symbiotic and mutualistic relationship with the host as well as enteric pathogens that are usually co-ingested with food (Cerf-Bensussan and Gaboriau-Routhiau, 2010; Rodriguez et al., 2015). Hence, different types of response are required, dependent on whether the antigen is profitable or harmful to the host (Mowat, 2003). How is it possible to stay permeable for the uptake of nutrients but simultaneously preventing the entry of commensal bacteria, pathogens and harmful macromolecules? This remarkable function is achieved by a dynamic, selective permeable barrier. While the oesophagus is lined by a multilayered stratified squamous epithelium (Grace et al., 1985), the remaining parts of the gastrointestinal tract are covered by a single layer of polarized columnar epithelial cells that are tightly connected by a set of intercellular junctional complexes (Capaldo et al., 2014; Farquhar and Palade, 1963a). The major part of digestion and absorption of nutrients takes place in the small intestine, divided into the sections duodenum, jejunum and ileum, as well as in the large intestine (Helander and Fandriks, 2014; Moog, 1981). In order to achieve a high efficiency in digestion and absorption, the intestinal epithelium is organized in a three-dimensional structure consisting of crypts and villi in the small intestine and crypts in the colon, which enlarges the surface area to approximately 32 m² (Helander and Fandriks, 2014). To carry out the diversity of functions, four major types of intestinal epithelial cells (IECs) are present in the intestinal epithelium (Fig.1). Enterocytes make up the largest portion and are created primarily for specific digestive functions and absorption of nutrients such as ions, water, sugar, peptides and lipids (Clevers, 2013; van der Flier and Clevers, 2009). Goblet cells secrete highly glycosylated mucins into the intestinal lumen, thereby creating a thick fluid

that protects the intestinal wall from digestive enzymes and forms the first line of defense against microorganisms from the gut (Johansson et al., 2013; Kim and Ho, 2010). The major intestinal mucin produced by goblet cells is MUC2 that belongs to the gel-forming mucins. This group of mucins forms large polymers consisting of glycosylated mucin domains that are resistant to endogenous proteases, which allows the intestine to digest food without digesting itself (Johansson et al., 2013). In addition, transmembrane mucins that are produced by enterocytes, as well, form a thin layer called the glycocalyx that covers the apical side of IECs. Beyond their assumed role in protection, transmembrane mucins are also believed to be involved in apical cell surface sensing and signaling (Hattrup and Gendler, 2008; Singh and Hollingsworth, 2006). Paneth cells, which are present only in the small intestine, produce antimicrobial peptides (AMPs) including alpha-defensins, lysozymes and Reg3 proteins (Bevins and Salzman, 2011; Clevers and Bevins, 2013). AMPs have bactericidal activity and eradicate bacteria, thereby shaping the composition of the commensal microbiota and protecting against infections (Muniz et al., 2012). Moreover, AMPs function in recruiting and activating immune cells as well as modulate their maturation and differentiation (Funderburg et al., 2007; Navid et al., 2012; Rodriguez-Garcia et al., 2009). Enteroendocrine cells function as chemoreceptors and following stimulation, they release intestinal hormones like gastrin, motilin or somatostatin directly into the bloodstream (Cox, 2016; Noah et al., 2011). In addition, progenitor stem cells reside in the crypt base, also called crypts of Lieberkühn, and differentiate into mature IECs while migrating up along the crypt-villus axis, thereby renewing the intestinal epithelium every 4-5 days (Clevers, 2013). Together, these specialized IECs lineages form a dynamic, physical and biochemical barrier.

Lamina propria, which is present in close contact below the intestinal epithelium, contains blood vessels, immune cells such as intra-epithelial lymphocytes, macrophages, dendritic cells, B- and T-cells and connects the epithelium to the smooth muscle layer which is responsible for gut movement such as peristalsis (Collins and Bhimji, 2018). Muscle contractions and digestive functions are coordinated by the enteric nervous system (ENS) that cooperates with the central nervous system (CNS) and consists of the myenteric and submucosal plexus (Furness, 2012). Of note here are the enteric glial cells (EGCs), which are located also in proximity to the IECs (Yu and Li, 2014). They release specific mediators such as glial cell-derived neurotrophic factor (GDNF) or

transforming growth factor (TGF) β 1 and play an important role in the maintenance of both, ENS and epithelial barrier integrity (Abdo et al., 2010; Neunlist et al., 2014).

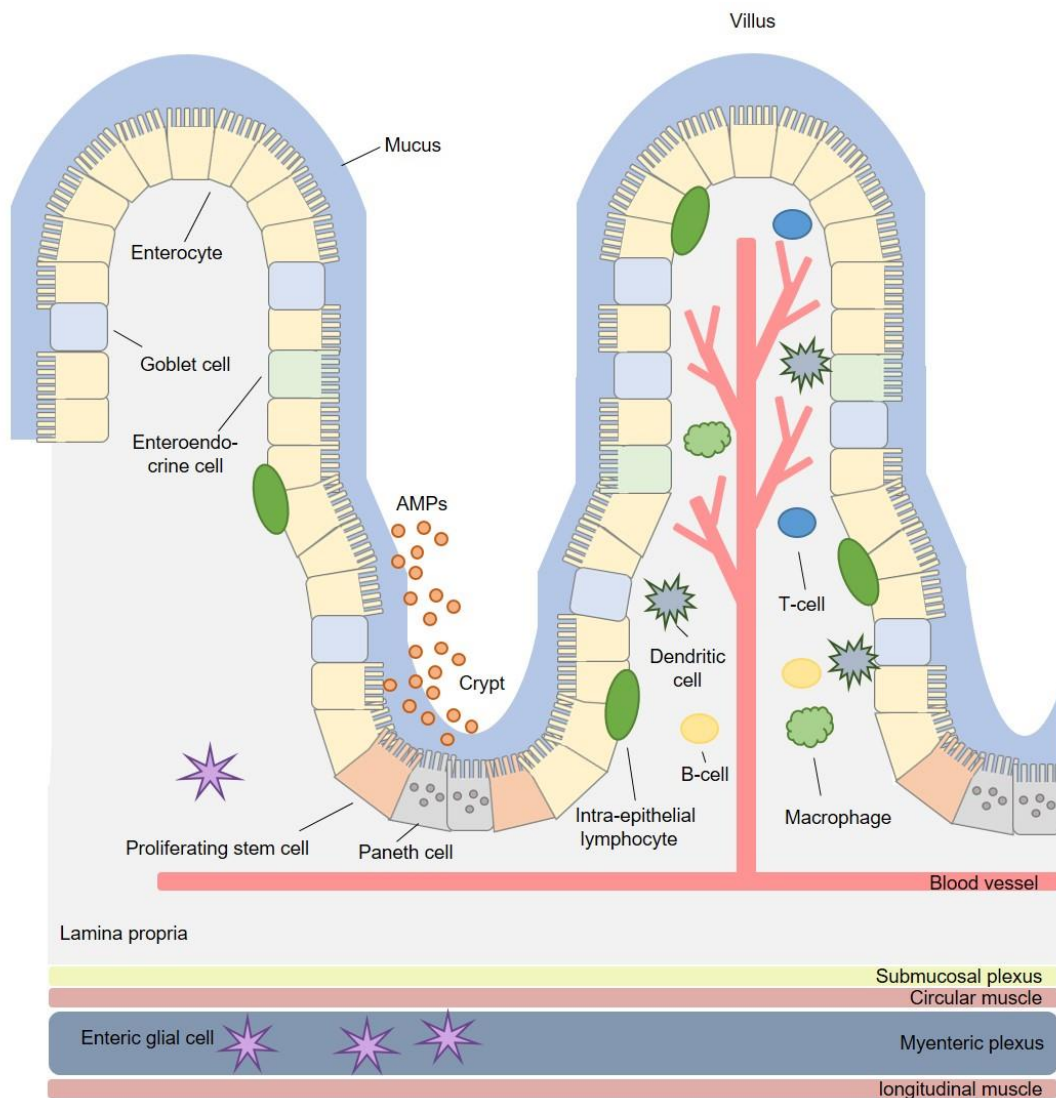


Figure 1: Schematic overview of the cellular composition and three-dimensional organization of the epithelium in the small intestine. The intestinal epithelium includes absorptive enterocytes, mucus secreting goblet cells, hormone releasing enteroendocrine cells, antimicrobial peptides (AMPs) - producing paneth cells and proliferating stem cells, which together form a dynamic barrier that separates the mucosal tissue from the luminal gut microbiota. A three-dimensional structure consisting of crypts and villi increases the surface area and ensures highly efficient digestion and absorption. The epithelium is in close contact to the lamina propria that connects the epithelial cells to the muscle layer and contains blood vessels and immune cells.

1.2 Intestinal epithelial intercellular junctions

In order to achieve a functional barrier, the paracellular space between IECs must be sealed. Three different types of intercellular junctions namely tight junctions (TJs), adherens junctions (AJs) and desmosomes hold the IECs together and form the “terminal bar” by sealing the paracellular space (Capaldo et al., 2014; Farquhar and Palade, 1963a) (Fig.2). In addition, clusters of intercellular plasma membrane channels called gap junctions (GJ) allow communication between adjacent cells through a passage route for ions and small metabolites of less than 2 kilodalton (kDa)(Staehelin, 1972).

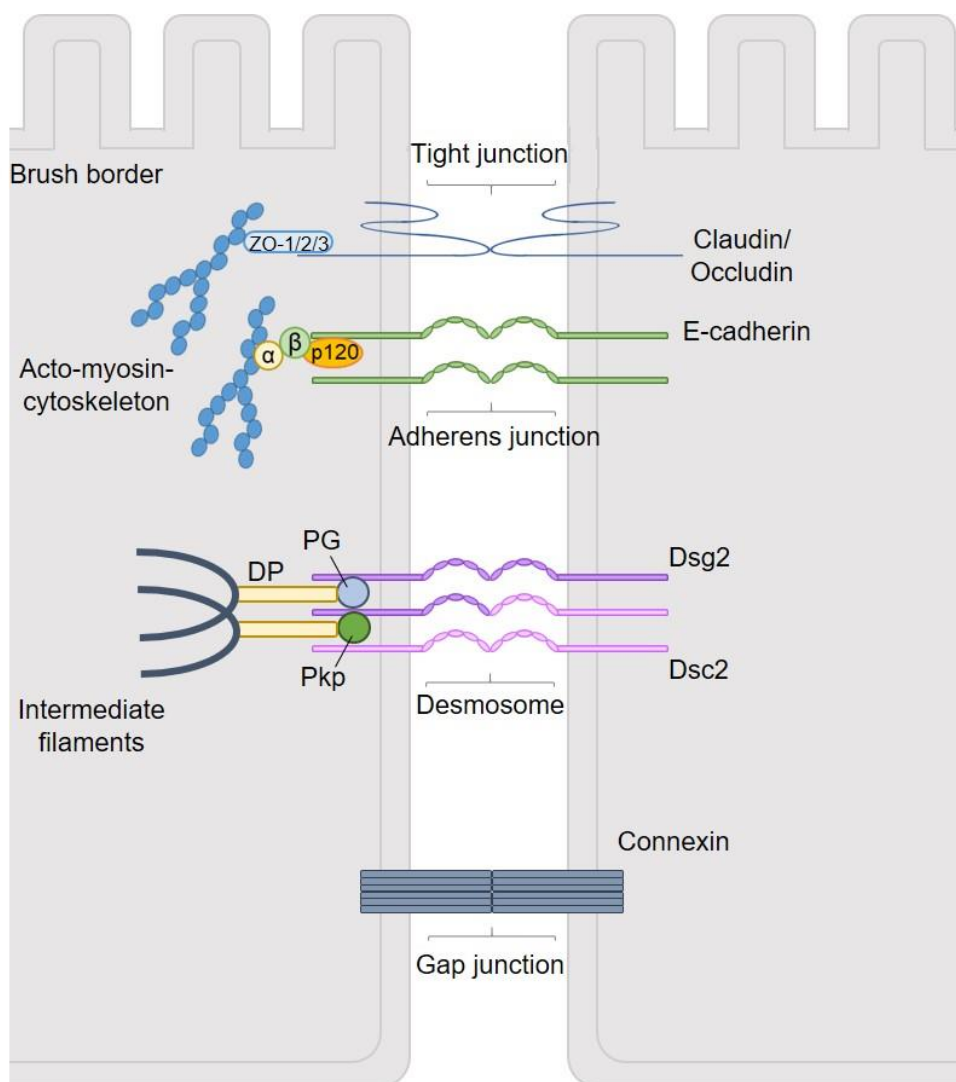


Figure 2: Structure of intercellular junctional complexes in the intestinal epithelium. Intestinal epithelial cells (IEC) are connected through a set of adhesion complexes including tight junctions (TJ), adherens junctions (AJ), desmosomes and gap junctions (GJ). TJ and AJ are tethered to the acto-myosin cytoskeleton, while desmosomes are linked to the intermediate filament cytoskeleton and provide strong intercellular cohesion.

1.2.1 Tight junctions

TJs are the most apical junctional complexes and besides restricting paracellular diffusion based on size and charge, they maintain apicobasal cell polarity through their function as fence that restricts diffusion of lipids and proteins between the apical and basolateral sides of the cell (Cereijido et al., 1998; Tsukita and Furuse, 2000). The main protein components of tight junctions include the small tetraspan proteins of the claudin family, three MARVEL domain proteins including occludin, tricellulin and MARVELD3 as well as the junctional adhesion molecules (JAMs) (Furuse et al., 1996; Kubota et al., 1999; Martin-Padura et al., 1998; Tsukita and Furuse, 2000). The cytoplasmic C-terminal domains of the transmembrane proteins bind to the junctional plaque that is composed of adaptor proteins such as zonula occludens 1 (ZO1), which contain multiple protein-protein interaction motifs and connect the junctional membrane proteins with F-actin and microtubules (Stevenson et al., 1986; Van Itallie and Anderson, 2014). Claudins are the most well understood TJ proteins. They comprise at least 27 members with sizes ranging from 20 to 27 kDa and are expressed in a tissue specific manner (Mineta et al., 2011; Tsukita et al., 2001). According to their channel- and barrier-forming properties, claudins are grouped into either anion- or cation-selective paracellular channels and further into tight claudins when increasing barrier tightness such as claudin 4 (Cld4) and leaky claudins when increasing paracellular permeability such as claudin 2 (Cld2) (Amasheh et al., 2002; Krug et al., 2014). As they can oligomerize in cis and trans, diverse combinations are possible that influence barrier function (Koval, 2013).

1.2.2 Adherens junctions

AJs are located directly beneath TJs and due to their close structural and functional proximity, both together are also referred to as the apical junctional complex (AJC). AJs are calcium-dependent multiprotein complexes, consisting of classical cadherins such as E-cadherin (Ecad), N-cadherin (Ncad), VE-cadherin (VEcad) and P-cadherin (Pcad), which initiate intercellular contacts through homo- or heterophilic binding of cadherins on opposing cells (Adams et al., 1998; Pokutta et al., 1994). Classical cadherins are expressed in tissue specific manner. For instance Ncad is present in muscle cells and

neurons, while VEcad can be found in endothelial cells and Ecad is the key transmembrane protein in epithelial cells (Niessen et al., 2011). Their binding is essential for the differentiation into an epithelial cell, as loss of Ecad binding results in an epithelial to mesenchymal transition and thus impairs barrier function (Pal et al., 2018). Cadherin-cadherin interaction occur via their extracellular domains (EDs) and is highly dependent on extracellular Ca^{2+} that rigidifies the ED and allows interaction (Nagar et al., 1996). The occurrence of several Ca^{2+} binding pockets with different affinities, enables cadherins to respond dynamically to changes in junctional Ca^{2+} levels (Prasad and Pedigo, 2005). Moreover, a highly conserved tryptophan residue that is present in the first ED and inserts into the hydrophobic pocket of the partner cadherin influences binding by forming a so-called strand-swapped dimeric structure (Shapiro et al., 1995). The cytoplasmic domain of these transmembrane proteins interact with catenins such as α -catenin, β -catenin and p120^{ctn}, which couple the cadherin complex to the actin cytoskeleton (Perez-Moreno and Fuchs, 2006). With this, AJs confer mechanical strength to adjacent epithelial cells and stabilize cell-cell adhesion. Additionally, through interaction with numerous other cytoskeletal linker molecules as well as adaptor proteins (Padmanabhan et al., 2015), AJs regulate the actin cytoskeleton and are involved in intracellular signaling as well as transcriptional regulation (Rubsam et al., 2017a).

1.2.3 Desmosomes

Desmosomes (which is a composition of the Greek words “desmos”, meaning bond and “soma”, meaning body) are the least studied type of intercellular junctions and considered to provide primarily the mechanical strength to intercellular cohesion (Green and Simpson, 2007). Similar to AJs, they are composed of transmembrane glycoproteins of the cadherin family that mediate calcium-dependent cell-cell adhesion via their EDs in a homo- or heterophilic manner. In human epithelial tissues, seven isoforms of desmosomal cadherins, desmoglein 1-4 (Dsg1-4) and desmocollin 1-3 (Dsc1-3) are expressed in a tissue- and differentiation- specific pattern. While stratified epithelia such as the human epidermis, express all desmosomal cadherin isoforms, the simple columnar epithelium of the human intestine contains Dsg2 and Dsc2 only (Holthofer et al., 2007;

Koch et al., 1992). A common feature shared by all desmosomal cadherins is their molecular organization (Fig. 3). Their ED consists of four extracellular cadherin repeats (ECs 1-4) and a membrane proximal extracellular anchor (EA) sequence, followed by a single-pass transmembrane (TM) domain. While the extracellular repeats of the cadherin superfamily are pretty well conserved in classical and desmosomal cadherins, unique features are attributed to the cytoplasmic tails (Hulpiau and van Roy, 2009). Both, desmogleins and desmocollins, contain a membrane proximal intracellular anchor (IA) domain and an intracellular cadherin-like sequence (ICS) that associates with the armadillo family plaque proteins plakoglobin (PG) and plakophilin (Pkp). These proteins in turn interact with desmoplakin (DP) that anchors the multiprotein complex to the intermediate filament cytoskeleton (Holthofer et al., 2007; Koch et al., 1990; Owen and Stokes, 2010). Desmocollins occur in two isoforms, of which one contains a truncated ICS domain. In addition, desmogleins contain an extended C-terminal unique region (DUR) with unknown features that is composed of an intracellular proline-rich linker (IPL), a repeat unit domain (RUD) and a desmoglein terminal domain (DTD) (Koch et al., 1990).

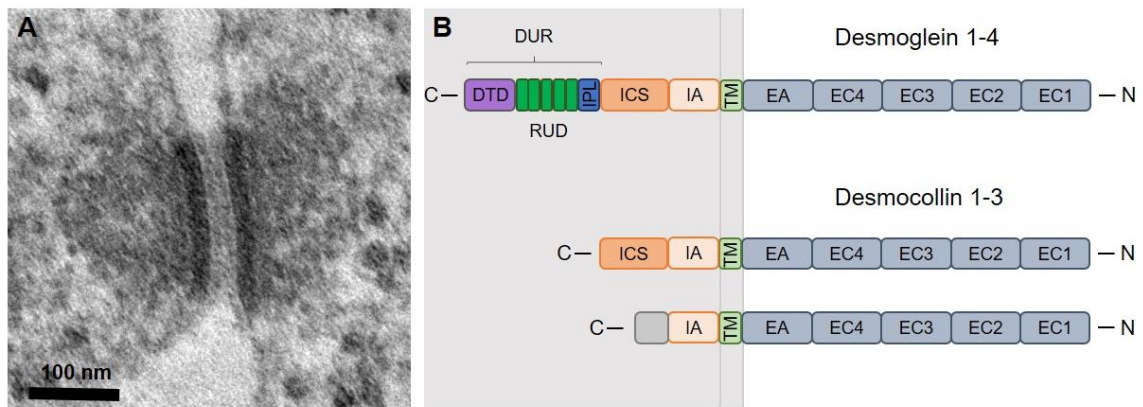


Figure 3: Molecular composition of a desmosome. (A) Electron micrograph of a desmosome from cultured Caco2 cells. (B) Desmosomal cadherins consist of four extracellular cadherin repeats (EC), a single pass transmembrane domain (TM) and a cytoplasmic tail that comprises an intracellular anchor (IA) and an intracellular cadherin-like sequence (ICS) that associates with plaque proteins. Desmogleins have an additional desmoglein unique region (DUR) composed of an intracellular proline-rich linker (IPL), a repeat unit domain (RUD) and a desmoglein terminal domain (DTD).

1.2.4 Gap junctions

GJs allow direct communication between two cells through providing a conduit for the passage of small metabolites and ions. They are constructed of transmembrane proteins called connexins (Cxs) that interact in a homo- and heterophilic way and can form homo- and heterotypic channels. Two hemichannels consisting of six Cxs each form a GJ, of which permeability is determined by the composition of Cxs isoforms (De Maio et al., 2002; Segretain and Falk, 2004). Furthermore, Cxs interact with numerous proteins such as cytoskeletal components, junctional molecules from AJ or TJ and enzymes like kinases or phosphatases (Giepmans, 2004). Intercellular communication via GJ is required for maintaining epithelial cell homeostasis and function (Vinken et al., 2006). Furthermore, they are assumed to play an important role in several pathophysiological processes. A recent study demonstrates that hetero-cellular communication via GJ between IECs and inflammatory cells such as macrophages contributes to the dysregulation of intestinal epithelial barrier in inflammatory bowel disease (IBD) (Al-Ghadban et al., 2016).

1.3 Regulation of the intestinal barrier and intercellular adhesion

The intestinal epithelial tissue renews every 4-5 days and thus shows the highest turnover rate in adult mammals (Clevers, 2013; Mayhew et al., 1999). Within the crypt, progenitor stem cells proliferate and differentiate into mature IECs that migrate along the crypt-villus axis toward the villus tip region, or surface epithelial cuff in the colon, where dying epithelial cells are shed, a process that is called cell extrusion (Rosenblatt et al., 2001). Cell proliferation and shedding must be tightly regulated to assure the integrity of the intestinal barrier and maintain its properties. Hence, it is reasonable that under inflammatory conditions, when epithelial proliferation and cell turnover are enhanced, an increased risk of barrier leakage is observed (Cliffe et al., 2005). However, how can adherent cells in an epithelium proliferate and extrude without compromising the epithelial barrier function? The key lies in the regulation of intercellular junctions. Here, several strategies are conceivable.

1.3.1 Regulation of intercellular adhesion via specific expression and turnover of adhesion molecules

First, the type and amount of expressed adhesion molecules determines the strength of cell-cell adhesion. It is widely recognized that a huge number of narrow tight junctions is present in intestinal villi with a mature barrier, while more leaky junctions are found in the crypts where cell proliferation takes place (Hollander, 1999). Altered expression of tight junction proteins is also observed in a variety of gastrointestinal disorders that are characterized by a leaky barrier (Oshima and Miwa, 2016). For instance, expression of occludin as well as sealing claudins 5 and 8 is reduced in colon biopsies from patients with Crohn's disease (CD) (Zeissig et al., 2007), whereas the pore-forming claudin 2 has been shown to be upregulated in samples from patients suffering from ulcerative colitis (UC) and CD (Heller et al., 2005; Zeissig et al., 2007). The same holds true for the expression of components from other intercellular junctions. Dsg2 was found to be reduced in the mucosa of CD patients (Spindler et al., 2015) and loss of Ecad is nowadays commonly considered as a hallmark of epithelial to mesenchymal transition in tumor progression (Pal et al., 2018). However, transcriptional regulation of adhesion molecules

accounts rather for long-term changes and cannot induce rapid changes in intercellular adhesion, since the metabolic half-life of adhesion proteins ranges from approximately 4 hours for claudins to around five to ten hours for cadherins and up to 12 hours for occludin (McCrea and Gumbiner, 1991; Shore and Nelson, 1991; Van Itallie et al., 2004; Wong and Gumbiner, 1997). A more dynamic regulation of available amount of adhesion molecules is achieved through endocytosis and degradation. In line with this, deregulated cadherin internalization has been demonstrated to play a role in various diseases associated with loss of epithelial integrity (Kowalczyk and Nanes, 2012). While desmosomal cadherins show a rapid turnover, as shown for Dsc2 with a fluorescence recovery time of only 30 min after photobleaching, their cytoplasmic plaques seem to be exceptionally stable (Windoffer et al., 2002). Furthermore, the composition of desmosomal plaques also regulates desmosome dynamics. While Pkp3 renders desmosomes to be more dynamic and is found at early desmosomes for instance during wound healing, incorporation of Pkp1 results in stable and hyperadhesive desmosomes to stabilize intercellular adhesion (Keil et al., 2016; Tucker et al., 2014). A recent study shows, that this incorporation is regulated through association of Pkp1 and Pkp3 with 14-3-3 proteins, which depends on the Pkp phosphorylation status (Rietscher et al., 2018).

1.3.2 Regulation of intercellular adhesion via the extracellular domain of transmembrane adhesion proteins

A second strategy for regulation of intercellular adhesion involves modulation of the existing adhesion complexes including direct inhibition of binding between transmembrane proteins through conformational changes, steric hindrance or cleavage of extracellular domains (Fig.4). Several studies using adhesion proteins with mutations in their extracellular domains report decreased adhesion properties, highlighting the importance of a functional ED for proper adhesion (Buck et al., 2018; Dieding et al., 2017; Gunzel and Yu, 2013; Samuelov and Sprecher, 2015).

1.3.2.1 Inhibition of binding through conformational changes

The importance of cadherin ED conformation is obvious regarding the fact that calcium binding-induced conformational changes are required for cadherin-cadherin interaction (Pokutta et al., 1994). Furthermore, several Ca^{2+} binding pockets with different affinities allow adjustment of binding properties dependent on junctional Ca^{2+} levels (Prasad and Pedigo, 2005). However, for desmosomes, this approach of regulation plays rather a role in wound healing, since desmosomes in mature tissues appear in a so-called hyper-adhesive Ca^{2+} -independent state and thus are resistant to disruption by reduced Ca^{2+} concentration (Garrod et al., 2005). A recent study, reporting that arrhythmogenic cardiomyopathy related mutations in Dsg2 ED influence the cadherin binding kinetics (Dieding et al., 2017), underlines the importance of proper ED function for adhesive properties of cadherins. Modulation of ED conformational changes plays also a role in TJ adhesion. For instance, an enterotoxin produced by the food-poisoning bacterium *Clostridium perfringens*, has been reported to target the extracellular domain of Cld4, thereby inducing a conformational change that disrupts the claudin assembly in TJ, which causes diarrhea (Shinoda et al., 2016).

1.3.2.2 Inhibition of binding through steric hindrance

Binding inhibition through steric hindrance is well known from the autoimmune disease pemphigus, whereby autoantibodies targeting the adhesive domains of Dsg1 and Dsg3 interfere with desmoglein trans-interaction, leading to skin blisters (Amagai and Stanley, 2012). However, beside steric hindrance, autoantibody-mediated signaling events are required to induce impaired keratinocyte cohesion in pemphigus (Waschke and Spindler, 2014). Furthermore, multifunctional modulators such as Galectins inhibit cell adhesion through steric hindrance when binding monovalently to one of the interacting domains, albeit bivalent galectin might also enhance adhesion by cross-linking the ED (Hughes, 2001). For instance, binding of Galectin-3 to the ED of Dsg2 has been shown to stabilize the desmosomal cadherin and intercellular adhesion in intestinal epithelial cells (Jiang et al., 2014).

1.3.2.3 Inhibition of binding through extracellular cleavage of ED

Regulation of intercellular junctions through extracellular cleavage of the transmembrane domains is on the one hand a vital mechanism to regulate epithelial homeostasis through loosening intercellular junctions for modulation of cell migration, induction of cell proliferation or to prevent the formation of unintended cell aggregates (Huguenin et al., 2008; Lochter et al., 1997; McCawley and Matrisian, 2001). On the other hand, bacterial proteases target junctional proteins thereby disrupting barrier integrity and in pathological states including inflammation and cancer, many proteases for junctional proteins are misregulated, which underlines the importance of this regulatory mechanism (Nava et al., 2013). For instance, a serine protease released by *Staphylococcus aureus* cleaves the ED of Dsg1, which disrupts cell-cell adhesion and results in Staphylococcal scalded skin syndrome or bullous impetigo (Amagai et al., 2000; Hanakawa et al., 2002). A zinc-containing metalloprotease produced by *Vibrio cholerae* targets TJs and disrupts epithelial barrier function through cleavage of the occludin ED (Wu et al., 2000). Also AJ are targeted by bacterial proteases such as the HtrA protease from *Helicobacter pylori* that cleaves the ED of Ecad (Hoy et al., 2012). By now, a huge number of proteases has been identified for all types of intercellular junctions present in the intestinal epithelium and many of them are upregulated in IBD (Menzel et al., 2006; Ravi et al., 2007). For instance, matrixmetalloproteinase (MMP) as well as a disintegrin and metalloproteinase domain-containing protein (ADAM) can cleave classical cadherins as well as Dsg2 (Bech-Serra et al., 2006; Lochter et al., 1997; Maretzky et al., 2005; Nava et al., 2013; Noe et al., 2001) and their activities are upregulated in several pathological conditions including inflammation, cancers, vascular disorders and autoimmune diseases (Gialeli et al., 2011; Rocks et al., 2008). However, beside disruption of adhesion, cleavage of the ED releases a functional ectodomain fragment that additionally modulates cellular processes. In this context, Dsg2 ectodomain shedding has been shown to compromise the mucosal barrier and to enhance IEC proliferation through activation of growth factor receptors (Kamekura et al., 2015). Also in skin epithelium, shed cadherin fragments have been reported to inhibit intercellular adhesion (Klessner et al., 2009; Lorch et al., 2004; Maretzky et al., 2005; Reiss et al., 2005). Moreover, increased soluble fragments of Ecad, Ncad and nectin are detected in cancer

tissues of patients and thus are meanwhile considered as biomarkers (Chung et al., 2011; Derycke et al., 2006; Fabre-Lafay et al., 2005; Katayama et al., 1994).

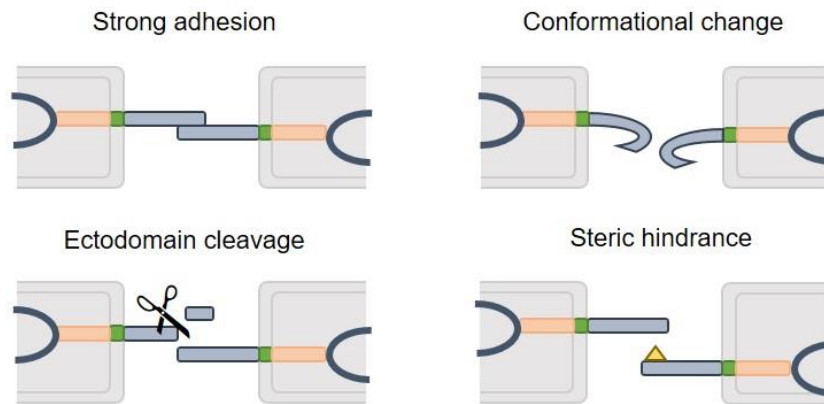


Figure 4. Regulation of intercellular adhesion through direct inhibition of binding between ED of adhesion molecules. Transmembrane adhesion molecules interact via their ED in a homo- or heterophilic manner, thereby mediating strong intercellular adhesion. Interaction is inhibited through conformational changes of the ED, protease-mediated cleavage of the ED, whereby the cleaved fragment also exerts biological functions and steric hindrance for example through autoantibodies or small molecules such as lectins.

1.3.3 Regulation of intercellular adhesion via the cytoplasmic tail of adhesion proteins

Although it is the ED of the transmembrane junctional proteins that mediates interaction with their respective binding partners on adjacent cells, also the cytoplasmic tail is an important site for regulation of intercellular adhesion (Fig. 5). To provide mechanical strength, adhesion complexes are associated with the cytoskeleton, which in case of TJ and AJ is the actin cytoskeleton and in case of desmosomes, the intermediate filament cytoskeleton. Hence, the cytoskeletal anchorage is a favorable target site for regulation of the adhesive strength and for opening of the intercellular space by contraction of the cytoskeleton. Important to mention here are the Rho family GTPases that modulate actin cytoskeleton dynamics and have emerged as crucial regulators of intestinal barrier function (Citalan-Madrid et al., 2013). Both, barrier stabilizing and destabilizing effects for these GTPases have been shown such as RhoA and Cdc42 mediated support of TJ formation as well as barrier disruption through RhoA induced myosin light chain phosphorylation and actin-myosin contraction (Itoh et al., 2012; Terry et al., 2011;

Yamada and Nelson, 2007). Along this line, reduced barrier function in CD is assumed to be induced by increased expression of myosin light chain kinase (MLCK) in response to $\text{TNF}\alpha$ (Turner, 2006). Moreover, retraction of the keratin intermediate filament network is a hallmark of the autoimmune disease pemphigus vulgaris that is characterized by skin blisters, which result from loss of cell-cell adhesion (Spindler et al., 2018). Furthermore, keratinocytes deficient of all keratin filaments showed impaired Dsg3 binding properties and membrane stability (Vielmuth et al., 2018). In this context, another important signaling molecule, p38 mitogen-activated protein kinase (p38MAPK) has been shown to regulate the anchorage of the desmosomal complex to the keratin filament cytoskeleton and its activation is linked to keratin retraction (Berkowitz et al., 2005; Spindler et al., 2013; Waschke et al., 2006). In addition, p38MAPK is also involved in regulation of intercellular adhesion in the intestinal epithelium and is supposed to play an important role in the pathogenesis of CD. In this regard, $\text{TNF}\alpha$, the central cytokine in CD, has been shown to increase the activity of p38MAPK, which was accompanied by loss of Dsg2 and TJ remodeling (Spindler et al., 2015). The p38MAPK signaling pathway and its interrelationship with desmosomal cadherins is described in detail below. Finally, the cytoplasmic tails modulate intercellular adhesion through regulation of cadherin turnover as tail-tail interactions have been demonstrated to stabilize the protein and inhibit endocytosis (Chen et al., 2012).

1.3.4 Regulation of intercellular adhesion via receptor tyrosine kinase signaling

Regulation of intercellular adhesion is required for proper cell homeostasis and has to be adjusted dynamically in response to environmental stimuli. Central in transmitting extracellular stimuli, are the receptor tyrosine kinases (RTK) that have emerged as key regulators of fundamental cellular processes including differentiation, proliferation and migration (Ullrich and Schlessinger, 1990). In humans, 58 RTKs are expressed, with all having a similar molecular architecture consisting of an extracellular region with ligand binding domains, a single transmembrane helix and a cytoplasmic region containing a protein tyrosine kinase domain as well as further carboxy terminal and juxtamembrane regulatory regions (Lemmon and Schlessinger, 2010). A growing number of studies

provide evidence that RTKs associate with intercellular junctions and influence cell-cell adhesion but vice versa also junctional proteins control RTKs (McClatchey and Yap, 2012; McCrea et al., 2015; McLachlan and Yap, 2007). Mechanisms how RTKs regulate intercellular adhesion, include phosphorylation of multiple components of the adhesion complex in a direct manner or via activation of kinases such as Src, Abl, PAK and CK1/2 (Bertocchi et al., 2012; Escobar et al., 2015; Hoschuetzky et al., 1994; Ji et al., 2009; Shibamoto et al., 1994). It is assumed, that this modification weakens cell adhesion by disrupting the cytoskeleton anchorage (Bertocchi et al., 2012; McCrea et al., 2015) or by inducing protein endocytosis (Cadwell et al., 2016). In this study, particular attention is given to the epidermal growth factor (EGF) receptor (EGFR) that has been demonstrated to regulate function of desmogleins (Klessner et al., 2009; Lorch et al., 2004) and is described in detail below.

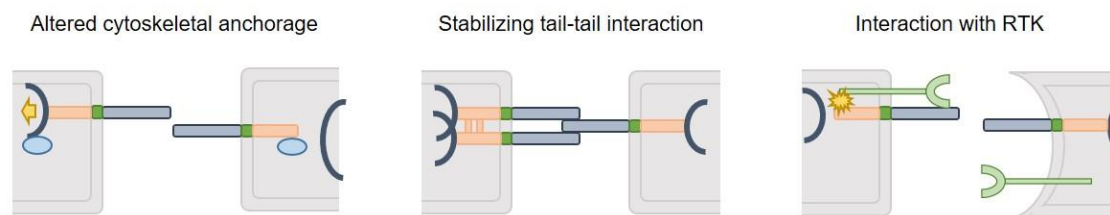


Figure 5. Modulation of the transmembrane adhesion protein cytoplasmic tail regulates intercellular adhesion. Adhesion proteins are tethered to the cytoskeleton via their cytoplasmic tail, which provides mechanical strength to the intercellular junction. Contraction of the cytoskeleton as well as disruption of cytoskeleton anchorage, both mediated by a range of signaling molecules, weakens intercellular adhesion. Tail-tail interaction of desmosomal cadherins stabilizes the proteins and prevents internalization. RTKs regulate intercellular adhesion via direct or indirect phosphorylation of the junctional proteins, which results in disruption of cytoskeleton anchorage or internalization.

Thus far, many signaling molecules have been identified to interact with intercellular junctions. In general, junctional complexes are meanwhile accepted as signaling platforms that are targeted by various signaling mechanisms but also themselves modulate epithelial homeostasis including cell proliferation, differentiation, migration and regulated shedding (Chiasson-MacKenzie and McClatchey, 2018; Muller et al., 2008; Rubsam et al., 2017a).

1.3.5 Desmosomes as signaling hubs

There is increasing evidence that desmosomes do not only provide mechanical strength to intercellular adhesion but also integrate mechanical and biochemical pathways to regulate cellular functions. Although cells are held together by three types of intercellular junctions, inactivation of desmosomal components such as Dsg2, Dsc3 or DP are embryonic lethal in mice, indicating their important function in tissue morphogenesis (Den et al., 2006; Eshkind et al., 2002; Gallicano et al., 1998). Over the last years, desmosomal contacts have emerged as critical signaling hubs (Spindler and Waschke, 2014). Since to date no enzymatic activity has been accredited to the intracellular tail of desmogleins, interaction with signaling components is required for signal transduction. In keratinocytes, extradesmosomal Dsg3 has been reported to strengthen cell cohesion via modulation of p38MAPK through the formation of a signaling complex together with Ecad, β -catenin and Src (Rotzer et al., 2015). Activation of p38MAPK through desmosomal signaling is also a well-known event in the autoimmune disease pemphigus, where autoantibody binding to the ED of Dsg1 and Dsg3 induces phosphorylation of p38MAPK (Berkowitz et al., 2008b; Berkowitz et al., 2005). Furthermore, several other signaling molecules have been shown to be activated by pemphigus autoantibodies such as the protein kinase C (PKC), Src, Erk and cAMP signaling (Esaki et al., 1995; Seishima et al., 1995; Walter et al., 2017), suggesting that desmosomal cadherins transmit extracellular stimuli and trigger signaling inside the cell (Muller et al., 2008). A well-known environmental stimulus are for instance inflammatory cytokines like interferon- γ (IFN γ) and TNF α , which are released during mucosal inflammation as known for the pathogenesis of IBD (Koch and Nusrat, 2012; Nava et al., 2010; Rogler and Andus, 1998). In respond to inflammatory cytokines, Dsg2 ED cleavage has been reported. Here, the cleaved fragments bind to human epidermal growth factor receptor family members HER2 and HER3, which results in activation of MAPK and Akt/mTOR downstream signaling pathways (Kamekura et al., 2015).

However, signaling occurs also independently of the extracellular portion, as shown for Dsg1, where direct interaction of the Dsg1 cytoplasmic tail and EGFR suppress EGFR activation and subsequent Erk1/2 signaling, to promote differentiation (Getsios et al., 2009). Further, the release and translocation of otherwise tied desmosomal components

regulates signaling pathways, as shown for PG that inhibits the expression of β -catenin genes in the nucleus, thereby controlling the canonical Wnt pathway (Ben-Ze'ev et al., 2000; Garcia-Gras et al., 2006). Likewise, the plakophilins, in addition to their role as architectural component in desmosomal plaques, are known to be present in the cytoplasm or nucleus, where they influence translational as well as transcriptional processes through direct interaction with RNA binding proteins or transcription factors, respectively (Hofmann et al., 2006; Mertens et al., 1996; Munoz et al., 2014). In addition, the release of cleaved fragments from the intracellular desmoglein domains are able to induce signaling as shown recently for Dsg2, of which intracellular fragments regulate apoptosis in IECs (Yulis et al., 2018). Similarly, the cleaved intracellular fragments of Dsg1 and Dsg3 have been reported to regulate apoptosis (Dusek et al., 2006; Weiske et al., 2001). Furthermore, the intracellular C-terminal fragment of Dsg2 has been found to be enriched in extracellular vesicles secreted by keratinocytes, thus influencing intercellular signaling. Moreover, Dsg2 modulated biogenesis of the extracellular vesicles via caveolin-1 and lipid rafts (Overmiller et al., 2017). Previously, Dsg2 has already been demonstrated to displace caveolin-1, EGFR and Src from lipid rafts leading to their enhanced activity (Overmiller et al., 2016).

Given their tight association with the cytoskeleton, it is easily comprehensible that desmosomes control also the cytoskeletal network and thereby integrate mechanical pathways to attune tissue structure and function (Rubsam et al., 2017a). However, this involves not only regulation of the directly associated intermediate filament cytoskeleton, but also includes regulation of the actin cytoskeleton and actin-based junctions. For instance, keratinocytes deficient for DP have a reduced number of desmosomes that are not linked to keratins anymore and in addition, they have less AJs (Vasioukhin et al., 2001b). Vice versa, loss of classical cadherins from AJ or α -catenin also impairs AJ as well as desmosome assembly (Michels et al., 2009; Tinkle et al., 2008; Vasioukhin et al., 2001a). In addition, extradesmosomal Dsg3 signaling complexes have been shown to bind to actin and recruitment of DP to the desmosomal plaque requires actomyosin, which raises the possibility that actin is important for desmosome assembly (Godsel et al., 2010; Tsang et al., 2012). Desmosome-mediated regulation of the actin organization involves inter alia the plaque protein Pkp2 that regulates actin remodeling and

localization of active RhoA to cell-cell contacts (Godsel et al., 2010). Furthermore, it can be concluded that TJ are under control of desmosomes. DP was demonstrated to regulate claudin expression (Sumigray et al., 2014) and an antibody targeting the ED of Dsg2 induced increased permeability accompanied with alterations of TJ component distribution, while Ecad was unaltered (Schlegel et al., 2010). However, the underlining mechanism remains unclear, so far.

1.3.6 p38MAPK signaling pathway

The p38MAPK is an important player involved in the regulation of intercellular adhesion (Spindler and Waschke, 2014) and has been associated with a variety of vital functions (Fig. 6). So far, four splice variants of p38MAPK are known, of which p38 α and p38 β are ubiquitously expressed whereas p38 γ as well as p38 δ expression is dependent on the type of tissue (Hanks and Hunter, 1995). Activation of p38MAPK includes extracellular stimuli such as UV light, heat, osmotic shock, inflammatory cytokines and growth factors (Foltz et al., 1997; Han et al., 1994; Lee et al., 1994; Raingeaud et al., 1995; Rouse et al., 1994). Further complexity comes from the vast number of extracellular activators, of which some can do both, activate as well as inactivate the kinase dependent on the type of cell. For instance, insulin activates p38MAPK in adipocytes but downregulates the kinase in chick forebrain neuron cells (Heidenreich and Kummer, 1996; Sweeney et al., 1999). Moreover, several upstream kinases regulate p38MAPK activity (Zarubin and Han, 2005) with MKK3 and MKK6 from the MAP kinase kinase (MAPKK) family being the two main kinases known to activate p38MAPK (Enslin et al., 1998). Furthermore, a MAPKK-independent mechanism of p38MAPK activation has been reported, involving autophosphorylation of p38MAPK upon binding to transforming growth factor- β -activated protein kinase 1 binding protein (TAB1) (Ge et al., 2002). In addition, Rho family GTP-binding proteins such as RhoA, Rac1 and Cdc42 also contribute to p38MAPK activation (Bagrodia et al., 1995; Kyriakis and Avruch, 2001; Zhang et al., 1995). Downregulation of p38MAPK activity is achieved by dephosphorylation through phosphatases from the MAP kinase phosphatase (MPK) family as well as some other types of phosphatases such as serine/threonine protein

phosphatase type 2C (PP2C) (Sun et al., 1993; Takekawa et al., 1998). Substrates of p38MAPK include downstream kinases, transcription factors as well as components of the cytoskeleton such as keratins and regulate cell metabolism, apoptosis, survival, migration, inflammation, cell growth, proliferation and cell differentiation (Daly et al., 1999; Dieckgraefe et al., 1997; Sharma et al., 2003; Xia et al., 1995; Zarubin and Han, 2005). Furthermore, a growing number of studies reports a role for p38MAPK in regulating cell adhesion. Thus, p38MAPK-mediated keratin retraction paralleled with decreased cell cohesion, is a well-known phenomenon in pemphigus (Berkowitz et al., 2005; Spindler et al., 2013). This process involves EGFR activation and inhibition of RhoA activity, which results in reduced insertion of keratin filaments at cell junctions (Bektas et al., 2013; Waschke, 2008). Furthermore, p38MAPK is also known to bind directly to Dsg3 and PG and activation of p38MAPK has been associated with increased desmosomal turnover in a clathrin- and dynamin-independent manner (Delva et al., 2008; Mao et al., 2009; Saito et al., 2012; Schulze et al., 2012; Spindler et al., 2013). In addition, increased activity of p38MAPK upon stimulation with TNF α induced loss of cell cohesion and increased permeability in cultured IECs (Spindler et al., 2015).

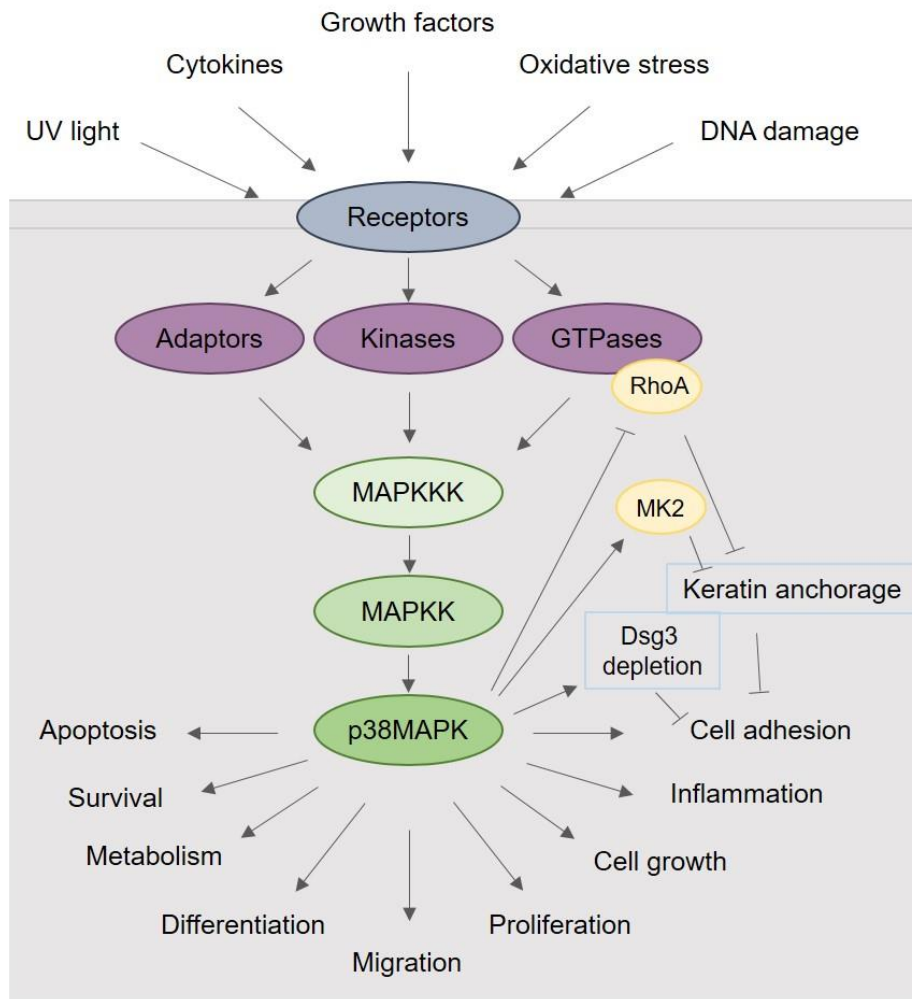


Figure 6. The p38MAPK signaling pathway and associated functions. Activation of the p38MAPK signaling pathway includes stimulation with UV light, cytokines, growth factors, oxidative stress or DNA damage. Upon stimulation, a cascade of several kinases is activated resulting in phosphorylation of p38MAPK, which in turn regulates a variety of cellular functions. Among others, activation of p38MAPK inhibits anchorage of the keratin filament cytoskeleton via RhoA and MK2, resulting in impaired cell adhesion. In addition, active p38MAPK promotes Dsg3 depletion, further destabilizing cell adhesion.

1.3.7 EGFR signaling pathway

Beside its plethora of functions including cell growth, differentiation, proliferation and motility (Ceresa and Peterson, 2014), increasing evidence indicate that EGFR plays a central role in regulating intercellular adhesion. Moreover, EGFR has already been shown to regulate function of desmogleins and vice versa (Blay and Brown, 1985; Getsios et al., 2009; Kamekura et al., 2014; Klessner et al., 2009; Lorch et al., 2004; Overmiller et al., 2016). The EGFR belongs to the ErbB/HER protein-tyrosine kinase family, of which four members are known in vertebrates, HER1-4 that are expressed at the cell surface of numerous cell types (Hynes and Lane, 2005). The extracellular region comprises four domains I-IV, of which the domains I and III bind to activating ligands. Domain II contains a dimerization arm that is masked through intramolecular interactions with domain IV resulting in a tethered conformation that inhibits dimerization (Bouyain et al., 2005; Burgess et al., 2003; Cho and Leahy, 2002; Ferguson et al., 2003). Ligand binding induces a conformational change that unmask the dimerization arm and allows homophilic as well as heterophilic interaction with a second ligand-bound receptor molecule to form functional dimers or oligomers (Burgess et al., 2003; Roskoski, 2014). So far, seven different ligands are known to bind to EGFR, of which EGF is considered to bind with high affinity (Harris et al., 2003; Wilson et al., 2009). All ligands are produced as transmembrane precursor proteins and have to be cleaved by cell surface proteases to be released as mature growth factors that bind to EGFR (Harris et al., 2003). Since production of EGF is controlled locally, in contrast to being delivered systematically like it is the case for hormones, it is possible that different organs execute their own EGF-mediated programs (Conte and Sigismund, 2016; Singh and Harris, 2005). Receptor dimerization induces activation of the EGFR tyrosine kinase domain (TKD) and succeeding cross-phosphorylation of cytoplasmic receptor domains that serve as docking sites for several adaptor proteins containing Src homology-2 (SH2) and phosphotyrosine-binding (PTB) domains (Honegger et al., 1989; Kaplan et al., 2016; Ogiso et al., 2002; Shoelson, 1997; Sudol, 1998; Ullrich and Schlessinger, 1990). Recruited proteins include for example Src homology domain-containing adaptor protein C (Shc), growth factor receptor-bound protein 2 (Grb2) phospholipase C γ (PLC γ) or kinases such as Src, phosphatidylinositol-3-kinase (PI3K), phosphatases such

as PTP1B, SHP1 and SHP2 and ubiquitin ligases such as Cbl (Olayioye et al., 2000). The kinase Src has additionally been shown to phosphorylate EGFR on tyrosine residue 845 (Y845) in a ligand independent manner (Moro et al., 2002). Over hundred interaction partners for EGFR have been identified so far and the number is still growing (Morandell et al., 2008). Specificity of the docking site is defined by the phosphorylated tyrosine residue, of which approximately twenty residues have been identified as docking sites that trigger various signaling cascades. The major signaling cascades involve Ras/Raf/MEK/ERK/MAPK and PI3K/Akt pathways (Singh and Harris, 2005) but further pathways have been reported such as PLC γ /PKC, signal transducer and activator of transcription (STAT), c-Jun terminal kinase (JNK) as well as p38MAPK (Andl et al., 2004; Johnson et al., 2005; Kloth et al., 2002) (Fig. 7). Vice versa, p38MAPK is also a feedback regulator of EGFR and controls its expression (Frey et al., 2006; Vergarajauregui et al., 2006). Furthermore, EGFR is internalized upon ligand binding via clathrin-coated endocytic vesicles that fuse with early endosomes where the EGFR is sorted for recycling or degradation (Bakker et al., 2017). While trafficking, signaling continues and EGFR is also known to function as transcription factor in the nucleus (Brand et al., 2013; Francavilla et al., 2016; Haugh et al., 1999; Kamio et al., 1990; Vieira et al., 1996; Wu et al., 2012). The EGFR pathway controls a series of biological functions such as cell proliferation, differentiation, survival, migration, angiogenesis and cell adhesion (Baselga and Hammond, 2002; Laskin and Sandler, 2004; Morandell et al., 2008; Yarden and Sliwkowski, 2001). Moreover, EGFR is suggested to regulate cell extrusion, wound healing and migration in the intestinal epithelium (Blay and Brown, 1985; Miguel et al., 2017; Polk, 1998). These processes require precise regulation of intercellular adhesion and thus it comes as no surprise that several studies linked the EGFR to desmosomal function. In keratinocytes, Dsg1 was shown to co-localize with EGFR, thus suppressing its activity to promote differentiation (Getsios et al., 2009). Another study reported positive regulation of EGFR by Dsg2 thereby stimulating cell-growth and migration (Overmiller et al., 2016) and Dsg2 turnover is under control of EGFR signaling (Klessner et al., 2009). There is also evidence for direct interaction of Dsg2 and EGFR (Tong et al., 2014). In addition, desmosomal plaque proteins have been linked to the EGFR pathway, such as Pkp2 that enhances ligand-dependent as well as ligand-independent receptor dimerization and activation (Arimoto et al., 2014).

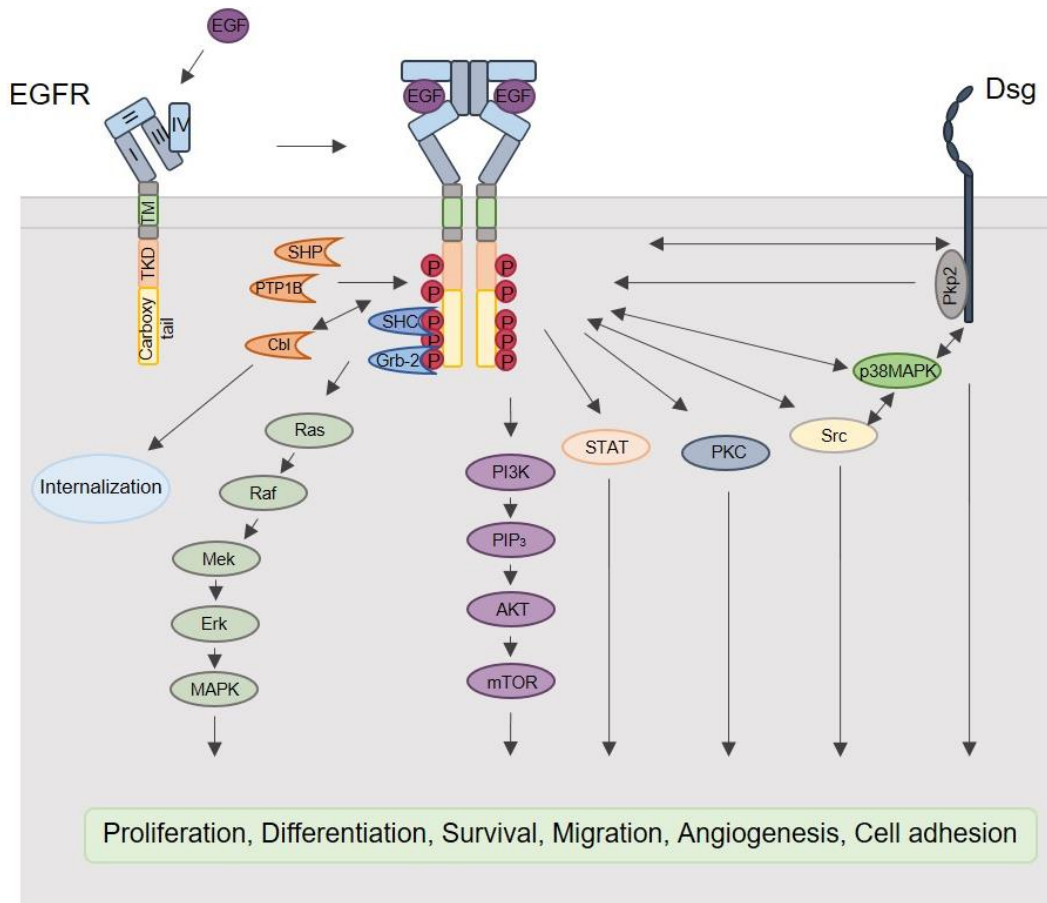


Figure 7. The EGFR signaling pathway and associated functions. The EGFR appears as monomer in a tethered conformation that is opened upon ligand binding, which allows receptor dimerization followed by cross-phosphorylation of the cytoplasmic tail tyrosine residues. Several adaptor proteins as well as kinases, phosphatases and ubiquitin ligases are recruited dependent on the type of phosphorylation that results in activation of various signaling cascades controlling vital cellular functions. Ligand binding also induces receptor internalization. Besides, EGFR is also linked to desmosomal components.

1.3.8 Glial cell-derived neurotrophic factor

The intestinal epithelial barrier function is additionally regulated by the ENS, which is a network of glial and neuronal cells and through sympathetic and parasympathetic pathways liaises closely with the CNS (Furness, 2012). Increasing evidence attribute a key role in regulating barrier function to the EGCs that release specific mediators such as GDNF or TGF β 1 hence controlling the maintenance of both, ENS and epithelial barrier integrity (Abdo et al., 2010; Neunlist et al., 2014). Ablation of EGCs has been

demonstrated to impair intestinal barrier function in mice (Bush et al., 1998; Cornet et al., 2001) and functional as well as morphological abnormalities similar to inflammatory bowel diseases were observed in mice with reduced GDNF levels (Brun et al., 2013; von Boyen et al., 2004; Zhang et al., 2010b). GDNF is a growth factor belonging to the cysteine-knot superfamily and signals through a receptor complex consisting of the RTK RET (rearranged during transfection) and one of four GDNF family receptors (GFR α 1-4) (Takahashi, 2001). Downstream targets of the activated receptor complex include p38MAPK, Erk, Akt and PKA (Allen et al., 2013; Granholm et al., 2000; Takahashi, 2001). In general, GDNF influences the proliferation of glial cells as well as neurons during development of the ENS (Wang et al., 2010), but additionally GDNF is reported to have strong anti-apoptotic effects on colonic epithelial cells (Steinkamp et al., 2003; Zhang et al., 2010b). Moreover, GDNF is suggested to directly affect junctional proteins such as claudin 5 that is upregulated by the growth factor in the blood-brain barrier (Shimizu et al., 2012). Along this line, a recent study demonstrated a positive effect on barrier maturation and wound healing in IECs involving enhanced maturation of TJ and on top, suggests enterocytes to represent another source for GDNF in the intestine (Meir et al., 2015b). However, it is unclear what stimulus induces GDNF expression in enterocytes. Here, toll-like receptor 2 (TLR-2) that is activated by pathogen-associated molecular patterns (PAMPs) and damage-associated molecular patterns (DAMPs), has been shown to be required for secretion of GDNF in EGCs (Walsh et al., 2013). Hence, it can be envisioned that GDNF regulates the intestinal barrier properties in pathophysiological inflammatory states such as IBD.

1.4 Inflammatory bowel disease

Dysfunction of the intestinal epithelial barrier is a hallmark of IBD including ulcerative colitis (UC) and CD, which affect mostly young people (Martini et al., 2017). While CD can impact any part of the gastrointestinal tract, UC is limited to the mucosa of the colon (Feakins, 2014). Up to 40% of first-degree relatives of patients suffering from CD display an altered permeability in the small intestine without showing symptoms of IBD, indicating that multiple genetic as well as environmental factors contribute to a complex pathogenesis (Geremia et al., 2014; Hollander et al., 1986; Peeters et al., 1997; Uhlig, 2013). Due to an uncontrolled immune response to gut microbiota, which results from compromised barrier functions, IBD was classified as an autoimmune disease, for a long time. However, nowadays the disturbed adaptive immunity is considered rather as consequence than as cause of intestinal inflammation (Jager et al., 2013). An increased secretion of the inflammatory cytokine $\text{TNF}\alpha$ is believed to be a critical factor that links the observed increased intestinal permeability and immune reaction (Sanders, 2005). However, $\text{TNF}\alpha$ also affects junctional components such as Dsg2 that has been shown to disappear from cell borders upon stimulation with $\text{TNF}\alpha$. In addition, claudins were deregulated with a reduction of Cld1 and upregulation of Cld2 (Spindler et al., 2015). At least in part, these effects were triggered by activation of p38MAPK. Alterations in TJ integrity is a well-known phenomenon in patients suffering from CD (Mankertz and Schulzke, 2007; Zeissig et al., 2007). Likewise, AJ are affected in CD with an observed dislocation of Ecad (Muisse et al., 2009). Furthermore, several signaling molecules such as RhoA or MLCK that are linked to regulation of intercellular adhesion, have been reported to be dysregulated in patients with IBD (Blair et al., 2006; Lopez-Posadas et al., 2016). Hence, not only changes in composition of intercellular junctions play a key role in the pathogenesis of IBD but also signaling related to intercellular junctions. Treatment of IBD is currently focused on immunomodulators and anti-inflammatory agents to control the inappropriate immune response as well as inflammation that harms the intestinal epithelium (Cohen et al., 2012). However, there are considerable side-effects and not all patients respond to the therapy, which underlines the need for new therapeutic approaches (MacDonald et al., 2012; Rutgeerts et al., 2009). Hence, a deeper knowledge on the pathophysiology of IBD might provide new therapeutic options.

1.5 Aim of this study

For a long time, desmosomes have been considered to provide primarily the mechanical strength to intercellular cohesion. However, a growing number of studies point also towards a role in regulating signaling cascades. Especially tissues with a high turnover rate such as the human intestinal epithelium require a precise regulation of intercellular adhesion to allow cell extrusion and proliferation, while maintaining the epithelial barrier function. Many signaling pathways are known to be central during intestinal tissue homeostasis, however only little is known about their interplay with desmosomal components. Thus, the main objective of this PhD thesis was to explore whether the desmosomal cadherin Dsg2 modulates signaling pathways beside its adhesive properties in simple epithelia of the intestine.

For this purpose, WT as well as Dsg2 deficient cultured enterocytes were analyzed regarding deregulated signaling pathways as well as their intercellular cohesion and barrier properties. To ascertain the suitability of cultured enterocytes as a model for the intestinal epithelium, cells were characterized concerning the establishment of junctional complexes and compared to human tissue from the intestine using transmission as well as scanning electron microscopy.

Although, being the core adhesive molecule of desmosomes, the appearance of extradesmosomal cadherins has been reported. Thus, another goal was to clarify the question whether extradesmosomal Dsg2 is present in IECs, which was addressed utilizing high resolution microscopy as well as biochemical approaches.

To elucidate binding properties of Dsg2, atomic force microscopy (AFM) was established on living enterocytes. Using this approach several modulators of different signaling cascades were tested regarding their ability to influence Dsg2 binding.

A crucial regulator of the intestinal homeostasis is EGFR that has already been linked to regulation of junctional complexes. Hence, a further aim was to explore a putative cooperation of Dsg2 and EGFR in intestinal barrier regulation. For this, co-localization studies, biochemical assays, interaction studies and functional assays were performed in cultured cells as well as human tissue samples.

Since Dsg2 is assumed to contribute to the pathogenesis of CD, another goal was to elucidate its role in this context. To this end, human tissue samples from CD patients were analyzed with regard to ultrastructural changes of desmosomes. Moreover, the interrelationship of Dsg2 and GDNF, which is a potential key player in IBD, was characterized with AFM.

2 Results

2.1 Desmoglein 2 regulates the intestinal epithelial barrier via p38 mitogen-activated protein kinase

SCIENTIFIC REPORTS

OPEN

Desmoglein 2 regulates the intestinal epithelial barrier via p38 mitogen-activated protein kinase

Hanna Ungewiß¹, Franziska Vielmuth¹, Shintaro T. Suzuki², Andreas Maiser³, Hartmann Harz³, Heinrich Leonhardt³, Daniela Kugelmann¹, Nicolas Schlegel⁴ & Jens Waschke¹

Intestinal epithelial barrier properties are maintained by a junctional complex consisting of tight junctions (TJ), adherens junctions (AJ) and desmosomes. Desmoglein 2 (Dsg2), an adhesion molecule of desmosomes and the only Dsg isoform expressed in enterocytes, is required for epithelial barrier properties and may contribute to barrier defects in Crohn's disease. Here, we identified extradesmosomal Dsg2 on the surface of polarized enterocytes by Triton extraction, confocal microscopy, SIM and STED. Atomic force microscopy (AFM) revealed Dsg2-specific binding events along the cell border on the surface of enterocytes with a mean unbinding force of around 30pN. Binding events were blocked by an inhibitory antibody targeting Dsg2 which under same conditions activated p38MAPK but did not reduce cell cohesion. In enterocytes deficient for Dsg2, p38MAPK activity was reduced and both barrier integrity and reformation were impaired. Dsc2 rescue did not restore p38MAPK activity indicating that Dsg2 is required. Accordingly, direct activation of p38MAPK in Dsg2-deficient cells enhanced barrier reformation demonstrating that Dsg2-mediated activation of p38MAPK is crucial for barrier function. Collectively, our data show that Dsg2, beside its adhesion function, regulates intestinal barrier function via p38MAPK signalling. This is in contrast to keratinocytes and points towards tissue-specific signalling functions of desmosomal cadherins.

The internal surface of the gut is covered by a single layer of polarized enterocytes, forming the intestinal epithelium that operates as a selective barrier which protects the organism against luminal pathogens but allows uptake of nutrients. Barrier properties are established by three types of intercellular junctions, tight junctions (TJ), adherens junctions (AJ) and desmosomes which together form the "terminal bar" by sealing the paracellular space^{1,2}. TJ composed of claudins, occludin and a range of additional transmembrane proteins, are located in the most apical part where they seal the intercellular cleft³. Beneath, AJ formed by E-cadherin (E-cad) and a set of associated proteins mediate mechanical strength between epithelial cells and in addition are also involved in epithelial polarization, differentiation, migration and tissue morphogenesis⁴. The third and least studied type of intercellular junctions are the desmosomes, composed of the cadherin family members desmoglein (Dsg) and desmocollin (Dsc), which interact in homo- and heterophilic fashion via their extracellular domains (ED) and are associated with the intermediate filament cytoskeleton through specific desmosomal plaque proteins, namely plakoglobin (PG), plakophilins (Pkp) and desmoplakin (DP)⁵. Desmosomal cadherins are expressed as multiple isoforms in a tissue- and differentiation-specific manner. Layer specific expression pattern of all human isoforms (Dsg1-4 and Dsc1-3) can be observed in stratified epithelia such as the human epidermis whereas desmosomes in the simple columnar epithelium of the human intestine are composed of Dsg2 and Dsc2 only⁶⁻⁹.

Desmosomes are assumed to play the leading role in intercellular cohesion¹⁰. Beyond, they are also implicated in modulating fundamental cellular processes such as proliferation, apoptosis or organization of the cytoskeleton¹¹. We have previously shown that desmosomal adhesion is required for intestinal epithelial barrier function¹². The maintenance and turn-over of junctional complexes has to be regulated tightly during the rapid cell renewal of every 4–5 days in the intestinal epithelium¹³. On the other hand, increased intestinal permeability is associated

¹Department I, Institute of Anatomy and Cell Biology, Ludwig-Maximilians-Universität München, Pettenkoferstr. 11, 80336, Munich, Germany. ²Department of Bioscience, School of Science and Technology, Kwansai Gakuin University, Sanda-shi, Hyogo-ken, 669-1337, Japan. ³Department of Biology II, Ludwig-Maximilians-Universität München, Großhaderner Str. 2, 82152, Planegg-Martinsried, Germany. ⁴Department of General, Visceral, Vascular and Paediatric Surgery, Julius-Maximilians-Universität, Oberdürrbacher Str. 6, 97080, Würzburg, Germany. Correspondence and requests for materials should be addressed to J.W. (email: jens.waschke@med.uni-muenchen.de)

Received: 16 December 2016

Accepted: 16 June 2017

Published online: 24 July 2017

with severe inflammatory disorders such as Crohn's disease (CD)^{14–17}. Especially, Dsg2 has already been shown to play a role in inflammation¹⁸ and in the pathogenesis of CD as it was strongly reduced in the mucosa of patients suffering from CD whereas the AJ molecule E-cadherin was unaffected¹⁹. Tumor necrosis factor- α (TNF- α), which is a central cytokine in CD, resulted in impaired barrier properties whereas a tandem peptide stabilizing desmosomal adhesion rescued barrier function. Interestingly, similar to TNF- α , a Dsg2-specific antibody targeting the ED of Dsg2 increased permeability¹². However, it is unclear how this effect is achieved. It is likely that some amount of antibody permeates across TJs and directly inhibits transinteraction of Dsg2 within desmosomes, which compromises barrier integrity.

Another possibility could be that Dsg2 is expressed outside of desmosomes on the cell surface, accessible to the Dsg2-specific antibody and binding resulted in activation of signalling pathways. Desmogleins have already been shown to mediate signalling events²⁰, however, nothing is known about extradesmosomal Dsg2 on the cell surface of enterocytes. In contrast, in keratinocytes extradesmosomal Dsg3 but not Dsg2 has been found in a signalling complex together with E-cadherin, β -catenin and Src²¹ where Dsg3 strengthens cell cohesion via modulation of mitogen-activated protein kinase (p38MAPK)²².

Bearing in mind that Dsg2 is the only Dsg isoform expressed in enterocytes and in view of our previous finding that it may contribute to the pathogenesis of CD, we investigated whether Dsg2 plays a role in modulating signalling cascades and cell cohesion in enterocytes, in this study. For the recent study, we used DLD1 cells deficient for Dsg2 and or Dsc2 under conditions where they were polarized similar to the well-established model of Caco2 cells used in our previous studies. Here, we show for the first time that extradesmosomal Dsg2 is expressed on the surface of polarized cultured enterocytes. Moreover, our data identify a novel role for Dsg2 in regulating p38MAPK as this kinase was activated after application of the Dsg2-specific antibody and reduced levels of p38MAPK activity were detected in Dsg2 knockout cells. Furthermore, activation as well as inhibition of p38MAPK led to barrier-destabilization, suggesting that a well-balanced level of p38MAPK activity is crucial for barrier properties. Collectively, our data provides evidence that Dsg2 regulates barrier properties in enterocytes via modulating the p38MAPK signalling cascade.

Results

Polarized cultured enterocytes displayed extradesmosomal Dsg2 at the cell surface. To explore the adhesive and signalling function of Dsg2 in the intestine, we used Caco2 and DLD1 cell lines. Both form an enterocyte-like epithelial cell monolayer with fully formed junctional complexes and characteristic microvilli on the cell surface (Fig. S1A) resembling a human specimen from the terminal ileum (Fig. S1B). Immunostaining of the junctional components Dsg2 and Claudin4 (Cld4) revealed linear localization at the cell border with junctional complexes being present at the most apical part of the intercellular cleft (Fig. 1A and S1C). Moreover, constant protein levels of junctional components (Fig. S1D) as well as constant transepithelial resistance (TER) values (Fig. S1E) revealed mature barrier properties. By using structured illumination microscopy (SIM), we observed that Dsg2 is also located at the free cell surface which is characterized by microvilli (Fig. 1B). Furthermore, SIM allowed distinguishing between desmosomal Dsg2 which is in close proximity to DP and extradesmosomal Dsg2 which is found solitary. Sandwich-like arrangement of Dsg2 and DP was observed at the lower lateral cell borders whereas apically, Dsg2 was found primarily separate from DP (Fig. 1C). Additionally, by using stimulated emission depletion microscopy (STED), we identified clusters on the cell surface consisting of Dsg2 and DP molecules as well as single Dsg2 molecules (Fig. 1D). These results were confirmed biochemically by triton extraction which separates the cell lysate into a soluble fraction and an insoluble fraction which is considered to be cytoskeleton-bound and to contain desmosomal components. In contrast to DP, which was detected in the insoluble fraction only, Dsg2 was found in both the insoluble as well as the soluble fraction (Fig. 1E) in line with extradesmosomal localization of Dsg2. Taking together, our findings reveal that Dsg2 is present outside of desmosomes on the cell surface in addition to its typical localization to serve as adhesion molecule in desmosomes.

Dsg2-specific binding events were detected on the surface of living enterocytes. Since immunostaining revealed Dsg2-specific spots on the cell surface, we next applied AFM on living cells to characterize Dsg2-specific binding events similar as shown recently for Dsg3^{23,24}. The AFM topography image of DLD1 cells closely resembled the scanning electron microscopy (SEM) image of these cells (Fig. S2A) and allows specific measurements at cell borders which appeared elevated in the topography image. For each experiment, 2–3 areas at cell borders were selected for each condition, with 1000 recorded force-distance curves for each area. Under control conditions, binding events with a frequency of around 14,5% were detected which were more prominent close to the cell border (Fig. 2A). Peak fit analysis of unbinding force in DLD1 cells revealed a distribution-peak at 30,4 pN (Fig. 2B). To demonstrate specificity of binding events, an inhibitory Dsg2-specific antibody was added after control measurements^{12,25}. The antibody significantly reduced the binding frequency by around 40% (Fig. 1C). Specificity of the Dsg2-specific antibody was verified in a cell-free AFM setup, where it significantly blocked homophilic Dsg2 interaction to a similar extent (Fig. 2D). Similarly, siRNA-mediated silencing of Dsg2 expression resulted in significantly reduced binding frequency (Fig. S2B). Next, the antibody was applied in a dispase-based cell dissociation assay to investigate its effect on cell adhesion. Application for 24 h resulted in increased cell monolayer fragmentation compared to controls in both DLD1 and Caco2 monolayers (Fig. 2E and S2C). Depletion of Dsg2 using siRNA yielded similar results in both DLD1 and Caco2 cells (Fig. S2D). These observations further confirm the presence of extradesmosomal Dsg2 on the cell surface which specifically can be targeted by an anti Dsg2 antibody which is capable of reducing cell cohesion.

Inhibition of Dsg2 binding activated p38MAPK which is critical for enterocyte cohesion. In addition to their adhesive functions, desmosomal cadherins have already been shown to regulate p38MAPK signalling in keratinocytes^{22,26,27}. Hence, we investigated the effect of inhibited Dsg2 binding on p38MAPK activity

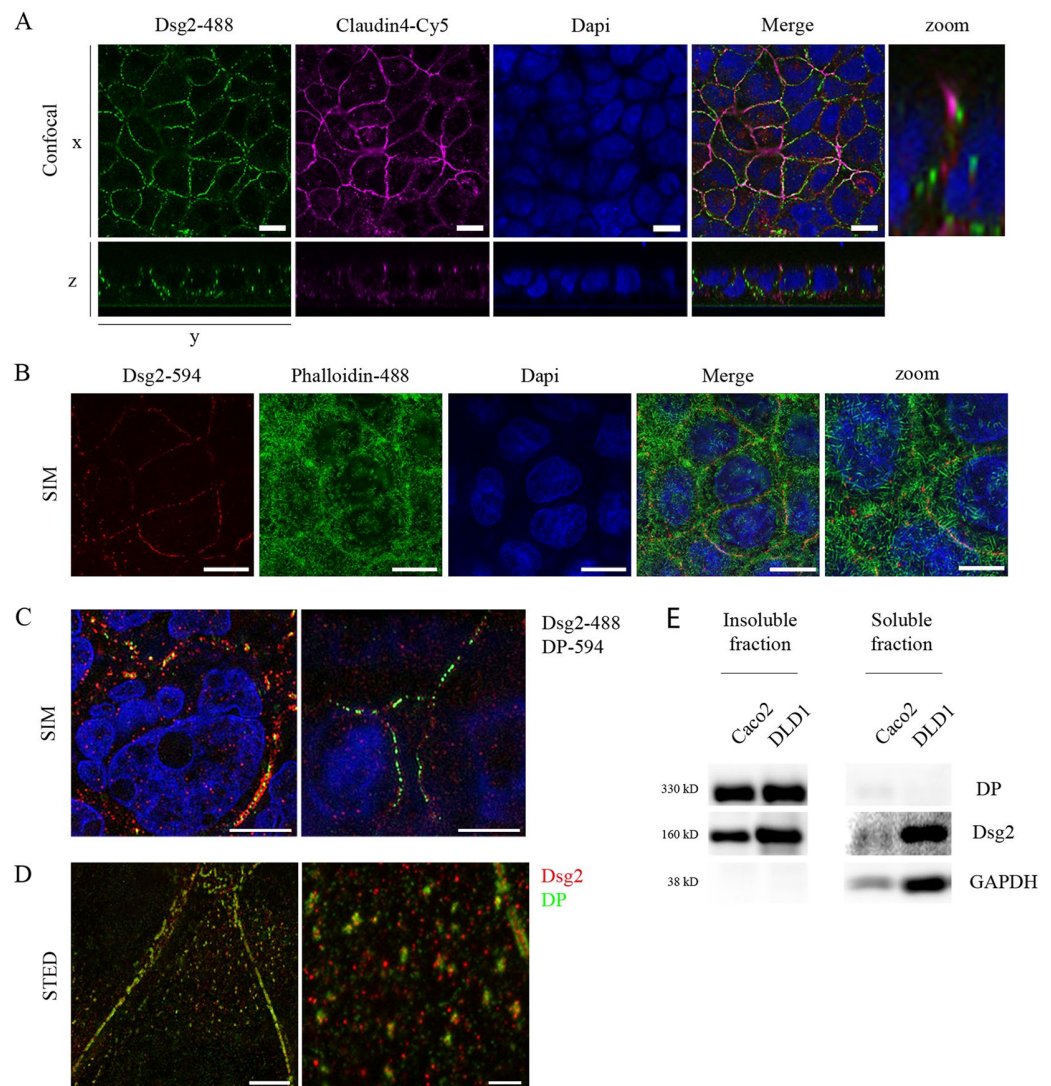


Figure 1. Extradesmosomal Dsg2 is present at the cell surface of polarized cultured enterocytes. Cells were grown on coverslips for several days after reaching confluency, fixed with 2% PFA and stained for junctional components. (A) Confocal microscopy analysis of Caco2 cells shows linear and apical localization of the junctional components Dsg2 and Cld4 at cell borders. Scale bar, 10 μ m. (B) Analysis with SIM shows Dsg2 being located at same level as microvilli, visualized with Alexa488-phalloidin, at the surface of Caco2 cells. Shown is a Z-projection. Bar, 5 μ m. (C) Apical fraction of Dsg2 (right panel) is not co-localizing with DP in contrast to lower layers (left panel) where both can be found in close proximity as analysed via SIM. Scale bar, 5 μ m. (D) Both, clusters consisting of Dsg2 and DP as well as single Dsg2 molecules are present on the cell surface of DLD1 cells, as revealed by STED. Scale bar, 5 μ m (left panel), 1 μ m (right panel). (E) Dsg2 was detected in both, the Triton X-100-soluble and -insoluble fraction in contrast to DP being present only in the insoluble fraction. GAPDH served as loading control. Cropped blots are displayed and full-length blots are included in the supplementary information.

in enterocytes. After incubation with the Dsg2-specific antibody for 30 min, we observed activation of p38MAPK (Fig. 3A and B). Depletion of Dsg2 by siRNA did not cause p38MAPK activation but rather resulted in reduced level of p38MAPK activity (Fig. S3A), which is similar to DLD1 cells lacking Dsg2 (see below). Next, we examined whether the activity of p38MAPK is important for cell cohesion. Blocking of p38MAPK with the inhibitor SB202190 as well as activation of p38MAPK with anisomycin resulted in increased cell monolayer fragmentation (Fig. 3C). Moreover, application of the p38MAPK inhibitor together with the Dsg2-specific antibody also increased fragmentation (Fig. 3C). Intriguingly, short incubation with the Dsg2-specific antibody for 30 min was sufficient to activate p38MAPK but not to reduce cell cohesion (Fig. S3B), suggesting that binding to extradesmosomal Dsg2 may induce p38MAPK signalling. In contrast, incubation for 24 h increased cell monolayer fragmentation and was accompanied with elevated p38MAPK activity (Fig. S3C). Together, these data indicate that

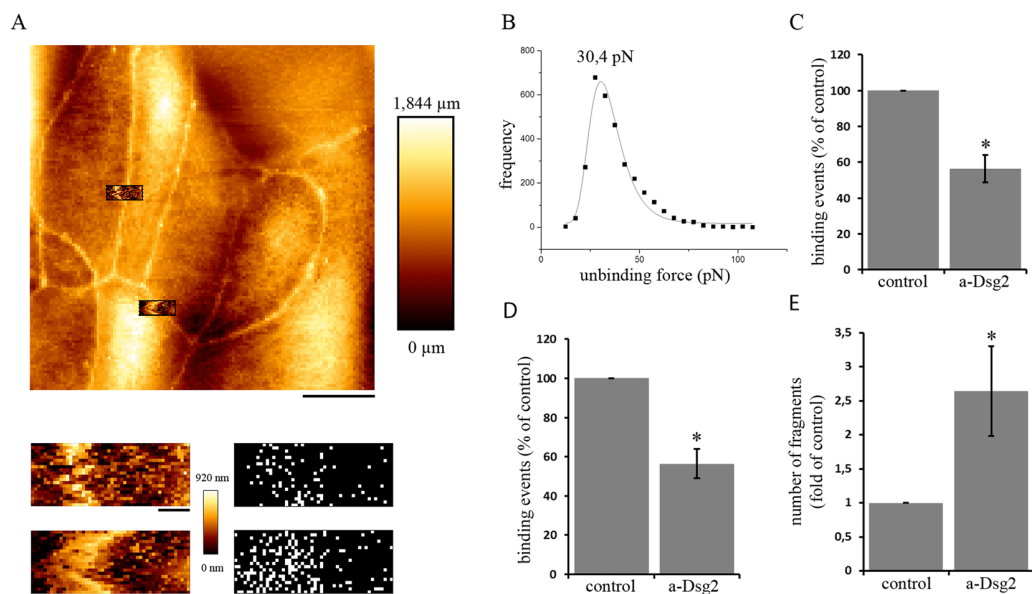


Figure 2. Dsg2-specific binding events can be detected on the surface of enterocytes. (A) Dsg2 force measurements were performed on living DLD1 cells at 37 °C. Cell topography was imaged to select specific areas at cell borders (upper panel). Force measurements revealed binding events along the cell border (lower panel) Bar, 10 μ m (upper panel), 1 μ m (lower panels). (B) Peak fit analysis of unbinding force resulted in a distribution-peak of 30,4 pN. (C) Application of a Dsg2-specific antibody significantly reduced the amount of binding events on living DLD1 cells as well as (D) in a cell-free setup (shown are means \pm SE, n = 3, *p < 0,05). (E) Dsg2-specific antibody increased cell monolayer fragmentation in a disperse-based cell dissociation assay. (Shown is mean \pm SE, n = 9, *p < 0,05 compared to control).

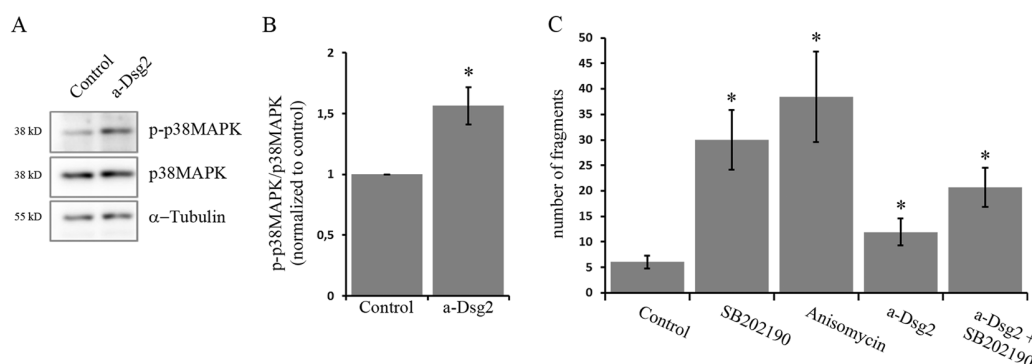


Figure 3. Inhibition of Dsg2 binding resulted in increased p38MAPK activity which is critical for enterocyte cohesion. (A) Western blot analysis after incubation of DLD1 cells with a Dsg2-specific antibody for 30 min revealed increased phosphorylation of p38MAPK. Cropped blots are displayed and full-length blots are included in the supplementary information. (B) Band intensity of detected p-p38MAPK was quantified using ImageJ and normalized to control (shown is mean \pm SE, n = 6, *p < 0,05 compared to control). (C) DLD1 cells were treated with the p38MAPK inhibitor SB202190 or the activator anisomycin and analysed in a disperse-based cell dissociation assay. Both resulted in increased cell monolayer fragmentation. (Shown is mean \pm SE, n = 3, *p < 0,05 compared to control).

inhibition of Dsg2 binding activates p38MAPK which is critical for enterocyte cohesion and that the level of activated p38MAPK has to be well-balanced.

Balance of p38MAPK activity is critical for intestinal barrier function. We have previously shown that Dsg2 is required for maintenance of intestinal barrier function¹². Therefore, we next sought to explore the role of Dsg2 during barrier recovery. To this end, we performed Ca^{2+} -switch experiments which allowed us to induce barrier recovery under well-defined conditions²⁸. TER values of confluent monolayers dropped during 1 h of EGTA-mediated Ca^{2+} depletion by around 50% and rose immediately after addition of $CaCl_2$ (Fig. 4A and S4A). After about two hours of repletion, TER values reached again control levels indicating that reformation

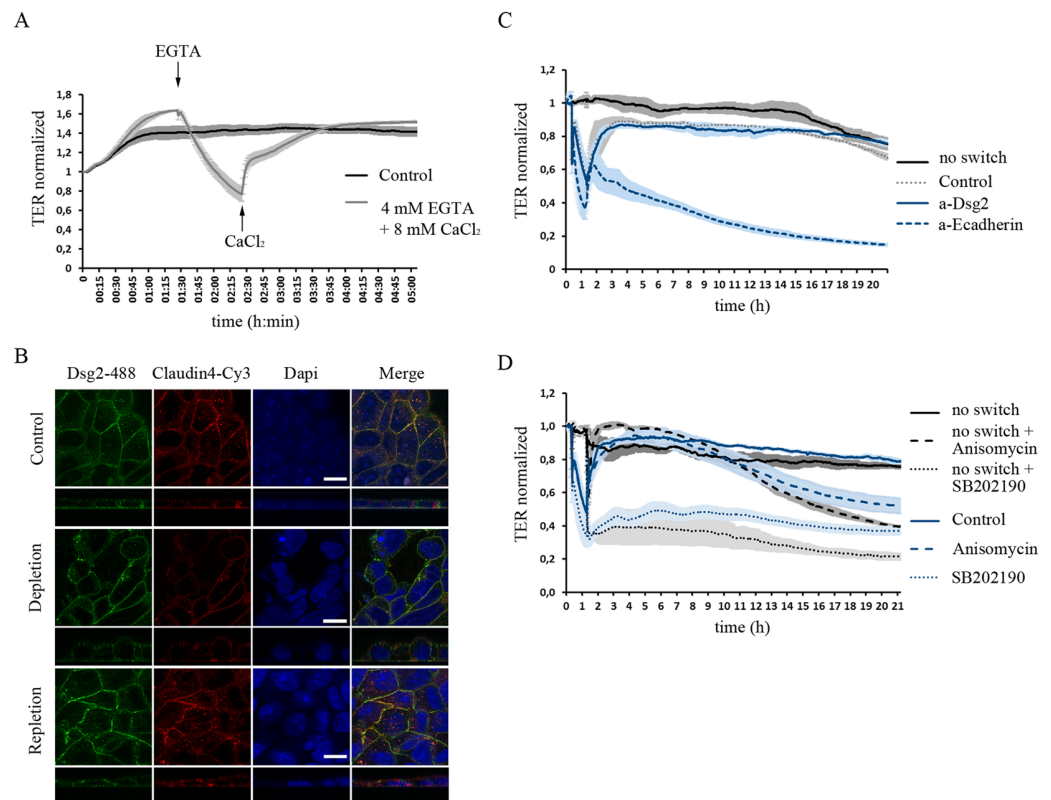


Figure 4. Well-balanced p38MAPK activity is critical for intestinal barrier function. Ca²⁺-switch assay with confluent DLD1 cells. (A) TER values decrease during depletion with 4 mM EGTA for 1 h and increase to back to control values during 2 h of repletion with 8 mM CaCl₂. (B) Immunostaining of Dsg2 and Cld4 shows reduced and fragmented staining as well as gaps after 1 h depletion and similar staining to control condition after 2 h repletion. (C) Barrier reformation is not disturbed after application of a Dsg2-specific antibody but is impaired after addition of an inhibitory anti E-cadherin antibody. (D) TER values decrease after inhibition of p38MAPK with SB202190 and also barrier reformation is impaired in the Ca²⁺-switch experiment. Activation of p38MAPK via anisomycin has no effect in the short run but also induces reduction of TER values after about 10 h. (shown are representative graphs for at least three independent experiments).

of junctional complexes is completed. In line with this, immunostaining of Dsg2, E-cad and Cld4 displayed fragmentation and reduction at cell borders during depletion accompanied with formation of intercellular gaps (Fig. 4B and S4B–D). After two hours of repletion, immunostaining was similar to controls (Fig. 4B and S4C). To examine the role of Dsg2 during barrier recovery, we next applied the Dsg2-specific antibody at the end of depletion together with CaCl₂. Interestingly, barrier recovery was not disturbed (Fig. 4C). In contrast, application of an inhibitory E-cad-specific antibody abolished barrier recovery. Next, we applied SB202190 at the end of depletion which in DLD1 cells, prevented barrier reformation and moreover also resulted in barrier disruption without Ca²⁺-switch (Fig. 4D). Similarly, in Caco2 cells, inhibition of p38MAPK significantly delayed barrier recovery (Fig. S4E and S4F). Activation of p38MAPK via anisomycin had no immediate effect on barrier function and recovery (Fig. 4D). However, 10 h after application of anisomycin TER values dropped indicating that a well-balanced level of activated p38MAPK is crucial for barrier maintenance. In summary, our findings support an indispensable role of p38MAPK in barrier reformation and maintenance.

Dsg2 regulates p38MAPK activity which is required for barrier properties. Since the activation of p38MAPK via the Dsg2-specific antibody indicated that Dsg2 regulates p38MAPK activity, we hence determined alterations in p38MAPK signalling in DLD1 cells lacking desmosomal cadherins. Comparison of baseline TER values of wildtype (wt) and knockout cells revealed a significant reduction when desmosomal cadherins were absent (Fig. 5A). Interestingly, no difference was observed when both Dsg2 and Dsc2 were missing or when Dsc2 was re-expressed indicating that Dsg2 was critical for barrier properties. Similarly, in cells lacking Dsg2 chelation of Ca²⁺ had a more severe impact on cell junction disruption with values around 70% lower than wt values at the end of depletion (Fig. 5B). Interestingly, in both DLD1 cells missing Dsg2 and Dsc2 as well as in cells with Dsc2 rescue levels of p-p38MAPK but not total p38MAPK were reduced (Fig. 5D and E). This is similar to DLD1 cells where Dsg2 expression was suppressed by siRNA (Fig. S3A). This indicates that Dsg2 but not Dsc2 regulates the activity of p38MAPK. Finally, we investigated how the loss of desmosomal cadherins affects barrier recovery. Time for repletion was about 4–5 times higher in cells lacking Dsg2 and Dsc2 compared to wildtype (Fig. 5F and G). However, anisomycin to activate p38MAPK during Ca²⁺-switch experiments facilitated repletion in

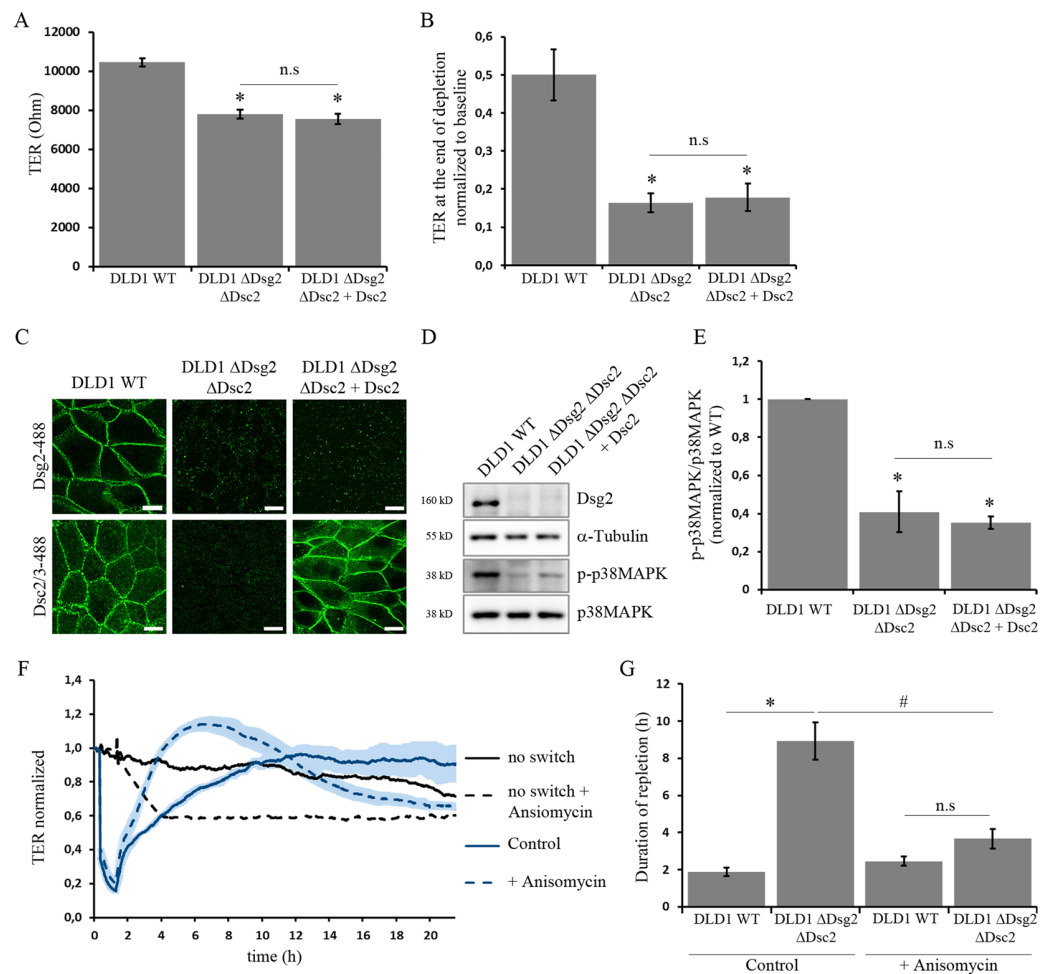


Figure 5. Dsg2 regulates p38MAPK activity which is required for barrier properties. **(A)** Comparison of baseline TER values between wildtype and knockout cells revealed reduced TER in DLD1 cells lacking Dsg2 (shown is mean \pm SE, $n \geq 10$, $*p < 0,05$ compared to control, n.s not significant). **(B)** During Ca^{2+} depletion for 1 h TER values of Dsg2-deficient cells decreased stronger compared to wildtype cells. (Shown is mean \pm SE, $n \geq 6$, $*p < 0,05$ compared to control, n.s not significant). **(C)** Wildtype and knockout cells grown on coverslips were stained for Dsg2 and Dsc2 to confirm knockout. Scale bar, 10 μ m **(D)**. Level of p-p38MAPK in Dsg2 and Dsc2 knockout cells was analysed via Western blot. Loss of Dsg2 and Dsc2 resulted in reduced level of p-p38MAPK which was not restored by Dsc2 rescue. α -Tubulin served as loading control. Cropped blots are displayed and full-length blots are included in the supplementary information. **(E)** Band intensity of detected p-p38MAPK was quantified using ImageJ and normalized to control (shown is mean \pm SE, $n \geq 3$, $*p < 0,05$ compared to control, n.s not significant). **(F)** Time for complete repletion during Ca^{2+} -switch experiments was compared between wildtype and double knockout of Dsg2 and Dsc2. Loss of desmosomal cadherins resulted in a prolonged repletion time which was rescued by activation of p38MAPK via anisomycin (shown is mean \pm SE, $n \geq 6$, $*p < 0,05$ compared to wildtype under control conditions, # $p < 0,05$ compared to Δ Dsg2 Δ Dsc2 under control conditions, n.s not significant). **(G)** Treatment with anisomycin reduced repletion time in Δ Dsg2 Δ Dsc2 knockout cells. Representative graph for at least four independent Ca^{2+} -switch experiments is shown.

Δ Dsg2 Δ Dsc2 cells resulting in times to recovery similar to wt cells (Fig. 5F and G). In summary, these data identify a new role for Dsg2 in regulating p38MAPK activity which is required for barrier properties in enterocytes.

Discussion

In this study we demonstrate that Dsg2 is required for cell cohesion of enterocytes and maintenance of intestinal epithelial barrier function. For this function, regulation of p38MAPK appears to be critical, especially for barrier recovery. We detected reduced levels of activated p38MAPK in enterocytes deficient for Dsg2 and Dsc2 which was accompanied by both impaired barrier integrity as well as delayed barrier reformation. Reduced activity of p38MAPK was not restored with a Dsc2 rescue indicating that Dsg2 is required. However, barrier reformation was accelerated with direct activation of p38MAPK demonstrating that Dsg2-mediated activation of p38MAPK is crucial for barrier function. Furthermore, we identified extradesmosomal Dsg2 on the surface of polarized enterocytes. Application of an antibody targeting the ED of Dsg2 reduced binding events in AFM experiments

and under same conditions activated p38MAPK but was not effective to reduce cell cohesion, indicating that extradesmosomal Dsg2 may be involved in the regulation of p38MAPK signalling.

In previous studies, we have characterized mechanisms regulating desmosomal adhesion in keratinocytes. However, desmosomal cadherins show tissue-specific expression patterns^{6–9}, which implies that they may have distinct functional properties within different tissues. In keratinocytes we found that Dsg2 is less important for cell cohesion compared to Dsg3²⁹ and beyond that, activated p38MAPK reduces intercellular cohesion and forms a complex with Dsg3 but not Dsg2^{22, 30}. In line with this, depletion of Dsg2 did not cause p38MAPK activation. In contrast, this study reveals that in enterocytes active p38MAPK is indispensable for barrier reformation and maintenance. Moreover, Dsg2 appears to regulate the activity of this kinase. However, by immunoprecipitation we did not find Dsg2 being associated with p38MAPK (data not shown).

Previously, we have shown that Dsg2 is required for intestinal barrier properties. Both, an antibody directed against Dsg2 as well as siRNA-mediated Dsg2 depletion resulted in loss of cell cohesion and reduced barrier function^{12, 19, 22}. Since Dsg2 was missing at cell junctions in patients suffering from CD and a Dsg-specific tandem peptide ameliorated barrier dysfunction in response to TNF- α , which is regarded as a central cytokine in CD pathogenesis, we concluded that impaired Dsg2 may contribute to pathogenesis of inflammatory bowel diseases (IBD)¹⁹. This is supported by the finding that cytokines in IBD via matrix metalloproteinase 9 (MMP9) and a disintegrin and metalloproteinase domain-containing protein 10 (ADAM10) cause ectodomain cleavage of Dsg2, the products of which further compromised barrier integrity¹⁸. Thus, we were surprised that the Dsg2-specific antibody was not effective to inhibit barrier reformation in Ca²⁺-switch experiments, in contrast to an inhibitory E-cad-specific antibody which prevented barrier recovery completely. With this, it can be speculated that homophilic Dsc2 interactions can compensate for inhibited Dsg2 binding and are sufficient to restore barrier properties. Otherwise, it is also possible that AJ account for barrier establishment while desmosomes have rather regulatory function during epithelial homeostasis via p38MAPK. Studies from the literature showing that E-cad is clearly present at cell borders already at beginning of confluency¹² support this hypothesis.

As outlined above, previous studies have shown that a specific antibody binding the ED of Dsg2 disrupted intestinal epithelial barrier properties¹². Although, it is likely that this effect is to some extent caused by direct interference of Dsg2 binding within desmosomes, it is also possible that the Dsg2-specific antibody bound to extradesmosomal Dsg2 thereby inducing signalling events leading to reduced barrier properties. This is especially intriguing since extradesmosomal Dsg molecules have been proposed to serve as signalling hubs³¹. In this study, we demonstrated for the first time that Dsg2 is present outside of desmosomes on the surface of polarized cultured enterocytes. Using SIM and STED, we identified distinct Dsg2 spots on the cell surface as well as clusters consisting of Dsg2 and DP. Moreover, specific interaction between Dsg2-coated tips and the surface of living enterocytes was measured with AFM and application of the Dsg2-specific antibody resulted in decreased binding frequency, under conditions where it did not reduce cell cohesion in a dispase-based cell dissociation assay but significantly increased p38MAPK phosphorylation. Collectively, these findings suggest that the Dsg2-specific antibody binds to extradesmosomal Dsg2 on the cell surface thereby inducing p38MAPK signalling. However, incubation for 24 h reduced cell cohesion, indicating that it most likely interfered with desmosomal Dsg2 binding under these conditions. Along with a possible signalling function, Dsg2 is known to be a receptor for adenoviruses of which binding triggers intracellular signalling^{32, 33} also pointing towards the appearance of extradesmosomal Dsg2 on the cell surface as desmosomal Dsg2 is inaccessible for adenoviruses in polarized epithelial cells. Interestingly, Adenovirus 3 is supposed to bind to the ED 3 and 4 leading to an activation of members of the MAPK pathway^{32, 33}. This is in accordance with our data, since the Dsg2-specific antibody is also directed against the ED 3 and induced p38MAPK activation, which was paralleled by reduced cell cohesion in a dispase-based cell dissociation assay. Considering that there is no enzymatic activity of the intracellular tail of Dsg2 known to date, the question arises how signalling cascades can be activated. A recent study demonstrated that soluble Dsg2 fragments activate the Akt/mTOR and MAPK pathway through binding to HER2 and HER3 receptors¹⁸. In this line shedding of the Dsg2 ED upon binding to the virus was reported³², supporting the idea of Dsg2 fragments acting as ligands for other receptors. An alternative mechanism for activating signalling pathways may involve displacing proteins from lipid rafts as it has just been reported for Dsg2 in keratinocytes³⁴. Furthermore, our data demonstrate that activity of p38MAPK has to be regulated tightly. Inhibition of p38MAPK impaired barrier reformation during Ca²⁺-switch experiments and augmented cell monolayer fragmentation. Direct activation of p38MAPK with anisomycin facilitated barrier recovery in Dsg2-deficient cells, in which baseline p38MAPK activity was reduced. However, in the course of several hours treatment with anisomycin impaired barrier function also. This is in line with our previous data, as treatment with TNF α activated p38MAPK which resulted in loss of cell cohesion and increased permeability as well as reduction of Dsg2 at the cell borders¹⁹.

Finally, our experiments also may give some insight into the pathogenesis of CD. As previously shown, Dsg2 is decreased in samples from patients suffering from CD¹⁹. However, it is unclear whether this is primary or secondary to lesion formation in CD and nothing is known about the underlying mechanisms leading to reduction of Dsg2. Our findings that extradesmosomal Dsg2 is present on the cell surface of enterocytes and Dsg2 modulates the p38MAPK signalling cascade could uncover a new mechanism in the development of CD. Dsg2 may act as a sensor to transmit extracellular stimuli thereby controlling intestinal barrier maintenance. In this scenario, it can be speculated that inappropriate transmission of environmental signals could lead to severe inflammatory responses and facilitate the development of CD. Further studies are necessary to prove this hypothesis.

Materials and Methods

Cell Culture. The two human intestinal epithelial cell lines Caco2 (ATTC, LGC Standards, Wesel, Germany) and DLD1 (kind gift of Shintaro T. Suzuki, Kwansei Gakuin University, Japan) were used. Caco2 cells were cultured in Eagle's minimal essential medium (ATCC) and DLD1 cells were maintained in Dulbecco's modified Eagle medium (Life Technologies, Carlsbad, CA) with both media being supplemented by 10% fetal bovine serum

(Biochrom, Berlin, Germany), 50 U/ml penicillin and 50 U/ml streptomycin (both AppliChem, Darmstadt, Germany). Both cell lines were cultivated in a humidified atmosphere containing 5% CO₂ at 37 °C and used for experiments after reaching full confluence.

Test Reagents. SB202190 (Calbiochem, Darmstadt, Germany) was used to inhibit p38MAPK at 30 μM for 24 h and anisomycin (Sigma-Aldrich, Munich, Germany) was applied at 60 μM for 24 h to activate p38MAPK. For inhibition of Dsg2 binding a specific monoclonal mouse antibody directed against the second and third ED of Dsg2 (clone 10G11, Acris, Herford, Germany) without sodium azide was applied at 1:50. Following primary antibodies were used: mouse anti Dsg2 (clone 10G11) and rabbit anti Dsg2 (rb5, both Progen, Heidelberg, Germany), rabbit anti DP (NW6, USA, self-made), mouse anti Dsc2/3 (clone 7G6, Life Technologies, Carlsbad, CA), rabbit anti Claudin-4, rabbit anti Claudin-1 and rabbit anti Claudin-2 (all from Life Technologies, Carlsbad, CA), mouse anti E-cadherin (clone 36, BD Bioscience, Heidelberg, Germany), mouse anti GAPDH (Santa Cruz Biotechnology, Santa Cruz, CA), mouse anti α-tubulin (Abcam, Cambridge, UK), rabbit anti p38MAPK, rabbit anti phospho-Thr180/182 p38MAPK, (Cell Signaling, Danvers, MA, USA). As secondary antibodies HRP-conjugated goat anti-mouse or goat anti-rabbit (Dianova, Hamburg, Germany) were used for western blot analysis, Cy2-, Cy3- or Alexa488-labeled goat anti-mouse or goat anti-rabbit antibodies (Dianova, Hamburg, Germany) were used for confocal microscopy, Alexa488-labeled goat anti-mouse (Dianova, Hamburg, Germany) and Alexa594-labeled goat anti-rabbit (Life Technologies, Carlsbad, CA) were used for SIM and Star580- and Star635P-labeled antibodies (Abberior) were used for STED. For visualization of F-Actin Alexa488-labeled phalloidin (Life Technologies, Carlsbad, CA) was applied and nuclei were counterstained with DAPI (Sigma-Aldrich, Munich, Germany).

Immunofluorescence. After grown to confluency on glass coverslips, cells were fixed with 2% paraformaldehyde in PBS for 10 min and subsequently permeabilized with 0.5% TritonX-100 in PBS containing 0.02% Tween20 (PBS-T) for 10 min. After blocking in 2% BSA in PBS-T for 1 h cells were incubated with primary antibodies for 1 h (all steps were performed at room temperature) and subsequently after 3 washing steps with PBS-T with secondary antibodies also for 1 h. For confocal microscopy coverslips were mounted on glass slides with 60% glycerol in PBS, containing 1.5% *N*-propyl gallate (Serva, Heidelberg, Germany) and images were acquired using a Leica SP5 confocal microscope with a 63 x NA 1.4 PL APO objective (both Leica, Wetzlar, Germany).

Structured illumination microscopy (SIM). After immunostaining, cells were mounted in VECTASHIELD (Vector Laboratories) and SIM images were acquired with a DeltaVisionOMX V3 microscope system (General Electric) equipped with a 100 × 1.4 oil immersion objective UPlanSApo (Olympus), 405 nm, 488 nm and 593 nm laser (DIC) and Cascade II camera (Photometrics). Reconstruction was done with the SoftWorx software (Vers. 6.0 Beta 19, unreleased) and additionally images were aligned with a self-written Fiji macro.

Stimulated emission depletion microscopy (STED). After immunostaining, cells were mounted in 2.5% DABCO in MOWIOL/HEPES (self-made solution) and imaged with an Abberior 3D STED confocal microscope. Star580 and Star635P (both from Abberior) were excited at 594 nm and 638 nm respectively using pulsed diode lasers (PDL 594, Abberior Instruments; PiL063X, Advanced Laser Diode Systems). Fluorescent molecules were depleted at 775 nm with a pulsed fibre laser (PFL-P-30-775B1R, MPB Communications) and emission was detected with an avalanche photodiode detector at 605–625 and 650–720 nm range.

Western Blot. Cells were grown in 24-well plates and after treatment with respective reagents lysed using SDS lysis buffer containing (containing 25 mM HEPES, 2 mM EDTA, 25 mM NaF and 1% SDS) supplemented with a protease-inhibitor cocktail (Roche, Mannheim, Germany) and subsequently sonicated. After protein amount determination using a BCA Protein Assay Kit (Pierce/Thermo Scientific, Waltham, MA, USA) cell lysates were mixed with 3x Laemmli buffer and resolved by reducing SDS-PAGE. Following, proteins were transferred to a nitrocellulose membrane (Life Technologies, Carlsbad, CA) according to the standard protocols and membranes were probed with primary antibodies. Afterwards, HRP-conjugated secondary antibodies (Dianova, Hamburg, Germany) were applied and detected with an ECL reaction system (self-made solution).

TritonX-100 Protein Extraction. Cell monolayer grown in 6-well plates were washed with ice cold PBS and incubated in a Triton buffer (containing 0.5% Triton X-100, 50 mM MES, 25 mM EGTA and 5 mM MgCl₂) for 15 min on ice under gentle shaking. To separate the cytoskeletal protein fraction (Triton-insoluble) from the non-cytoskeletal protein fraction (Triton-soluble), cell lysates were centrifuged at 13,000 rpm for 5 min. After resuspending the pellets in SDS lysis buffer followed by sonication, protein concentration of both fractions was defined as described above and lysates were analysed via Western blot.

Atomic Force Microscopy (AFM). Dsg2 interactions on the surface of living enterocytes were analysed with atomic force microscopy (AFM), using a Nanowizard III AFM (JPK Instruments, Berlin, Germany) mounted on an optical microscopy (Carl Zeiss, Jena, Germany). The principle of AFM force spectroscopy was described in detail before²³. Briefly, the sharp tip on a flexible cantilever was functionalized with recombinant Dsg2-Fc containing the complete ED of Dsg2 using a flexible polyethylene glycol linker (Gruber Lab, Institute of Biophysics, Linz, Austria) as outlined elsewhere³⁵. While measurements, the tip is repetitively lowered onto the enterocyte cell monolayer and retracted again. Thereby binding events between the molecule on the tip and a molecule on the cell surface can be detected as the tip is hold back near the cell surface during the retraction movement in case of interaction. When the retraction force overcomes the binding strength of the interaction the tip jumps back into neutral position. AFM topography images of 50 × 50 μm were acquired at the beginning of each experiment in a force curve-based imaging mode (QI- mode) with a setpoint adjusted to 0.5 nN, a z-length of 1500 nm and a pulling speed of 50 μm/s. For force mapping to detect specific binding events a small area of 2 × 5 μm was chosen

and a map consisting of 20×50 pixels with each pixel representing one force-distance curve was recorded. Hereby, relative setpoint was set to 0,5 nN, a z-length of $2 \mu\text{m}$ was used for the DLD1 cells and $3 \mu\text{m}$ for the Caco2 cells with a pulling speed of $4 \mu\text{m/s}$ for the DLD1 cells and $5 \mu\text{m/s}$ for Caco2 cells. Measurements were performed in respective cell culture medium at 37°C . For cell-free AFM measurements Dsg2 coated mica sheets (SPI Supplies, West Chester, USA) were used instead of cell monolayers. Setpoint was adjusted to the same value as for cell-based experiments to produce comparable results. The z-length was set to $0,3 \mu\text{m}$ and a pulling speed of $1 \mu\text{m/s}$ was used. For each condition 400 force-distance curves were measured on an area of $25 \mu\text{m} \times 25 \mu\text{m}$.

Dispase-based Dissociation Assay. Confluent Caco2 and DLD1 cell monolayer grown in 24-well plates were incubated with test reagents, washed with Hank's buffered saline solution (HBSS; Sigma-Aldrich) and treated with $150 \mu\text{l}$ of the enzyme dispase II ($2,4 \text{ U/ml}$ in HBSS, Sigma-Aldrich) at 37°C to detach the whole cell monolayer from the well bottom. For Caco2 cells additionally 1% Collagenase I (Thermo Scientific, Waltham, MA, USA) was added. DLD1 cell monolayer detached from the well bottom after 30 min and Caco2 cell monolayer after 1,5 h. After stopping the reaction with $200 \mu\text{l}$ HBSS cell monolayer were sheared by pipetting 3 times using an electrical pipet. Finally, resulting fragments were counted under a binocular microscope (Leica). For every condition 3–4 wells out of a 24-well plate were counted and each experiment was repeated at least 3 times.

Measurement of transepithelial resistance. To assess epithelial barrier integrity, the transepithelial resistance (TER) was measured with an ECIS model Z theta (Applied Biophysics, Troy, NY) as described previously³⁶. For this, cells were cultured on 8-well electrode arrays (Ibidi, 8W10E) with sensing areas consisting of working electrodes at each well bottom and a counter electrode. Via the electrolytes of the cell culture medium above the cells, the electrodes are electrically connected. By application of a non-invasive alternating current ($<1 \mu\text{A}$) to the electrodes, the ECIS device measures the associated voltage drop across the system and determines the electrical resistance of the cell covered electrodes. A drop in TER values mirrors barrier breakdown. At the beginning of measurements medium was exchanged ($300 \mu\text{l}$) and baseline TER at 400 Hz for Caco2 cells and 800 Hz for DLD1 cells, was measured until values reached a plateau. Then, different test reagents were added and resistance was monitored every minute for the next 24 h.

Calcium Switch Assay. To analyse cell junctional disassembly and reassembly, Caco2 and DLD1 cells were grown on 8-well electrode arrays (Ibidi, 8W10E) and TER was monitored every minute. After measurement of baseline TER for about 20 min, Ca^{2+} ions were depleted using 4 mM EGTA for 1 h thereby inducing disruption of Ca^{2+} -dependent cell junctions. With the addition of 8 mM CaCl_2 , reformation of cell junctions was induced and validated based on changes in TER values.

Statistics. All experiments were repeated at least 3 times. Quantification of band intensity was performed using ImageJ (National Institutes of Health, Bethesda, MD). Statistical analysis was performed using a two-tailed *t* test for 2-sample group analysis and one-way ANOVA followed by bonferroni correction for multiple sample groups.

Human samples. Human specimens were obtained from terminal ileum of patients that required right hemicolectomy in which the surgical resection routinely involves a part of the healthy small intestine. All experiments were performed in accordance with relevant guidelines and regulations. All patients had given their informed consent before surgery, and the study was approved by the Ethical Board of the University of Würzburg (proposal numbers 113/13 and 46/11). For TEM analyses samples were fixed with 2.5% glutaraldehyde, cut into $\sim 1\text{mm}^3$ pieces and further processed as described above.

Data Availability. The datasets generated during and/or analysed during the current study are available from the corresponding author on reasonable request.

References

- Farquhar, M. G. & Palade, G. E. JUNCTIONAL COMPLEXES IN VARIOUS EPITHELIA. *The Journal of Cell Biology* **17**, 375 (1963).
- Capaldo, C. T., Farkas, A. E. & Nusrat, A. Epithelial adhesive junctions. *F1000Prime Rep* **6**, 1, doi:10.12703/P6-1 (2014).
- Tsukita, S., Furuse, M. & Itoh, M. Multifunctional strands in tight junctions. *Nature reviews. Molecular cell biology* **2**, 285–293, doi:10.1038/35067088 (2001).
- Ivanov, A. I. & Naydenov, N. G. Dynamics and regulation of epithelial adherens junctions: recent discoveries and controversies. *International review of cell and molecular biology* **303**, 27–99, doi:10.1016/b978-0-12-407697-6.00002-7 (2013).
- Owen, G. R. & Stokes, D. L. Exploring the Nature of Desmosomal Cadherin Associations in 3D. *Dermatology research and practice* **2010**, 930401, doi:10.1155/2010/930401 (2010).
- Garrod, D. & Chidgey, M. Desmosome structure, composition and function. *Biochimica et biophysica acta* **1778**, 572–587, doi:10.1016/j.bbame.2007.07.014 (2008).
- Holthofer, B., Windoffer, R., Troyanovsky, S. & Leube, R. E. Structure and function of desmosomes. *International review of cytology* **264**, 65–163, doi:10.1016/s0074-7696(07)64003-0 (2007).
- Koch, P. J., Goldschmidt, M. D., Zimbelmann, R., Troyanovsky, R. & Franke, W. W. Complexity and expression patterns of the desmosomal cadherins. *Proc Natl Acad Sci U S A* **89**, 353–357 (1992).
- Mahoney, M. G. *et al.* Delineation of diversified desmoglein distribution in stratified squamous epithelia: implications in diseases. *Experimental dermatology* **15**, 101–109, doi:10.1111/j.1600-0625.2006.00391.x (2006).
- Dubash, A. D. & Green, K. J. Desmosomes. *Current biology: CB* **21**, R529–531, doi:10.1016/j.cub.2011.04.035 (2011).
- Spindler, V. & Waschke, J. D. Cadherins and Signaling: Lessons from Autoimmune Disease. *Cell Communication & Adhesion* **21**, 77–84, doi:10.3109/15419061.2013.877000 (2014).
- Schlegel, N. *et al.* Desmoglein 2-mediated adhesion is required for intestinal epithelial barrier integrity. *Am J Physiol Gastrointest Liver Physiol* **298**, G774–783, doi:10.1152/ajpgi.00239.2009 (2010).
- Vereecke, L., Beyaert, R. & van Loo, G. Enterocyte death and intestinal barrier maintenance in homeostasis and disease. *Trends Mol Med* **17**, 584–593, doi:10.1016/j.molmed.2011.05.011 (2011).

14. Gibson, P. R. Increased gut permeability in Crohn's disease: is TNF the link? *Gut* **53**, 1724–1725, doi:10.1136/gut.2004.047092 (2004).
15. Jager, S., Stange, E. F. & Wehkamp, J. Inflammatory bowel disease: an impaired barrier disease. *Langenbeck's archives of surgery* **398**, 1–12, doi:10.1007/s00423-012-1030-9 (2013).
16. Laukoetter, M.-G. Role of the intestinal barrier in inflammatory bowel disease. *World Journal of Gastroenterology* **14**, 401, doi:10.3748/wjg.14.401 (2008).
17. Rowlands, B. J., Soong, C. V. & Gardiner, K. R. The gastrointestinal tract as a barrier in sepsis. *British medical bulletin* **55**, 196–211 (1999).
18. Kamekura, R. *et al.* Inflammation-induced desmoglein-2 ectodomain shedding compromises the mucosal barrier. *Mol Biol Cell* **26**, 3165–3177, doi:10.1091/mbc.E15-03-0147 (2015).
19. Spindler, V. *et al.* Loss of Desmoglein 2 Contributes to the Pathogenesis of Crohn's Disease. *Inflamm Bowel Dis* **21**, 2349–2359, doi:10.1097/MIB.0000000000000486 (2015).
20. Waschke, J. The desmosome and pemphigus. *Histochem Cell Biol* **130**, 21–54, doi:10.1007/s00418-008-0420-0 (2008).
21. Rotzer, V. *et al.* E-cadherin and Src associate with extradesmosomal Dsg3 and modulate desmosome assembly and adhesion. *Cell Mol Life Sci* **72**, 4885–4897, doi:10.1007/s00018-015-1977-0 (2015).
22. Hartlieb, E., Rötzer, V., Radeva, M., Spindler, V. & Waschke, J. Desmoglein 2 Compensates for Desmoglein 3 but Does Not Control Cell Adhesion via Regulation of p38 Mitogen-activated Protein Kinase in Keratinocytes. *The Journal of Biological Chemistry* **289**, 17043–17053, doi:10.1074/jbc.M113.489336 (2014).
23. Vielmuth, F., Hartlieb, E., Kugelmann, D., Waschke, J. & Spindler, V. Atomic force microscopy identifies regions of distinct desmoglein 3 adhesive properties on living keratinocytes. *Nanomedicine* **11**, 511–520, doi:10.1016/j.nano.2014.10.006 (2015).
24. Vielmuth, F., Waschke, J. & Spindler, V. Loss of Desmoglein Binding Is Not Sufficient for Keratinocyte Dissociation in Pemphigus. *J Invest Dermatol* **135**, 3068–3077, doi:10.1038/jid.2015.324 (2015).
25. Schlipp, A. *et al.* Desmoglein-2 interaction is crucial for cardiomyocyte cohesion and function. *Cardiovascular research* **104**, 245–257, doi:10.1093/cvr/cvu206 (2014).
26. Berkowitz, P. *et al.* Desmosome signaling. Inhibition of p38MAPK prevents pemphigus vulgaris IgG-induced cytoskeleton reorganization. *J Biol Chem* **280**, 23778–23784, doi:10.1074/jbc.M501365200 (2005).
27. Berkowitz, P. *et al.* p38MAPK inhibition prevents disease in pemphigus vulgaris mice. *Proceedings of the National Academy of Sciences of the United States of America* **103**, 12855–12860, doi:10.1073/pnas.0602973103 (2006).
28. Kugelmann, D., Waschke, J. & Radeva, M. Y. Adducin is involved in endothelial barrier stabilization. *PLoS one* **10**, e0126213, doi:10.1371/journal.pone.0126213 (2015).
29. Hartlieb, E. *et al.* Desmoglein 2 is less important than desmoglein 3 for keratinocyte cohesion. *PLoS one* **8**, e53739, doi:10.1371/journal.pone.0053739 (2013).
30. Spindler, V. *et al.* Peptide-mediated desmoglein 3 crosslinking prevents pemphigus vulgaris autoantibody-induced skin blistering. *J Clin Invest* **123**, 800–811, doi:10.1172/JCI60139 (2013).
31. Waschke, J. & Spindler, V. Desmosomes and extradesmosomal adhesive signaling contacts in pemphigus. *Medicinal research reviews* **34**, 1127–1145, doi:10.1002/med.21310 (2014).
32. Wang, H. *et al.* Intracellular Signaling and Desmoglein 2 Shedding Triggered by Human Adenoviruses Ad3, Ad14, and Ad14P1. *J Virol* **89**, 10841–10859, doi:10.1128/JVI.01425-15 (2015).
33. Wang, H. *et al.* Desmoglein 2 is a receptor for adenovirus serotypes 3, 7, 11 and 14. *Nat Med* **17**, 96–104, doi:10.1038/nm.2270 (2011).
34. Overmiller, A. M. *et al.* c-Src/Cav1-dependent activation of the EGFR by Dsg2. *Oncotarget* **7**, 37536–37555, doi:10.18632/oncotarget.7675 (2016).
35. Andreas, E. *et al.* A new simple method for linking of antibodies to atomic force microscopy tips. *Bioconjugate Chem.* **18**, 1176–1184 (2007).
36. Baumer, Y., Drenckhahn, D. & Waschke, J. cAMP induced Rac 1-mediated cytoskeletal reorganization in microvascular endothelium. *Histochem Cell Biol* **129**, 765–778, doi:10.1007/s00418-008-0422-y (2008).

Acknowledgements

The authors thank K. Green (Northwestern University) for providing the DP-specific antibody NW6. This work was funded by grants of the Deutsche Forschungsgemeinschaft: the priority program DFG_SPP1782 to JW and NS and the Nanosystems Initiative Munich (NIM) to HL.

Author Contributions

H.U. and J.W.: Study concept and design; H.U. and A.M.: Acquisition of data; H.U., J.W., D.K., F.V. and H.L.: Analysis and interpretation of data; H.U.: Writing of the manuscript, preparation of figures and statistical analysis; H.U., J.W., N.S. and H.L.: Obtained funding and supervision; S.T.S. and H.H.: Technical or material support; H.U., J.W., D.K. and F.V.: Critical revision of the manuscript for important intellectual content; All authors reviewed the manuscript.

Additional Information

Supplementary information accompanies this paper at doi:10.1038/s41598-017-06713-y

Competing Interests: The authors declare that they have no competing interests.

Publisher's note: Springer Nature remains neutral with regard to jurisdictional claims in published maps and institutional affiliations.



Open Access This article is licensed under a Creative Commons Attribution 4.0 International License, which permits use, sharing, adaptation, distribution and reproduction in any medium or format, as long as you give appropriate credit to the original author(s) and the source, provide a link to the Creative Commons license, and indicate if changes were made. The images or other third party material in this article are included in the article's Creative Commons license, unless indicated otherwise in a credit line to the material. If material is not included in the article's Creative Commons license and your intended use is not permitted by statutory regulation or exceeds the permitted use, you will need to obtain permission directly from the copyright holder. To view a copy of this license, visit <http://creativecommons.org/licenses/by/4.0/>.

© The Author(s) 2017

Supplementary material to the manuscript

Title: Desmoglein 2 regulates the intestinal epithelial barrier via p38 mitogen-activated protein kinase

Authors: Hanna Ungewiß¹, Franziska Vielmuth¹, Shintaro T. Suzuki², Andreas Maiser³, Hartmann Harz³, Heinrich Leonhardt³, Daniela Kugelmann¹, Nicolas Schlegel⁴, Jens Waschke^{1*}

Author affiliation:

¹Department I, Institute of Anatomy and Cell Biology, Ludwig-Maximilians-Universität München, Pettenkoferstr. 11, 80336 Munich, Germany

²Department of Bioscience, School of Science and Technology, Kwansai Gakuin University, Sanda-shi, Hyogo-ken 669-1337, Japan

³Department of Biology II, Ludwig-Maximilians-Universität München, Großhaderner Str. 2, 82152 Planegg-Martinsried, Germany

⁴Department of General, Visceral, Vascular and Paediatric Surgery, Julius-Maximilians-Universität, Oberdürrbacher Str. 6, 97080 Würzburg, Germany

Supplemental Material and Methods

Transmission Electron Microscopy (TEM)

Cell monolayer were fixed with 1% glutaraldehyde at 37°C for 1 h, then washed three times with PBS and incubated with 2% osmiumtetroxid solution for 1 h at 4°C. Afterwards, samples were dehydrated through an ethanol series from 20 to 100% followed by embedding with epon for 24 hours at 80°C. Finally, ultrathin sections (60 - 80 nm) were cut with a diamond knife and staining was performed with a saturated solution of uranyl acetate for 40 min and lead citrate for 5 min. Images were acquired with the transmission electron microscope Libra 120 (Zeiss, Oberkochen, Germany).

Scanning Electron Microscopy (SEM)

For scanning electron microscopy, cell monolayer were fixed and dehydrated as described for TEM. Afterwards, samples were dried with carbon dioxide under excess pressure of around 86 bar (Critical point dryer K850, Quorum Technologies, UK) and subsequently sputtered with gold at 30 mA for 60 s (Cressington 108auto) under argon atmosphere. Images were acquired using the scanning electron microscope Leo 1550 (Zeiss Oberkochen, Germany).

siRNA-mediated Silencing of Dsg2

Human siRNA oligo pools specific for Dsg2 as well as non-target controls were purchased from Dharmacon/GE Healthcare (Freiburg, Germany). Cells were transfected at 90% confluency using Turbofect (Thermo Scientific, Waltham, MA) as a transfection reagent according to manufacturer's protocols. Medium was exchanged after 24 hours and experiments were performed after 48 hours.

Supplementary figure legends

Figure S1. Caco2 cells were cultured for 2 days, 4 days or 6 days after confluency and analysed via transmission and scanning electron microscopy, confocal microscopy, Western blot and TER. (A) Characteristic junctional complexes as well as microvilli were present already on day 2. Scale bar, 1 μm (left and central panels), 2 μm (right panel) (B) Electron microscopy images of human terminal ileum specimens show tight junctions (TJ), adherens junctions (AJ) and desmosomes (D) at the apical

part of the intercellular cleft. Desmosomes can also be found in lower regions of the intercellular cleft. Scale bar, 1000 nm (left panel), 500 nm (right panel) (C) Immunostaining of junctional components reveals linear localization of Dsg2, Cld1 and Cld4 already on day 2, staining for Cld2 decreases in the time course of differentiation. Scale bar, 10 μ m. (D) Western blot analysis reveals unaltered protein level of junctional components from day 2 till day 6. α -Tubulin serves as loading control. (E) TER measurements reveal constant values between day 2 and day 6. (n = 4, n.s not significant)

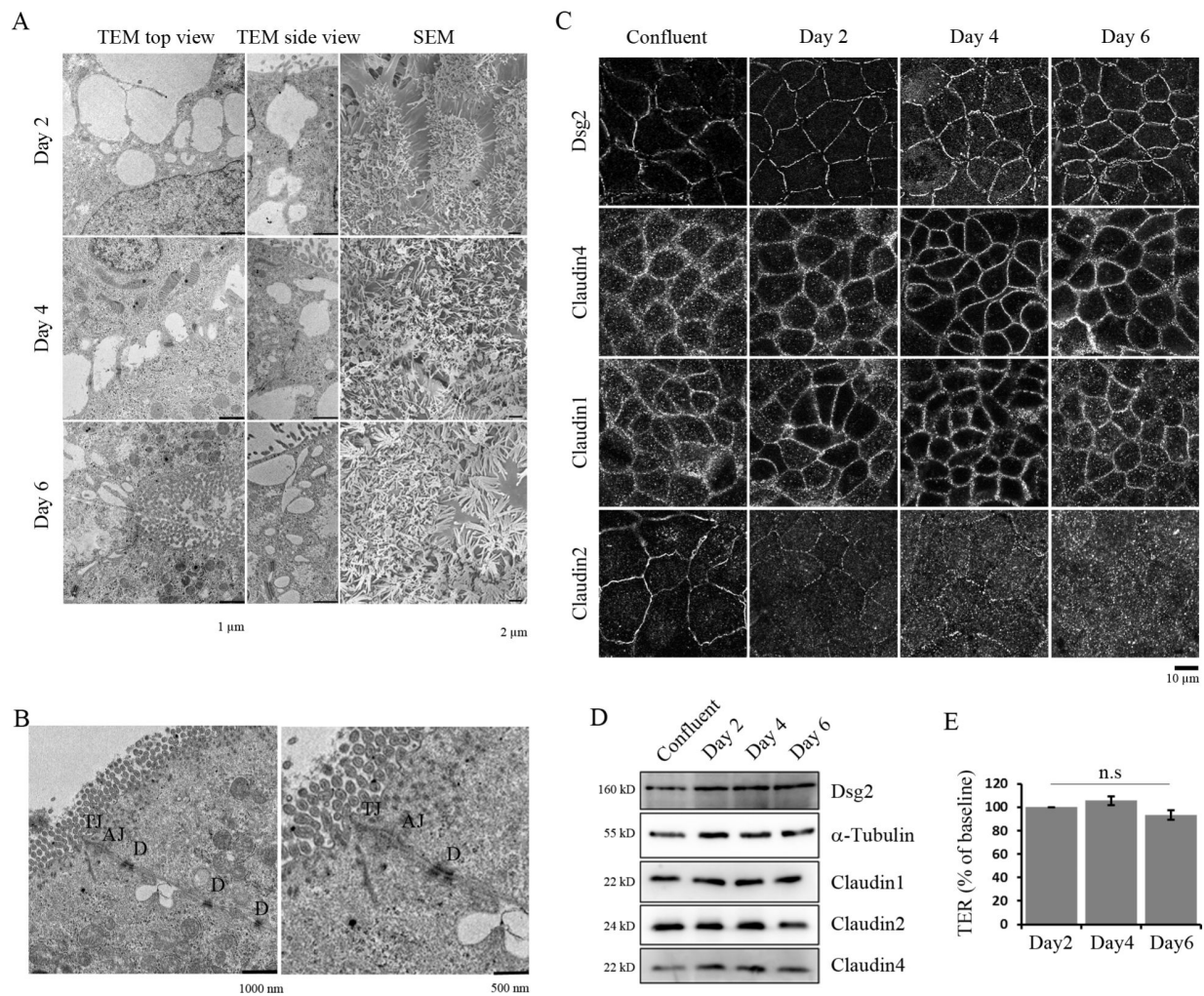
Figure S2. (A) AFM topography image and scanning microscopy image of DLD1 cells closely resemble each other. Scale bar, 2 μ m (left panel), 10 μ m (right panel). (B) siRNA-mediated silencing of Dsg2 reduces amount of binding events on living DLD1 cells. (siNT = non-target siRNA; shown is mean \pm SE, n = 4, * p < 0,05) (C) Dsg2-specific antibody increases cell monolayer fragmentation of Caco2 cells in a dispase-based cell dissociation assay (shown is mean \pm SE, n = 4, * p < 0,05). (D) siRNA-mediated silencing of Dsg2 increases cell monolayer fragmentation of DLD1 and Caco2 cells in a dispase-based cell dissociation assay. (shown is mean \pm SE, n = 4, * p < 0,05)

Figure S3. (A) siRNA mediated silencing of Dsg2 reduces phosphorylation of p38MAPK. (B) Dsg2-specific antibody did not increase cell monolayer fragmentation in a dispase-based cell dissociation assay after 30 min of incubation (shown is mean \pm SE, n = 4, n.s = not significant compared to control). (C) Western blot analysis after incubation of DLD1 cells with a Dsg2-specific antibody for 24 h revealed increased phosphorylation of p38MAPK. Band intensity of detected p-p38MAPK was quantified using ImageJ and normalized to control (shown is mean \pm SE, n = 3, * p < 0,05 compared to control).

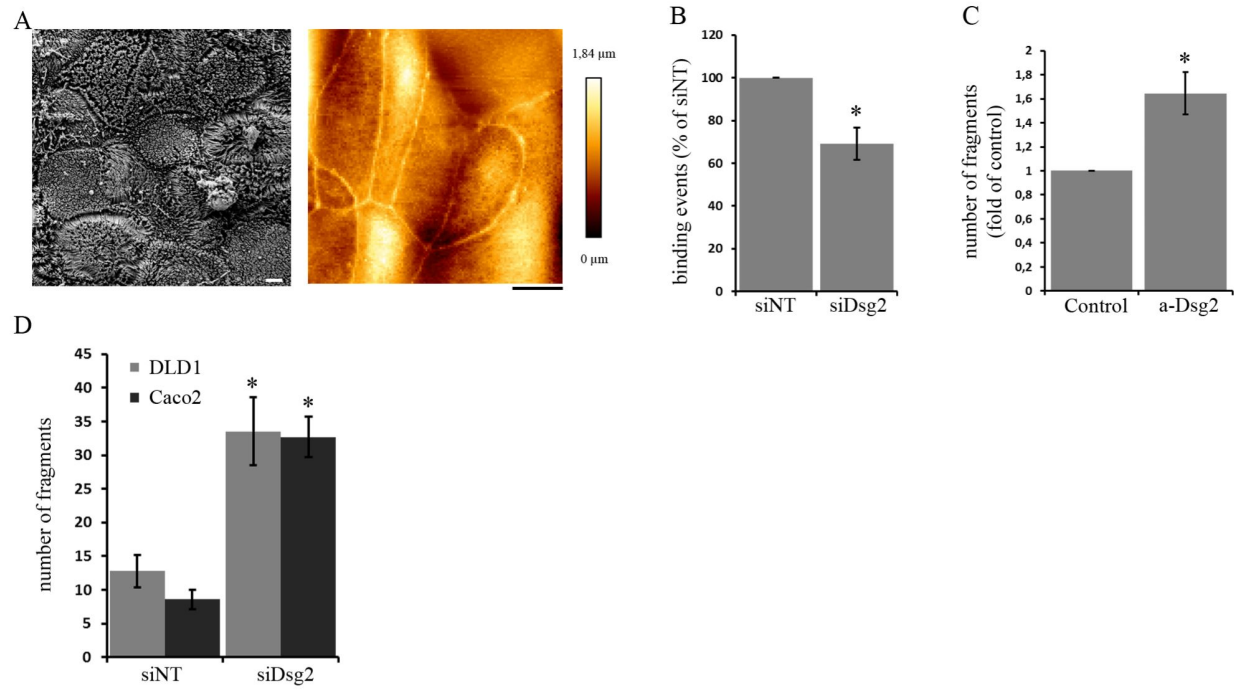
Figure S4. (A) TER values of Caco2 cells decrease during depletion with 4 mM EGTA for 1 h and increase back to control values during 2 h of repletion with 8 mM CaCl₂. (Representative graph for n > 3 is shown). (B) Immunostaining of Dsg2 and E-cadherin during Ca²⁺-switch experiments in DLD1 cells reveals reduction and fragmentation after 1 h depletion and similar staining to control condition after 2 h repletion. Scale bar, 10 μ m. (C-D) Immunostaining of junctional components during Ca²⁺-switch experiments in Caco2 cells reveals reduction and fragmentation as well as gap formation after 1 h depletion and similar staining to control condition after 2 h repletion. Scale bar, 10 μ m. (E) Barrier

reformation in Caco2 cells is impaired after inhibition of p38MAPK with SB202190 in the Ca²⁺-switch experiment while addition of anisomycin has no effect (Representative graph for 6 independent experiments is shown). (D) Time for repletion during Ca²⁺-switch experiments was compared between control condition and application of anisomycin or SB202190. Inhibition of p38MAPK with SB202190 significantly delayed the repletion time while application of anisomycin resulted in a repletion time similar to control condition (shown is mean \pm SE, n=6, * p < 0,05 compared to control condition, n.s not significant).

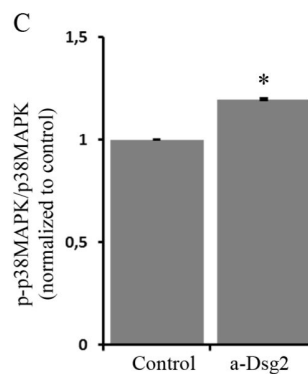
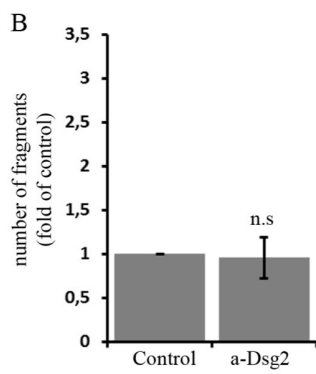
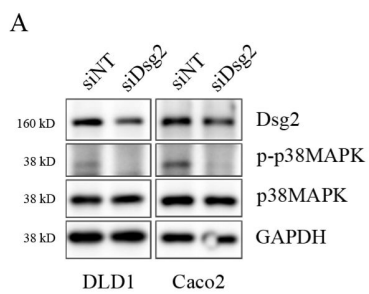
Supplemental Figure 1



Supplemental Figure 2

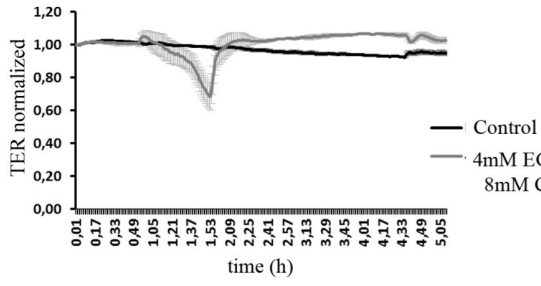


Supplemental Figure 3

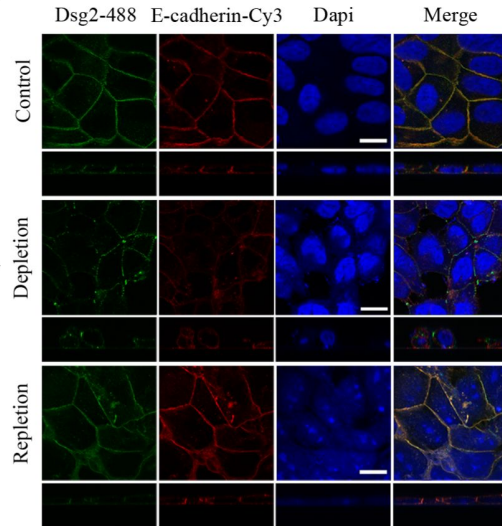


Supplemental Figure 4

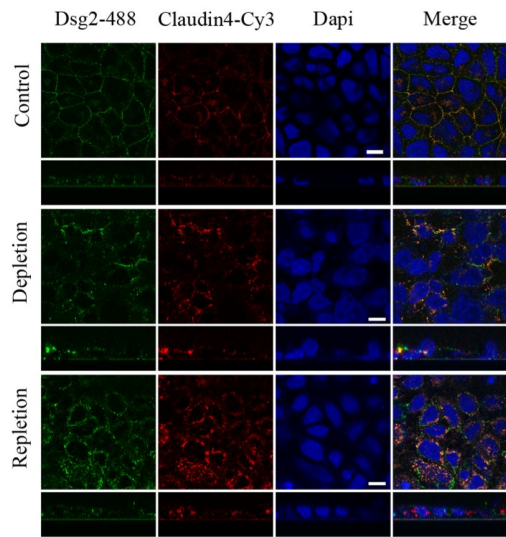
A



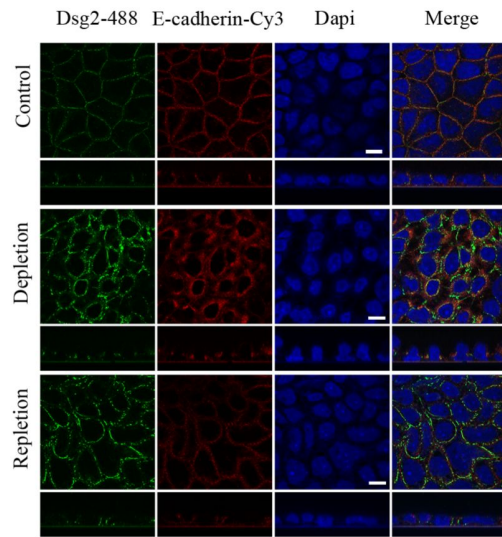
B



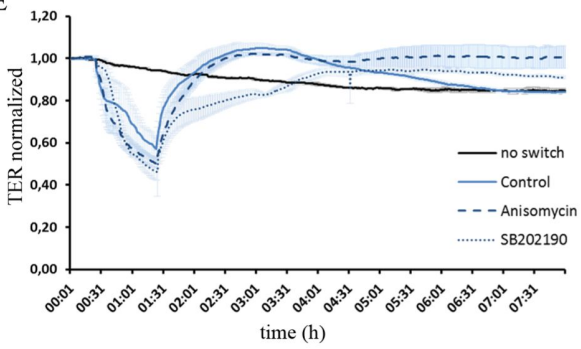
C



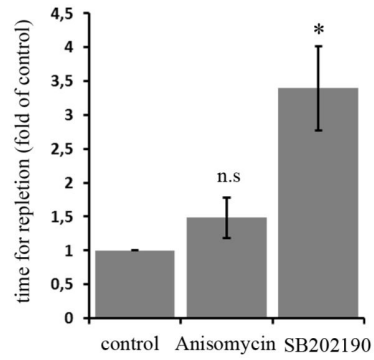
D

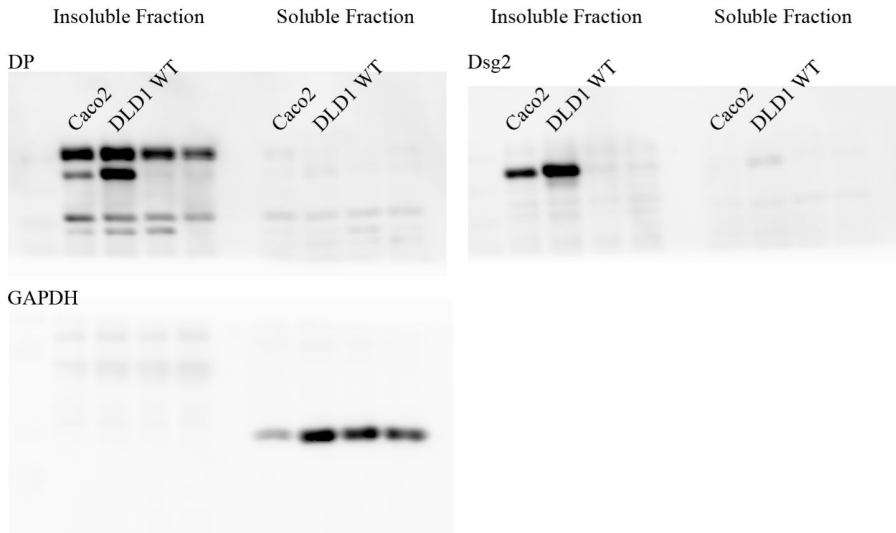


E

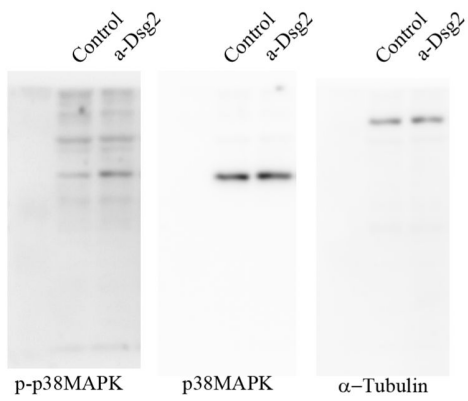


F

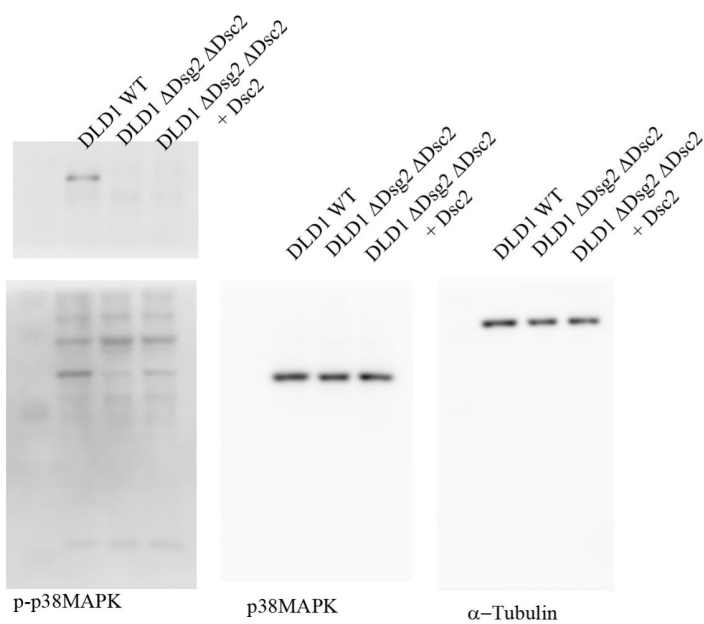




Full length blot for Desmoplakin, Desmoglein 2 and GAPDH displayed in figure 1E



Full length blot for p-p38MAPK, p38MAPK and α -Tubulin displayed in figure 3A



Full length blot for Dsg2, p-p38MAPK, p38MAPK and α -Tubulin displayed in figure 5D

2.2 Dsg2 via Src-mediated transactivation shapes EGFR signaling towards cell adhesion



Dsg2 via Src-mediated transactivation shapes EGFR signaling towards cell adhesion

Hanna Ungewiß¹ · Vera Rötzer¹ · Michael Meir² · Christina Fey³ · Markus Diefenbacher⁴ · Nicolas Schlegel² · Jens Waschke¹

Received: 8 February 2018 / Revised: 19 June 2018 / Accepted: 3 July 2018
© Springer Nature Switzerland AG 2018

Abstract

Rapidly renewing epithelial tissues such as the intestinal epithelium require precise tuning of intercellular adhesion and proliferation to preserve barrier integrity. Here, we provide evidence that desmoglein 2 (Dsg2), an adhesion molecule of desmosomes, controls cell adhesion and proliferation via epidermal growth factor receptor (EGFR) signaling. Dsg2 is required for EGFR localization at intercellular junctions as well as for Src-mediated EGFR activation. Src binds to EGFR and is required for localization of EGFR and Dsg2 to cell–cell contacts. EGFR is critical for cell adhesion and barrier recovery. In line with this, Dsg2-deficient enterocytes display impaired barrier properties and increased cell proliferation. Mechanistically, Dsg2 directly interacts with EGFR and undergoes heterotypic-binding events on the surface of living enterocytes via its extracellular domain as revealed by atomic force microscopy. Thus, our study reveals a new mechanism by which Dsg2 via Src shapes EGFR function towards cell adhesion.

Keywords Desmosomes · Desmosomal cadherins · Intestinal barrier · Cell adhesion

Abbreviations

AFM	Atomic force microscopy
AJ	Adherens junction
Cld4	Claudin 4
Dsc2	Desmocollin 2
Dsg2	Desmoglein
DP	Desmoplakin

Ecad	E-cadherin
EGFR	Epidermal growth factor receptor
MAPK	Mitogen-activated protein kinase
PG	Plakoglobin
Pkp	Plakophilin
RTK	Receptor tyrosine kinase
STED	Stimulated emission depletion microscopy
TER	Transepithelial resistance
TJ	Tight junction
WT	Wild type

Electronic supplementary material The online version of this article (<https://doi.org/10.1007/s00018-018-2869-x>) contains supplementary material, which is available to authorized users.

✉ Jens Waschke
jens.waschke@med.uni-muenchen.de

¹ Department I, Institute of Anatomy and Cell Biology, Ludwig Maximilians University Munich, Pettenkoferstr. 11, 80336 Munich, Germany

² Department of General, Visceral, Vascular and Paediatric Surgery, Julius-Maximilians-Universität, Oberdürrbacher Str. 6, 97080 Würzburg, Germany

³ Department for Tissue Engineering and Regenerative Medicine, University Hospital Würzburg, Röntgenring 11, 97070 Würzburg, Germany

⁴ Department of Biochemistry and Molecular Biochemistry, University of Würzburg, Am Hubland, 97074 Würzburg, Germany

Introduction

Epithelial tissues represent the interface between the organism and the environment, and thus, maintenance of epithelial barrier function is indispensable to prevent entry of pathogens or harmful macromolecules. This is, in particular, crucial for the gastrointestinal epithelium, which comprises a huge surface and faces a plethora of bacteria present in the gut but simultaneously needs to stay permeable to enable the uptake of nutrients and essential macromolecules [1, 2]. Aggravating this situation, the intestinal epithelial tissue shows the highest turnover rate in adult mammals and is exposed to notable mechanical stress

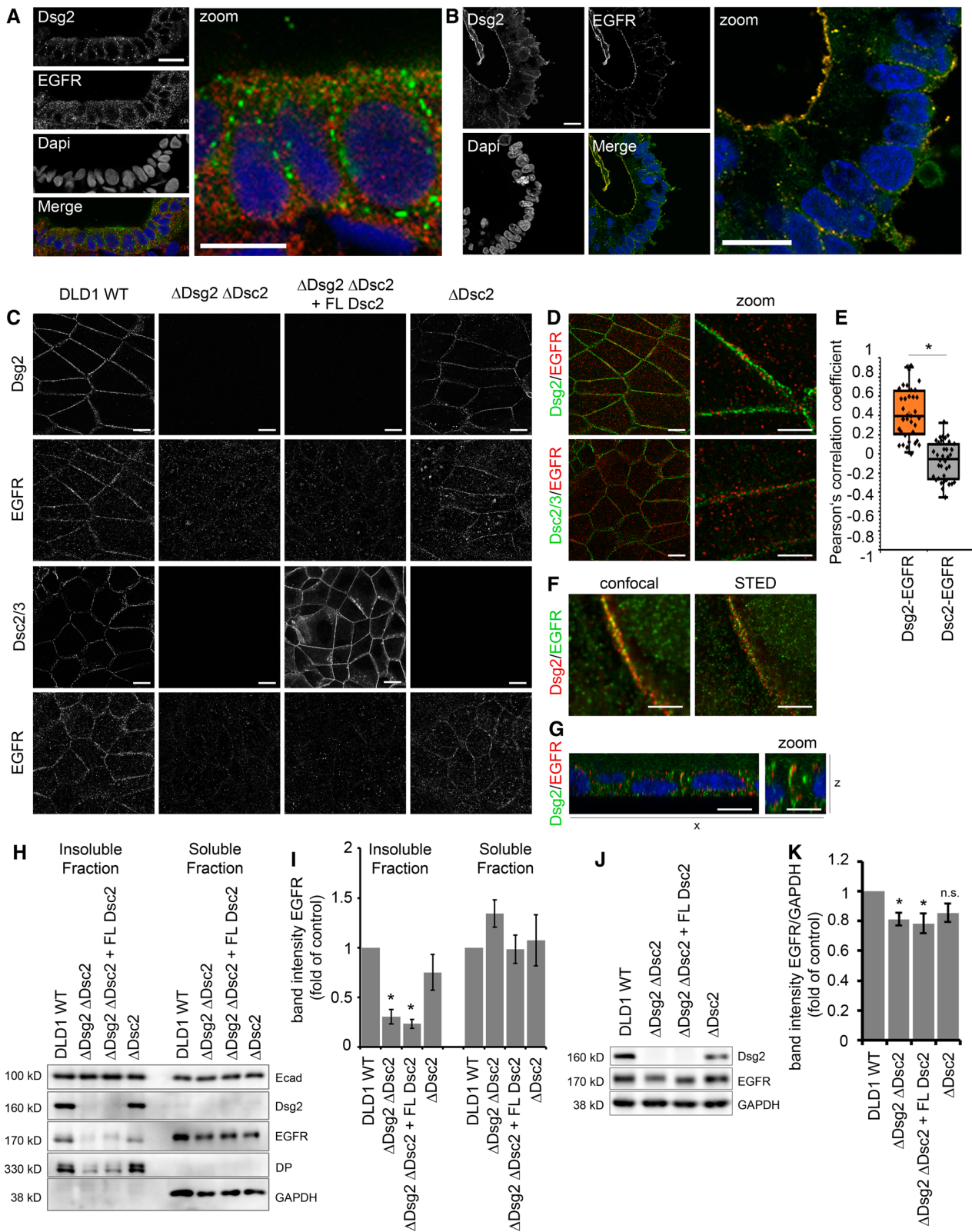


Fig. 1 Dsg2 knockout results in mislocalization and reduced protein levels of EGFR in intestinal epithelial cells. **a** Immunostaining for Dsg2 (green) and EGFR (red) in patient tissue sections of the colon revealed co-localization of both proteins. Four independent patient tissue samples were analyzed. Shown is representative image of a section from the colon. Bar 10 μm . **b** Immunostaining for Dsg2 (green) and EGFR (red) in human enteroids revealed co-localization of both proteins along the cell borders as well as on the surface facing the lumen. Shown is representative image for ten enteroids. Bar 10 μm . **c** Confluent cell monolayer of DLD1 cells grown on coverslips were immunostained for EGFR, Dsg2, and Dsc2/3. Loss of Dsg2 but not Dsc2/3 results in a major loss of EGFR staining at cell borders. Bar 10 μm . **d** Merged images of immunofluorescence staining of Dsg2, EGFR, and Dsc2/3 show co-localization of Dsg2 and EGFR but not Dsc2/3 and EGFR. Bar 10 μm (left panel) and 5 μm (right panel). **e** Evaluation of the Pearson correlation coefficient of EGFR confirms a co-localization of EGFR with Dsg2 but not Dsc2. Shown are boxplots with each point representing one analyzed area along the cell border. $*p < 0.05$. **f** STED super resolution microscopy analysis of Dsg2 and EGFR co-immunostaining shows co-localization. Bar 5 μm . **g** $x-z$ image of Dsg2 and EGFR co-immunostaining shows specific co-localization at the apical site of cell contacts. Bar 10 μm (left panel) and 5 μm (right panel). **h** EGFR is absent in the Triton X-100 insoluble fraction when Dsg2 is missing in contrast to Ecad that is not affected by Dsg2 knockout. GAPDH served as loading control. **i** Band intensity of detected EGFR was measured from five independent experiments, showing a significant reduction of EGFR in the insoluble fraction in Dsg2-deficient DLD1 cells. Results are shown as mean \pm SE. $*p < 0.05$. **j** Total protein level of EGFR in DLD1 cells were assessed by western blotting that revealed reduced EGFR levels in Dsg2-deficient cells. GAPDH served as loading control. **k** Band intensity of detected EGFR was quantified from at least ten independent experiments, demonstrating a significant reduction of total EGFR protein levels upon Dsg2 knockout. Shown are mean \pm SE. $*p < 0.05$

resulting from gastrointestinal motility [3, 4]. Hence, precise regulation of intercellular adhesion and proliferation is required to preserve barrier integrity. This function is achieved by a set of adhesion complexes including tight junctions (TJ), adherens junctions (AJ), and desmosomes that tightly connect the polarized enterocytes within the simple columnar epithelium, thereby sealing the paracellular space [5, 6]. Initially, desmosomes were considered to primarily provide the mechanical strength in intercellular cohesion [7]. However, growing evidence suggests that desmosomal cadherins beside their adhesive function actively coordinate signaling pathways, hence mediating proliferation, differentiation, and apoptosis [8–11]. Desmosomal cadherins are transmembrane glycoproteins which interact via their extracellular domains (ED) in a homo- and heterophilic manner, while their tails associate with the plaque proteins plakoglobin (PG), plakophilin (Pkp), and desmoplakin (DP), thereby anchoring the desmosomal complex to the intermediate filament cytoskeleton. Thus, these components constitute the adhesive core of desmosomes [12]. Seven isoforms of desmosomal cadherins are expressed in human epithelial tissues, of which the intestinal epithelium contains Desmoglein 2 (Dsg2)

and Desmocollin 2 (Dsc2) only [13–15]. A recent study reports that Dsc2 alone is sufficient to form a functional desmosomal plaque in enterocytes [16]. However, Dsg2 is required for intestinal epithelial barrier properties and abnormal expression of Dsg2 is implicated in colon cancer and inflammatory disorders such as Crohn's disease [17–20]. In addition, it was shown that Dsg2 besides its role in cellular adhesion has an essential signaling function in regulating p38 mitogen-activated protein kinase (MAPK) signaling in enterocytes [20].

The mechanism by which desmosomal cadherins regulate signaling pathways is an emerging focus of research. Given that the intracellular tail of desmogleins has no enzymatic activity, transduction of signaling requires interaction with signaling components such as kinases. In this context, several molecular mechanisms have been proposed such as matrix metalloprotease-mediated shedding of Dsg2 external domain fragments which may act as ligands for receptor tyrosine kinases (RTK) [21] or displacing kinases from lipid rafts, thereby promoting their activation [22]. The common denominator in both scenarios is the involvement of RTK which are already known to associate with classical cadherins, and thus, both molecules are modulated mutually [23, 24]. Depending on the phosphorylation site, specific signaling molecules can be recruited which, in turn, modulate a variety of downstream signaling cascades [25–29]. Of particular interest to this study is the epidermal growth factor receptor (EGFR) which has been shown to modulate function of desmogleins [30, 31] as well as to be modulated by desmogleins [9, 22, 32]. Furthermore, EGFR is suggested to regulate cell migration, wound healing, and cell extrusion in intestinal epithelial cells [33–35]. Albeit, all these processes require regulation of intercellular junctions; the role of desmosomal cadherins in this context has only been marginally explored.

In this study, we examined how Dsg2 and EGFR cooperate in regulating intestinal epithelial homeostasis to assure barrier integrity. We show that Dsg2 modulates EGFR localization as well as protein level and Src-dependent activation, which both were reduced in Dsg2-deficient DLD1 and Caco2 cells. Here, we demonstrate, for the first time, that Dsg2 and EGFR interact directly using atomic force microscopy (AFM) both on living enterocytes as well as in a cell-free setup. Moreover, these binding events were inhibited by ligand binding to EGFR and depend on EGFR tyrosine kinase activity. In addition, inhibition of EGFR tyrosine kinase activity impaired barrier formation and intercellular adhesion. Furthermore, loss of Dsg2 increased cell proliferation, which was restored after inhibition of EGFR activity. Collectively, our data suggest a new signaling complex consisting of Dsg2 and EGFR which stabilizes the adhesive state of intestinal epithelial cells.

Results

Loss of Dsg2 reduces EGFR levels and prevents its localization to cell borders

Increasing evidence suggests that desmosomal cadherins beyond their adhesive function are actively involved in regulating signaling cascades. Previously, we demonstrated that Dsg2 regulates barrier integrity in human intestinal cells via p38MAPK signaling [20]. In addition, several studies on keratinocytes linked desmogleins to differentiation and proliferation through regulation of growth factor signaling cascades [8, 9]. We, therefore, asked how desmosomal cadherins influence EGFR signaling in human intestinal cells. First, we performed immunostaining for Dsg2 and EGFR in human colon samples to investigate whether these proteins can be found in close proximity. EGFR is assumed to be located primarily in the basolateral membrane of enterocytes, whereas Dsg2 was shown to be present as part of desmosomes in the basolateral membrane but also outside of desmosomes in the apical membrane, at least in cultured enterocytes [20, 36, 37]. Interestingly, we observed EGFR staining at the basolateral membrane as well as at the apical surface and distinct spots of Dsg2 staining all along the cell borders (Fig. 1a). Besides, a small fraction of apical EGFR staining was overlapping with immunostaining for Dsg2 resulting in yellow spots. Similarly, we observed overlapping staining for EGFR and Dsg2 in human enteroids with an even more pronounced EGFR staining at the apical cell membrane facing the enteroid lumen (Fig. 1b). Using human colon carcinoma DLD1 cells deficient for Dsg2 and/or Dsc2 [16], we next investigated whether localization and protein levels of EGFR are controlled by desmosomal cadherins. DLD1 wild-type (WT) cells in immunostaining displayed linear localization of EGFR along cell borders similar to Dsg2 (Fig. 1c, upper panels) and Dsc2 (Fig. 1c, lower panels). To examine whether desmosomal cadherins affect the localization of EGFR, we immunostained DLD1 cells deficient for Dsg2, Dsc2, or both cadherins. Cells deficient for both, Dsg2 and Dsc2, showed almost complete loss of EGFR staining at cell borders (Fig. 1c, second column). Similar results were obtained using WT and Dsg2-deficient Caco2 cells (Fig. S1A). Reconstitution of Dsc2 was not sufficient to restore this phenotype (Fig. 1c, third column), suggesting that Dsg2 is required for recruiting EGFR to cell borders. In line with this, loss of Dsc2 did not affect EGFR localization (Fig. 1c, fourth column). Moreover, merged images of Dsg2 (green) and EGFR (red) staining revealed co-localization at cell borders with a Pearson correlation coefficient of around 0.4 pointing towards positive correlation of overlapping

staining (Fig. 1d, e). In contrast, no correlation between EGFR and Dsc2 staining was observed, as indicated by a correlation coefficient of 0 (Fig. 1d, e). Using STED super resolution microscopy, we analyzed EGFR and Dsg2 localization more closely and found overlapping staining for EGFR and Dsg2 even at high resolution (Fig. 1f) confirming their close co-localization. Furthermore, we observed co-localization all along the cell border but more pronounced at the most apical part of the intercellular cleft (Fig. 1g). In accordance to the immunostaining, triton extraction resulted in a significant reduction of EGFR in the insoluble fraction when Dsg2 was absent (Fig. 1h, i) raising the possibility of a putative signaling complex consisting of Dsg2 and EGFR maybe at sites of desmosomes. Importantly, immunoblotting for Ecad did not result in any changes upon loss of Dsg2 or of Dsc2 (Fig. 1h), suggesting that AJ stay unaffected. Moreover, total protein expression levels of EGFR were reduced significantly in cells deficient for Dsg2 but not Dsc2 (Fig. 1j, k), indicating that Dsg2 might be important for EGFR stability. Similarly, EGFR protein levels were reduced in Dsg2-deficient Caco2 cells (Fig. S1 B–E).

Dsg2 and EGFR interact directly via their extracellular domains

Given the first hints pointing towards a signaling complex consisting of Dsg2 and EGFR, we next investigated whether there is direct interaction. To this end, we conducted AFM on living DLD1 cells using an AFM cantilever coated with recombinant Dsg2-Fc containing the complete extracellular domain of Dsg2 similar as shown recently [20]. First, AFM topography images were created to select specific areas at cell borders for further adhesion measurements (Fig. 2a, upper panel). For interaction studies, the functionalized AFM tip was repetitively lowered on the cell surface, thereby creating an adhesion map consisting of 1000 force–distance curves for each selected area, with each white pixel representing one positive-binding event (Fig. 2a, lower panel). Intriguingly, these binding events were blocked significantly when applying an inhibitory antibody against the extracellular domain of EGFR (Fig. 2a, b), indicating that measured binding events under control conditions partly reflect heterophilic Dsg2–EGFR interaction. To verify that measured binding events were Dsg2-specific, an inhibitory antibody against the extracellular domain of Dsg2 was applied, which reduced the binding events to a similar extent (Fig. 2b), similar as published previously [20]. In addition, we performed cell-free AFM experiments with Dsg2-coated AFM tips on mica sheets functionalized with either recombinant Dsg2-Fc or recombinant EGFR-Fc containing the complete extracellular domain to validate homophilic or heterophilic interactions. Binding frequency was similar when

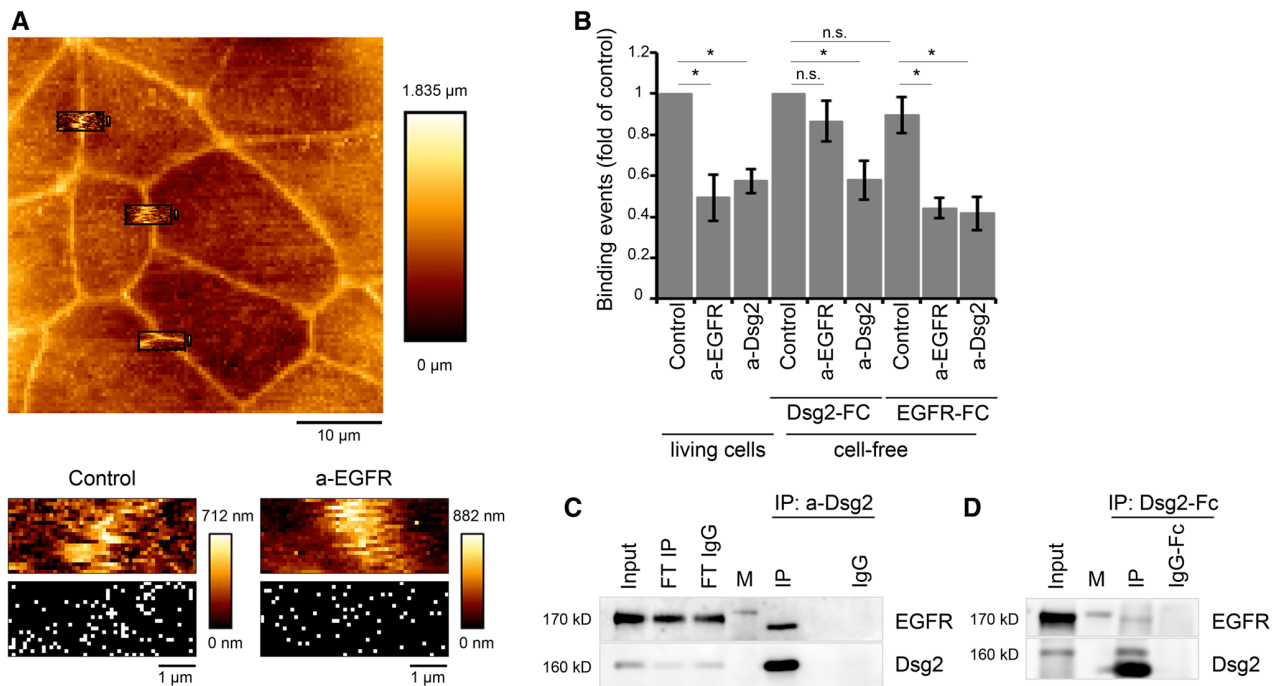


Fig. 2 Dsg2 and EGFR form heterophilic interactions via their extracellular domains. **a** AFM cell topography image was created to select specific areas along the cell borders for Dsg2 adhesion measurements (upper panel). Adhesion measurements using a Dsg2-coated AFM tip generated adhesion maps with each white pixel representing one binding event (lower panel). **b** Treatment with an inhibitory EGFR-specific antibody significantly reduced the amount of Dsg2 binding events on living cells similar to an inhibitory anti-Dsg2 antibody. Cell-free AFM measurements using a Dsg2 coated tip and mica sheets coated either with Dsg2 or with EGFR revealed a similar

binding frequency of homophilic Dsg2–Dsg2 and heterophilic Dsg2–EGFR interactions, which were significantly blocked by respective antibodies applied to the mica sheet. Graph shows fold-change values from at least three independent experiments \pm SE. * $p < 0.05$. **c** Co-immunoprecipitation was performed with DLD1 cell lysates and an anti-Dsg2 antibody for immunoprecipitation (IP) of endogenous Dsg2. Immunoblotting for EGFR revealed co-IP of both proteins. *FT* flow through. **d** Pull-down assay was performed with DLD1 cell lysates and a Dsg2-Fc fusion protein. Immunoblotting for EGFR revealed co-IP of Dsg2-Fc and EGFR

measured Dsg2–Dsg2 or Dsg2–EGFR interaction under the same conditions (Fig. 2b), suggesting that both interactions can occur. Application of the inhibitory EGFR-specific antibody did not reduce homophilic Dsg2 interactions (Fig. 2b), demonstrating that it does not bind un-specifically to Dsg2. In contrast, heterophilic Dsg2–EGFR binding was significantly reduced similar to AFM measurements on living cells (Fig. 2b) underlining the specificity of measured binding events. Bearing in mind that the inhibitory EGFR-specific antibody blocks the ligand-binding site of EGFR, these data further raise the possibility that this binding site might be important for heterophilic EGFR–Dsg2 binding. Application of the inhibitory Dsg2-specific antibody reduced both homophilic Dsg2–Dsg2 as well as heterophilic Dsg2–EGFR interactions (Fig. 2b). Given that the antibody is directed against the extracellular domains 3 and 4 of Dsg2, this result indicates that these subdomains may be required for EGFR–Dsg2 interaction. In addition, we also examined endogenous association between EGFR and Dsg2 in DLD1 cells using co-immunoprecipitation studies. In line with the AFM-based adhesion studies, interaction of EGFR and Dsg2

was detected in DLD1 cells (Fig. 2c). Moreover, we performed a pull-down assay using the recombinant Dsg2-Fc, which also resulted in co-precipitation of EGFR and thus further indicates an interaction of EGFR with the extracellular domain of Dsg2 (Fig. 2d).

Ligand binding to EGFR prevents its interaction with Dsg2 at the cell surface

The canonical EGFR signaling pathway involves binding of growth factors to EGFR resulting in receptor dimerization and subsequent cross-phosphorylation of cytoplasmic receptor domains [25, 26, 28, 29]. Therefore, we applied EGF during AFM measurements on living DLD1 cells resulting in a significant reduction of binding frequency (Fig. 3a, b). This prompted us to ask whether EGF-mediated receptor dimerization reduced binding to Dsg2 maybe through masking the binding site. Alternatively, the subsequent auto-phosphorylation might induce decreased Dsg2–EGFR interaction. Hence, we treated the cells with erlotinib, a specific EGFR tyrosine kinase inhibitor to assess whether the

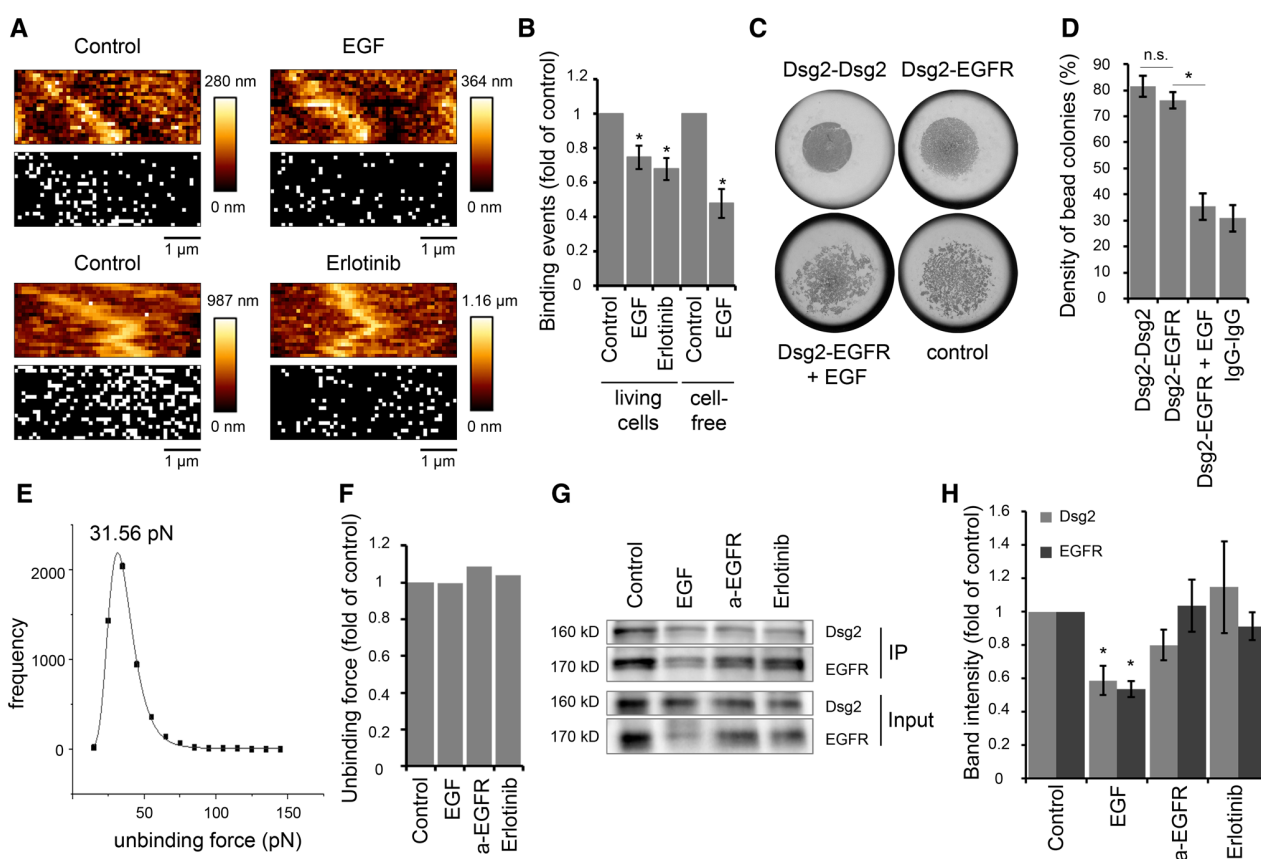


Fig. 3 EGF reduces Dsg2-specific binding events on the cell surface of living DLD1 cells. **a** Dsg2 adhesion measurements were performed on living DLD1 cells under control conditions and after incubation with EGF or erlotinib. Shown are topography images of selected areas at cell borders and adhesion maps with each white pixel representing one binding event. **b** Quantification shows a significant reduction of binding events on living DLD1 cells after incubation with both, EGF or erlotinib. Application of EGF also reduced the amount of binding events in the cell-free AFM setup with a Dsg2-coated tip and EGFR-coated mica sheets. Graph bars represent fold-change values \pm SE from at least four independent experiments. $*p < 0.05$. **c** Peak fit analysis of measured unbinding forces revealed a distribution peak of 31.56 pN under control conditions. **d** Distri-

bution-peak values of unbinding forces measured on DLD1 cells under control conditions and after incubation with EGF, anti-EGFR antibody, or erlotinib were compared and revealed similar values for all conditions. Graph shows distribution-peak values normalized to control. **e**, **f** Hanging drop bead aggregation assay confirms blockade of interaction between Dsg2 and EGFR through EGF. Beads coated with a human IgG Fc fragment served as control. $*p < 0.05$; *n.s.* not significant. **g** Western blot analysis of surface biotinylation assay revealed reduced Dsg2 and EGFR levels on the surface of DLD1 cells after incubation with EGF. **h** Quantification of Dsg2 and EGFR band intensity from at least seven independent experiments shows a significant reduction of surface protein levels only after incubation with EGF. Graph bars represent fold-change values \pm SE. $*p < 0.05$

tyrosine kinase activity of EGFR affects its binding to Dsg2. Indeed, the inhibitor resulted in reduced binding frequency (Fig. 3a, b), indicating that EGFR kinase activity is important. However, EGF also reduced the binding frequency in cell-free AFM measurements with a Dsg2-coated cantilever on EGFR-coated mica sheets (Fig. 3b), which raises the possibility that Dsg2–EGFR interaction might be also inhibited through steric hindrance upon EGF binding to EGFR. Results from hanging drop bead aggregation assays that revealed a similar inhibitory effect of EGF on interaction of Dsg2- and EGFR-coated beads support this hypothesis (Fig. 3c, d). Next, we analyzed the measured interactions with regard to their unbinding forces to gain insight into

the molecular interaction mechanism. Peak fit analysis of measured unbinding force curves under control conditions revealed a distribution peak at 31.56 pN (Fig. 3e) which is in accordance with previously measured unbinding forces using a Dsg2-coated AFM tip on living enterocytes [20]. Interestingly, unbinding forces were similar after application of EGF, the inhibitory EGFR-specific antibody or erlotinib (Fig. 3f). Given that, EGFR is internalized following ligand binding [38, 39], we hypothesized that reduced binding frequency might be due to less available EGFR at the cell surface. Therefore, we performed surface biotinylation assays. As expected, incubation with EGF reduced EGFR levels at the cell surface (IP) as well as in total lysate (Input)

(Fig. 3g, h). Interestingly, Dsg2 cell surface levels were also reduced after EGF treatment (Fig. 3g, h), indicating that EGFR and Dsg2 might stabilize one another at the cell surface. In contrast, the inhibitory EGFR-specific antibody as well as Erlotinib had no significant effect on cell surface protein levels of Dsg2 and EGFR (Fig. 3g, h), suggesting that reduced AFM-binding frequency is attributable to inhibition of direct binding. In summary, our data demonstrate that interaction of Dsg2 and EGFR is disrupted upon ligand binding to EGFR as well as after inhibition of the tyrosine kinase activity, suggesting that both direct binding via their extracellular domains as well as ligand-independent activation of EGFR might be involved in this interaction.

Loss of Dsg2 reduces Src-dependent phosphorylation of EGFR

Inhibition of EGFR kinase activity reduced EGFR binding to Dsg2. Hence, we asked whether loss of Dsg2 might reduce phosphorylation of EGFR. As we hypothesized that ligand-independent activation of EGFR is involved in Dsg2–EGFR complex formation and it has been shown that EGFR is phosphorylated on Y845 in an EGF-independent manner [40], we focused on this phosphorylation site. Indeed, DLD1 cells deficient for Dsg2 displayed lower levels of

Y845 phosphorylation (Fig. 4a, b). Similarly, loss of Dsg2 in Caco2 cells reduced phosphorylation of EGFR at this site (Fig. S2A and B). Reconstitution of Dsc2 in DLD1 cells deficient for both desmosomal cadherins did not restore the level of phosphorylation. Moreover, loss of Dsc2 alone had no significant effect on phosphorylation levels (Fig. 4a, b), suggesting that Dsg2 and not Dsc2 is required for phosphorylation. Usually, the phosphorylation at Y845 is catalyzed by the tyrosine kinase Src [41–43], which has already been reported to play a role in cell adhesion signaling [40, 44, 45]. Interestingly, Src localization to cell borders remained unchanged upon loss of Dsg2 (Fig. S2C). Furthermore, also protein levels of total and phosphorylated Src as well as distribution in the triton-soluble and -insoluble fractions were not affected (Figs. S2D and S2E). However, inhibition of Src activity using the Src-specific inhibitors PP2 and KX2-391 resulted in reduced and fragmented EGFR and Dsg2 immunostaining at cell borders in DLD1 cells (Fig. 4c). Intriguingly, where remaining both proteins were still co-localizing. Since Src is reported to associate with Dsg3 [45], we next performed immunoprecipitation to investigate whether it also forms a complex with Dsg2 and EGFR. Surprisingly, we found Src only associated with EGFR but not Dsg2 in DLD1 cells (Fig. 4d). Altogether, these data indicate that Src acts upstream of Dsg2 and EGFR; Src activity is required

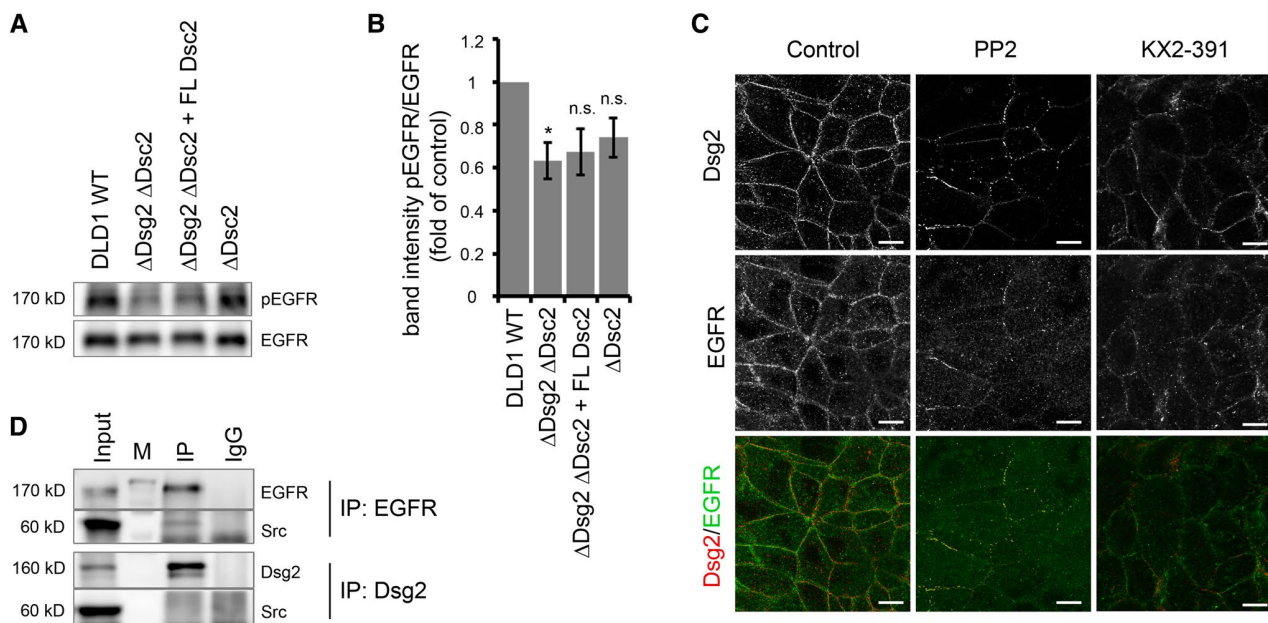


Fig. 4 Dsg2 knockout reduces Src-dependent phosphorylation of EGFR. **a** Level of phosphorylated EGFR at Y845 in DLD1 cells deficient for Dsg2 and Dsc2 was analyzed via Western blot. Loss of Dsg2 resulted in reduced level of pEGFR, which was not rescued by reconstitution of Dsc2. **b** Intensity of bands detected by a pEGFR-specific antibody was quantified using ImageJ and normalized to total EGFR. Shown are fold-change values \pm SE of six independent experiments.

* $p < 0.05$; n.s. not significant. **c** Immunostaining of Dsg2 and EGFR in DLD1 cells showed reduced and fragmented staining of both proteins at the cell border after application of the Src inhibitors PP2 and KX2-391. Bar 10 μ m. **d** DLD1 cell lysates were used for immunoprecipitation of EGFR (upper panels) or Dsg2 (lower panels) and subjected to western blot analysis for Src, revealing a co-IP of Src with EGFR but not with Dsg2

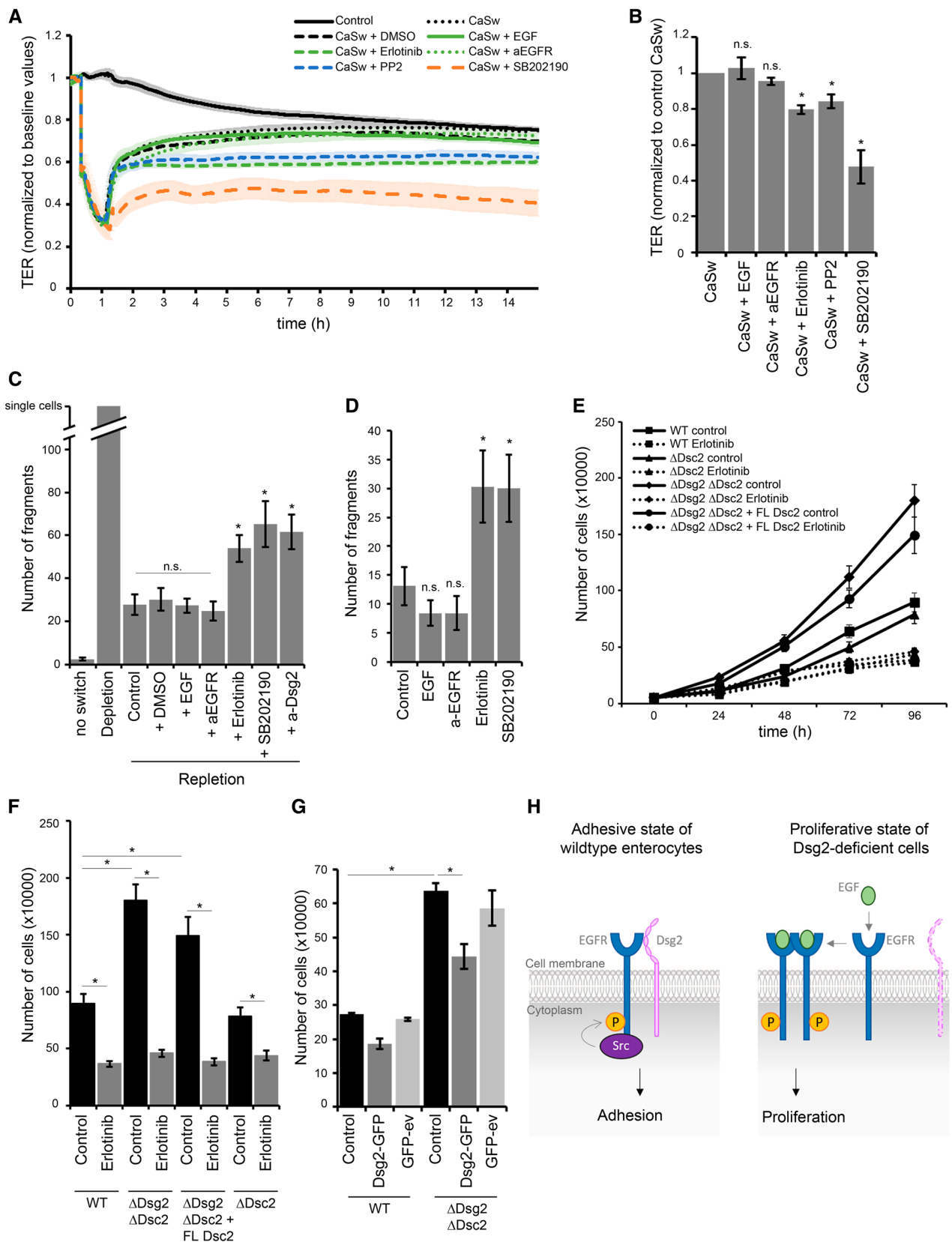


Fig. 5 Dsg2 regulates EGFR activity, thereby suppressing proliferation and supporting an adhesive state in enterocytes. **a** Barrier recovery of DLD1 WT cells after Ca^{2+} switch was monitored via TER measurements showing impaired barrier recovery after inhibition of EGFR, Src and p38MAPK activity with respective inhibitors. Inhibitors were applied together with CaCl_2 after 1 h depletion with EGTA. **b** TER values were quantified after 10 h of repletion with respective inhibitors and normalized to control repletion with respective vehicle. Repletion with erlotinib, PP2, and SB202190 resulted in significantly reduced TER values compared to control. Shown are fold-change values \pm SE of 4–6 independent experiments. $*p < 0.05$; *n.s.* not significant. **c** Cell adhesion of DLD1 cells was analyzed in a disperse-based dissociation assay after Ca^{2+} switch and treatment with several inhibitors. Treatment with erlotinib, PP2, and SB202190 during repletion significantly increased monolayer fragmentation compared to control repletion with respective vehicle. Shown is mean \pm SE of six independent experiments. $*p < 0.05$; *n.s.* not significant. **d** Confluent DLD1 cell monolayer were treated with EGF, a-EGFR, erlotinib, or SB202190, and analyzed for cell adhesion in a disperse-based cell dissociation assay. Inhibition of EGFR and p38MAPK activity significantly increased number of fragments in contrast to EGF and the EGFR-specific antibody. Shown is mean \pm SE of five independent experiments. $*p < 0.05$; *n.s.* not significant. **e** Cell proliferation was determined by cell counting. 50,000 cells were seeded for each cell line with or without erlotinib and cells were counted after 24, 48, 72, and 96 h. **f** Number of cells after 96 h was quantified. Shown is mean \pm SE of at least five independent experiments. $*p < 0.05$. **g** Cell proliferation was determined after Dsg2 reconstitution in DLD1 cells deficient for Dsg2 and Dsc2, 48 h after transfection. Shown is mean \pm SE of four independent experiments. GFP-ev empty vector, $*p < 0.05$. **h** Model of Dsg2-mediated regulation of EGFR. Dsg2 recruits EGFR to cell borders where it is phosphorylated by Src and induces downstream signaling, thereby strengthening adhesion maybe via p38MAPK. Loss of Dsg2 results in activation of the canonical EGFR signaling pathway resulting in proliferation

for proper localization of Dsg2 and EGFR to the cell borders and Src-mediated phosphorylation at Y845 stabilizes Dsg2–EGFR interaction.

Dsg2 via EGFR regulates the switch between adhesive and proliferative states in enterocytes

Finally, we were interested in the functional relevance of this new signaling complex. We have previously shown that loss of Dsg2 affects barrier properties via impaired downstream signaling of p38MAPK [20]. Here, we investigated whether EGFR signaling is involved in maintenance of barrier properties in intestinal cells. To explore its role during barrier recovery, we performed Ca^{2+} -switch experiments and applied several EGFR-modulating agents at initiation of repletion. Treatment of DLD1 WT cells with EGF as well as the inhibitory EGFR-specific antibody did not disturb barrier recovery, resulting in similar TER values compared to Ca^{2+} -switch alone (Fig. 5a, b). In contrast, application of erlotinib abolished barrier recovery significantly (Fig. 5a, b). Since we assume that Src activity is required for localization of EGFR to cell borders, we next tested whether inhibition

of Src using the inhibitor PP2 affects barrier recovery after Ca^{2+} switch. Similar to the effect of erlotinib, also Src inhibition prevented barrier reformation significantly (Fig. 5a, b). Furthermore, inhibition of p38MAPK with the inhibitor SB202190 hampered barrier recovery (Fig. 5a, b), similar as published previously [20], which led us to the assumption that p38MAPK might be regulated downstream of the Dsg2–EGFR signaling complex. We obtained similar results using Caco2 cells (Fig. S3A and B). Moreover, Ca^{2+} -switch experiments with DLD1 WT cells grown on filter inserts revealed no difference when applying EGF from apical side to basolateral side with both behaving similar to control conditions (Fig. S3C and D). Treatment with erlotinib in the trans-well system also disturbed barrier under both conditions, but recovery was even more affected by application from basolateral side (Fig. S3C and D). Furthermore, Ca^{2+} -switch experiments with DLD1 cells deficient for both Dsg2 and Dsc2 also revealed significantly impaired barrier recovery after inhibition of EGFR, Src, or p38MAPK, indicating that desmosomal cadherins are not the only target of these signaling pathways in the process of barrier recovery (Fig. S3E and F). Since barrier properties are maintained by TJ, effects on claudins may also be possible. Therefore, we performed immunostaining for Claudin 4 (Cld4) after 2 h repletion together with the respective mediator, which revealed linear staining along cell borders similar to control condition after repletion without any inhibitor or when supplemented with EGF or a-EGFR, whereas staining appeared irregular after repletion in the presence of erlotinib, PP2, or SB202190 (Fig. S3G). Next, we analyzed whether the stability of newly formed cell junctions differs after repletion with EGFR-modulating agents compared to control, using a disperse-based cell dissociation assay. Application of EGF and the inhibitory EGFR-specific antibody had no effect on cell adhesion after Ca^{2+} switch (Fig. 5c) as well as when applied on a confluent monolayer (Fig. 5d). However, inhibition of EGFR tyrosine kinase activity using erlotinib increased the number of fragments significantly after Ca^{2+} switch (Fig. 5c) and disrupted cell adhesion of a confluent cell monolayer (Fig. 5d). Similar, inhibition of Dsg2 binding using the Dsg2-specific antibody and inhibition of p38MAPK with SB202190 increased cell monolayer fragmentation after Ca^{2+} switch as well as under normal conditions (Fig. 5c, d), further indicating that the Dsg2–EGFR complex might regulate a downstream signaling cascade that includes p38MAPK. Several studies implicate a role for Dsg2 in regulating downstream signaling cascades linked to proliferation [8, 22, 32]. In addition, the pivotal function of the EGFR is to drive cell growth and survival [46–48]. Therefore, we investigated whether loss of Dsg2 and, as a consequence, disruption of the Dsg2–EGFR complex affect cell proliferation. Indeed, DLD1 cells deficient for Dsg2 and Dsc2 showed significantly increased cell proliferation

compared to WT cells (Fig. 5e, f). Stable reconstitution of Dsc2 in cells deficient for both desmosomal cadherins did not revert proliferation rate and loss of Dsc2 only did not result in increased proliferation compared to WT cells (Fig. 5e, f), suggesting that Dsg2 and not Dsc2 mediates this effect. Treatment with the EGFR tyrosine kinase inhibitor erlotinib diminished cell proliferation under all conditions resulting in values similar to WT cells (Fig. 5e, f). A similar result was obtained using WT and Dsg2-deficient Caco2 cells (Fig. S3 H). These data suggest that increased cell proliferation caused by loss of Dsg2 was mediated through EGFR tyrosine kinase activity. In addition, we performed Dsg2 rescue experiments with transient re-expression of Dsg2-GFP to corroborate the effect on proliferation upon loss of Dsg2. Using confocal microscopy, we confirmed the successful expression of Dsg2-GFP that was found linearly along cell borders in DLD1 double knockout as well as Dsg2-deficient Caco2 cells (Fig. S3I). Analysis of proliferation revealed that transient re-expression of Dsg2 was sufficient to reduce the increased proliferation rate in Dsg2-deficient DLD1 and Caco2 cells (Fig. 5g; Fig. S3J).

Altogether, our study has identified a new role for Dsg2 in regulating EGFR activity in intestinal epithelial cells via a novel signaling complex consisting of Dsg2, EGFR, and Src. In this model, EGFR binds to Dsg2 and is phosphorylated by Src, which results in increased adhesion maybe via modulating p38MAPK signaling. In cells deficient for Dsg2, unbound EGFR is activated by ligand binding that leads to dimerization and cross-phosphorylation, thereby inducing pro-proliferative signaling pathways (Fig. 5h).

Discussion

Although many cellular processes regulated by EGFR require a break-up of intercellular junctions and desmosomes are considered to play the leading role in intercellular cohesion, only little is known about the functional interplay of EGFR and desmosomal cadherins. In this study, we propose a new mechanism of EGFR regulation in intestinal epithelial cells via a signaling complex consisting of Dsg2, EGFR, and Src. We demonstrate, for the first time, that Dsg2 and EGFR interact directly via their extracellular domains and that ligand binding as well as inhibition of EGFR tyrosine kinase activity prevent this interaction in AFM measurements. In addition, inhibition of EGFR tyrosine kinase activity significantly reduced cell adhesion, suggesting that the Dsg2-EGFR complex stabilizes desmosomal adhesion. Dsg2 is required for EGFR to localize to cell borders where it binds to Src. In line with this, we detected reduced level of Src-mediated phosphorylation of EGFR at Y845 in Dsg2-deficient cells. Moreover, inhibition of Src activity impaired barrier formation, which was accompanied by fragmented

immunostaining of Dsg2 and EGFR at cell borders. Furthermore, loss of Dsg2 enhanced cell proliferation that was restored by inhibition of EGFR kinase activity, indicating that Dsg2 modulates EGFR activity, thereby regulating the switch between adhesive and proliferative states in intestinal epithelial cells.

Our data are in line with the previous studies reporting reduced phosphorylation of EGFR on Y845 upon loss of Dsg2 [22, 32]. EGFR phosphorylation at Y845 is usually catalyzed by Src and regulates a variety of cellular functions through the activation of several downstream events [41–43]. Increased levels of Src and EGFR can be found in various cancer cells, and Y845 phosphorylation-mediated signaling is linked to higher cancer malignancy due to enhanced cell transformation, motility, and invasion [42, 49–52]. Moreover, Src-mediated phosphorylation at Y845 has been reported to promote anti-apoptotic and pro-proliferative cell functions [53–56]. In accordance, recently published data show that reduced level of EGFR Y845 phosphorylation after Dsg2 downregulation suppresses cell proliferation [22, 32]. However, our study provides evidence that loss of Dsg2 and corresponding reduction of EGFR Y845 phosphorylation enhanced cell proliferation of intestinal epithelial DLD1 cells as well as of Caco2 cells. One has to consider that EGFR signaling highly depends on its spatial compartmentalization that determines the biological outcome [57]. After ligand-mediated activation at the cell surface, EGFR molecules are internalized and traverse different routes of the endosome network, while signaling continues [58–61]. EGFR is also known to act as transcription factor in the nucleus [62, 63]. Our data indicate a new mechanism by which EGFR directly interacts with Dsg2 at cell borders, thereby signaling towards adhesion and suppressing proliferation. We observed that this direct interaction is blocked using specific antibodies directed against the extracellular domains of EGFR or Dsg2 in cell-free AFM measurements. A previous study reported that Dsg2 ectodomains, which are capable of binding to the same region as the Dsg2-specific antibody used in this study, inhibit intercellular adhesion and, in addition, increase intestinal epithelial cell proliferation [21], which fits well to our proposed model. Particular attention should be given to the close co-localization of Dsg2 and EGFR which we found not only in cell culture, but similarly in human enteroids as well as in human samples which supports the physiological relevance of direct interaction between Dsg2 and EGFR. Several studies reporting the presence of EGFR in the apical membrane in intestinal cells [64–66] where Dsg2 is located support these observations. Another study suggests EGFR activation through Dsg2-mediated disruption of EGFR association with lipid rafts without direct interaction of EGFR and Dsg2 [22]. Thus, presumably, a different signaling complex is formed, resulting in a different biological function. However, this

study was performed in keratinocytes which express more than one desmoglein isoform. This is in contrast to intestinal epithelial cells with only Dsg2 and Dsc2 being expressed [67, 68]. Hence, it is conceivable that desmosomal cadherins exert distinct functions in different tissues. In line with this, in keratinocytes, EGFR was shown to co-localize with Dsg1 that suppressed EGFR activity to promote differentiation [9]. A recent study demonstrated a similar mechanism, by which the classical cadherin Ecad recruits EGFR to AJ and suppresses its activity to foster barrier stability [69]. This is in line with our proposed model, where Dsg2 localizes EGFR to cell borders, thereby suppressing its proliferative activity and strengthening cell adhesion. Similarly, Dsg2 has been reported to support differentiation and thus to act as tumor suppressor gene in gastric cancer [70]. Furthermore, our data indicate that this effect is mediated by increased EGFR phosphorylation at Y845 which appears to be important for the formation of the Dsg2–EGFR signaling complex. Studies from the literature, demonstrating that Y845 phosphorylation induces cell cycle arrest and inhibits growth, also support our hypothesis [71, 72]. Interestingly, another group demonstrated that downregulation of Dsc2 increases proliferation in colon cancer cells, while downregulation of Dsg2 reduces proliferation, which is in contrast to our study [32, 73]. However, this study was conducted in cancer cells harboring a mutation that results in deregulated β -catenin signaling and increased expression of pro-proliferative genes [74, 75]. Given that the EGFR and β -catenin pathways are known to interact at multiple levels ranging from transcriptional to posttranscriptional regulation [76–81], deregulated signaling events downstream of these pathways may account for the different impact on proliferation after Dsg2 downregulation. Similar to our study, EGFR Y845 phosphorylation was reduced upon loss of Dsg2, which points toward comparable EGFR regulation but different downstream signaling. We observed increased proliferation rate in both DLD1 and Caco2 cells upon loss of Dsg2.

Previously, we have shown that Dsg2 regulates intestinal barrier properties via p38MAPK that is activated upon loss of Dsg2 [20]. However, it is still an open question how Dsg2 regulates this signaling pathway. MAPK cascades are known to be downstream targets of the EGFR and increased p38MAPK phosphorylation after EGF stimulation has been reported previously [82, 83]. Furthermore, Src-dependent p38MAPK activation has been shown to modulate the EGF-stimulated response towards migration instead of proliferation during wound closure in intestinal epithelial cells [84]. Hence, a signaling cascade consisting of Src being upstream of the Dsg2–EGFR complex and p38MAPK being regulated downstream of this complex, thereby supporting the adhesive state of intestinal epithelial cells, is conceivable. However, our data do not rule out the possibility that other targets including adhesion molecules as well as other signaling

cascades may be coordinated by Dsg2 together with EGFR. For instance, EGFR regulation has recently been linked to AJ [69] and we observed irregular staining of the TJ protein Cld4 after EGFR inhibition. Furthermore, it has been reported that the apical and basolateral fractions of EGFR exert differential signaling functions [85]. Although we observed no difference in outcome when applying EGFR-modulating agents from apical side to basolateral side in this study, future studies may gain more insight into the molecular mechanism underlying the EGFR-mediated regulation of intestinal barrier properties.

Taken together, we propose a new mechanism of EGFR regulation that is important for intestinal epithelial cell homeostasis. Deregulation of any of the involved proteins has potential to induce intestinal disorders such as inflammatory bowel disease (IBD) or cancer. Thus, EGFR signaling has been shown to be reduced in IBD patients, while upregulated levels are often found in various types of cancers, indicating that a precise regulation of EGFR activity is crucial to maintain intestinal barrier integrity [42, 86]. In line with this, growth factors such as EGF promote wound healing in IBD but are also involved in the formation of neoplasia [87–89]. Likewise, Dsg2 is reduced in the mucosa of patients suffering from Crohn's disease and is implicated in oncogenesis [17, 19]. In addition, tumor necrosis factor α (TNF α), a cytokine implicated in the pathogenesis of Crohn's disease, has been reported to modulate EGFR activity, as well [90, 91]. Hence, understanding the molecular mechanism of EGFR regulation in intestinal cells might provide the molecular basis for new therapeutic approaches for the treatment of IBD or cancer in the future.

Materials and methods

Cell culture

DLD1 and Caco2 cells were cultured in Dulbecco's modified Eagle medium (Life Technologies, Carlsbad, CA, USA) supplemented by 10% fetal bovine serum (Biochrom, Berlin, Germany), 50 U/mL penicillin, and 50 U/mL streptomycin (both AppliChem, Darmstadt, Germany), and cultivated in a humidified atmosphere containing 5% CO₂ at 37 °C. Experiments were performed 4 days after reaching full confluence. DLD1 knockout cells were generated in the lab of Suzuki (Kwansei Gakuin University, Japan) [16] using the CRISPR/Cas9 system with the pX330 vector (Addgene, Cambridge, MA, USA) according to the method described by Cong et al. [92]. Briefly, human cDNAs for Dsg2 and Dsc2 were obtained by polymerase chain reaction (PCR) with nucleotide sequences that are published in the GenBank, and amplified and cloned into the expression vector pEF1 (Invitrogen, Carlsbad, CA, USA) accompanied with

the introduction of an HA tag at the C-terminus. DLD1 cells were co-transfected with the CRISPR/Cas9 construct and the expression vector pCAG-Flag-IRESpuro (Addgene, Cambridge, MA, USA) using the lipofectamine LTX protocol. Puromycin was used for screening, resultant colonies were picked and cultured, and the expression of target protein was analyzed by immunoblotting. In addition, deletion of the target gene was confirmed by amplification of genomic DNA by PCR and subsequent sequencing. For stable expression of full-length Dsc2, cells were transfected with the DNA construct using the Lipofectamine LTX protocol and screened in the presence of G418 (400 µg/mL) for about 2 weeks, followed by immunoblot analysis.

Human tissue samples

Colon samples were obtained from patients who required right or left hemi-colectomy due to colon carcinoma in which the surgical resection routinely involves a part of the healthy small intestine or colon, respectively. All patients gave their written informed consent prior surgery to inclusion in the study and ethical approval was given by the Ethical Board of the University of Würzburg (proposal numbers 113/13, 46/11, 42/16). Tissue samples were collected in a standardized procedure via the Interdisciplinary Bank of Biomaterials and Data Würzburg (IBDW) as described in detail previously [93]. For immunostaining, tissue samples were fixed in 4% paraformaldehyde, embedded in paraffin, and sectioned (1 µm).

Enteroids

Intestinal epithelial cells (IECs) were isolated from healthy human full-wall gut resections, 1 cm² in size as described previously [94]. Briefly, villi were scraped off the muscle-free mucosa using a sterile glass slide. The remaining tissue was transferred into a 50 mL falcon tube with 20 mL 4 °C cold HBSS (Sigma-Aldrich, St. Louis, MO, USA) and vortexed for 5 s, and the supernatant discarded. This washing step was repeated until the supernatant was completely cleared of cell debris. Afterward, the tissue was incubated in 4 °C cold 2 mM EDTA/HBSS solution (Sigma-Aldrich, St. Louis, MO, USA) for 30 min at 4 °C under gentle rotation on a shaker. Subsequently, the tissue was washed once in 20 mL HBSS by manually inverting the tube five times. The mucosa was transferred in a new tube with 10 mL HBSS and manually shaken five times. This shaking procedure was repeated four times always using a new tube. Each cell fraction was checked for the amount and size of crypts within small drops under the microscope. The supernatants containing the most vital appearing crypts were pooled and centrifuged at 350g for 3 min at room temperature (RT). Pellet was resuspended in 10 mL basal medium, DMEM-F12 Advanced

(Invitrogen, Carlsbad, CA, USA) supplemented with N2, B27, Anti-Anti, 10 mM HEPES, 2 mM GlutaMAX-I (all from Invitrogen, Carlsbad, CA, USA), and 1 mM *N*-acetylcysteine (Sigma-Aldrich, St. Louis, MO, USA), and the crypt number was estimated in a 10 µL drop by microscopy. Crypts were centrifuged in a nonstick 1.5 mL tube at 350g for 3 min at RT and the supernatant was removed. The tube with the cell pellet was placed on ice until further use. The pellet was resuspended in an appropriate amount of cold Matrigel (Corning, Hickory, NC, USA), that is, 5000 crypts/mL. Drops of 50 µL per well were seeded in a 24-well plate and incubated for 10–20 min until the Matrigel was well solidified. The culture medium contained a mixture of 50% fresh basal medium and 50% Wnt3A-conditioned medium.

Furthermore, the following growth factors were added: 500 ng/mL hR-Spondin 1 (PeproTech, Rocky Hill, NY, USA). 100 ng/mL IECs were isolated from human small intestinal tissue and expanded as organoid culture for 3–4 weeks.

Test reagents

Epidermal growth factor receptor activity was inhibited using either a specific mouse anti-EGFR antibody (C225, sodium azide free, Merck Millipore, Darmstadt, Germany) at 0.5 µg/mL for 1 h or the tyrosine kinase activity inhibitor erlotinib (Santa Cruz Biotechnology, Santa Cruz, CA, USA) at 2.5 µM for 1 h. For positive stimulation of EGFR activity, the growth factor EGF (Sigma-Aldrich, Munich, Germany) was used at 20 ng/mL for 1 h. Cells were cultured in serum-free medium for 1 h prior to treatment with EGFR-modulating agents. PP2 (Calbiochem, Darmstadt, Germany) and KX2-391 (Biozol, Germany) were used at 10 µM for 1 h to inhibit Src activity and SB202190 (Calbiochem, Darmstadt, Germany) was used at 30 µM for 1 h to inhibit p38 MAPK. Dsg2 binding was inhibited using a specific monoclonal mouse antibody directed against the second and third extracellular repeat domains of Dsg2 (clone 10G11, sodium azide free, Progen, Heidelberg, Germany) applied 1:50. For western blot analysis and immunofluorescence staining, following primary antibodies were used: mouse anti-Dsg2 (clone 10G11) and rabbit anti-Dsg2 (rb5, both Progen, Heidelberg, Germany), mouse anti-Dsc2/3 (clone 7G6) and rabbit anti Claudin-4 (both Life Technologies, Carlsbad, CA, USA), rabbit anti-DP I/II (H-300), rabbit anti-EGFR (clone 1005-G), mouse anti-EGFR (clone A-10) and mouse anti-GAPDH (all from Santa Cruz Biotechnology, Santa Cruz, CA, USA), mouse anti- α -tubulin (Abcam, Cambridge, UK), and rabbit anti-phospho-EGFR Tyr845 and rabbit anti-Src (both from Cell Signaling, Danvers, MA, USA). HRP-conjugated goat anti-mouse or goat anti-rabbit (Dianova, Hamburg, Germany) secondary antibodies were used for western blot analysis. Cy3- or Alexa488-labeled

goat anti-mouse or goat anti-rabbit antibodies (Dianova, Hamburg, Germany) were used for confocal microscopy, and Star580- and Star635P-labeled antibodies (Abberior) were used for STED. F-actin was visualized using Alexa488-labeled phalloidin (Life Technologies, Carlsbad, CA, USA) and nuclei were counterstained with DAPI (Sigma-Aldrich, Munich, Germany).

Immunofluorescence

Cells were grown on 12 mm glass cover slides, fixed with 2% paraformaldehyde in PBS for 10 min and, subsequently, permeabilized with 0.5% TritonX-100 in PBS containing 0.02% Tween20 (PBS-T) for 10 min following 1 h of blocking in 2% BSA in PBS-T. Human tissue samples embedded in paraffin were sectioned in 1 μ m slices and immunostaining was performed after removal of paraffin using 100% Xylol followed by an ethanol series from 100 to 70% and sera dest at the end. Then, samples were permeabilized with 0.1% TritonX-100 in PBS-T for 30 min followed by blocking in 2% BSA in PBS-T. Primary and secondary antibodies were incubated for 1 h at room temperature each. Paraffin sections were incubated with primary antibodies at 4 °C over night. For confocal microscopy, coverslips were placed on glass slides with 60% glycerol in PBS, containing 1.5% *N*-propyl gallate (Serva, Heidelberg, Germany). Image acquisition was performed using a Leica SP5 confocal microscope with a 63 \times NA 1.4 PL APO objective (both Leica, Wetzlar, Germany). Co-localization analysis was performed by generating an intensity plot profile for each channel using the ImageJ software and calculating the Pearson's correlation coefficient between the intensity distributions of two molecules of interest. To this end, 35 cell borders from 7 independent experiments were selected.

Stimulated emission depletion microscopy (STED)

After immunostaining, cells were mounted in 2.5% DABCO in MOWIOL/HEPES (self-made solution). Images were acquired with an Abberior 3D STED confocal microscope. Star580 and Star635P (both from Abberior) were excited at 594 and 638 nm, respectively, using pulsed diode lasers (PDL 594, Abberior Instruments; PiL063X, Advanced Laser Diode Systems). Depletion of fluorescent molecules was conducted at 775 nm with a pulsed fibre laser (PFL-P-30-775B1R, MPB Communications) and emission was detected with an avalanche photodiode detector at 605–625 and 650–720 nm range.

Western blot

Cells were lysed with SDS lysis buffer (25 mM HEPES, 2 mM EDTA, 25 mM NaF, and 1% SDS) supplemented

with a protease-inhibitor cocktail (Roche, Mannheim, Germany) followed by sonication and heating to 95 °C for 10 min in Laemmli buffer with 50 mM dithiothreitol (Applichem). Protein amount was determined using a BCA Protein Assay Kit (Pierce/Thermo Scientific, Waltham, MA, USA) and equivalent protein concentrations were resolved by reducing SDS-PAGE. After protein transfer to a nitrocellulose membrane (Life Technologies, Carlsbad, CA, USA) according to the standard protocols, membranes were probed with primary antibodies overnight at 4 °C followed by incubation with secondary antibodies for 2 h at room temperature. Bands were detected with an ECL reaction system (self-made solution) using the Amersham Imager 600 (GE Healthcare Life Sciences, Germany).

TritonX-100 protein extraction

Cells were washed with ice-cold PBS and incubated in a Triton buffer (0.5% Triton X-100, 50 mM MES, 25 mM EGTA, and 5 mM MgCl₂) supplemented with 1 mM PMSF (Roth, Germany), Aprotinin, Pepstatin A (both Applichem, Germany), and Leupeptin (VWR, Germany) for 15 min on ice under gentle shaking. Subsequently, cell lysates were centrifuged at 13,000 rpm for 5 min to separate the insoluble from the soluble fraction and pellets were resuspended in SDS lysis buffer followed by sonication. Protein concentration of both fractions was calculated as described above and equivalent amounts of protein were used for western blot analysis.

Cell surface biotinylation

Cells grown in six-well plates were treated with test reagents, washed with ice-cold HBSS, and incubated with 0.25 mM membrane-impermeable EZ-Link Sulfo-NHS-Biotin (Thermo Fischer Scientific, Waltham, USA) for 1 h on ice to prevent internalization. Excess biotin was quenched by washing three times with ice-cold 100 mM Glycin followed by three times washing with ice-cold HBSS. Cells were lysed in lysis buffer (50 mM NaCl, 10 mM PIPES, 3 mM MgCl₂, and 1% Triton X-100) for 15 min on ice followed by 5 min centrifugation at 13,000 rpm and measurement of protein concentration of the recovered cell lysate supernatants as described above. For precipitation of biotin-labeled proteins, a protein amount of 500 μ g was incubated with NeutrAvidin (High Capacity)-agarose beads (Thermo Fischer Scientific, Waltham, USA) over night at 4 °C. After four times washing with lysis buffer, cell surface proteins were eluted in Laemmli buffer containing 50 mM dithiothreitol at 95 °C and subjected to Western blot analysis.

Co-immunoprecipitation

Cell monolayers were washed with ice-cold HBSS and incubated with RIPA buffer (50 mM Tris–HCl, 150 mM NaCl, 0.1% SDS, 1% NP-40, and 0.1 mM EDTA) supplemented with a protease-inhibitor cocktail (Roche, Mannheim, Germany) for 30 min on ice while shaking. Cells were scraped and centrifuged at 13,000 rpm for 5 min at 4 °C, and protein concentration of the lysate was determined as described above. Cell lysates were precleared with protein-G beads (Santa Cruz Biotechnology, Santa Cruz, CA, USA) for 1 h at 4 °C, followed by incubation with 1 µg of respective antibody or IgG control for 3 h at 4 °C with gentle rotation. Subsequently, protein-G beads were added and incubated over night at 4 °C. For pull-down assays with Dsg2-Fc, beads were incubated with 0.15 mg/mL Dsg2-Fc in HBSS at 4 °C over night, washed three times with RIPA buffer to remove unbound protein, and incubated with cell lysates at 4 °C again over night. After three times washing with RIPA buffer, immunocomplexes were boiled in 20 µL Laemmli buffer containing 50 mM dithiothreitol at 95 °C for 10 min and subjected to Western blot analysis.

Atomic force microscopy (AFM)

Atomic force microscopy measurements were performed with a Nanowizard III AFM (JPK Instruments, Berlin, Germany) mounted on an optical microscopy (Carl Zeiss, Jena, Germany). The whole setup was placed on a Halcyonics i4 anti-vibration table (Accurion, Goettingen, Germany) in a closed hood to protect measurements from environmental noise. The application of AFM force microscopy on living cells was described in detail before [95]. All measurements were conducted in cell culture medium at 37 °C. For Dsg2 adhesion studies, recombinant Dsg2-Fc (self-made) containing the complete extracellular domain (ED) of Dsg2 was linked to flexible Si₃N₄ AFM cantilevers (MLCT probes, Bruker, Calle Tecate, CA, USA) via a flexible bifunctional polyethylene glycol linker (Gruber Lab, Institute of Biophysics, Linz, Austria) as described elsewhere [96]. Prior to adhesion measurements on living cells, AFM topography images of 50 × 50 µm and 128 × 128 pixels were created using a force curve-based imaging mode (QI-mode) with a setpoint adjusted to 0.5 nN, a *z* length of 1500 nm, and a pulling speed of 50 µm/s. Adhesion measurements were performed in the force spectroscopy mode with a relative setpoint of 0.5 nN, a *z* length of 2 µm, and a pulling speed of 4 µm/s. The same cantilever was used under control conditions and after incubation for 1 h with inhibitory antibodies or EGFR-modulating agents. For each condition, several areas of 2 × 5 µm were selected with 1000 recorded force–distance curves per area. Cell-free AFM measurements were carried out with mica sheets (SPI Supplies, West

Chester, USA) instead of cell monolayers, functionalized with either Dsg2-Fc or EGFR-Fc (Sino Biological). To produce comparable results, setpoint was adjusted to the same value as for cell-based experiments. For each condition, several areas of 25 µm × 25 µm with 400 force–distance curves per area were measured using a *z* length of 0.3 µm and a pulling speed of 1 µm/s. Acquired AFM data were processed using the JPK processing software. Analysis of unbinding force distribution was performed with Origin Pro 2016, 93G (Northampton, MA, USA).

Hanging drop bead aggregation assay

Protein-G-coated polystyrene microbeads (Dynabeads, diameter 2.8 µm; Thermo Fisher Scientific) were coated with recombinant Dsg2- or EGFR-Fc and aggregation assays were carried out as described previously [95]. Briefly, beads were washed with 100 mM sodium phosphate buffer (pH 8.1), blocked with 5% BSA for 1 h at RT, and incubated with 0.15 mg/mL Dsg2-, EGFR-Fc or control-Fc part of human IgGs (Merck Millipore, Darmstadt, Germany) over night at 4 °C under slow overhead rotation. Following washing steps, beads were incubated with 500 mM dimethyl adipimidate-2 HCl (DMA, Thermo Fisher Scientific) for 45 min at RT to covalently cross-link protein-G with Fc parts. After incubation with 200 mM ethanolamine (pH 8.0) for 2 h at RT and several washing steps, about 0.3 µg beads were resuspended in 10 µL HBSS containing 1.8 mM Ca²⁺. Then, beads were allowed to aggregate in a hanging drop on the underside of a culture dish lid at 37 °C for 1 h, followed by 1 h incubation with EGF. After shaking on an orbital shaker at 1000 rpm for 3 min, a ratio was calculated from of the area covered with beads and the area of total bead extent and expressed as density of bead colonies in percentage.

Calcium switch assay

Cells were incubated with 4 mM EGTA for 1 h, thereby inducing disruption of Ca²⁺-dependent cell junctions. Reformation of cell junctions was induced by addition of 8 mM CaCl₂ supplemented with test reagents or the respective vehicle. Time course of junctional disassembly and reassembly was monitored by measuring the transepithelial resistance (TER) of cells grown on eight-well electrode arrays (Ibidi, 8W10E) with an ECIS model Z theta (Applied Biophysics, Troy, NY, USA) at 800 Hz for DLD1 cells and 400 Hz for Caco2 cells. In addition, cells were grown on filter inserts (Corning, PET membrane, pore size 0.4 µm) and measured with the ECIS 8W Trans-Filter Adapter. Stability of reformed cell junctions was analyzed using a dispase-based cell dissociation assay.

Dispase-based dissociation assay

Dissociation assays were performed in 24-well plates. After treatment with test reagents, cell monolayer were washed with Hank's buffered saline solution (HBSS; Sigma-Aldrich) and incubated with 150 μ L dispase II (2.4 U/mL in HBSS, Sigma-Aldrich) at 37 °C for 25 min. Reaction was stopped by adding 200 μ L HBSS and a defined shear stress was applied by pipetting three times with an electrical pipet. Resulting fragments were counted using a binocular microscope (Leica). Every condition was performed in duplicates and each experiment was repeated at least four times.

Proliferation assay

Cellular proliferation was ascertained by counting the number of cells using a Neubauer chamber (Laboroptik, Lancing, UK). 50,000 cells were seeded in 24-well plates in complete DMEM with erlotinib (2.5 μ M) or DMSO and counted after 24, 48, 72, and 96 h. Medium was changed every day.

Transfection with Dsg2-GFP

The plasmid encoding for human wild-type Dsg2 with a C-terminal eGFP tag [97] was kindly provided by Katja Gehmlich (University of Oxford, UK). 50,000 cells were seeded and transfected right away with 1 μ g endotoxin-free Dsg2-GFP plasmid DNA or the GFP empty vector [98] (pDEST-eGFP-N1, Addgene plasmid # 31796, gift from Robin Shaw, Cedars-Sinai Heart Institute, Los Angeles, USA) using TurboFect™ (Life Technologies) according to the manufacturer's protocol and incubated for 48 h. Medium was changed 8 h after transfection.

Statistics

All experiments were repeated at least three times. Band intensity was quantified using ImageJ (National Institutes of Health, Bethesda, MD, USA). For statistical analysis, two-tailed Student's *t* test was used to analyze two-sample groups and one-way ANOVA followed by Bonferroni correction was used for multiple sample groups. Results are shown as mean \pm SE. A *p* value of < 0.05 was considered significant.

Acknowledgements This work was supported by the DFG priority program SPP 1782. DLD1 cells were a gift from S.T. Suzuki (Kwansei Gakuin University, Japan). STED microscopy was performed in the lab of H. Leonhardt (Ludwig-Maximilians-University, Munich). The authors would like to thank Andreas Meiser and Hartmann Harz for their assistance in STED sample preparation and image acquisition.

Author contributions HU and JW designed the study. HU performed and analyzed the experiments. VR performed the hanging drop bead aggregation assay. MM obtained and prepared the human tissue samples. CF generated the enteroids. MD generated the Dsg2-deficient

Caco2 cell line. All authors interpreted the data. HU wrote the manuscript and prepared the figures. All authors reviewed the manuscript.

Compliance with ethical standards

Conflict of interest The authors declare that they have no conflict of interest.

References

1. Cerf-Bensussan N, Gaboriau-Routhiau V (2010) The immune system and the gut microbiota: friends or foes? *Nat Rev Immunol* 10:735–744
2. Helander HF, Fandriks L (2014) Surface area of the digestive tract—revisited. *Scand J Gastroenterol* 49:681–689
3. Gayer CP, Basson MD (2009) The effects of mechanical forces on intestinal physiology and pathology. *Cell Signal* 21:1237–1244
4. Sancho E, Battle E, Clevers H (2004) Signaling pathways in intestinal development and cancer. *Annu Rev Cell Dev Biol* 20:695–723
5. Capaldo CT, Farkas AE, Nusrat A (2014) Epithelial adhesive junctions. *F1000Prime Rep* 6:1
6. Farquhar MG, Palade GE (1963) Junctional complexes in various epithelia. *J Cell Biol* 17:375
7. Green KJ, Simpson CL (2007) Desmosomes: new perspectives on a classic. *J Invest Dermatol* 127:2499–2515
8. Brennan D, Hu Y, Joubes S, Choi YW, Whitaker-Menezes D, O'Brien T, Uitto J, Rodeck U, Mahoney MG (2007) Suprabasal Dsg2 expression in transgenic mouse skin confers a hyperproliferative and apoptosis-resistant phenotype to keratinocytes. *J Cell Sci* 120:758–771
9. Getsios S, Simpson CL, Kojima S, Harmon R, Sheu LJ, Dusek RL, Cornwell M, Green KJ (2009) Desmoglein 1-dependent suppression of EGFR signaling promotes epidermal differentiation and morphogenesis. *J Cell Biol* 185:1243–1258
10. Nava P, Laukoetter MG, Hopkins AM, Laur O, Gerner-Smidt K, Green KJ, Parkos CA, Nusrat A (2007) Desmoglein-2: a novel regulator of apoptosis in the intestinal epithelium. *Mol Biol Cell* 18:4565–4578
11. Spindler V, Waschke J (2014) Desmosomal cadherins and signaling: lessons from autoimmune disease. *Cell Commun Adhes* 21:77–84
12. Owen GR, Stokes DL (2010) Exploring the nature of desmosomal cadherin associations in 3D. *Dermatol Res Pract* 2010:930401
13. Holthofer B, Windoffer R, Troyanovsky S, Leube RE (2007) Structure and function of desmosomes. *Int Rev Cytol* 264:65–163
14. Koch PJ, Goldschmidt MD, Zimbelmann R, Troyanovsky R, Franke WW (1992) Complexity and expression patterns of the desmosomal cadherins. *Proc Natl Acad Sci USA* 89:353–357
15. Waschke J (2008) The desmosome and pemphigus. *Histochem Cell Biol* 130:21–54
16. Fujiwara M, Nagatomo A, Tsuda M, Obata S, Sakuma T, Yamamoto T, Suzuki ST (2015) Desmocollin-2 alone forms functional desmosomal plaques, with the plaque formation requiring the juxtamembrane region and plakophilins. *J Biochem* 158:339–353
17. Biedermann K, Vogelsang H, Becker I, Plaschke S, Siewert JR, Hoffer H, Keller G (2005) Desmoglein 2 is expressed abnormally rather than mutated in familial and sporadic gastric cancer. *J Pathol* 207:199–206
18. Schlegel N, Meir M, Heupel WM, Holthofer B, Leube RE, Waschke J (2010) Desmoglein 2-mediated adhesion is required for intestinal epithelial barrier integrity. *Am J Physiol Gastrointest Liver Physiol* 298:G774–G783

19. Spindler V, Meir M, Vigh B, Flemming S, Hutz K, Germer CT, Waschke J, Schlegel N (2015) Loss of desmoglein 2 contributes to the pathogenesis of Crohn's disease. *Inflamm Bowel Dis* 21:2349–2359
20. Ungewiss H, Vielmuth F, Suzuki ST, Maiser A, Harz H, Leonhardt H, Kugelmann D, Schlegel N, Waschke J (2017) Desmoglein 2 regulates the intestinal epithelial barrier via p38 mitogen-activated protein kinase. *Sci Rep* 7:6329
21. Kamekura R, Nava P, Feng M, Quiros M, Nishio H, Weber DA, Parkos CA, Nusrat A (2015) Inflammation-induced desmoglein-2 ectodomain shedding compromises the mucosal barrier. *Mol Biol Cell* 26:3165–3177
22. Overmiller AM, McGuinn KP, Roberts BJ, Cooper F, Brennan-Crispi DM, Deguchi T, Peltonen S, Wahl JK 3rd, Mahoney MG (2016) c-Src/Cav1-dependent activation of the EGFR by Dsg2. *Oncotarget* 7:37536–37555
23. Wheelock MJ, Johnson KR (2003) Cadherins as modulators of cellular phenotype. *Annu Rev Cell Dev Biol* 19:207–235
24. Yap AS, Crampton MS, Hardin J (2007) Making and breaking contacts: the cellular biology of cadherin regulation. *Curr Opin Cell Biol* 19:508–514
25. Honegger AM, Kris RM, Ullrich A, Schlessinger J (1989) Evidence that autophosphorylation of solubilized receptors for epidermal growth factor is mediated by intermolecular cross-phosphorylation. *Proc Natl Acad Sci USA* 86:925–929
26. Kaplan M, Narasimhan S, de Heus C, Mance D, van Doorn S, Houben K, Popov-Celeketic D, Damman R, Katrukha EA, Jain P et al (2016) EGFR dynamics change during activation in native membranes as revealed by NMR. *Cell* 167(1241–1251):e1211
27. Lemmon MA, Schlessinger J (2010) Cell signaling by receptor tyrosine kinases. *Cell* 141:1117–1134
28. Ogiso H, Ishitani R, Nureki O, Fukai S, Yamanaka M, Kim JH, Saito K, Sakamoto A, Inoue M, Shirouzu M et al (2002) Crystal structure of the complex of human epidermal growth factor and receptor extracellular domains. *Cell* 110:775–787
29. Ullrich A, Schlessinger J (1990) Signal transduction by receptors with tyrosine kinase activity. *Cell* 61:203–212
30. Klessner JL, Desai BV, Amargo EV, Getsios S, Green KJ (2009) EGFR and ADAMs cooperate to regulate shedding and endocytic trafficking of the desmosomal cadherin desmoglein 2. *Mol Biol Cell* 20:328–337
31. Lorch JH, Klessner J, Park JK, Getsios S, Wu YL, Stack MS, Green KJ (2004) Epidermal growth factor receptor inhibition promotes desmosome assembly and strengthens intercellular adhesion in squamous cell carcinoma cells. *J Biol Chem* 279:37191–37200
32. Kamekura R, Kolegraff KN, Nava P, Hilgarth RS, Feng M, Parkos CA, Nusrat A (2014) Loss of the desmosomal cadherin desmoglein-2 suppresses colon cancer cell proliferation through EGFR signaling. *Oncogene* 33:4531–4536
33. Blay J, Brown KD (1985) Epidermal growth factor promotes the chemotactic migration of cultured rat intestinal epithelial cells. *J Cell Physiol* 124:107–112
34. Miguel JC, Maxwell AA, Hsieh JJ, Harnisch LC, Al Alam D, Polk DB, Lien CL, Watson AJ, Frey MR (2017) Epidermal growth factor suppresses intestinal epithelial cell shedding through a MAPK-dependent pathway. *J Cell Sci* 130:90–96
35. Polk DB (1998) Epidermal growth factor receptor-stimulated intestinal epithelial cell migration requires phospholipase C activity. *Gastroenterology* 114:493–502
36. Bishop WP, Wen JT (1994) Regulation of Caco-2 cell proliferation by basolateral membrane epidermal growth factor receptors. *Am J Physiol* 267:G892–G900
37. Scheving LA, Shiurba RA, Nguyen TD, Gray GM (1989) Epidermal growth factor receptor of the intestinal enterocyte. Localization to laterobasal but not brush border membrane. *J Biol Chem* 264:1735–1741
38. Carpenter G, Cohen S (1976) ¹²⁵I-labeled human epidermal growth factor. Binding, internalization, and degradation in human fibroblasts. *J Cell Biol* 71:159–171
39. Levkowitz G, Waterman H, Zamir E, Kam Z, Oved S, Langdon WY, Beguinot L, Geiger B, Yarden Y (1998) c-Cbl/Sli-1 regulates endocytic sorting and ubiquitination of the epidermal growth factor receptor. *Genes Dev* 12:3663–3674
40. Moro L, Dolce L, Cabodi S, Bergatto E, Boeri Erba E, Smeriglio M, Turco E, Retta SF, Giuffrida MG, Venturino M et al (2002) Integrin-induced epidermal growth factor (EGF) receptor activation requires c-Src and p130Cas and leads to phosphorylation of specific EGF receptor tyrosines. *J Biol Chem* 277:9405–9414
41. Biscardi JS, Maa MC, Tice DA, Cox ME, Leu TH, Parsons SJ (1999) c-Src-mediated phosphorylation of the epidermal growth factor receptor on Tyr845 and Tyr1101 is associated with modulation of receptor function. *J Biol Chem* 274:8335–8343
42. Maa MC, Leu TH, McCarley DJ, Schatzman RC, Parsons SJ (1995) Potentiation of epidermal growth factor receptor-mediated oncogenesis by c-Src: implications for the etiology of multiple human cancers. *Proc Natl Acad Sci USA* 92:6981–6985
43. Sato K, Sato A, Aoto M, Fukami Y (1995) c-Src phosphorylates epidermal growth factor receptor on tyrosine 845. *Biochem Biophys Res Commun* 215:1078–1087
44. Balanis N, Yoshigi M, Wendt MK, Schiemann WP, Carlin CR (2011) beta3 integrin-EGF receptor cross-talk activates p190RhoGAP in mouse mammary gland epithelial cells. *Mol Biol Cell* 22:4288–4301
45. Rotzer V, Hartlieb E, Vielmuth F, Gliem M, Spindler V, Waschke J (2015) E-cadherin and Src associate with extradesmosomal Dsg3 and modulate desmosome assembly and adhesion. *Cell Mol Life Sci* 72:4885–4897
46. Bogdan S, Klambt C (2001) Epidermal growth factor receptor signaling. *Curr Biol* 11:R292–R295
47. Bowman T, Garcia R, Turkson J, Jove R (2000) STATs in oncogenesis. *Oncogene* 19:2474–2488
48. Massague J, Pandiella A (1993) Membrane-anchored growth factors. *Annu Rev Biochem* 62:515–541
49. Chung BM, Dimri M, George M, Reddi AL, Chen G, Band V, Band H (2009) The role of cooperativity with Src in oncogenic transformation mediated by non-small cell lung cancer-associated EGF receptor mutants. *Oncogene* 28:1821–1832
50. Jung J, Kim HY, Kim M, Sohn K, Kim M, Lee K (2011) Translationally controlled tumor protein induces human breast epithelial cell transformation through the activation of Src. *Oncogene* 30:2264–2274
51. Jung O, Choi YJ, Kwak TK, Kang M, Lee MS, Ryu J, Kim HJ, Lee JW (2013) The COOH-terminus of TM4SF5 in hepatoma cell lines regulates c-Src to form invasive protrusions via EGFR Tyr845 phosphorylation. *Biochim Biophys Acta* 1833:629–642
52. Kannangai R, Sahin F, Torbenson MS (2006) EGFR is phosphorylated at Ty845 in hepatocellular carcinoma. *Mod Pathol* 19:1456–1461
53. Cvriljevic AN, Akhavan D, Wu M, Martinello P, Furnari FB, Johnston AJ, Guo D, Pike L, Cavenee WK, Scott AM et al (2011) Activation of Src induces mitochondrial localisation of de2-7EGFR (EGFRvIII) in glioma cells: implications for glucose metabolism. *J Cell Sci* 124:2938–2950
54. Nair VD, Sealfon SC (2003) Agonist-specific transactivation of phosphoinositide 3-kinase signaling pathway mediated by the dopamine D2 receptor. *J Biol Chem* 278:47053–47061
55. Ray RM, Bhattacharya S, Johnson LR (2007) EGFR plays a pivotal role in the regulation of polyamine-dependent apoptosis in intestinal epithelial cells. *Cell Signal* 19:2519–2527

56. Tice DA, Biscardi JS, Nickles AL, Parsons SJ (1999) Mechanism of biological synergy between cellular Src and epidermal growth factor receptor. *Proc Natl Acad Sci USA* 96:1415–1420
57. Bakker J, Spits M, Neeffjes J, Berlin I (2017) The EGFR odyssey—from activation to destruction in space and time. *J Cell Sci* 130:4087–4096
58. Francavilla C, Papetti M, Rigbolt KT, Pedersen AK, Sigurdsson JO, Cazzamali G, Karemore G, Blagoev B, Olsen JV (2016) Multilayered proteomics reveals molecular switches dictating ligand-dependent EGFR trafficking. *Nat Struct Mol Biol* 23:608–618
59. Haugh JM, Huang AC, Wiley HS, Wells A, Lauffenburger DA (1999) Internalized epidermal growth factor receptors participate in the activation of p21(ras) in fibroblasts. *J Biol Chem* 274:34350–34360
60. Vieira AV, Lamaze C, Schmid SL (1996) Control of EGF receptor signaling by clathrin-mediated endocytosis. *Science* 274:2086–2089
61. Wu P, Wee P, Jiang J, Chen X, Wang Z (2012) Differential regulation of transcription factors by location-specific EGF receptor signaling via a spatio-temporal interplay of ERK activation. *PLoS One* 7:e41354
62. Brand TM, Iida M, Luthar N, Starr MM, Huppert EJ, Wheeler DL (2013) Nuclear EGFR as a molecular target in cancer. *Radiother Oncol* 108:370–377
63. Kamio T, Shigematsu K, Sou H, Kawai K, Tsuchiyama H (1990) Immunohistochemical expression of epidermal growth factor receptors in human adrenocortical carcinoma. *Hum Pathol* 21:277–282
64. Gonnella PA, Siminoski K, Murphy RA, Neutra MR (1987) Trans-epithelial transport of epidermal growth factor by absorptive cells of suckling rat ileum. *J Clin Invest* 80:22–32
65. Kelly D, McFadyen M, King TP, Morgan PJ (1992) Characterization and autoradiographic localization of the epidermal growth factor receptor in the jejunum of neonatal and weaned pigs. *Reprod Fertil Dev* 4:183–191
66. Yoo BK, He P, Lee SJ, Yun CC (2011) Lysophosphatidic acid 5 receptor induces activation of Na(+)/H(+) exchanger 3 via apical epidermal growth factor receptor in intestinal epithelial cells. *Am J Physiol Cell Physiol* 301:C1008–C1016
67. Garrod D, Chidgey M (2008) Desmosome structure, composition and function. *Biochim Biophys Acta* 1778:572–587
68. Mahoney MG, Hu Y, Brennan D, Bazzi H, Christiano AM, Wahl JK 3rd (2006) Delineation of diversified desmoglein distribution in stratified squamous epithelia: implications in diseases. *Exp Dermatol* 15:101–109
69. Rubsam M, Mertz AF, Kubo A, Marg S, Jungst C, Goranci-Buzhala G, Schauss AC, Horsley V, Dufresne ER, Moser M et al (2017) E-cadherin integrates mechanotransduction and EGFR signaling to control junctional tissue polarization and tight junction positioning. *Nat Commun* 8:1250
70. Yashiro M, Nishioka N, Hirakawa K (2006) Decreased expression of the adhesion molecule desmoglein-2 is associated with diffuse-type gastric carcinoma. *Eur J Cancer* 42:2397–2403
71. Godek J, Sargiannidou I, Patel S, Hurd L, Rothman VL, Tuszyński GP (2011) Angiostatin inhibits breast cancer proliferation through activation of epidermal growth factor receptor and nuclear factor kappa (NF- κ B). *Exp Mol Pathol* 90:244–251
72. Sato K, Nagao T, Iwasaki T, Nishihira Y, Fukami Y (2003) Src-dependent phosphorylation of the EGF receptor Tyr-845 mediates Stat-p21waf1 pathway in A431 cells. *Genes Cells* 8:995–1003
73. Kolegraff K, Nava P, Helms MN, Parkos CA, Nusrat A (2011) Loss of desmocollin-2 confers a tumorigenic phenotype to colonic epithelial cells through activation of Akt/beta-catenin signaling. *Mol Biol Cell* 22:1121–1134
74. Rowan AJ, Lamlum H, Ilyas M, Wheeler J, Straub J, Papadopoulos A, Bicknell D, Bodmer WF, Tomlinson IP (2000) APC mutations in sporadic colorectal tumors: a mutational “hotspot” and interdependence of the “two hits”. *Proc Natl Acad Sci USA* 97:3352–3357
75. Yang J, Zhang W, Evans PM, Chen X, He X, Liu C (2006) Adenomatous polyposis coli (APC) differentially regulates beta-catenin phosphorylation and ubiquitination in colon cancer cells. *J Biol Chem* 281:17751–17757
76. Guturi KK, Mandal T, Chatterjee A, Sarkar M, Bhattacharya S, Chatterjee U, Ghosh MK (2012) Mechanism of beta-catenin-mediated transcriptional regulation of epidermal growth factor receptor expression in glycogen synthase kinase 3 beta-inactivated prostate cancer cells. *J Biol Chem* 287:18287–18296
77. Jean C, Blanc A, Prade-Houdellier N, Ysebaert L, Hernandez-Pigeon H, Al Saati T, Haure MJ, Coluccia AM, Charveron M, Delabesse E et al (2009) Epidermal growth factor receptor/beta-catenin/T cell factor 4/matrix metalloproteinase 1: a new pathway for regulating keratinocyte invasiveness after UVA irradiation. *Cancer Res* 69:3291–3299
78. Lu Z, Ghosh S, Wang Z, Hunter T (2003) Downregulation of caveolin-1 function by EGF leads to the loss of E-cadherin, increased transcriptional activity of beta-catenin, and enhanced tumor cell invasion. *Cancer Cell* 4:499–515
79. Tan X, Apte U, Micsenyi A, Kotsagrelis E, Luo JH, Ranganathan S, Monga DK, Bell A, Michalopoulos GK, Monga SP (2005) Epidermal growth factor receptor: a novel target of the Wnt/beta-catenin pathway in liver. *Gastroenterology* 129:285–302
80. van Veelen W, Le NH, Helvensteijn W, Blonden L, Theeuwes M, Bakker ER, Franken PF, van Gurp L, Meijlink F, van der Valk MA et al (2011) beta-catenin tyrosine 654 phosphorylation increases Wnt signalling and intestinal tumorigenesis. *Gut* 60:1204–1212
81. Yue X, Lan F, Yang W, Yang Y, Han L, Zhang A, Liu J, Zeng H, Jiang T, Pu P et al (2010) Interruption of beta-catenin suppresses the EGFR pathway by blocking multiple oncogenic targets in human glioma cells. *Brain Res* 1366:27–37
82. Vergarajauregui S, San Miguel A, Puertollano R (2006) Activation of p38 mitogen-activated protein kinase promotes epidermal growth factor receptor internalization. *Traffic* 7:686–698
83. Frey MR, Dise RS, Edelblum KL, Polk DB (2006) p38 kinase regulates epidermal growth factor receptor downregulation and cellular migration. *EMBO J* 25:5683–5692
84. Frey MR, Golovin A, Polk DB (2004) Epidermal growth factor-stimulated intestinal epithelial cell migration requires Src family kinase-dependent p38 MAPK signaling. *J Biol Chem* 279:44513–44521
85. Kuwada SK, Lund KA, Li XF, Cliften P, Amsler K, Opresko LK, Wiley HS (1998) Differential signaling and regulation of apical vs. basolateral EGFR in polarized epithelial cells. *Am J Physiol* 275:C1419–C1428
86. Alexander RJ, Panja A, Kaplan-Liss E, Mayer L, Raicht RF (1995) Expression of growth factor receptor-encoded mRNA by colonic epithelial cells is altered in inflammatory bowel disease. *Dig Dis Sci* 40:485–494
87. Beck PL, Podolsky DK (1999) Growth factors in inflammatory bowel disease. *Inflamm Bowel Dis* 5:44–60
88. Potten CS, Owen G, Hewitt D, Chadwick CA, Hendry H, Lord BI, Woolford LB (1995) Stimulation and inhibition of proliferation in the small intestinal crypts of the mouse after in vivo administration of growth factors. *Gut* 36:864–873
89. Janmaat ML, Giaccone G (2003) The epidermal growth factor receptor pathway and its inhibition as anticancer therapy. *Drugs Today (Barc)* 39(Suppl C):61–80
90. Kaiser GC, Polk DB (1997) Tumor necrosis factor alpha regulates proliferation in a mouse intestinal cell line. *Gastroenterology* 112:1231–1240
91. McElroy SJ, Frey MR, Yan F, Edelblum KL, Goettel JA, John S, Polk DB (2008) Tumor necrosis factor inhibits ligand-stimulated

- EGF receptor activation through a TNF receptor 1-dependent mechanism. *Am J Physiol Gastrointest Liver Physiol* 295:G285–G293
92. Cong L, Ran FA, Cox D, Lin S, Barretto R, Habib N, Hsu PD, Wu X, Jiang W, Marraffini LA et al (2013) Multiplex genome engineering using CRISPR/Cas systems. *Science* 339:819–823
93. Geiger Joerg BS, Stefan Kircher, Michael Neumann, Andreas Rosenwald, Roland Jahns (2018) Hospital-integrated biobanking as a service—the Interdisciplinary Bank of Biomaterials and Data Wuerzburg (IBDW). *Open J Bioresour* 5:6
94. Schweinlin M, Wilhelm S, Schwedhelm I, Hansmann J, Rietscher R, Jurowich C, Walles H, Metzger M (2016) Development of an advanced primary human in vitro model of the small intestine. *Tissue Eng Part C Methods* 22:873–883
95. Vielmuth F, Hartlieb E, Kugelmann D, Waschke J, Spindler V (2015) Atomic force microscopy identifies regions of distinct desmoglein 3 adhesive properties on living keratinocytes. *Nano-medicine* 11:511–520
96. Andreas E, Linda W, Christian R, Jürgen W, Martin H, Rong Z, Ferry K, Dieter B et al (2007) A new simple method for linking of antibodies to atomic force microscopy tips. *Bioconjugate Chem.* 18:1176–1184
97. Gehmlich K, Asimaki A, Cahill TJ, Ehler E, Syrris P, Zachara E, Re F, Avella A, Monserrat L, Saffitz JE et al (2010) Novel missense mutations in exon 15 of desmoglein-2: role of the intracellular cadherin segment in arrhythmogenic right ventricular cardiomyopathy? *Heart Rhythm* 7:1446–1453
98. Hong TT, Smyth JW, Gao D, Chu KY, Vogan JM, Fong TS, Jensen BC, Colecraft HM, Shaw RM (2010) BIN1 localizes the L-type calcium channel to cardiac T-tubules. *PLoS Biol* 8:e1000312

Supplementary material to the manuscript

Title: Dsg2 via Src-mediated transactivation shapes EGFR signaling towards cell adhesion

Authors: Hanna Ungewiß¹, Vera Rötzer¹, Michael Meir², Christina Fey³, Markus Diefenbacher⁴,
Nicolas Schlegel², Jens Waschke¹

Author affiliation:

¹ Department I, Institute of Anatomy and Cell Biology, Ludwig Maximilians University Munich, Pettenkoferstr. 11, 80336 Munich, Germany

² Department of General, Visceral, Vascular and Paediatric Surgery, Julius-Maximilians-Universität, Oberdürrbacher Str. 6, 97080 Würzburg, Germany

³ Department for Tissue Engineering and Regenerative Medicine, University Hospital Würzburg, Röntgenring 11, 97070 Würzburg, Germany

⁴ Department of Biochemistry and Molecular Biochemistry, University of Würzburg, Am Hubland, 97074 Würzburg, Germany

Supplementary Methods

Generation of Dsg2 knockout in Caco2 cells by using the CRISPR/Cas9 system

Disruption of the Dsg2 gene was carried out with the CRISPR/Cas9 system. Two sgRNA targeting exon 3 and exon 13 of human Dsg2 were designed using the Chopchop-web based sgRNA design tool [1] and subcloned into the lentiviral vectors pLentiCRISPR v2 (kind gift from Feng Zhang, Addgene plasmid # 52961) and pLKO5.sgRNA.EFS.GFP (kind gift from Benjamin Ebert, Addgene plasmid # 57822) respectively. HEK293T cells were used for production of lentiviral particles employing the second generation lentiviral packaging system comprising pPAX and pMD2 packaging plasmids. Caco2 cells were infected with viral supernatant containing both viral particles, CrisprV2 and LKO-sgRNA-EFS GFP accompanied with the addition of polybrene. Infected cells were selected using Puromycin

(15µg/ml) for 1 week and positive clones were sorted for GFP-expression using FACS. Deletion of the target gene in single clones was assessed by immunoblotting and qPCR.

Table 1: Primers used for synthesis of the Dsg2 construct and used for qPCR

<i>Primer name</i>	<i>Sequence</i>
hDSG2-1 f	caccgCTTTGGCGCCCTTTCCGCAA
hDSG2-1 r	aaacTTGCGGAAAGGGCGCCAAAGc
hDSG2-2 f	caccgCTAAACATCCTCATTTAGTG
hDSG2-2 r	aaacCACTAAATGAGGATGTTTAGc
<i>qPCR primer</i>	<i>Sequence</i>
DSG2 f	Aattgcgctcatgatttgg
DSG2 r	Gcaatggcacatcagcagta

Supplementary figure legends

Fig. S1 (A) Immunostaining for Dsg2 and EGFR in confluent Caco2 cell monolayer displayed linear localization of Dsg2 and EGFR along the cell borders in Caco2 WT cells, which was not present in Dsg2 deficient Caco2 cells. Bar 10 µm (B) Triton X-100 protein extraction revealed reduced amount of EGFR in the insoluble fraction upon loss of Dsg2 in Caco2 cells. GAPDH served as loading control. (C) Band intensity of detected EGFR was analyzed from 4 independent experiments, resulting in a significant reduction of EGFR in both fractions in Dsg2-deficient Caco2 cells. Results are shown as means ± SE * p < 0.05 (D) Total protein level of EGFR in Caco2 cells was assessed by Western blotting resulting in reduced levels of EGFR in Dsg2-deficient Caco2 cells. GAPDH served as loading control. (E) Band intensity of detected EGFR bands was quantified from 5 independent experiments, showing a significant reduction of total EGFR protein levels upon loss of Dsg2 in Caco2 cells. Results are shown as means ± SE. * p < 0.05

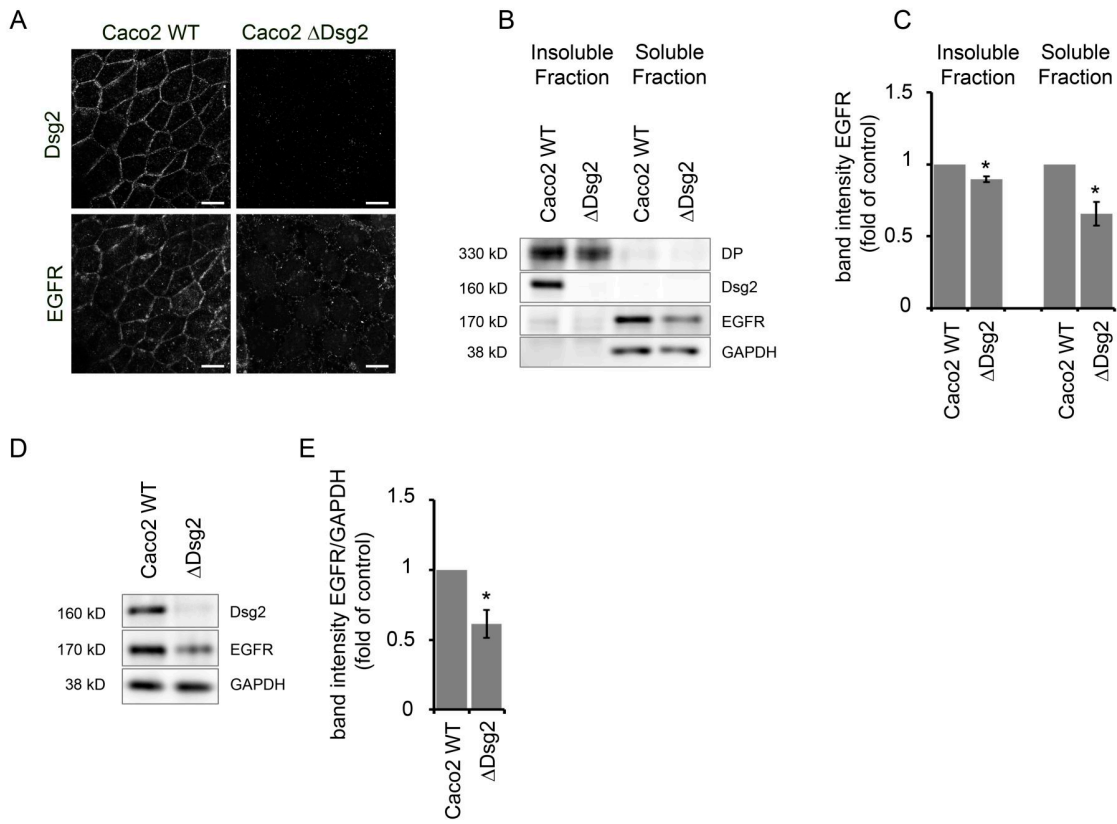
Fig. S2 (A) Phosphorylation of EGFR at Y845 in Caco2 cells was analyzed via Western blot. Reduced level of phosphorylation were observed in cells deficient for Dsg2. (B) Band intensity for detected pEGFR was quantified and normalized to total EGFR. Shown are fold change values \pm SE of 6 independent experiments. * $p < 0.05$ (C) Immunostaining for Src in DLD1 cells deficient for Dsg2 and/or Dsc2 revealed similar localization of Src at cell borders in all cell lines independent of Dsg2 expression. Alexa-phalloidin was used to visualize cell borders. Bar 10 μm (D) Western blot analysis of whole cell lysates of DLD1 cells revealed unaltered protein levels of total Src as well as phosphorylated Src in all knockout cell lines. GAPDH was used as loading control. Shown is representative blot of 3 independent experiments. (E) Src is present in the TritonX-100 insoluble fraction despite loss of Dsg2 and similar in all DLD1 knockout cell lines. GAPDH was used as loading control. Shown is representative blot of 3 independent experiments.

Fig. S3 (A) Barrier recovery of Caco2 cells after Ca^{2+} -switch was monitored by measuring the TER showing impaired barrier recovery after inhibition of EGFR, Src and p38MAPK activity with respective inhibitors. Inhibitors were applied together with CaCl_2 after 1 h depletion with EGTA. (B) TER values were quantified 10 h after repletion with respective inhibitors revealing significantly reduced TER values after repletion with Erlotinib, PP2 and SB202190 compared to control repletion with respective vehicle. Shown are fold change values \pm SE of 6 independent experiments. * $p < 0.05$; n.s. = not significant (C) Barrier recovery of DLD1 WT cells grown on filter inserts was analyzed via TER measurements. Test reagents were applied together with CaCl_2 from the apical or basolateral site of cell monolayer, which resulted in impaired barrier recovery after inhibition of apical as well as of basolateral localized EGFR. (D) TER values were quantified 8 h after repletion showing significantly decreased values in the presence of Erlotinib compared to control repletion. Shown are fold change values \pm SE of 4 independent experiments. * $p < 0.05$; n.s. = not significant (E) Barrier recovery of DLD1 cells deficient for Dsg2 and Dsc2 after Ca^{2+} -switch was analyzed using TER measurements revealing impaired recovery after repletion with added inhibitors for EGFR, Src and p38MAPK activity. (F) TER values were quantified 10 h after repletion showing a significant reduction in the presence of Erlotinib, PP2 and SB202190. Shown are fold change values \pm SE of 6-8 independent experiments. * $p < 0.05$; n.s. = not significant (G) Ca^{2+} -switch assay was performed with confluent cell monolayer of DLD1 WT cells

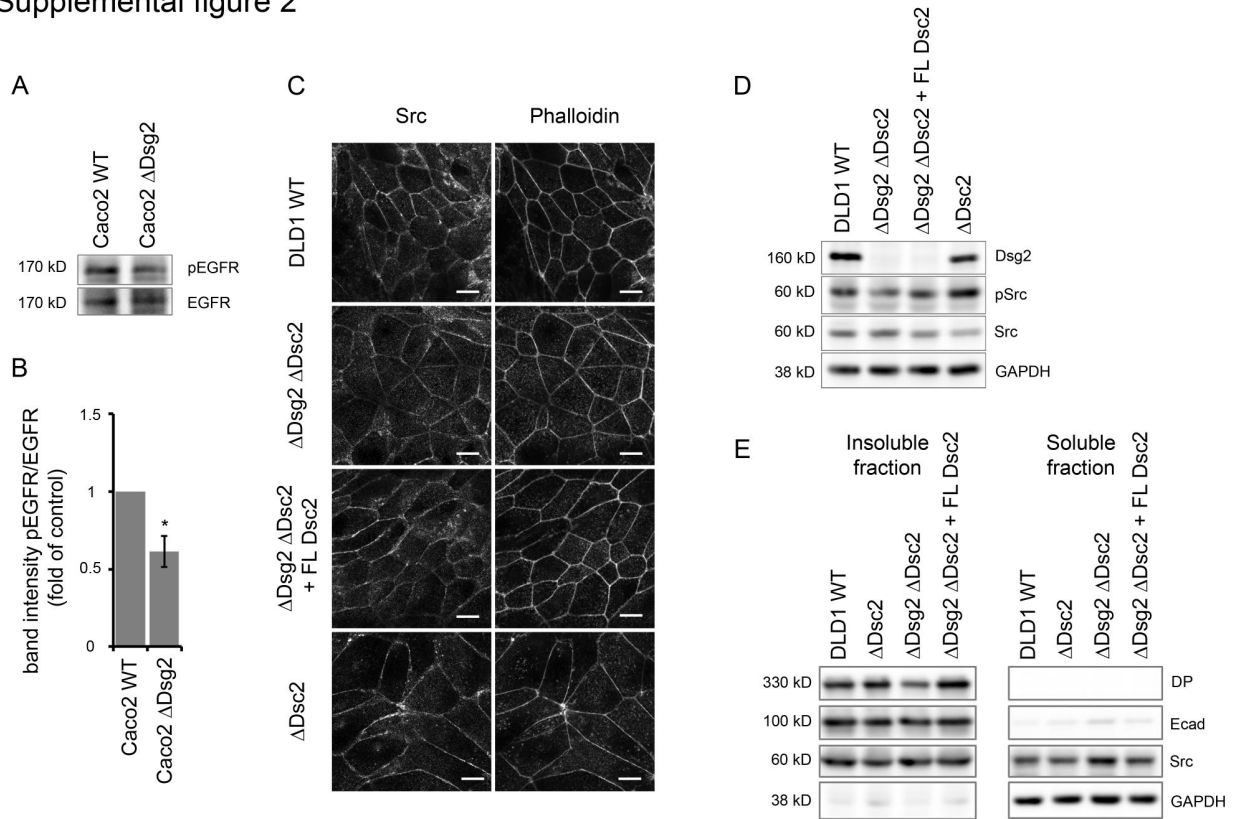
grown on coverslips and formation of TJ was assessed 2 h after repletion with several test reagents by immunostaining for Cld4. Alexa488-phalloidin was used to visualize cell borders. Bar 10 μ m. (H) DLD1 double knockout cells and Caco2 Dsg2-deficient cells were transfected with Dsg2-GFP or the GFP empty vector resulting in linear localization of Dsg2-GFP along the cell borders. Bar 10 μ m (I-J) Cell proliferation of Caco2 cells deficient for Dsg2 was determined by cell counting. 50000 cells were seeded and treated with Erlotinib (I) or transfected with Dsg2-GFP (J) and counted after 48 h. Shown is mean \pm SE of 4 (I) and 5 (J) independent experiments. GFP-ev = empty vector, * $p < 0.05$

1. Labun, K., Montague, T.G., Gagnon, J.A., Thyme, S.B., and Valen, E. (2016). CHOPCHOP v2: a web tool for the next generation of CRISPR genome engineering. *Nucleic Acids Res* 44, W272-276.

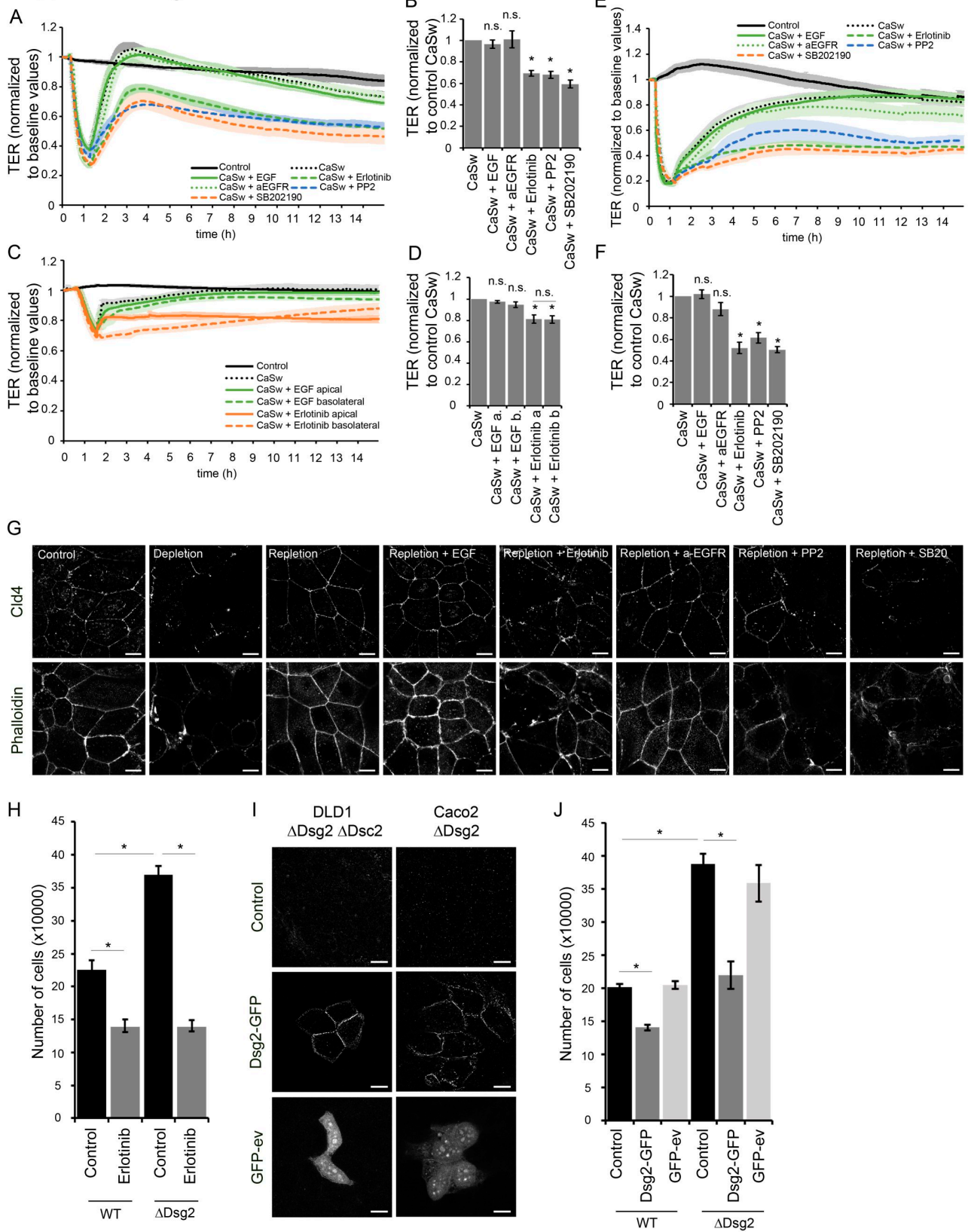
Supplemental figure 1



Supplemental figure 2



Supplemental figure 3



2.3 Desmoglein 2, but not Desmocollin 2, protects intestinal epithelia from injury

Desmoglein 2, but not desmocollin 2, protects intestinal epithelia from injury

Annika Gross¹, Lotta A. P. Pack¹, Gabriel M. Schacht¹, Sebastian Kantz², Hanna Ungewiss³, Michael Meir⁴, Nicolas Schlegel⁴, Christian Preisinger⁵, Peter Boor⁶, Nurdan Güldiken¹, Claudia A. Krusche², Gernot Sellge¹, Christian Trautwein¹, Jens Waschke⁴, Arnd Heusers⁸, Rudolf E. Leube², Pavel Strnad¹

Running title: Desmosomal cadherins in the intestine

¹Department of Medicine III and IZKF, University Hospital Aachen, Aachen, Germany

²Institute of Molecular and Cellular Anatomy, RWTH Aachen University, Aachen, Germany

³Institute of Anatomy, Faculty of Medicine, LMU Munich, Munich, Germany

⁴Department of Surgery I, University of Würzburg, Würzburg, Germany

⁵IZKF Proteomics Facility, University Hospital Aachen, Aachen, Germany

⁶Institute of Pathology and Department of Nephrology, University Hospital Aachen, Aachen, Germany

⁸Max-Delbrück-Center of Molecular Medicine, Berlin, Germany

Corresponding author:

Pavel Strnad, MD

Department of Internal Medicine III and IZKF

RWTH Aachen

Pauwelsstraße 30, D-52074 Aachen

Tel.: +49(241) 80-35324

Fax: +49(241) 80-82455

E-mail: pstrnad@ukaachen.de

Disclosures: The authors declare that they do not have any conflict of interest to disclose.

Keywords: desmosome/heat shock protein/apical junctional complex/tight junction/adherens junction

Abbreviations:

β Tub, β -tubulin; AJ, adherens junction; AJC, apical junctional complex; APC, adenomatous polyposis coli; BrdU, 5-bromo-2-deoxyuridine; CD, Crohn's Disease; CFU, colony forming units; *C. rod.*, *Citrobacter rodentium*; Dsc, desmocollin; Dsg, desmoglein; Dsp, desmoplakin; DSS, dextran sodium sulphate; EGFR, epidermal growth factor receptor; FITC, fluorescein isothiocyanate; fl, floxed; Gal3, Galectin 3; H&E, hematoxylin and eosin; Hsp70, heat shock protein 70; IEC, intestinal epithelial cells; IL-1 β , interleukin 1 β ; IL-22, interleukin-22; KO, knockout; LGR5, leucine-rich repeat-containing G-protein coupled receptor 5; K, keratin; LI, large intestine; min, multiple intestinal neoplasia; MLC, myosin II regulatory light chain; MLCK, MLC kinase; MLN, mesenteric lymph node; MPO, myeloperoxidase; mRNA, messenger RNA; PAS, periodic acid-Schiff; PCNA, proliferating-cell-nuclear-antigen; PG, plakoglobin (γ -catenin); Pkp2, plakophilin 2; Rspo1, r-spondin1; RT-PCR, reverse transcriptase polymerase chain reaction; SI, small intestine; STAT3, signal transducer and activator of transcription 3; TJ, tight junction; TNF α , tumor necrosis factor alpha; ZO-1, zonula occludens-1

Abstract:

Desmosomes are the least understood intercellular junctions in the intestinal epithelia and provide cell-cell adhesion via the cadherins desmoglein (Dsg)2 and desmocollin (Dsc)2. We studied these cadherins in Crohn's disease (CD) patients and in newly generated conditional villin-Cre DSG2 and DSC2 knockout mice (DSG2 Δ IEC; DSC2 Δ IEC). CD patients exhibited altered desmosomes and reduced Dsg2/Dsc2 levels. The intestines of both transgenic animal lines were histopathologically inconspicuous. However, DSG2 Δ IEC, but not DSC2 Δ IEC mice displayed an increased intestinal permeability, a wider desmosomal space as well as alterations in desmosomal and tight junction components. After dextran sodium sulfate (DSS)-treatment and *C. rodentium* exposure, DSG2 Δ IEC mice developed a more pronounced colitis, an enhanced intestinal epithelial barrier disruption leading to a stronger inflammation and activation of epithelial pSTAT3 signaling. No susceptibility to DSS-induced intestinal injury was noted in DSC2 Δ IEC animals. Dsg2 interacted with the cytoprotective chaperone Hsp70. Accordingly, DSG2 Δ IEC mice had lower Hsp70 levels in the plasma membrane compartment, whereas DSC2 Δ IEC mice displayed a compensatory recruitment of galectin 3, a junction-tightening protein. Our results demonstrate that Dsg2, but not Dsc2 is required for the integrity of the intestinal epithelial barrier *in vivo*.

Introduction

Epithelial cell layers in general provide an efficient barrier against the hostile environment. The intestinal epithelium has to facilitate both, protection of the underlying tissue from invading microorganisms and efficient uptake of nutrients and solutes. Intercellular junctions constitute a crucial part of this barrier and consist of tight junctions (TJs), adherens junctions (AJs) and desmosomes that together form the apical junctional complex (AJC).¹ TJs are the primary structures sealing the intercellular space. However, pro-inflammatory signaling in epithelial cells alters the TJ composition leading to reduced barrier function, thereby contributing to the pathogenesis of multiple prevalent intestinal disorders such as inflammatory bowel disease, celiac disease or infectious gastroenteritis.^{2,3} This process is driven by molecular remodeling that results in decreased levels of claudin 1 and occludin and increased amounts of claudins 2 and 15.^{1,4} AJs are established mediators of cell-cell adhesion and play an important role in cell polarization and differentiation via the associated Wnt/ β -catenin pathway.¹

Desmosomes represent the least studied AJC component. They are, similar to AJs, important for cell adhesion and cytoskeletal anchorage.⁵ Their importance becomes evident in inherited cardiomyopathies that are caused by mutation in desmosomal genes and blistering skin disorders elicited by desmosomal autoantibodies. Desmosomes are also altered in microbial infections in that their constituents are cleaved by bacterial toxins and become targeted in adenoviral respiratory infections.⁶⁻⁸ Desmosomes bear structural similarities with hemidesmosomes that with the help of integrins connect the cells to the extracellular matrix. The crucial importance of hemidesmosomes was recently demonstrated in mice with intestinal epithelial cell-specific $\alpha 6$ integrin ablation that develop colitis with spontaneous progression into high-grade intestinal carcinoma.⁹

To connect the cells, desmosomes comprise transmembrane proteins termed desmosomal cadherins. These are subdivided into the desmoglein and desmocollin type (gene names: DSGs/DSCs, protein names: Dsgs/Dscs). While homo- and heterophilic interactions between the extracellular Dsg and Dsc domains have been described, the latter are preferred and accordingly, both protein types are needed for cellular adhesion.^{5,10} Dsgs/Dscs are expressed in a cell type-specific pattern with Dsc2 and Dsg2 being the

most wide-spread family members and the major desmosomal cadherins of digestive epithelia.⁶ On the cytoplasmic side, Dsg2/Dsc2 are connected to the armadillo proteins plakoglobin (PG) and plakophilin 2 (Pkp2), which, together with desmoplakin (Dsp), facilitate the attachment to the keratin cytoskeleton.^{5, 6}

Despite their presumed biological importance, only *in vitro* studies addressed the role of desmosomal cadherins in the intestine so far. The data available up to date suggest that although they are both functionally and structurally similar, they also display unique properties.^{6, 11-13} For example, DSG2 knockdown resulted in a compensatory up-regulation of Dsc2, whereas DSC2 loss did not lead to alterations in Dsg2 protein levels.¹⁴ Moreover, Dsg2 but not Dsc2 was cleaved during intestinal epithelial cell apoptosis and DSG2 down-regulation inhibited this cell death pathway.¹⁵ In addition to experimental data pointing towards a functional importance of desmosomes, a selective decrease of Dsg2 was reported in patients with Crohn's disease.¹⁶ In cultured epithelial cells, this down-regulation was associated with increased permeability that was prevented by stabilization of desmosomal adhesion.¹⁶ These disease-related changes coupled with their established *in vitro* biological function as well as the crucial importance of intercellular junctions^{1, 9} prompted us to analyze the *in vivo* properties of desmosomal cadherins in the intestine. To that end, we generated conditional villin-Cre mediated DSG2 knockout and DSC2 knockout (DSG2 Δ IEC/DSC2 Δ IEC) mice and analyzed desmosomal alterations in Crohn's disease patients.

In summary, we demonstrate that intestinal DSG2 but not DSC2 is required for the integrity of the intestinal epithelial barrier *in vivo*. These data might be of human relevance, since Crohn's disease patients display altered desmosomes as well as reduced desmosomal cadherin levels.

Results

Since patients with Crohn's disease were reported to have reduced intestinal Dsg2 levels,¹⁶ we performed transmission electron microscopy that revealed an altered ultrastructure of the apical junctional complex (Suppl. Fig. 1A). In particular, TJs lacked proper membrane annealing, while desmosomes were sometimes missing and/or exhibited irregular or asymmetric plaques with reduced intermediate filament insertion. In contrast, AJ were largely unaltered (Suppl. Fig. 1A). In line with that and previous findings,¹⁶ a significant reduction in both desmosomal cadherins, i.e. Dsg2 and Dsc2, was seen, whereas no obvious alterations were detected in E-cadherin (Suppl. Fig. 1B, C).

Next, we directly addressed the biological relevance of desmosomal cadherins in the newly generated intestinal-specific knockouts. In agreement with previous reports,⁶ Dsg2 and Dsc2 were the only desmosomal cadherins expressed in the mouse intestine (Fig. 1A). Both cadherins were abundantly expressed in the intestine, while lower amounts were seen in other organs such as the kidney (Fig. 1B). The newly generated intestine-specific Dsg2 knockout (DSG2 Δ IEC) displayed a selective and efficient deletion of Dsg2 in both small and large intestine (Fig. 1C, D, Suppl. Fig. 2A-D) and no upregulation of other desmoglein and desmocollin isoforms was observed (Suppl. Fig. 3A). Immunofluorescence staining confirmed the loss of Dsg2 while Dsc2/plakoglobin staining was retained and demonstrated an unaltered desmosome distribution (Fig. 2A). DSG2 Δ IEC mice developed normally, displayed normal weight gain and colon length (Suppl. Fig. 4). No diarrhea was observed. Histological examination revealed a morphologically inconspicuous small and large intestine with correctly differentiated and localized cell types (Fig. 2B, Suppl. Fig. 5A,B and data not shown). Unaltered levels of the stem cell markers LGR5 and R-spondin and no changes in the basal cell proliferation were noted (Suppl. Fig. 5C,D Suppl. Fig. 6). No inflammation was observed at any analyzed time point (Suppl. Fig. 7 and not shown). Electron microscopy revealed largely normal desmosomal plaques whereas the intercellular space between the junctions was significantly wider in the small and large intestine (Fig. 2C, Suppl. Fig. 8). Biochemical analysis illustrated profound changes in other desmosomal components with up-regulation of Dsc2 and down-regulation of Dsp and PG, while the levels of Pkp2 and

keratin 8 (K8) were not altered (Fig. 2D, Suppl. Fig. 9). The same alterations were observed in small and large intestine and the changes likely occurred at the posttranscriptional level since the mRNA expression of all analyzed desmosomal genes was unaltered (Fig. 2E and data not shown). Immunoblotting revealed decreased levels of occludin and claudin 1 that are often reduced in situations leading to barrier dysfunction, while no differences were observed in the tight junction proteins claudin 7 and 15 and the adherens junction protein E-cadherin (Suppl. Fig. 10A). Immunofluorescence staining revealed a normal distribution of tight and adherens junction proteins (Suppl. Fig. 10B). Myosin II regulatory light chain (MLC) phosphorylation, that constitutes a key regulator of tight junction permeability, did not differ between DSG2 Δ IEC and DSG2 fl/fl control mice (Suppl. Fig. 10C). In line with the described changes in epithelial junctions, DSG2 Δ IEC mice had an increased intestinal permeability (Fig. 2F).

Given that DSG2 Δ IEC mice did not show a spontaneous intestinal injury, we tested their susceptibility to DSS colitis. Even at low DSS doses, DSG2 Δ IEC animals developed a profound weight loss with bloody diarrhea and intestinal lesions (Fig. 3A-C). As an additional sign of tissue destruction, DSS-treated DSG2 Δ IEC mice had shorter colons (Fig. 3C). The histological examination revealed a marked epithelial loss with an edema, inflammatory reaction and goblet cell loss that resulted in significantly higher injury scores (Fig. 3D). The pronounced inflammation was confirmed by increased intestinal myeloperoxidase activity as well as by higher pro-inflammatory cytokine levels (Fig. 3E,F). Analysis of mesenteric lymph nodes demonstrated increased bacterial translocation (Fig. 3E).

To further delineate the mechanisms underlying the observed phenotype, we analyzed the effects of short-term DSS administration that led to modest histological changes (Fig. 4A). Compared to controls, DSG2 Δ IEC animals displayed a more profound epithelial cell loss into the intestinal lumen as demonstrated by higher levels of the epithelial marker K8 in the luminal content of the colon and by histological observation (Fig. 4A). In DSG2 Δ IEC mice, DSS treatment resulted in a marked increase in intestinal permeability, while only a moderate DSS effect was seen in DSG2 fl/fl mice (Fig. 2F, 4B). In line with the more pronounced epithelial leakiness, molecular analyses

demonstrated an increased mRNA expression of pro-inflammatory cytokines and an activated IL-22-STAT3 signaling (Fig. 4C-E). Immunostaining revealed that STAT3 was phosphorylated in the epithelial cells and is most likely responsible for the increased production of the antimicrobial peptide RegIII β (Fig. 4D,F). As another consequence of the increased intestinal leakiness, we detected elevated levels of cleaved caspase 1 in DSS-treated DSG2 Δ IEC mice suggesting enhanced inflammasome activation (Fig. 4E).

To test the susceptibility of DSG2 Δ IEC animals to infectious colitis, we exposed mice to the murine pathogen *C. rodentium*. In line with previous reports, the treatment did not lead to weight loss (Suppl. Fig. 11A).¹⁷ During the peak of infection, DSG2 Δ IEC animals displayed higher fecal *C. rodentium* CFU counts, however, both genotypes successfully cleared the infection around day 18 (Suppl. Fig. 11B). Histological analysis demonstrated characteristic epithelial detachment, crypt elongation and hyperproliferation that were more pronounced in DSG2 Δ IEC mice (Fig. 5A,B). The latter was confirmed by increased amounts of Ki-67 positive epithelial cells and higher PCNA expression (Fig. 5B,D, Suppl. Fig. 11C). No significant alterations in the amount of goblet cells were seen (Suppl. Fig. 11D). Among the *C. rodentium*-treated animals, DSG2 Δ IEC mice displayed a stronger inflammatory reaction, higher expression of pro-inflammatory cytokines and a higher epithelial cell stress response with activation of the STAT3 signaling pathway and its antimicrobial product RegIII β (Fig. 5C,D). Immunostaining revealed that STAT3 was phosphorylated to a large extent in epithelial cells (Fig. 5D). In contrast to previous *in vitro* studies,^{18, 19} untreated DSG2 Δ IEC mice displayed no obvious alteration in EGFR and p38 pathways (not shown). On the other hand, exposure of DSG2 Δ IEC mice to DSS or *C. rodentium* resulted in diminished EGFR and p38 levels (Suppl. Fig. 12A,B).

To better understand the biological significance of desmosomal cadherins, we also assessed the role of Dsc2. Similarly to DSG2 Δ IEC mice, DSC2 Δ IEC mice developed normally (Suppl. Figs. 13). Unlike in DSG2-deficient mice, no profound changes in other desmosomal or TJ components were observed (Fig. 6A,B, Suppl. Figs. 14) and plakoglobin immunofluorescence revealed an unaltered desmosomal distribution (Fig. 6B). Additionally, no upregulation of other desmocollin and desmoglein isoforms was noticed (Suppl. Fig. 15). Electron microscopy indicated a normal desmosomal ultrastructure (Fig. 6C). In line with that, DSC2 Δ IEC mice showed no alteration in

intestinal permeability (Fig. 6D). A morphologically inconspicuous small and large intestine with properly localized cell types was noted (Fig. 7A, Suppl. Fig. 16). In particular, the amount of goblet cells did not differ between DSC2 Δ IEC and DSC2 Δ / Δ mice (Suppl. Fig. 16). Moreover, in both genotypes, treatment with 2.4% DSS resulted in a comparable weight loss and a similar histological injury (Fig. 7A,B). In line with that, comparable levels of pro-inflammatory cytokines and antimicrobial peptides were noted (Fig. 7C and data not shown). To identify the mechanisms responsible for the different biological impact of DSG2 vs. DSC2 loss, we collected plasma membrane protein fractions. These identified reduced amounts of the cytoprotective chaperone Hsp70 in DSG2 Δ IEC but not DSC2 Δ IEC animals, while the established Dsg2-interacting protein Galectin 3₂₀ was enriched in the plasma membrane fractions of Dsc2-deficient, but not Dsg2-deficient animals (Fig. 7D). As a potential molecular explanation, Hsp70 co-immunoprecipitated with Dsg2 but not with Dsc2 (Fig. 7E and data not shown).

To further understand the ability of Dsg2/Dsc2 to compensate for the loss of its counterpart, we examined colorectal adenocarcinoma DLD1 cells lacking either one or both desmosomal cadherins.^{18, 21} Immunofluorescence and immunoblotting confirmed the knockout of both cadherins as well as a complete re-expression of full-length Dsc2 (FL Dsc2) in the double-knockout line (Suppl. Figure 17A,C). A simultaneous knockout of both cadherins resulted in a marked loss of membranous Dsp/PG staining, that was maintained in the lines lacking only one cadherin (Suppl. Figure 17B). Immunoblotting demonstrated that the altered Dsp staining pattern is not due to altered protein levels (Suppl. Figure 17C). With regard to functional properties, a knockdown of both cadherins resulted in a stronger decrease in the transepithelial electrical resistance (TER) than the loss of Dsc2 only, while a re-expression of Dsc2 was not sufficient to rescue the TER phenotype of double-knockout cells (Suppl. Figure 17D).

In summary, our findings uncover the differential biological relevance of the desmosomal cadherins Dsg2 and Dsc2 that are both reduced in the human intestinal injury (Fig. 1B, Fig. 7F).

Discussion

Our study analyzed the *in vivo* biological role of desmosomal cadherins in the intestine. We showed that desmosomal alterations as well as loss of Dsg2/Dsc2 occur in patients with Crohn's disease. Since these patients display a strong activation of TNF α signaling,²² our data are in line with previous findings implicating TNF α in the loss of Dsg2 signal.¹⁶ In that respect, the regulation of Dsg2 is reminiscent of the regulation of TJ proteins, which undergo a strong inflammation-induced remodeling.^{1,3,4} On the other hand, E-cadherin as a key component of adherens junctions remained unaltered in all conditions.

With regard to the biological importance of the desmosomal cadherins, DSG2 Δ IEC and DSC2 Δ IEC mice displayed morphologically normal desmosomes. In case of DSG2 Δ IEC animals, this is not surprising since previous reports demonstrated that Dsg2 is not essential for desmosomal assembly.^{23, 24} On the other hand, the previous data on Dsc2 were somewhat contradictory. It was reported to be indispensable for desmosomal assembly in an *in vitro* study,²⁴ however, Dsc2 knockdown in cancer cell lines did not result in altered Dsg2 levels.¹⁴ In addition to normal appearing desmosomes, neither DSG2 Δ IEC nor DSC2 Δ IEC animals show an obvious epithelial injury under basal conditions. This is in line with the intestinal desmoplakin KOs, that do not exhibit an obvious pathology either.²⁵ In contrast, cardiomyocyte-specific DSG2 ablation resulted in spontaneous arrhythmogenic cardiomyopathy²³ whereas deletion/mutation of other desmosomal cadherins led to defects in oral epithelia, skin and hair follicles.²⁶ Collectively, these data suggest that desmosomal cadherins are essential for integrity of mechanically challenged tissues, but are more dispensable in single-layered epithelia.

While untreated mice displayed no obvious phenotype, altered desmosomal and TJ protein composition, wider desmosomal space and increased intercellular permeability were noted in DSG2 Δ IEC but not DSC2 Δ IEC mice (Figure 7F). With regard to the desmosomal composition and permeability, our data are consistent with Dsg2/Dsc2 knockdowns performed in cancer cell lines and suggest that Dsg2 loss has a more profound impact on intercellular junctions than Dsc2 ablation.^{18, 19, 23} A potential explanation is that homophilic Dsg2 bonds, but not Dsc2 bonds are able to at least

partially compensate the ablation of the partner protein. In support of the latter, cell lines that lacked both Dsg2 and Dsc2 displayed similar TER as cells lacking Dsg2 only (Suppl. Figure 17D). Notably, although homophilic interactions of cadherins occur in epithelial cells, formation of heterophilic Dsg-Dsc interactions is preferred.^{10, 27} In addition to the strength of homophilic complexes, interactions with associated proteins might be also responsible for the differences between DSG2 Δ IEC and DSC2 Δ IEC mice. In particular, Hsp70 was found to interact with Dsg2 but not Dsc2 and accordingly, Dsg2 Δ IEC mice displayed lower Hsp70 levels in their plasma membrane protein fractions. This finding is intriguing since Hsp70 is an established stress-protective protein that ameliorates the development of intestinal injury^{28, 29} and is known to interact with keratins, i.e. structures that are functionally tightly linked to desmosomes.^{30, 31} However, further studies are needed to delineate the functional importance of the diminished Hsp70 levels in Dsg2 Δ IEC mice.

On the other hand, DSC2 Δ IEC mice (but not DSG2 Δ IEC mice) displayed an accumulation of galectin 3 in their plasma membrane fractions. Of note, galectin 3 constitutes an established Dsg2-binding protein and an important mediator of adhesive strength.²⁰ Therefore, a perturbation in Hsp70 might account for the phenotype seen in DSG2 Δ IEC mice, whereas galectin 3 may functionally compensate for the Dsc2 loss (Figure 7F). The reduced p38 levels seen in DSG2 Δ IEC mice exposed to DSS or *C. rodentium* might be also of importance, since p38 in intestinal epithelia protects from colitis development.³²

While the moderate impairment of intestinal barrier seen in untreated DSG2 Δ IEC mice is not sufficient to induce epithelial injury, it becomes more evident in the analyzed stress models. Two key events likely contribute to this finding: (i) inflammatory cytokines, in particularly TNF α , that are induced in the stress models,^{33, 34} further weaken the desmosomal adhesion,¹⁶ (ii) the injuries increase the leakiness of TJs that are known to constitute the major component of the intestinal barrier. The weakening of TJs is both a direct effect of an exposure to DSS/*C. rodentium* as well as a consequence of the resulting inflammatory reaction.^{1, 3, 4, 35-37} Moreover, our findings indicate that Dsg2 ablation promotes TJ leakiness by decreasing the levels of tightening TJ components. This is supported by previous in vitro studies in which loss of Dsg2-mediated adhesion led to disruption of TJ integrity.^{15, 38} Consequently, peptides strengthening desmosomal

adhesion may present a viable therapeutic strategy in situations with impaired desmosomes.¹⁶

The above described loss of epithelial barrier resulted in stronger bacterial translocation that induced the observed intestinal inflammation (Figure 7F). Two classic inflammatory pathways have been prominently activated: (i) production of pro-inflammatory cytokines IL-1 β and TNF α ; (ii) activation of IL-22-pSTAT3 signaling. IL-1 β /TNF α are known to be produced as a direct reaction to microbial components.^{39, 40} Their increased levels likely contribute to the stronger epithelial loss seen after DSS treatment thereby leading to a vicious cycle of inflammation and epithelial injury (Figure 7C).^{40, 41} On the other hand, IL-22 belongs to anti-inflammatory cytokines that protect from development of colitis in several models.^{40, 42, 43} It stimulates, via STAT3 activation, epithelial cell proliferation and regeneration and likely contributes to the hyperplasia that was observed in the *Citrobacter rodentium* model. Since both signaling pathways become activated as a consequence of increased epithelial permeability after Dsg2 loss, the balance between IL-1 β /TNF α and IL-22-pSTAT3 activation presumably dictates, whether DSG2 Δ IEC animals will display increased epithelial loss (as seen in the DSS model) or increased regeneration (*Citrobacter* model).

In summary, our findings reveal desmosomal alterations in patients with Crohn's disease and demonstrate the differential importance of the desmosomal cadherins Dsg2/Dsc2 for the desmosomal structure and susceptibility to intestinal injury (Figure 7F). Given that a TJ stabilizing agent showed promise in a clinical trial of celiac disease,⁴⁴ further studies are warranted to explore the therapeutic potential of desmosome-stabilizing peptides.¹⁶

Materials and Methods

Mouse experiments

Mice with conditional (intestine-specific) Desmoglein 2 (Dsg2) or Desmocollin 2 deletion were generated by crossing previously described DSG2 exon4/5 floxed (DSG2^{fl/fl}) and DSC2 exon2 floxed (DSC2^{fl/fl}) mice with mice expressing Cre under the control of the villin promotor (DSG2^{ΔIEC}/DSC2^{ΔIEC}).^{23, 45-47} All mice were on C57BL/6 background and kept under standardized conditions (12 hours day/night cycle, 21-24°C, humidity ~50%) with free access to food and water. To induce colitis, 10 weeks old sex-matched mice were exposed to dextran sodium sulfate (DSS, MP Biochemicals, Heidelberg, Germany) in the drinking water and sacrificed after four days (short-term DSS). Alternatively, DSS was administered for five days with a change to normal water afterwards and killing of animals at day 7 (long-term DSS). For DSG2^{ΔIEC} and DSC2^{ΔIEC} mice, we used 1.6% and 2.4% DSS, respectively. For an infectious model, *Citrobacter rodentium* strain DBS100⁴⁸ was grown in Luria-Bertani (LB) medium at 37 °C overnight by shaking (200 rpm). 9-10 weeks old sex-matched mice were infected by oral gavage with 1x10⁹ *C. rodentium* and analyzed 14 or 21 days thereafter. At indicated time points, stool was collected, homogenized in sterile phosphate buffered saline (PBS) (Digital Disruptor Genie, Scientific industries, New York, US) and plated in serial dilutions on MacConkey agar plates (Roth, Karlsruhe, Germany) to count colony forming units (CFU) of *Citrobacter rodentium*. Untreated, age- and sex-matched littermates were used as controls.

To examine intestinal permeability, mice were fasted for three hours and gavaged with 0.6 mg/g of body weight 4kD FITC-labelled dextran (Sigma-Aldrich, Steinheim, Germany). Four hours later, blood was collected retroorbitally and the fluorescence intensity in serum was measured (excitation: 492 nm; emission: 525 nm, Cytation3 imaging reader, BioTek, Bad Friedrichshall, Germany). The samples were prepared in duplicates and the results calculated according to the standard curve. All animals were weighted and sacrificed by an isoflurane overdose. In selected animals, the distal colon was analyzed via a mini-endoscope (Karl Storz, Tuttlingen, Germany). Rectal bleeding was examined using commercial hemoCARE fecal occult blood Guajak test using a

semi-quantitative scoring from 0 to 3 (0: no bleeding, 1: mild bleeding, 2: moderate bleeding, 3: severe bleeding). Mesenteric lymph nodes were dissected and homogenates were plated on Columbia sheep blood agar plates (Oxoid/Thermo Scientific, Munich, Germany) to evaluate the translocation of bacteria into the lymph nodes. Proximal intestinal parts were washed and stored as Swiss rolls in 4% formaldehyde for histological evaluation or embedded in O.C.T. compound (Tissue-Tek, Sakura, Staufen, Germany) for cryosectioning. Distal parts were washed and snap frozen in liquid nitrogen for biochemical and RNA analysis.

Human samples

As described in detail previously,³⁸ human specimens were obtained from terminal ileum of patients who suffered from refractory Crohn's Disease (CD) and/or had a complication that required surgical resection, such as stenosis, fistula, or abscesses. Control tissue samples of the terminal ileum were from patients that required right hemicolectomy in which the surgical resection routinely involves a part of the healthy small intestine (for further information see Suppl. table 1). For Western blot analyses, mucosa was mechanically dissected from the tissue immediately after the resection and transferred into lysis buffer containing 25 mmol/L HEPES, 2 mmol/L EDTA, 25 mmol/L NaF, and 1% sodium dodecyl sulfate. Specimens were homogenized with TissueLyzer (Qiagen, Hilden, Germany) and normalized with BCA assay (Thermo Fisher, Waltham, MA). Anti-Dsg2 (Invitrogen, Carlsbad, CA), anti-Dsc2 (Abcam, Cambridge, UK) and anti E-cadherin (BD Biosciences, Franklin Lakes, NJ) primary antibodies were combined with a horseradish peroxidase-labeled goat anti-mouse antibody (Dianova, Hamburg, Germany).

A second part of the tissue samples was fixed in 4% paraformaldehyde, embedded in paraffin and cut into 1 μ m thick sections. Immunostaining was performed as described previously⁴⁹ using rabbit anti-Dsg2 (Invitrogen), anti-Dsc2 (Abcam) and mouse anti-E-cadherin (BD Biosciences) antibodies in combination with a Cy3-labeled goat anti-mouse- and a Cy2-labeled goat anti-rabbit antibody (Both Dianova, Hamburg, Germany). To analyze the tissue architecture, all specimens were stained with Hematoxylin and Eosin (H&E).

Cell culture experiments

For the described experiments, we used previously published DLD1 cells with CRISPR/Cas9-mediated knockdown of Dsc2 (Δ Dsc2) or both desmosomal cadherins (Δ Dsg2 Δ Dsc2), as well as a cell line in that the knockout of both cadherins was followed by a re-expression of Dsc2 (Δ Dsg2 Δ Dsc2 + FL Dsc2).²¹ The cells were cultured in Dulbecco's modified Eagle's medium (Life Technologies, Carlsbad, CA) containing 10% fetal bovine serum (Biochrom, Berlin, Germany), 50 U/ml penicillin and 50 U/ml streptomycin (AppliChem, Darmstadt, Germany) in 5% CO₂ atmosphere at 37°C until they reached confluence.¹⁸

Biochemical methods

Total tissue lysates were prepared by homogenization of tissues in 3% SDS-containing buffer with protease and phosphatase inhibitors. To determine luminal protein composition, colon was removed, opened longitudinally and vigorously inverted fifteen times in PBS. The solution containing epithelial cells was centrifuged at 5000 rpm for 10 minutes at 4°C and the pellet was used for homogenization. DLD1 cells were grown in 24-well plates and lysed using 1% SDS lysis buffer supplemented with a protease-inhibitor cocktail (Roche, Mannheim, Germany). Same amounts of proteins were separated by SDS-polyacrylamide gel electrophoresis (SDS-PAGE) followed by transfer to PVDF/nitrocellulose membranes or staining with 0.1% Coomassie Brilliant Blue G-250. The membranes were incubated with specific primary and HRP-coupled secondary antibodies, which were then visualized by an enhanced chemiluminescence detection kit (GE Healthcare/Amersham Biosciences, UK). The antibodies used in this study are summarized in Suppl. table 3.

To determine myeloperoxidase (MPO) activity, colonic tissue was homogenized in ice-cold 50 mM potassium phosphate buffer containing 0.5% hexadecyltrimethylammonium bromide. Equal volume of cell lysis buffer was added and the homogenates were freeze-thawed twice. After centrifugation, supernatant was removed and supplemented with reaction buffer (with *o*-dianisidine hydrochloride and 0.001% H₂O₂) or standard solution. After three minutes of reaction time, the absorbance was spectrophotometrically measured at 450 nm (Cytation3 imaging reader). The

samples were prepared in duplicates and the results were calculated according to the standards.

Plasma membrane protein fractions from colon scrapings were extracted according to the manufacturer's protocol (Abcam, ab65400). Briefly, scrapings were homogenized in an appropriate volume of homogenization buffer containing protease inhibitor cocktail. Following centrifugation, the pellet that contains plasma membrane proteins was re-suspended in the provided upper phase solution. Plasma membrane proteins were purified by repeated addition of lower phase solution that was later on removed by centrifugation at low speed. Finally, the plasma membrane proteins were pelleted via high-speed centrifugation at +4°C. The membrane fraction was dissolved in 0.5% Triton-X-100/PBS that was supplemented with Laemmli buffer (0.2 M Tris pH 6.8, 40% glycerol, 8% sodium dodecyl sulfate, 7.2% β -mercaptoethanol, 0.02% bromophenol blue).

Immunoprecipitation

Total lysates were prepared by homogenization of colon scrapings in RIPA buffer (2.5 mM Tris-HCl pH 7.4, 0.025% sodium deoxycholate, 150 mM NaCl, 2 mM EDTA, 0.01% NP-40). After conjugation of Dsc2 or Dsg2 antibody to Protein G Dynabeads (Thermo Fisher) for 10 minutes, the lysates were added to the beads-antibody complex and the solution was incubated upon a gentle rotation for 2 hours at +4°C. A magnet was used to collect the beads that were washed three times with a supplied washing buffer. The supernatant was discarded, the proteins were eluted via heating in SDS-containing Laemmli buffer for 5 minutes at 95°C and further analysed by SDS-PAGE.

Histological analysis

The formaldehyde-fixed tissues were paraffin-embedded, cut into 3 μ m thick sections and stained with H&E or periodic acid-Schiff (PAS). For the latter, deparaffinized slides were oxidized in 2% periodic acid solution for 5 minutes. After washing in distilled water, a staining with Schiff reagent for 15 minutes was performed and followed by hematoxylin counterstaining. Finally, the sections were blued in 1M Tris buffer (pH 8). Images were recorded with a Zeiss light microscope (Zeiss, Germany) and AxioVision

Rel 4.8 software (Zeiss, Germany). PAS-positive cells were counted as a mean from at least thirty different crypts by ImageJ software.

A previously described semi-quantitative histopathological score⁵⁰ with minor modifications was used for evaluation of DSS-treated samples. The following parameters were assessed: (i) submucosa thickening/edema, (ii) inflammatory cell infiltration, (iii) goblet cell loss (each parameter with a score 0-3: 0: normal; 1: mild; 2: moderate; 3: severe), (iv) epithelial damage/erosion (0: normal; 2: <1/3 of total area with altered epithelial cell morphology; 4: >1/3 of total area with altered epithelial cell morphology and/or mild erosions; 6: <10% of ulcerative areas; 8: 10-20% of ulcerative areas, 10: >20% of ulcerative areas).

The *C. rodentium* exposed colons were semi-quantitatively scored. Following criteria were assessed: (i) epithelial detachment (0: normal, 0,5: low, 1: high); (ii) hyperplasia (0: normal, 1: low hyperplasia, 2: high hyperplasia); (iii) inflammation (0: normal, 1: moderate, 2: severe). Lengths of colonic crypts were measured in longitudinal orientation. At least 10 crypts per mouse were analysed and the results are presented as means. All analyses were performed in a blinded manner by AG and an experienced pathologist (PB).

Study approval

The animal experiments were approved by the state of North Rhine-Westphalia in Germany and the University of Aachen animal care committee and were conducted in compliance with the German Law for Welfare of Laboratory Animals. All CD patients had given their informed consent before surgery, and the study was approved by the Ethical Board of the University of Würzburg (proposal numbers 113/13 and 46/11).

Data analysis and statistical methods

Image quantifications were performed with ImageJ (National Institutes of Health, Bethesda, USA). Data were analyzed with an unpaired two-tailed Student's t-test or Mann-Whitney test where appropriate. P-values below 0.05 were considered as statistically significant.

For additional materials, see supplementary section.

Acknowledgements:

We are thankful to Adam Breitscheidel for his assistance with figure preparation. The expert technical assistance of Linda Schaub, Ingrid Breuer, Silvia Roubrocks, Ana Mandić, Sandra Jumpertz, Sabine Eisner and Silvia Koch is gratefully acknowledged. Our work was supported by a grant from the Interdisciplinary Centre for Clinical Research (IZKF) within the faculty of Medicine at the RWTH Aachen University, by Else Kröner Exzellenzstipendium (to P.S.), by the Deutsche Forschungsgemeinschaft (DFG) SFB TRR57 (to PS, PB and CT) and by the German Federal Ministry of Education and Research (BMBF01GM1518A to PB). The research on epithelial junctions is supported by the DFG Priority Program SPP 1782 to NS, PS, RL and JW.

Author contributions

Study was planned and designed by AG, REL, PS and the acquisition of data was performed by AG, LAPP, GMS, MM, PB, HU, CP. Analysis and interpretation of data were conducted by AG, NS, PB, GS, REL, JW, PS, CP. AG and PS drafted the manuscript and all authors contributed to the critical revision of the manuscript for important intellectual content. Statistical analysis was performed by AG and PS, who also obtained the funding and supervised the study. SK, CAK, GS, CT, REL, NG, AH provided technical or material support.

References:

1. Turner JR. Intestinal mucosal barrier function in health and disease. *Nature reviews Immunology* 2009; **9**(11): 799-809.
2. Barmeyer C, Schulzke JD, Fromm M. Claudin-related intestinal diseases. *Seminars in cell & developmental biology* 2015; **42**: 30-38.
3. Turner JR, Buschmann MM, Romero-Calvo I, Sailer A, Shen L. The role of molecular remodeling in differential regulation of tight junction permeability. *Seminars in cell & developmental biology* 2014; **36**: 204-212.
4. Capaldo CT, Nusrat A. Claudin switching: Physiological plasticity of the Tight Junction. *Semin Cell Dev Biol* 2015; **42**: 22-29.
5. Nekrasova O, Green KJ. Desmosome assembly and dynamics. *Trends in cell biology* 2013; **23**(11): 537-546.
6. Holthofer B, Windoffer R, Troyanovsky S, Leube RE. Structure and function of desmosomes. *International review of cytology* 2007; **264**: 65-163.
7. Wang H, Li ZY, Liu Y, Persson J, Beyer I, Moller T *et al.* Desmoglein 2 is a receptor for adenovirus serotypes 3, 7, 11 and 14. *Nature medicine* 2011; **17**(1): 96-104.
8. Brooke MA, Nitoiu D, Kelsell DP. Cell-cell connectivity: desmosomes and disease. *J Pathol* 2012; **226**(2): 158-171.
9. De Arcangelis A, Hamade H, Alpy F, Normand S, Bruyere E, Lefebvre O *et al.* Hemidesmosome integrity protects the colon against colitis and colorectal cancer. *Gut* 2016.
10. Harrison OJ, Brasch J, Lasso G, Katsamba PS, Ahlsen G, Honig B *et al.* Structural basis of adhesive binding by desmocollins and desmogleins. *Proceedings of the National Academy of Sciences of the United States of America* 2016; **113**(26): 7160-7165.
11. Garrod D, Chidgey M. Desmosome structure, composition and function. *Biochimica et biophysica acta* 2008; **1778**(3): 572-587.
12. Delva E, Tucker DK, Kowalczyk AP. The desmosome. *Cold Spring Harbor perspectives in biology* 2009; **1**(2): a002543.
13. Kowalczyk AP, Green KJ. Structure, function, and regulation of desmosomes. *Progress in molecular biology and translational science* 2013; **116**: 95-118.
14. Kolegraff K, Nava P, Helms MN, Parkos CA, Nusrat A. Loss of desmocollin-2 confers a tumorigenic phenotype to colonic epithelial cells through activation of Akt/beta-catenin signaling. *Molecular biology of the cell* 2011; **22**(8): 1121-1134.
15. Nava P, Laukoetter MG, Hopkins AM, Laur O, Gerner-Smidt K, Green KJ *et al.* Desmoglein-2: a novel regulator of apoptosis in the intestinal epithelium. *Molecular biology of the cell* 2007; **18**(11): 4565-4578.
16. Spindler V, Meir M, Vigh B, Flemming S, Hutz K, Germer CT *et al.* Loss of Desmoglein 2 Contributes to the Pathogenesis of Crohn's Disease. *Inflammatory bowel diseases* 2015; **21**(10): 2349-2359.
17. Raczynski AR, Muthupalani S, Schlieper K, Fox JG, Tannenbaum SR, Schauer DB. Enteric infection with *Citrobacter rodentium* induces coagulative liver necrosis and hepatic inflammation prior to peak infection and colonic disease. *PloS one* 2012; **7**(3): e33099.
18. Ungewiss H, Vielmuth F, Suzuki ST, Maiser A, Harz H, Leonhardt H *et al.* Desmoglein 2 regulates the intestinal epithelial barrier via p38 mitogen-activated protein kinase. *Scientific reports* 2017; **7**(1): 6329.
19. Kamekura R, Kolegraff KN, Nava P, Hilgarth RS, Feng M, Parkos CA *et al.* Loss of the desmosomal cadherin desmoglein-2 suppresses colon cancer cell proliferation through EGFR signaling. *Oncogene* 2014; **33**(36): 4531-4536.
20. Jiang K, Rankin CR, Nava P, Sumagin R, Kamekura R, Stowell SR *et al.* Galectin-3 regulates desmoglein-2 and intestinal epithelial intercellular adhesion. *The Journal of biological chemistry* 2014; **289**(15): 10510-10517.
21. Fujiwara M, Nagatomo A, Tsuda M, Obata S, Sakuma T, Yamamoto T *et al.* Desmocollin-2 alone forms functional desmosomal plaques, with the plaque formation

- requiring the juxtamembrane region and plakophilins. *Journal of biochemistry* 2015; **158**(4): 339-353.
22. Atreya R, Neumann H, Neufert C, Waldner MJ, Billmeier U, Zopf Y *et al.* In vivo imaging using fluorescent antibodies to tumor necrosis factor predicts therapeutic response in Crohn's disease. *Nature medicine* 2014; **20**(3): 313-318.
23. Kant S, Holthofer B, Magin TM, Krusche CA, Leube RE. Desmoglein 2-Dependent Arrhythmogenic Cardiomyopathy Is Caused by a Loss of Adhesive Function. *Circulation Cardiovascular genetics* 2015; **8**(4): 553-563.
24. Lowndes M, Rakshit S, Shafraz O, Borghi N, Harmon RM, Green KJ *et al.* Different roles of cadherins in the assembly and structural integrity of the desmosome complex. *Journal of cell science* 2014; **127**(Pt 10): 2339-2350.
25. Sumigray KD, Lechler T. Desmoplakin controls microvilli length but not cell adhesion or keratin organization in the intestinal epithelium. *Molecular biology of the cell* 2012; **23**(5): 792-799.
26. Thomason HA, Scothern A, McHarg S, Garrod DR. Desmosomes: adhesive strength and signalling in health and disease. *The Biochemical journal* 2010; **429**(3): 419-433.
27. Nie Z, Merritt A, Rouhi-Parkouhi M, Tabernero L, Garrod D. Membrane-impermeable cross-linking provides evidence for homophilic, isoform-specific binding of desmosomal cadherins in epithelial cells. *The Journal of biological chemistry* 2011; **286**(3): 2143-2154.
28. Samborski P, Grzymislowski M. The Role of HSP70 Heat Shock Proteins in the Pathogenesis and Treatment of Inflammatory Bowel Diseases. *Advances in clinical and experimental medicine : official organ Wroclaw Medical University* 2015; **24**(3): 525-530.
29. Tanaka K, Namba T, Arai Y, Fujimoto M, Adachi H, Sobue G *et al.* Genetic evidence for a protective role for heat shock factor 1 and heat shock protein 70 against colitis. *The Journal of biological chemistry* 2007; **282**(32): 23240-23252.
30. Osmani N, Labouesse M. Remodeling of keratin-coupled cell adhesion complexes. *Current opinion in cell biology* 2015; **32**: 30-38.
31. Hatzfeld M, Keil R, Magin TM. Desmosomes and Intermediate Filaments: Their Consequences for Tissue Mechanics. *Cold Spring Harbor perspectives in biology* 2017; **9**(6).
32. Otsuka M, Kang YJ, Ren J, Jiang H, Wang Y, Omata M *et al.* Distinct effects of p38alpha deletion in myeloid lineage and gut epithelia in mouse models of inflammatory bowel disease. *Gastroenterology* 2010; **138**(4): 1255-1265, 1265 e1251-1259.
33. Kojouharoff G, Hans W, Obermeier F, Mannel DN, Andus T, Scholmerich J *et al.* Neutralization of tumour necrosis factor (TNF) but not of IL-1 reduces inflammation in chronic dextran sulphate sodium-induced colitis in mice. *Clin Exp Immunol* 1997; **107**(2): 353-358.
34. Goncalves NS, Ghaem-Maghami M, Monteleone G, Frankel G, Dougan G, Lewis DJ *et al.* Critical role for tumor necrosis factor alpha in controlling the number of luminal pathogenic bacteria and immunopathology in infectious colitis. *Infection and immunity* 2001; **69**(11): 6651-6659.
35. Poritz LS, Garver KI, Green C, Fitzpatrick L, Ruggiero F, Koltun WA. Loss of the tight junction protein ZO-1 in dextran sulfate sodium induced colitis. *The Journal of surgical research* 2007; **140**(1): 12-19.
36. Flynn AN, Buret AG. Tight junctional disruption and apoptosis in an in vitro model of *Citrobacter rodentium* infection. *Microb Pathog* 2008; **45**(2): 98-104.
37. Nighot P, Al-Sadi R, Rawat M, Guo S, Watterson DM, Ma T. Matrix metalloproteinase 9-induced increase in intestinal epithelial tight junction permeability contributes to the severity of experimental DSS colitis. *American journal of physiology Gastrointestinal and liver physiology* 2015; **309**(12): G988-997.
38. Schlegel N, Meir M, Heupel WM, Holthofer B, Leube RE, Waschke J. Desmoglein 2-mediated adhesion is required for intestinal epithelial barrier integrity. *American journal of physiology Gastrointestinal and liver physiology* 2010; **298**(5): G774-783.

39. Kontoyiannis D, Pasparakis M, Pizarro TT, Cominelli F, Kollias G. Impaired on/off regulation of TNF biosynthesis in mice lacking TNF AU-rich elements: implications for joint and gut-associated immunopathologies. *Immunity* 1999; **10**(3): 387-398.
40. Neurath MF. Cytokines in inflammatory bowel disease. *Nature reviews Immunology* 2014; **14**(5): 329-342.
41. Carvalho FA, Nalbantoglu I, Ortega-Fernandez S, Aitken JD, Su Y, Koren O *et al.* Interleukin-1beta (IL-1beta) promotes susceptibility of Toll-like receptor 5 (TLR5) deficient mice to colitis. *Gut* 2012; **61**(3): 373-384.
42. Sabat R, Ouyang W, Wolk K. Therapeutic opportunities of the IL-22-IL-22R1 system. *Nature reviews Drug discovery* 2014; **13**(1): 21-38.
43. Pickert G, Neufert C, Leppkes M, Zheng Y, Wittkopf N, Warntjen M *et al.* STAT3 links IL-22 signaling in intestinal epithelial cells to mucosal wound healing. *The Journal of experimental medicine* 2009; **206**(7): 1465-1472.
44. Leffler DA, Kelly CP, Green PH, Fedorak RN, DiMarino A, Perrow W *et al.* Larazotide acetate for persistent symptoms of celiac disease despite a gluten-free diet: a randomized controlled trial. *Gastroenterology* 2015; **148**(7): 1311-1319 e1316.
45. el Marjou F, Janssen KP, Chang BH, Li M, Hindie V, Chan L *et al.* Tissue-specific and inducible Cre-mediated recombination in the gut epithelium. *Genesis* 2004; **39**(3): 186-193.
46. Madison BB, Dunbar L, Qiao XT, Braunstein K, Braunstein E, Gumucio DL. Cis elements of the villin gene control expression in restricted domains of the vertical (crypt) and horizontal (duodenum, cecum) axes of the intestine. *The Journal of biological chemistry* 2002; **277**(36): 33275-33283.
47. Rimpler U. Funktionelle Charakterisierung von Desmocollin 2 während der Embryonalentwicklung und im adulten Herzen in der Maus 2014.
48. Schauer DB, Falkow S. The eae gene of *Citrobacter freundii* biotype 4280 is necessary for colonization in transmissible murine colonic hyperplasia. *Infection and immunity* 1993; **61**(11): 4654-4661.
49. Meir M, Flemming S, Burkard N, Bergauer L, Metzger M, Germer CT *et al.* Glial cell line-derived neurotrophic factor promotes barrier maturation and wound healing in intestinal epithelial cells in vitro. *American journal of physiology Gastrointestinal and liver physiology* 2015; **309**(8): G613-624.
50. Chinen T, Komai K, Muto G, Morita R, Inoue N, Yoshida H *et al.* Prostaglandin E2 and SOCS1 have a role in intestinal immune tolerance. *Nature communications* 2011; **2**: 190.

Gross et al., Fig. 1

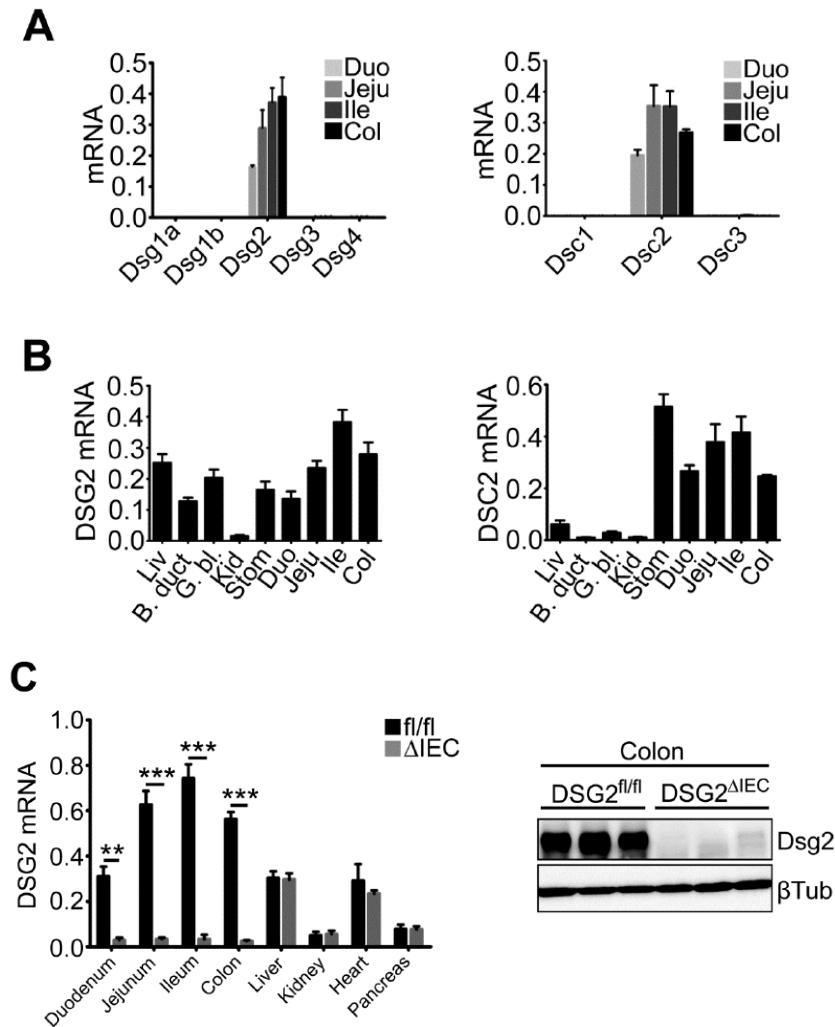


Figure 1. Dsg2 and Dsc2 are the major cadherins expressed in the intestine and DSG2-deficient animals (DSG2 Δ IEC) display an intestine-specific Dsg2 loss.

(A,B) Expression levels of DSG2, DSC2 as well as the other desmoglein and desmocollin family members were assessed by real time RT-PCR in the indicated mouse organs (n=4-5). (C) DSG2 mRNA expression was quantified in the highlighted mouse organs of DSG2 Δ IEC (Δ IEC) and DSG2^{fl/fl} (fl/fl) mice (n=4) by real time RT-PCR. Colonic desmoglein 2 (Dsg2) protein levels were assessed in both groups by immunoblotting (n=5). L7 (mouse ribosomal protein) gene and β -tubulin (β Tub) were used as an internal and a loading control, respectively. Dsg, desmoglein; Dsc, desmocollin; Liv, liver; B. duct, common bile duct; G.bl, gallbladder; Kid, kidney; Stom, stomach; Duo, duodenum; Jeju, jejunum; Ile, ileum; Col, colon. Two-tailed Student's t test was used for statistical analyses. **p<0.01, ***p<0.001.

Gross et al., Fig. 2

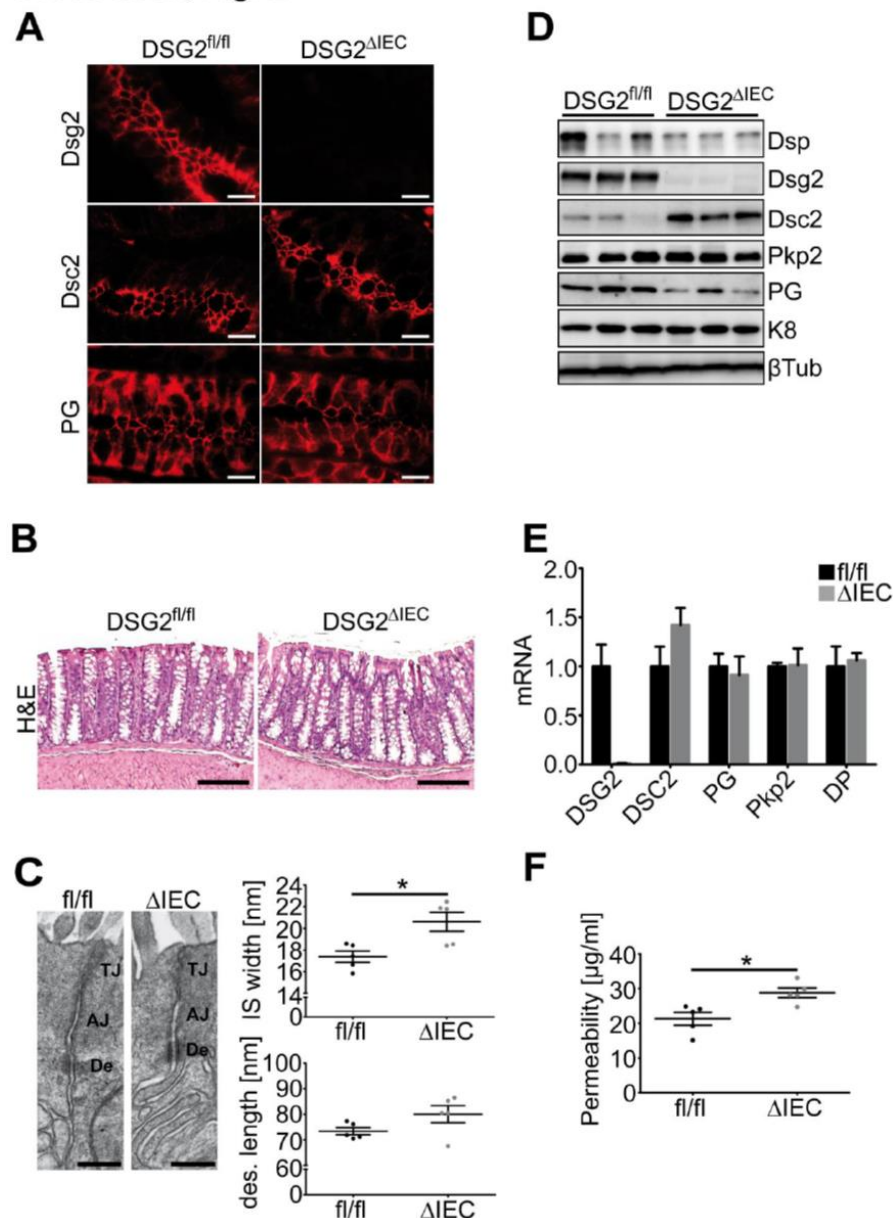


Figure 2. DSG2-deficient animals ($DSG2^{\Delta IEC}$) display an altered desmosomal protein composition, a wider desmosomal space width and increased intestinal permeability. (A) The distribution of Dsc2, plakoglobin (PG) and Dsg2 in the colon of $DSG2^{\Delta IEC}$ (ΔIEC) and $DSG2^{fl/fl}$ (fl/fl) mice was visualized by immunofluorescence. Scale bar = 20 μ m. (B) Hematoxylin and eosin (H&E) staining revealed an unperturbed overall colon architecture. (C) Desmosomal ultrastructure of colon samples was assessed by electron microscopy with subsequent quantification of the desmosomal intercellular space (IS) width and length of the desmosomal plaque (n=5). Scale bar = 200 nm. AJ, adherens junctions; De, desmosomes; TJ, tight junctions (D,E) Immunoblotting and

RT-PCR were employed to study the impact of Dsg2 loss on desmosomal composition in the colon (n=5). Dsc2, desmocollin 2; Dsp, desmoplakin; Pkp2, plakophilin 2; K8, keratin 8. (F) Administration of 4kD FITC-dextran with subsequent quantification of serum FITC levels was utilized as a measurement of intestinal permeability (n=5). Average mRNA expression in DSG2^{fl/fl} mice was arbitrarily set as 1 and levels in DSG2^{ΔIEC} mice are presented as ratio. L7 (mouse ribosomal protein) gene and β-tubulin (βTub) were used as an internal and a loading control, respectively. Data in C,F are shown as dot plots. Two-tailed Student's t test was used for statistical analyses. *p<0.05

Gross et al., Fig. 3

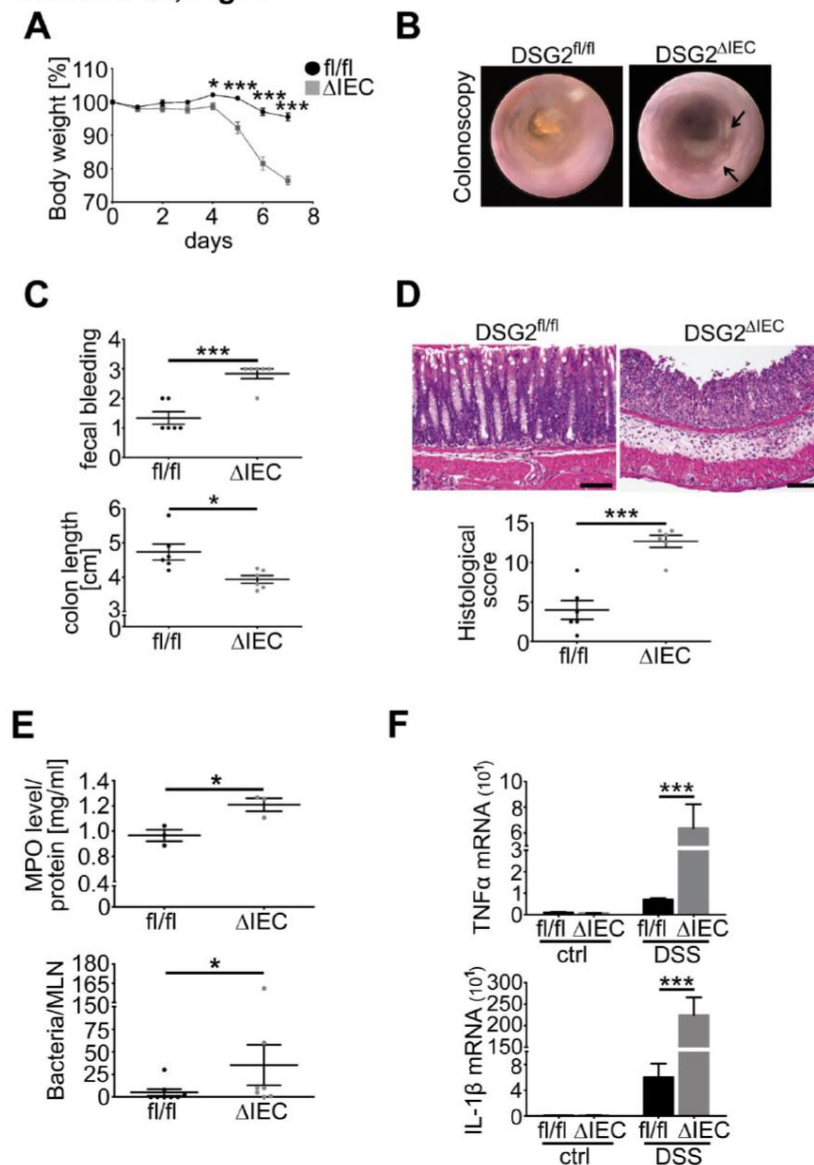


Figure 3. DSG2-deficient animals (DSG2 Δ IEC) exhibit an enhanced susceptibility to dextran sodium sulfate (DSS)-induced colitis. (A) Relative body weights of DSG2 Δ IEC (Δ IEC) mice (grey rectangles) and their floxed littermates (black circles, DSG2 fl/fl , fl/fl , $n=7$ each) were determined daily starting at the time of first DSS administration. (B-D) Macroscopic images of the colon mucosa obtained by colonoscopy, stool guaiac test with semi-quantitative scoring ($n=6$), colonic length and hematoxylin and eosin (H&E) staining of colon sections with morphometric quantification were used to assess the severity of colitis at day 7 after DSS administration ($n=6$). (E,F) The extent of colonic inflammation 7 days after DSS exposure was evaluated by myeloperoxidase (MPO) activity and real-time RT-PCR for TNF α and IL-1 β ($n=3-6$). The low cytokine expression in non-treated animals (ctrl) was arbitrarily set as 1. L7 (mouse ribosomal protein) gene was used as an internal control. Bacterial translocation into mesenteric lymph nodes (MLN) was quantified as the amount of colonies grown from total MLN homogenates on blood agar plates ($n=7-8$). Data in C,D,E are presented as dot plots. Two-tailed Student's t test was used for statistical analyses of DSS-treated animals. * $p<0.05$, *** $p<0.001$.

Gross et al., Fig. 4

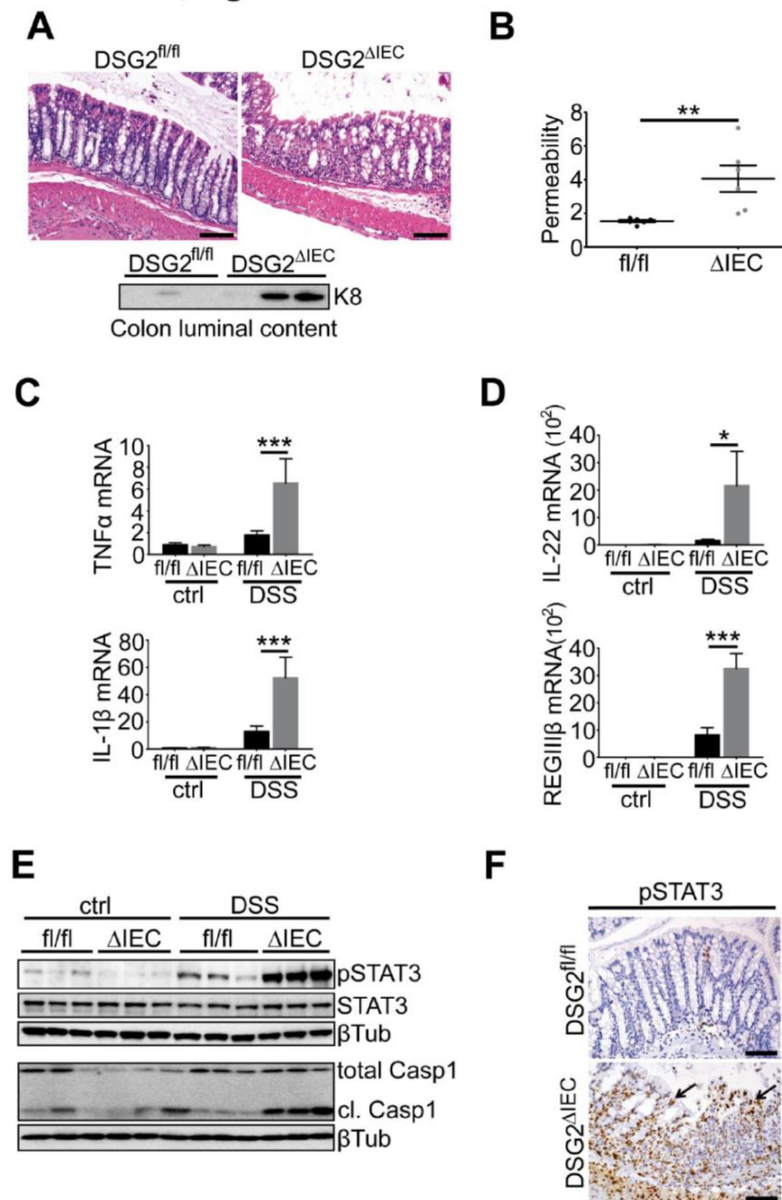


Figure 4. DSG2-deficient animals (DSG2 Δ IEC) subjected to dextran sodium sulfate (DSS) for four days display higher intestinal permeability and enhanced STAT3 signaling. (A) Hematoxylin and eosin (H&E) staining of colon sections from DSG2 Δ IEC (Δ IEC) mice and their floxed littermates (DSG2^{fl/fl} or fl/fl) was performed. Western Blot depicts the epithelial cell marker keratin 8 (K8) in the colonic luminal content. (B) Serum FITC levels were measured following gavage of 4kD FITC-dextran and presented as dot plots (n=6). (C-E) RT-PCR for TNF α , IL-1 β and IL-22 as well as the antimicrobial peptide REGIII β was performed (n=4-9). Activation of selected

signaling pathways was assessed by immunoblotting. The low cytokine expression in non-treated animals (ctrl) was arbitrarily set as 1. All other values are presented as ratio. L7 (mouse ribosomal protein) gene and β -tubulin (β Tub) were used as an internal and a loading control, respectively. (F) Immunohistochemistry visualizes phosphorylated STAT3 in colon sections of DSS-treated mice. Scale bar (A,F) = 100 μ m. Two-tailed Student's t test was used for statistical analysis of DSS-treated animals.* p <0.05, ** p <0.01, *** p <0.001.

Gross et al., Fig. 5

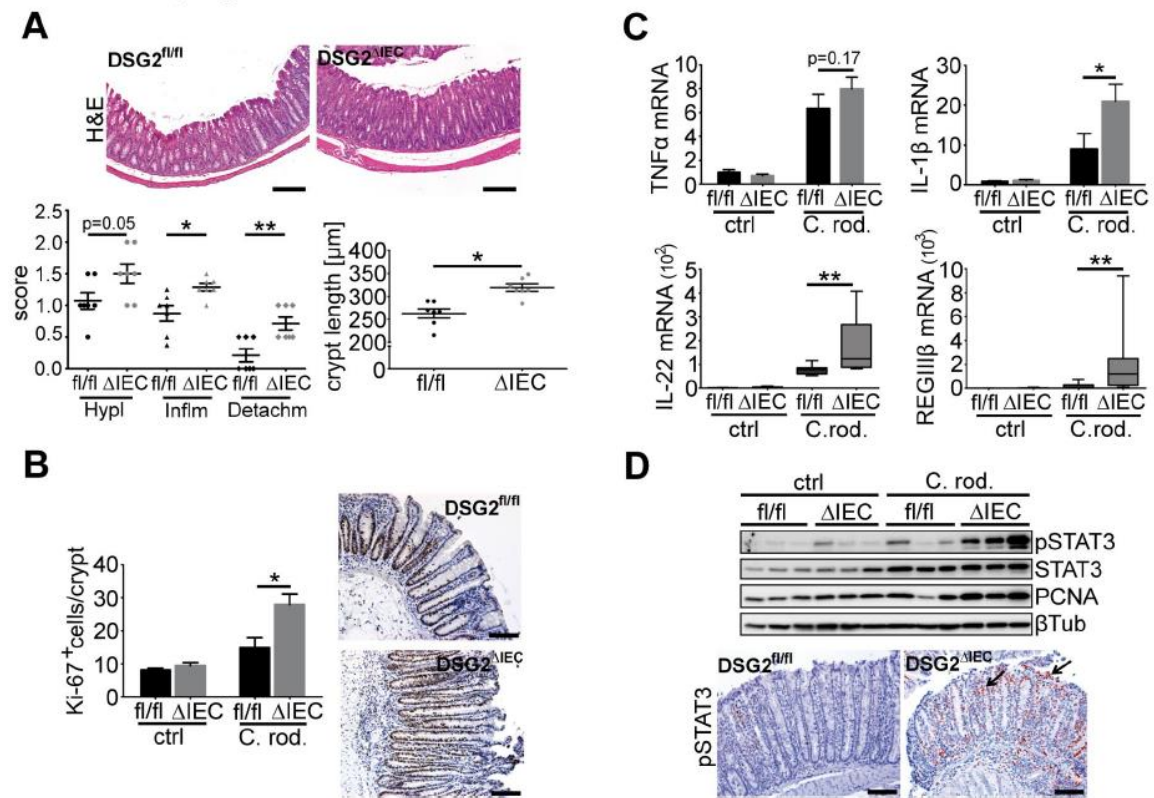


Figure 5. DSG2-deficient (DSG2 Δ IEC) mice exhibit enhanced susceptibility to *Citrobacter rodentium* (C. rod.)-induced colitis. (A) Hematoxylin and eosin (H&E) staining of colon sections with quantification of epithelial hyperplasia (HypI), detachment (Detachm) and inflammatory immune cell infiltration (Inflm) as well as colon crypt length determination was performed in DSG2 Δ IEC mice and their floxed littermates (DSG2^{fl/fl} or fl/fl) 14 days after oral infection with C. rod. (n=7). Scale bar = 200 μ m. Data are shown as dot plots. (B) Ki-67 immunohistochemistry with morphometric quantification visualize the proliferation in colon sections 14 days post infection with C. rod. (n=7). (C,D) Real time RT-PCR for the highlighted cytokines and the antimicrobial product REGIII β as well as immunoblotting for the indicated signalling molecules were conducted in untreated and in C. rod.-infected mice (n=4-7). L7 (mouse ribosomal protein) gene and β -tubulin (β Tub) were used as an internal and a loading control, respectively. mRNA expression in untreated fl/fl mice was arbitrarily set as 1 and other levels are presented as ratio. Immunohistochemistry illustrates phosphorylated STAT3 in colon sections of C. rod.- infected mice. Scale bar (B,D) =

100 μm . Two-tailed Student's t test (A,B, upper panels in C) or Mann-Whitney test (lower panels in C) were used for statistical analyses of *C.rod.*-exposed mice.* $p < 0.05$, ** $p < 0.01$.

Gross et al., Fig. 6

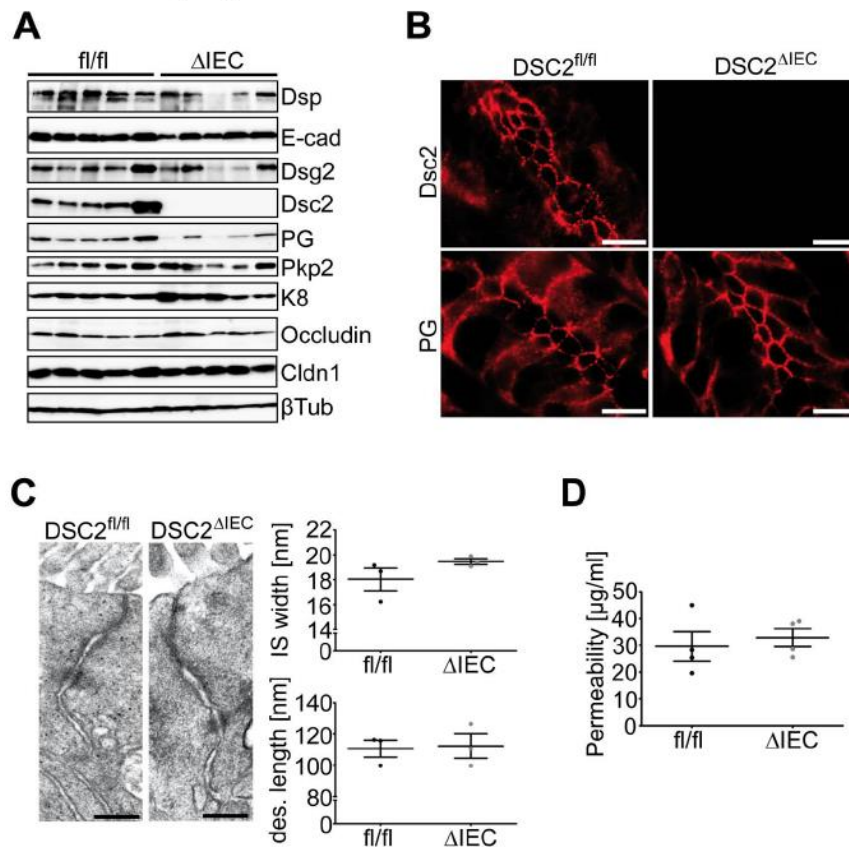


Figure 6. DSC2-deficient animals ($DSC2^{\Delta IEC}$) show an unaltered desmosomal plaque and no increased intestinal permeability. (A) Immunoblotting was performed on total colon lysates from $DSC2^{\Delta IEC}$ (ΔIEC) mice and their floxed littermates ($DSC2^{fl/fl}$, fl/fl) ($n=5$). β -tubulin (β Tub) was used as a loading control. (B) Immunofluorescence depicts the distribution of Dsc2 and plakoglobin (PG) in the colons of both genotypes. Scale bar = 20 μ m. (C) Desmosomal ultrastructure was assessed on colon samples by electron microscopy with subsequent quantification of the desmosomal intercellular space width and desmosomal length ($n=3$). Scale bar = 200 nm. IS = intercellular space. (D) 4kD FITC-dextran was administered and serum FITC levels were quantified as a measurement of intestinal permeability ($n=4$). Data in C,D are shown as dot plots. Cldn1, claudin 1; Dsp, desmoplakin; E-cad, E-cadherin; K8, keratin 8; PG, plakoglobin; Pkp2, plakophilin 2.

Gross et al., Fig. 7

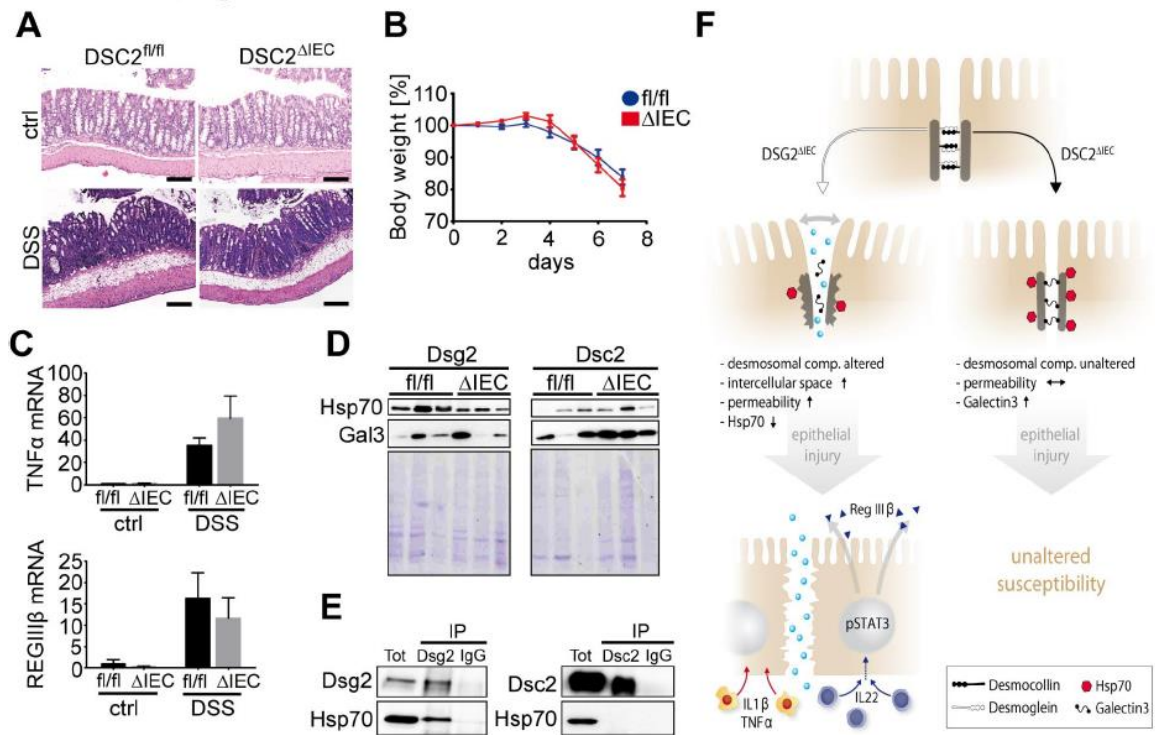


Figure 7. DSG2 Δ IEC and DSC2 Δ IEC mice display differential phenotypes as well as alterations in their plasma membrane proteome. (A) Overall colon architecture of *DSC2 Δ IEC* mice and corresponding floxed mice (*DSC2^{fl/fl}*) was evaluated prior to (ctrl) and 7 days after DSS exposure by hematoxylin and eosin (H&E) staining. Scale bar = 200 μ m. (B) The relative body weight of *DSC2 Δ IEC* mice (red rectangles, Δ IEC) and their floxed littermates (blue circles, *fl/fl*) was measured daily starting at the day of the first DSS administration (n=7). (C) The mRNA levels of the pro-inflammatory cytokine TNF α and the antimicrobial peptide REGIII β were evaluated prior to (ctrl) and 7 days after DSS exposure by real time RT-PCR. The cytokine expression in ctrl animals was arbitrarily set as 1. L7 (mouse ribosomal protein) gene was used as an internal control. (D) Plasma membrane protein fractions were isolated from colons of both genotypes and subjected to immunoblotting. Coomassie blue staining of blots was used as loading control. Gal3, Galectin 3; Hsp70, heat shock protein 70. (E) Colonic mucosa lysates from *fl/fl* animals were used for co-immunoprecipitation with Dsg2 (left panel) and Dsc2 (right panel), that was followed by immunoblotting. IgG-conjugated beads (IgG) and total lysates (Total) were used as a control and an input, respectively. (F) Schematic illustrates the molecular changes seen in *DSG2 Δ IEC* and *DSC2 Δ IEC* mice.

Supplementary material to the manuscript

Title: Desmoglein 2, but not desmocollin 2, protects intestinal epithelia from injury

Authors: Annika Gross¹, Lotta A. P. Pack¹, Gabriel M. Schacht¹, Sebastian Kantz, Hanna Ungewiss³, Michael Meir⁴, Nicolas Schlegel⁴, Christian Preisinger⁵, Peter Boor⁶, Nurdan Güldiken¹, Claudia A. Krusche², Gernot Sellge¹, Christian Trautwein¹, Jens Waschke⁴, Arnd Heusers⁸, Rudolf E. Leube², Pavel Strnad¹

Author affiliation:

¹Department of Medicine III and IZKF, University Hospital Aachen, Aachen, Germany

²Institute of Molecular and Cellular Anatomy, RWTH Aachen University, Aachen, Germany

³Institute of Anatomy, Faculty of Medicine, LMU Munich, Munich, Germany

⁴Department of Surgery I, University of Würzburg, Würzburg, Germany

⁵IZKF Proteomics Facility, University Hospital Aachen, Aachen, Germany

⁶Institute of Pathology and Department of Nephrology, University Hospital Aachen, Aachen, Germany

⁸Max-Delbrück-Center of Molecular Medicine, Berlin, Germany

Supplementary Materials and Methods

Immunohistochemistry

Deparaffinized sections were boiled in either citrate-based antigen unmasking solution pH 6 (Vector laboratories, Burlingame, USA) or EDTA-based retrieval solution pH 9 (DAKO, Hamburg, Germany). To reduce the endogenous peroxidase activity, slides were incubated with 3% H₂O₂ for 10 minutes. Based on supplier recommendations, the sections were blocked either with 2% BSA (bovine serum albumin) in Tris Base Saline Buffer with 0.1% Tween-20 (TBST) or 5% normal goat serum in PBS for 30 minutes. Afterwards, sections were incubated with anti-pSTAT3 (Tyr705, #9131, Cell Signalling, Leiden, Netherlands), anti-Ki-67 (M7249, Dako, Hamburg, Germany) or anti-Lysozyme (sc27958 (C-19), Santa Cruz, Heidelberg, Germany) antibody overnight at 4°C. After washing, biotinylated secondary antibodies (Vector laboratories) were applied for 30 minutes followed by incubation with the Vectastain working solutions as recommended by the manufacturer (Vectastain ABC Kit, Vector laboratories). Staining was developed with 3,3'-diaminobenzidine (DAB, Vector laboratories) and hematoxylin was used as a counterstain. Lysozyme-positive cells were counted as a mean in at least twenty different crypts.

Immunofluorescence staining

Immunofluorescence staining was performed on frozen, O.C.T.-embedded tissues, that were cut into 2-3 µm and 5 µm thick sections, respectively and DLD1 cells that were seeded on 12 mm glass cover slides and grown for 4 days after reaching full confluence. Tissue specimen and cells were fixed in pre-cooled acetone or 2% paraformaldehyde in PBST for 10 minutes, respectively. Paraformaldehyde-fixed samples were permeabilized with 0.5% Triton X-100 in PBST for another 10 minutes. Blocking was performed for 30 minutes at room temperature in 2% normal goat serum, 1% BSA, 0.1% cold fish skin gelatine, 0.1% Triton X-100, 0.05% Tween 20 in 1x PBS (tissue) or 2% BSA in PBST (cells). Afterwards the slides were exposed to following primary antibodies: anti-Desmoglein 2 (tissue),¹ anti-Desmoglein 2 (cells, #610121 (rb5), Progen, Heidelberg, Germany), anti-Desmocollin 2 (see below for details), anti-Desmocollin 2/3 (#326200, clone 7G6, Thermo Scientific, Munich, Germany), anti-Desmoplakin (NW6, gift from

Kathleen J. Green, Chicago, USA), anti-Plakoglobin (#61005 (PG 5.1.), Progen, Hamburg, Germany), anti-ZO-1(Mid) (#402200, Life technologies, USA) and anti-E-cadherin (#3195, Cell signaling, Leiden, Netherlands) overnight at 4°C. After washing and incubation with Cy3 or Alexa-Fluor 488/568-conjugated secondary antibodies (Dianova, Hamburg, Germany and Invitrogen, Molecular Probes, Eugene, OR, USA) for 1 hour in the dark, slides were washed and mounted. The immunofluorescence for γ -catenin (PG) was performed on paraffin-embedded colon sections. In brief, the sections were deparaffinized, washed and boiled in citrate-based antigen unmasking solution pH 6 (Vector laboratories). Anti- γ -catenin (PG) (sc30997 K-20, Santa Cruz, Heidelberg, Germany) and anti-goat Alexa-Fluor 568 (Invitrogen) were used as primary and secondary antibodies, respectively. The sections were covered with ProLong antifade reagent containing DAPI (Invitrogen). DLD1 cells were mounted with 60% glycerol in PBS containing 1.5% N-propyl gallate (Serva, Heidelberg, Germany). Fluorescence images were acquired with Zeiss microscope Axio Imager Z1 (Zeiss, Jena) or a Leica SP5 confocal microscope with a 63 x NA 1.4 PL APO objective (Leica, Wetzlar, Germany).

Transmission electron microscopy

Murine samples were cut into $\sim 1 \text{ mm}^3$ pieces and fixed by a three step process with the following fixatives: (i) 3.7% formaldehyde, 1% glutaraldehyde, 11.6 g $\text{NaH}_2\text{PO}_4 \cdot \text{xH}_2\text{O}$ and 2.7 g NaOH per liter ddH₂O for two hours; (ii) 1% OsO₄ for one hour; (iii) 0.5% uranylacetate/0.05 N sodium hydrogen maleate buffer (pH 5.2) for 2 hours (all at room temperature). Subsequently, tissues were dehydrated, embedded in araldite for 48 hours at 60°C and cut into 75 nm ultrathin sections that were treated with 3% uranylacetate for four minutes and with 80 mM lead citrate for three minutes to enhance the contrast. Images were acquired with an EM 10 (Zeiss) plus digital camera (Olympus) and iTEM software (Olympus). The intercellular space width and length were determined as a mean from at least ten different desmosomes per mouse.

Human samples were fixed with 2.5% glutaraldehyde and cut into $\sim 1 \text{ mm}^3$ pieces. After three washing steps with PBS, samples were incubated with 2% osmium tetroxide solution for 1 hour at 4°C and subsequently dehydrated through an ascending ethanol

series from 20 to 100%. Samples were embedded with epon for 24 hours at 80°C and ultrathin sections (60 - 80 nm) were cut with a diamond knife. Staining was performed with a saturated solution of uranyl acetate for 40 minutes and lead citrate for 5 minutes. Images were acquired with the transmission electron microscope Libra 120 (Zeiss, Oberkochen, Germany).

Quantitative real-time PCR

Total RNA was isolated using RNeasy Mini Kit (Qiagen, Hilden, Germany) according to the manufacturer's instructions and 1 µg was reverse-transcribed into cDNA using M-MLV Reverse Transcriptase Kit (Promega, Mannheim, Germany). Quantitative real-time PCR was performed with the 7300 Fast Real-Time PCR System (Applied Biosystems). Samples were analyzed in duplicates with the $\Delta\Delta C_t$ method relative to L7 ribosomal protein as an internal control. All levels are reported as means +/- SEM. The primers used in this study are summarized in Suppl. table 2.

Transepithelial Resistance Measurements (TER)

Cells were grown on 8-well electrode arrays (Ibidi, 8W10E) and baseline TER was measured with an ECIS model Z theta (Applied Biophysics, Troy, NY) at 800 Hz as described previously.²

Desmocollin 2 antibody generation

To generate a peptide-specific anti-Dsc2 antibody, an antigen was obtained by conjugation of the synthetic peptide with sequence SRRGAGYHHHTLDPC to ovalbumin. Guinea pigs were immunized by subcutaneous injection of 240 µg of the peptide diluted in complete Freund's adjuvant followed by three boostings with the same amount of antigen diluted in incomplete Freund's adjuvant being performed every two weeks. Serum was collected 14 days after the last immunization. To purify the Dsc2-specific antibodies, the serum was purified over a column that was adsorbed with the immunogenic peptide. After washing with 10 mM sodium phosphate (pH 6.8), the antibodies were retrieved with IgG Elution Buffer (Thermo Scientific, #21004). At the end, the solution was neutralized with 2 M K₂HPO₄.

Suppl. table 1: Overview of the analyzed human samples

Identification	Sex	Age	Medication	Disease history
control 1	M	62	no	Schwannoma coecum
control 2	F	77	no	Colon ascendens carcinoma
control 3	F	69	no	Colon ascendens carcinoma
control 4	F	56	no	Adenomatous polyposis
control 5	M	45	no	Non resectable coecum polyp
control 6	M	74	no	Colon ascendens carcinoma
control 7	M	72	no	Non resectable ascendens polyp
control 8	M	71	no	Non resectable coecum polyp
control 9	F	50	no	Neuroendocrine tumor ileum
control 10	F	66	no	Colon ascendens carcinoma
patient 1	M	26	Budesonide	Crohn's disease (terminal ileum)
patient 2	F	23	Prednisolone + AZT	Crohn's disease (Ileocecal)
patient 3	M	46	AZT + Prednisolone	Crohn's disease (terminal ileum)
patient 4	F	43	Adalimumab + MTX	Crohn's disease (Ileocecal)
patient 5	F	46	Budesonide	Crohn's disease (terminal ileum)
patient 6	F	32	Adalimumab	Crohn's disease (small intestine)
patient 7	M	25	Adalimumab	Crohn's disease (terminal ileum)
patient 8	M	55	Prednisolone	Crohn's disease (terminal ileum)
patient 9	F	24	Infliximab+ Mesalazine + Prednisolone	Crohn's disease (terminal ileum)
patient 10	F	41	Budesonide + Infliximab + AZT	Crohn's disease (small intestine)
patient 11	M	61	Prednisolone + Adalimumab	Crohn's disease (Ileocecal)
patient 12	F	34	Prednisolone	Crohn's disease (terminal ileum)

AZT=Azathioprin, MTX=Methotrexate

Suppl. table 2: Primers used for genotyping and quantitative Real Time PCR

Genotyping PCR Primer		
mDsg2	Forward	GGTAAATGCAGACGGATCAG
	Reverse	TGGGCTACACTCATAGGAAG
mDsc2	Forward	CCCTCCAGTCAGTGAAGTTA
	Reverse	TTTGATACCCAGCACACCTTT
mVillin-Cre	Forward	CCACGACCAAGTGACAGCAAT
	Reverse	TTCGGATCATCAGCTACACCA
Quantitative Real Time PCR Primer		
mDsg1a	Forward	GGCCTCGCCCTAACACTAA
	Reverse	AGGACCGAAGTGAACGTGT
mDsg1b	Forward	GGGAATATAAAGGAACAGTGCTATC
	Reverse	CACCACCATCTGAACCTGGTA
mutE4/E5-mDsg2	Forward	ACCGGGAAGAAACACCATATT
	Reverse	AGGGCTTTTCAGGTTGTTT
mDsg3	Forward	TGTTGCTATTGGCCCCACTT
	Reverse	ATCGGGCACTGGGATAAAGC
mDsg4	Forward	GGTAACTGGAGAAGTCCGC
	Reverse	TGAGCCCCTCACCAGTAGAT
mDsc1	Forward	CTCGGCTTGGTAAAAGGTG
	Reverse	ATGGGCGAACGTAGTCTTCAC
mDsc2	Forward	GCACTGGTCGTGTAGATCGT
	Reverse	CTCTGGCGTATACCCATCTG
mDsc3	Reverse	GTGGAGTTGTTACTGCCCGA
	Reverse	CCCAGGTGCTTCGGTATTT
mPG/JUP	Forward	TCCTGCACAACCTCTCTCAC
	Reverse	ACTGAGCATTCCGACTAGGG
mDSP	Forward	CTGGCAAACGAGACAAATCA
	Reverse	GATGCCAGCTGCAGTTCATA
mPkp2	Forward	TCAGCATAACCGAAGATGC
	Reverse	GGGAAAGATTCCGTGACAAA
mLGR5	Forward	CAGGCCGTCTGTGATCAGTT
	Reverse	GCAGCCTGACAACTGGGTA
mRspo1	Forward	GCTCGCCCAAGCTCTTCATT
	Reverse	CGGGCATCAAAGTATCCAGGT
mMuc2	Forward	GCTGACGAGTGGTTCGTGAATG
	Reverse	GATGAGGTGGCAGACAGGAGAC
mTNFa	Forward	TCAGCCTCTTCTCATTCTGCTT
	Reverse	AGGCCATTTGGAACTTCTCATC
mIL1b	Forward	TGAAGCAGCTATGGCAACTG
	Reverse	GGGTCCGTCAACTTCAAAGA
mIL6	Forward	ACAAAGCCAGAGTCTTCAGAGAGA
	Reverse	TGGTCTTGGTCCTTAGCCACTCC
mIL22	Forward	CAACTGTTGACACTTGTGCGAT
	Reverse	GCGGCCAAAGTCCCATAAG
mReg3b	Forward	TGCCTTAGACCGTGCTTTCT
	Reverse	AGGGCAACTTCACCTCACAT
mPCNA	Forward	TACAGCTTACTCTGCGCTCC
	Reverse	TTGGACATGCTGGTGAGGTT
mL7	Forward	GAAAGGCAAGGAGGAAGCTCATCT
	Reverse	AATCTCAGTGCGGTACATCTGCCT

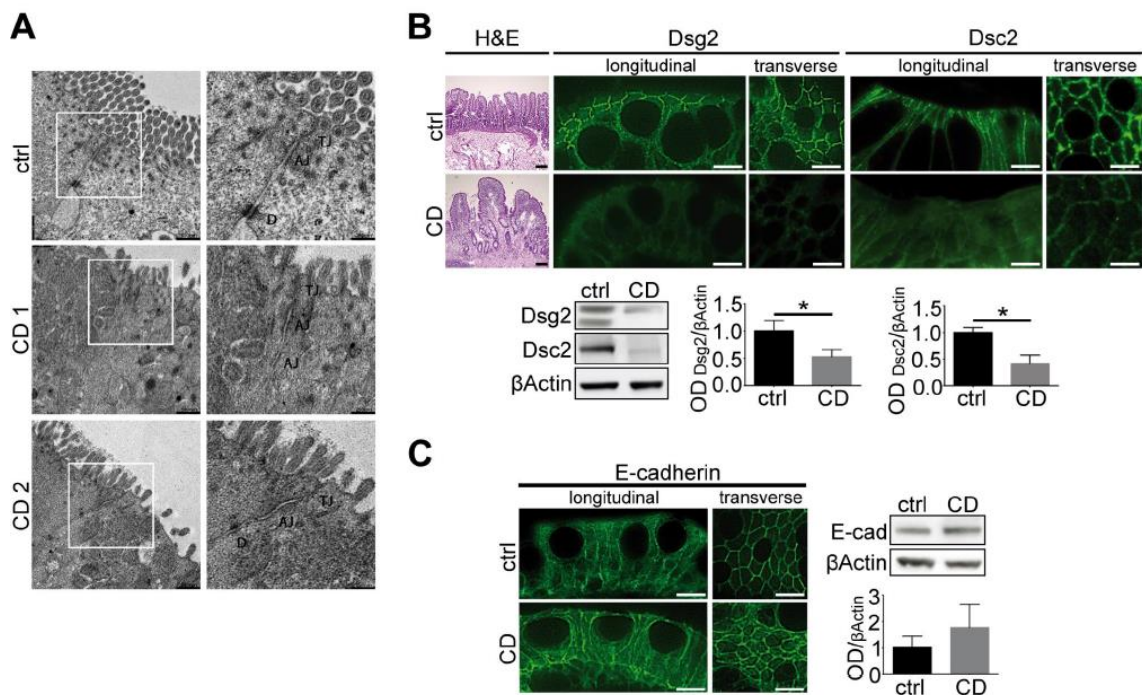
Suppl. table 3: Antibodies used for Western Blotting

Antibody	Host	Company
Claudin 1	rabbit	ab15098, Abcam, Cambridge, UK
Claudin 15	rabbit	389200, Life technologies, California, US
Claudin 2	mouse	325600, Life technologies, California, US
cleaved Caspase 1	mouse	IMG-5028, IMGENEX, San Diego, US
Desmocollin 2	guinea-pig	Institute of Molecular and Cellular Anatomy, RWTH Aachen, Germany
Desmocollin 2/3	mouse	326200 (7G6), Thermo Scientific, Munich, Germany
Desmoglein 2	rabbit	Institute of Molecular and Cellular Anatomy, RWTH Aachen, Germany
Desmoglein 2	rabbit	610121 (rb5), Progen, Heidelberg, Germany
Desmoplakin I/II	rabbit	sc33555 (H-300) Santa Cruz, Heidelberg, Germany
E-cadherin (CDH1)	rabbit	#3195, Cell signaling, Leiden, Netherlands
EGFR	Rabbit	#8690 (D13E1,XP), Cell signaling, Leiden, Netherlands
Galectin 3	Mouse	NB300-538 (A3A12), Novus Biologicals, Littleton, USA
Hsp70/Hsp72	Rabbit	ADI-SPA-812, Enzo Life Sciences, Lörrach, Germany
Keratin 8 (Clone Ks.8.7)	mouse	61038, Progen, Heidelberg, Germany
Occludin	rabbit	389200, Life technologies, California, US
p38 (MAPK)	Rabbit	#2646 (C74B9), Cell signaling, Leiden, Netherlands
PCNA	mouse	MS-106, Thermo Scientific, Munich, Germany
pEGFR (Y845)	rabbit	#2231, Cell signaling, Leiden, Netherlands
Plakophilin 2	goat	ab189323, Abcam, Cambridge, UK
pMLC2 (S19)	rabbit	#3671, Cell signaling, Leiden, Netherlands
pp38 MAPK (Thr180/Tyr182)	rabbit	#9211, Cell signaling, Leiden, Netherlands
pSTAT3 (Tyr705)	rabbit	#9131, Cell signaling, Leiden, Netherlands
STAT3	rabbit	sc7179 (H-190), Santa Cruz, Heidelberg, Germany
α Tubulin	mouse	ab4074, Abcam, Cambridge, UK
β Tubulin	mouse	T8328, Sigma-Aldrich, Steinheim, Germany
γ -catenin (PG)	goat	sc30997 (K-20) Santa Cruz, Heidelberg, Germany

Supplementary References

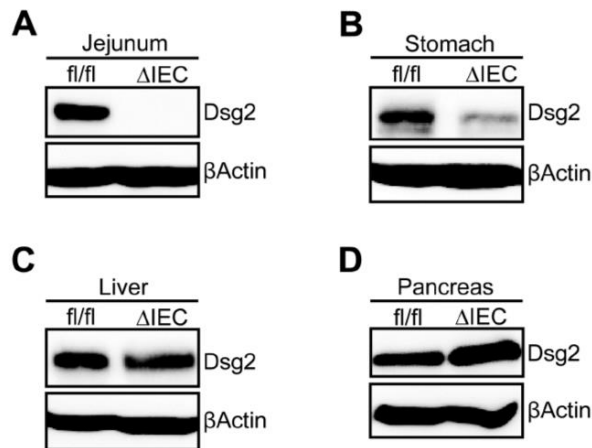
1. Schlegel N, Meir M, Heupel WM, Holthofer B, Leube RE, Waschke J. Desmoglein 2-mediated adhesion is required for intestinal epithelial barrier integrity. *American journal of physiology Gastrointestinal and liver physiology* 2010; **298**(5): G774-783.
2. Ungewiss H, Vielmuth F, Suzuki ST, Maiser A, Harz H, Leonhardt H et al. Desmoglein 2 regulates the intestinal epithelial barrier via p38 mitogen-activated protein kinase. *Scientific reports* 2017; **7**(1): 6329.

Gross et al., Suppl. Fig. 1



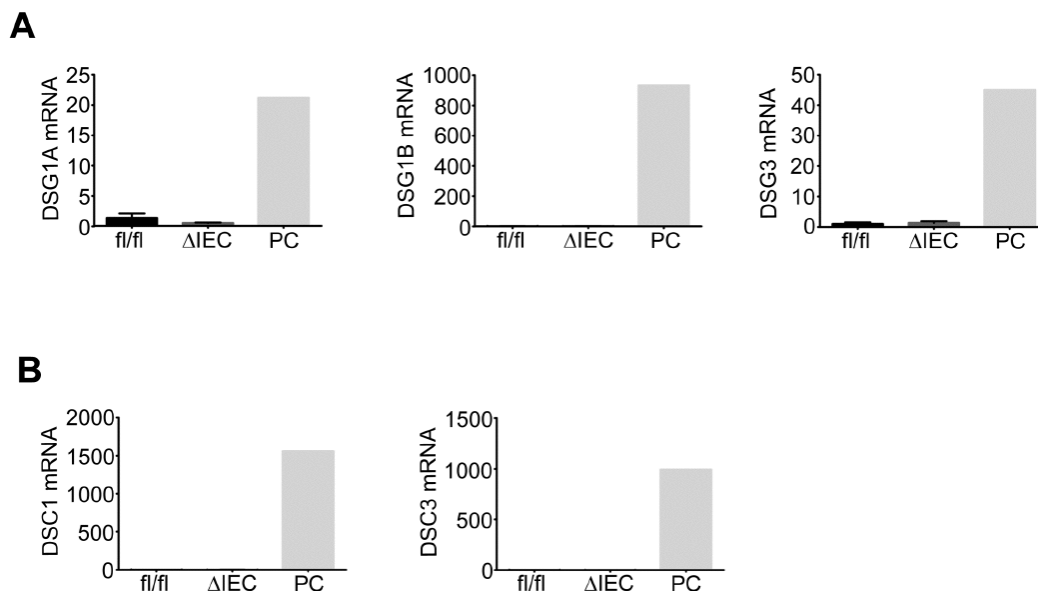
Supplementary Figure 1. Desmosomes are altered and desmosomal cadherins are reduced in patients with Crohn's disease. (A) Transmission electron microscopy images of terminal ileum specimens from patients with Crohn's disease (CD) and from a healthy control individual (ctrl). Scale bar = 500 nm (left panels) and 250 nm (right panels). (B,C) Terminal ileum specimens from patients with Crohn's disease (CD) (n=12) as well as from control individuals (ctrl) (n=10) were stained with antibodies against Dsg2, Dsc2 and E-cadherin. The corresponding protein lysates were subjected to immunoblotting with subsequent morphometric quantification. Hematoxylin and eosin (H&E) staining highlights the overall intestinal architecture. Scale bar immunofluorescence = 20 μm, scale bar H&E = 50 μm. Two-tailed Student's t test was used for statistical analyses. *p<0.05

Gross et al., Suppl. Fig. 2



Supplementary Figure 2. DSG2-deficient animals ($DSG2\Delta IEC$) reveal an intestine-specific Dsg2 loss. (A-D) Desmoglein 2 (Dsg2) protein levels were assessed in the indicated mouse organs of $DSG2\Delta IEC$ (ΔIEC) and $DSG2^{fl/fl}$ (fl/fl) mice by immunoblotting. β Actin was used as a loading control.

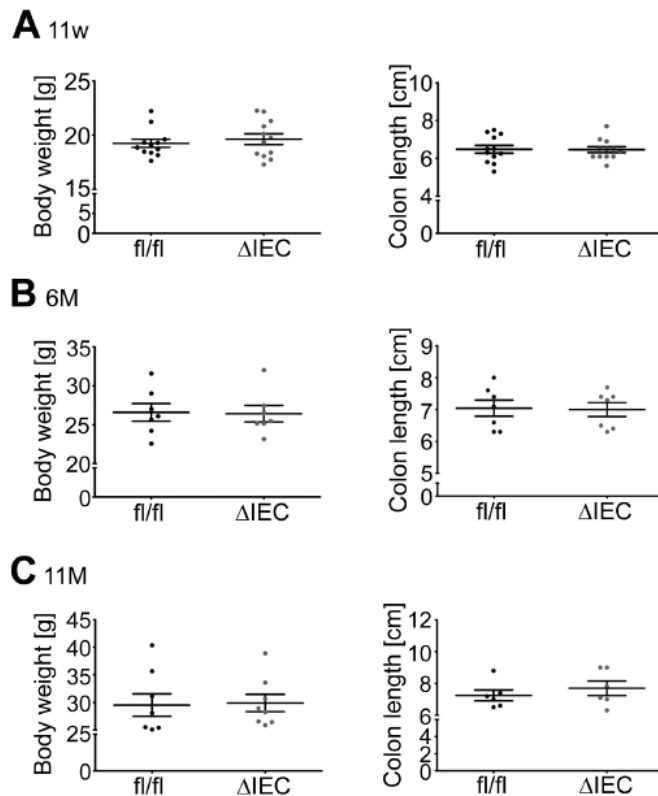
Gross et al., Suppl. Fig. 3



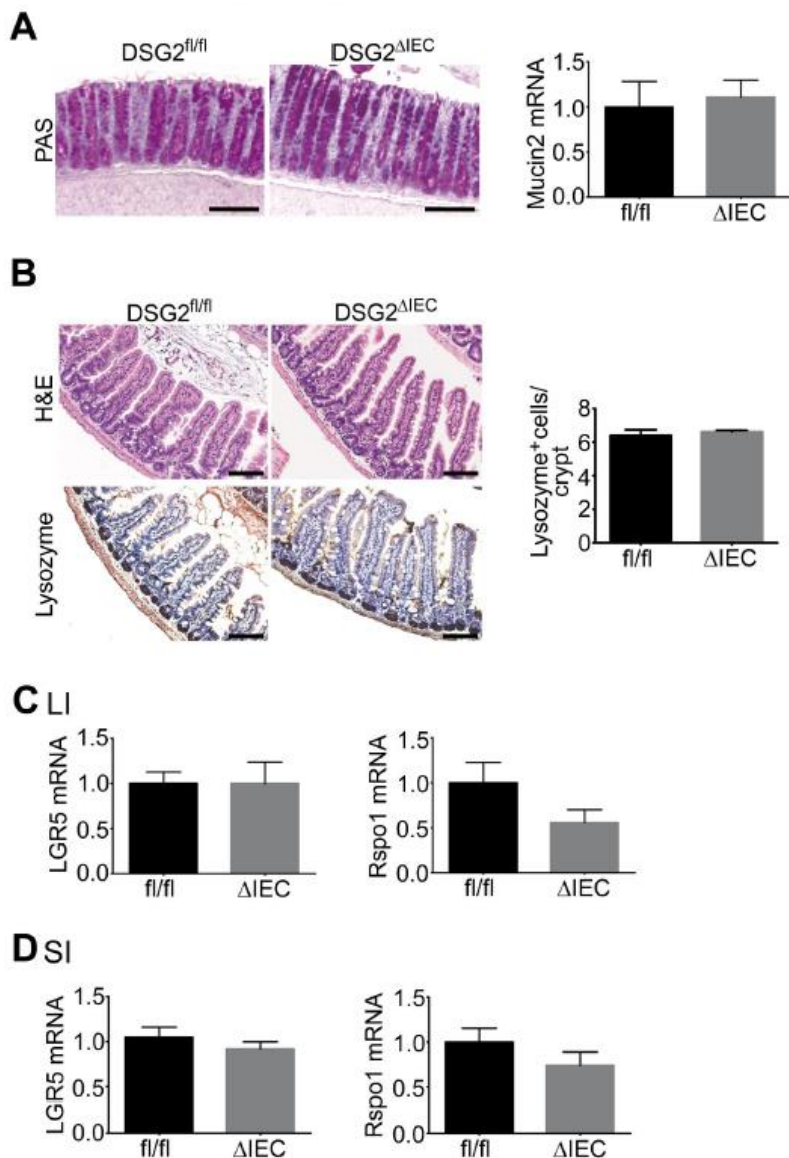
Supplementary Figure 3. Knockout of DSG2 does not alter the expression of other desmoglein and desmocollin isoforms. Expression levels of the desmoglein family members DSG1a, DSG1b and DSG3 (A) as well as the desmocollin members DSC1 and DSC3 (B) were assessed in the colon of $DSG2\Delta IEC$ (ΔIEC) and $DSG2^{fl/fl}$ (fl/fl) mice

by real time RT-PCR (n=3-4). Skin was used as a positive control (PC). L7 (mouse ribosomal protein) gene was used as an internal control. Average mRNA expression in fl/fl mice was arbitrarily set as 1 and levels in Δ IEC mice as well as the skin represent a ratio.

Gross et al., Suppl. Fig. 4



Supplementary Figure 4. DSG2-deficient animals ($\text{DSG2}_{\Delta\text{IEC}}$) display normal body weight and colon length. The body weights and the colon lengths of 11 weeks (11w), 6 months (6M) and 11 months (11M) old $\text{DSG2}_{\Delta\text{IEC}}$ (Δ IEC) mice and their floxed littermates (fl/fl) are displayed in form of dot plots (n=6-20).

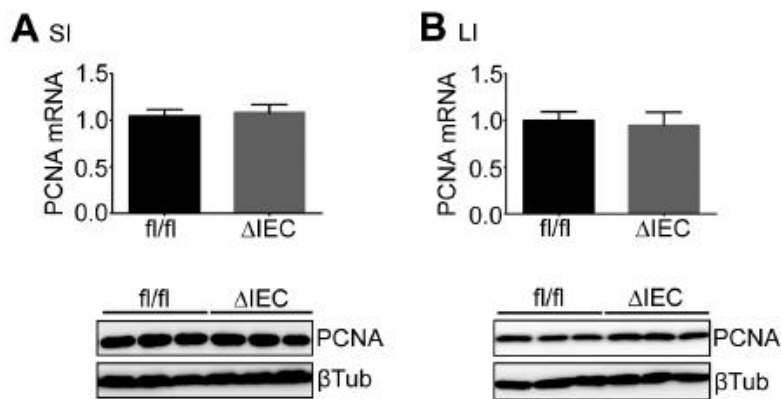
Gross et al., Suppl. Fig. 5

Supplementary Figure 5. Small and large intestine of DSG2-deficient animals (DSG2 Δ IEC) show no obvious defects in tissue morphology and differentiation.

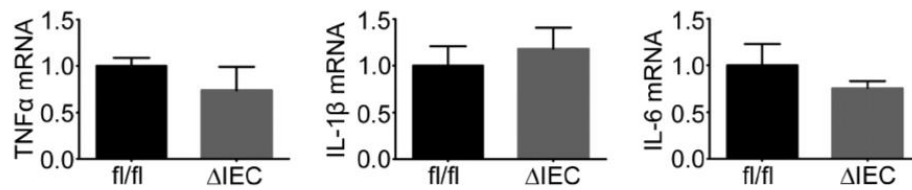
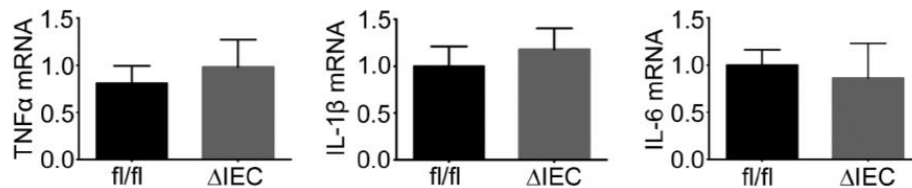
(A) Periodic acid-Schiff (PAS) staining demonstrated a similar amount of goblet cells in colons from DSG2 Δ IEC (Δ IEC) mice and their floxed littermates (DSG2 $^{fl/fl}$ or fl/fl). The results were confirmed by real time RT-PCR for mucin 2, a major goblet cell product (n=6). (B) Hematoxylin and eosin (H&E) staining demonstrates a regular architecture of the small intestine (SI). Immunohistochemistry for the small intestinal Paneth cell marker lysozyme with quantification of lysozyme-positive cells/crypt revealed no differences between both genotypes (n=4). Scale bar (A,B) = 100 μ m (C,D) Real time RT-PCR demonstrated similar expression levels of the stem cell markers LGR5 and R-

spondin 1 (*Rspo1*) in the transgenic animals. Small (SI) and large intestine (LI) were analysed (n=6-7). L7 (mouse ribosomal protein) gene was used as an internal control, respectively. Average mRNA expression in fl/fl mice was arbitrarily set as 1 and levels in Δ IEC mice represent a ratio.

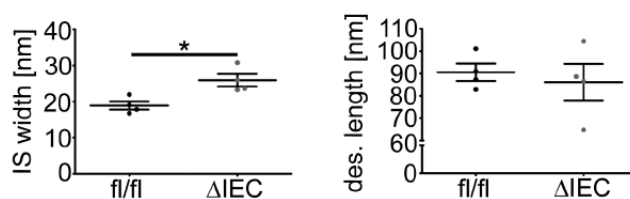
Gross et al., Suppl. Fig. 6



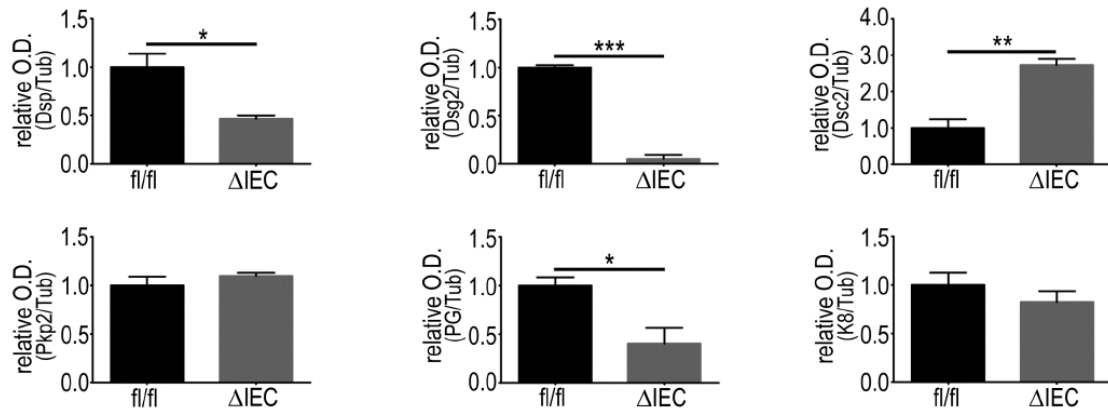
Supplementary Figure 6. DSG2-deficient animals ($DSG2_{\Delta IEC}$) show no changes in basal cell proliferation. To evaluate the proliferation grade in the small intestine (SI) and large intestine (LI) of $DSG2_{\Delta IEC}$ (Δ IEC) mice and their floxed littermates (fl/fl), the S-phase marker PCNA was assessed by real time RT-PCR (n=7) and immunoblotting. L7 (mouse ribosomal protein) gene and β -tubulin (β Tub) were used as an internal and a loading control, respectively. Average mRNA expression in fl/fl mice was arbitrarily set as 1 and levels in Δ IEC mice were presented as ratio.

Gross et al., Suppl. Fig. 7**A** SI**B** LI

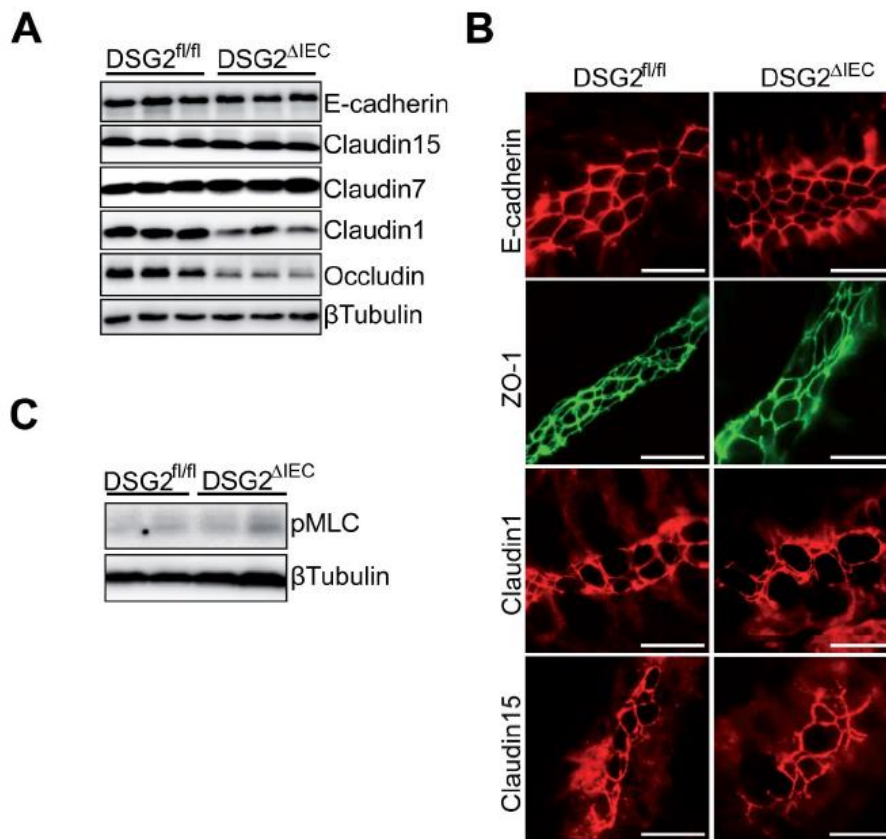
Supplementary Figure 7. DSG2-deficient animals (DSG2 Δ IEC) display no obvious inflammation under basal conditions. The inflammatory markers TNF α , IL-1 β and IL-6 were evaluated in the small (SI; A) and large intestine (LI; B) of 11 weeks old DSG2 Δ IEC (Δ IEC) mice and their floxed littermates (fl/fl) by real time RT-PCR (n=4-6). L7 (mouse ribosomal protein) gene was used as an internal control. Average mRNA expression in fl/fl mice was arbitrarily set as 1 and levels in Δ IEC mice were presented as ratio.

Gross et al., Suppl. Fig. 8

Supplementary Figure 8. DSG2-deficient animals (DSG2 Δ IEC) exhibit a wider desmosomal intercellular space in the small intestine. The desmosomal ultrastructure of small intestine samples from DSG2 Δ IEC (Δ IEC) and DSG2 $^{fl/fl}$ (fl/fl) mice was assessed by electron microscopy with quantification of the desmosomal intercellular space (IS) and the length of the desmosome (n=4). Data are shown as dot plots. Two-tailed Student's t test was used for statistical analysis. *p<0.05

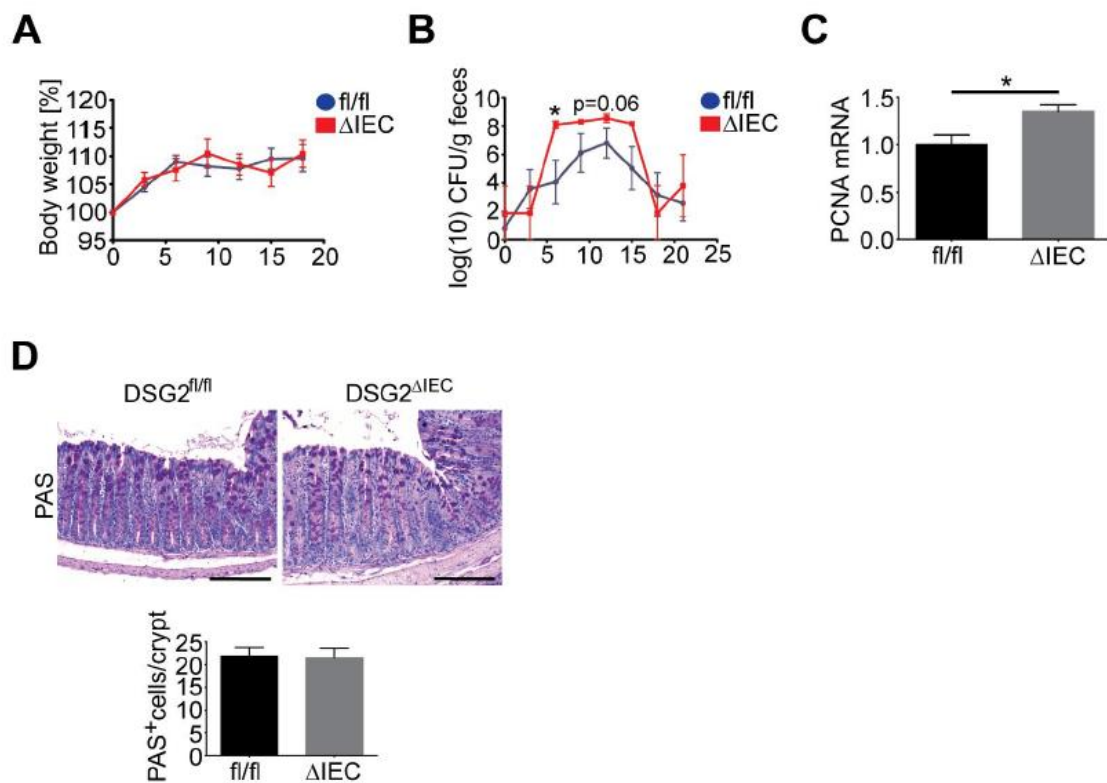
Gross et al., Suppl. Fig. 9

Supplementary Figure 9. DSG2-deficient animals (DSG2 Δ IEC) display an altered desmosomal protein composition. The OD (optical density) values from the immunoblots of colonic tissues from DSG2 Δ IEC (Δ IEC) mice and their floxed littermates (fl/fl) were normalized to the OD values of β -tubulin (n=3) (for representative pictures see Figure 2D). Average levels in fl/fl mice were arbitrarily set as 1 and the amounts in Δ IEC mice were presented as ratio. Dsp, desmoplakin; PG, plakoglobin; Pkp2, plakophilin 2; K8, keratin 8; Tub, β -tubulin. Two-tailed Student's t test was used for statistical analyses. *p<0.05, **p<0.01, ***p<0.001.

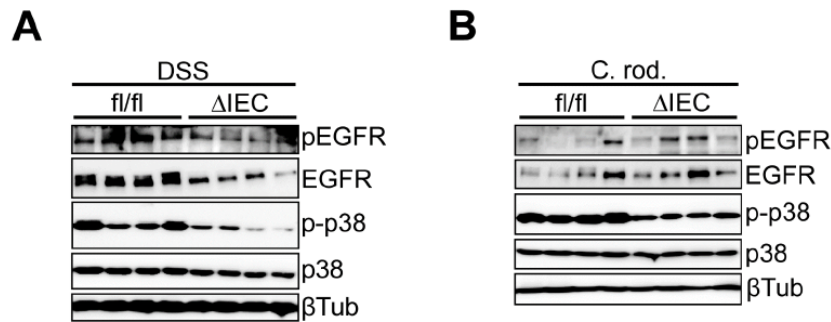
Gross et al., Suppl. Fig. 10

Supplementary Figure 10. DSG2-deficient animals (DSG2^{ΔIEC}) have altered levels of the tight junction proteins claudin 1 and occludin. (A,C) Immunoblotting was used to study the impact of Dsg2 deficiency on the composition of key tight/adherens junction proteins in the colons of DSG2^{ΔIEC} mice and their floxed littermates (DSG2^{fl/fl}). The activation of myosin II regulatory light chain (MLC) signalling as the regulator of tight junction permeability was also assessed. β-tubulin was used as a loading control. (B) The distribution of tight and adherens junctions in the colonic sections was visualized with antibodies against E-cadherin, ZO-1, Claudin 1 and Claudin 15, respectively. Scale bar = 20 μm. ZO-1, zonula occludens-1.

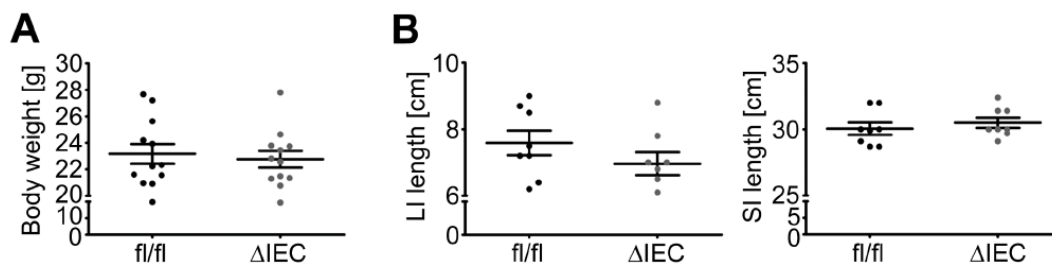
Gross et al., Suppl. Fig. 11



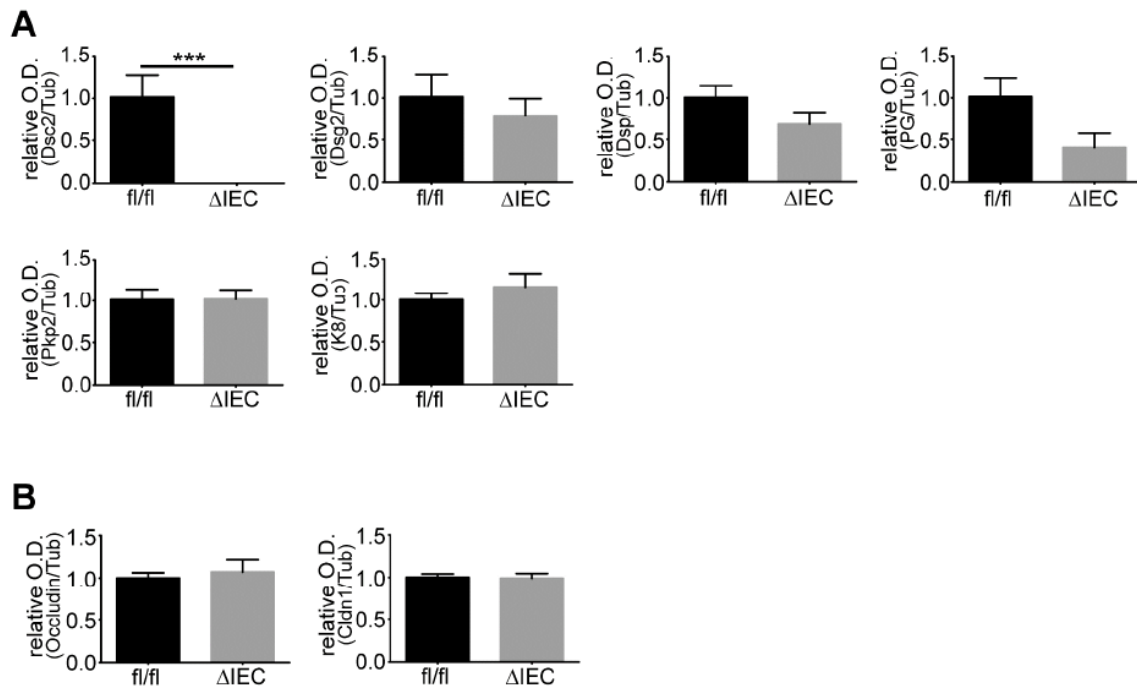
Supplementary Figure 11. DSG2-deficient animals (DSG2 Δ IEC) infected with *C. rodentium* display higher PCNA levels. (A) The relative body weight of DSG2 Δ IEC mice (red rectangles, Δ IEC) and their floxed littermates (blue circles, fl/fl) was measured (n=7). (B) *Citrobacter rodentium* colonization in the stool was quantified as the amount of colony forming units (CFUs) on MacConkey agar plates at the indicated days (n=5). (C) Colonic PCNA mRNA expression was assessed by real time RT-PCR (n=4-7). (D) Periodic acid-Schiff (PAS) staining with subsequent quantification of PAS-positive cells/crypt indicated a similar amount of goblet cells in colons from both genotypes (n=8). Real time RT-PCR and histological analysis were performed 14 days after oral infection with *C. rodentium*. L7 (mouse ribosomal protein) gene was used as an internal control. Average mRNA expression in fl/fl mice was arbitrarily set as 1 and levels in Δ IEC mice were presented as ratio. Two-tailed Student's t test were used for statistical analyses. *p<0.05

Gross et al., Suppl. Fig. 12

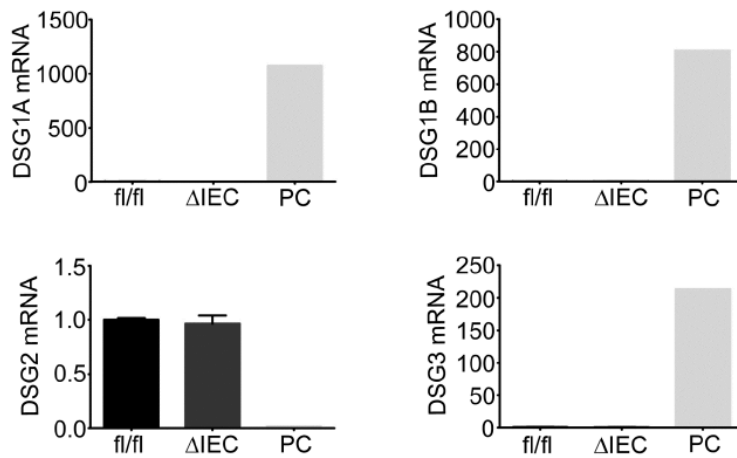
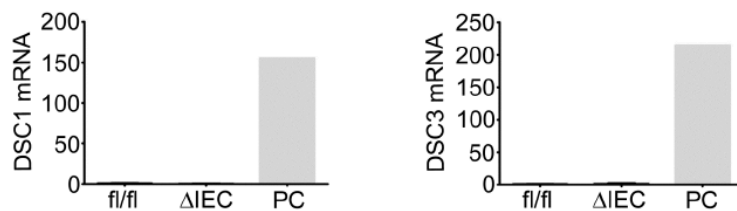
Supplementary Figure 12. DSG2-deficient animals ($DSG2_{\Delta IEC}$) do not show an activation of the analyzed signaling pathways. Immunoblotting revealed no obvious activation of EGFR and p38 signaling pathways in colons of DSG2-deficient (Δ IEC) mice compared to their floxed littermates (fl/fl). Mice were analysed after 4 days of DSS treatment or 14 days after exposure to *C. rodentium*. β -tubulin (β Tub) was used as a loading control. p, phospho.

Gross et al., Suppl. Fig. 13

Supplementary Figure 13. DSC2-deficient animals ($DSC2_{\Delta IEC}$) demonstrate normal body weight and small and large intestinal lengths. (A) The body weights of 11 weeks old $DSC2_{\Delta IEC}$ (Δ IEC) mice and their floxed littermates (fl/fl) were analysed (n=12). (B) The large (LI) and small intestinal (SI) lengths were measured in both genotypes (n=8). Data are shown as dot plots.

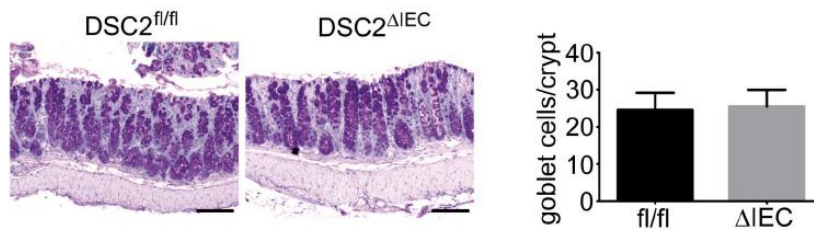
Gross et al., Suppl Fig. 14

Supplementary Figure 14. DSC2-deficient animals ($DSC2^{\Delta IEC}$) show no obvious alterations in the desmosomal and tight junction protein composition. (A,B) The OD (optical density) values were determined from the immunoblots of colonic tissues from $DSC2^{\Delta IEC}$ (ΔIEC) mice and control littermates (fl/fl). The values were normalized to the OD values of β -tubulin (n=5) (for representative pictures see Figure 6A,B). The values in fl/fl mice were arbitrarily set as 1 and levels in ΔIEC mice were presented as ratio. Cldn1, claudin 1; Dsp, desmoplakin; PG, plakoglobin; Pkp2, plakophilin 2; K8, keratin 8. Two-tailed Student's t test was used for statistical analyses. ***p<0.001.

Gross et al., Suppl. Fig. 15**A****B**

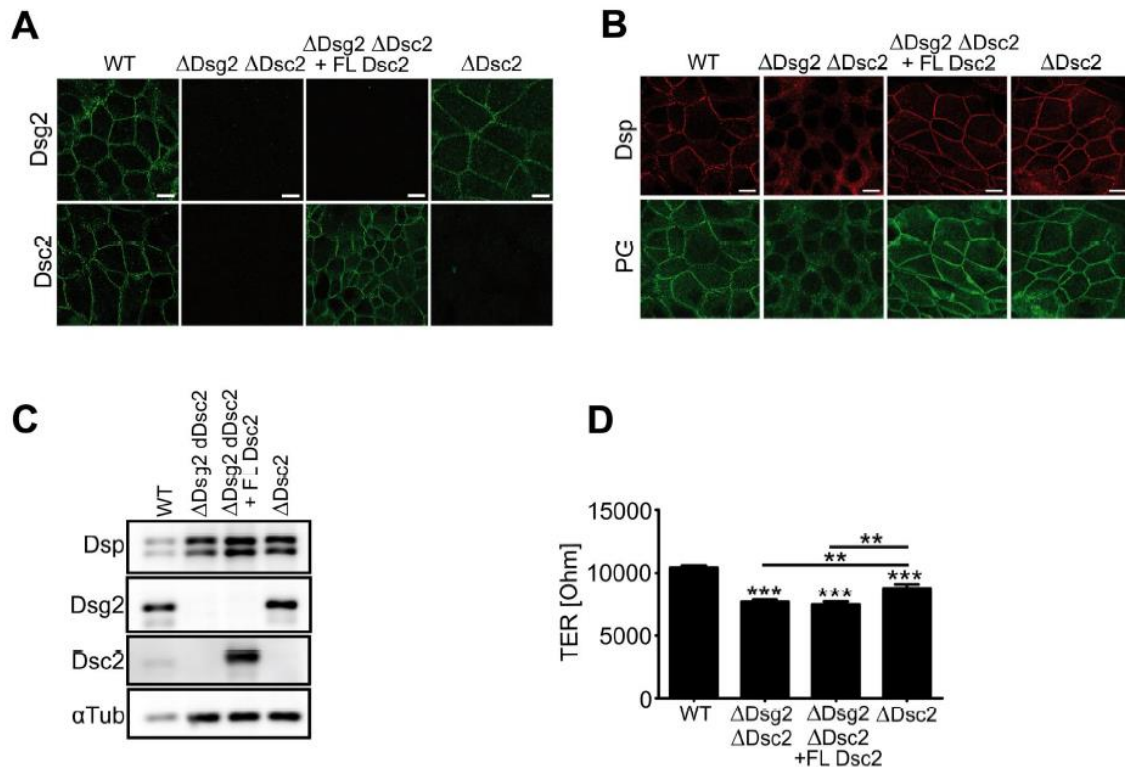
Supplementary Figure 15. Knockout of DSC2 does not alter the expression of other desmoglein and desmocollin isoforms. mRNA levels of the desmoglein family members DSG1a, DSG1b, DSG2 and DSG3 (A) as well as the desmocollin members DSC1 and DSC3 (B) were analyzed in the colon of DSC2 Δ IEC (Δ IEC) and DSC2 $^{fl/fl}$ (fl/fl) mice by real time RT-PCR (n=4). Skin was used as a positive control (PC) and L7 (mouse ribosomal protein) as an internal control. Average mRNA expression in fl/fl mice was arbitrarily set as 1 and levels in Δ IEC mice as well as the skin represent a ratio.

Gross et al., Suppl. Fig. 16



Supplementary Figure 16. DSC2-deficient animals ($DSC2^{\Delta IEC}$) display no alteration in the goblet cell amount. Periodic acid-Schiff (PAS) staining with subsequent quantification of PAS-positive cells/crypt showed a similar amount of goblet cells in colons of $DSC2^{\Delta IEC}$ (ΔIEC) and floxed control mice ($DSC2^{fl/fl}$ or fl/fl) (n=4). Scale bar = 200 μ m.

Gross et al., Suppl. Fig. 17



Supplementary Figure 17. Knockout DLD1 cells lacking both desmoglein 2 (Dsg2) and desmocollin 2 (Dsc2) display a loss of membranous desmoplakin

(Dsp) and plakoglobin (PG) staining and exhibit a decreased transepithelial electrical resistance (TER). (A, B) The distribution of Dsc2, Dsg2, plakoglobin (PG) and desmoplakin (Dsp) in DLD1 wildtype (WT) and knockout cell lines was visualized by immunofluorescence. Scale bar = 10 μ m. Δ Dsg2 Δ Dsc2 = knockout of both Dsg2/Dsc2, Δ Dsg2 Δ Dsc2 + FL Dsc2 = Dsg2/Dsc2 knockout + re-introduction of full length Dsc2, Δ Dsc2 = Dsc2 knockout. (B) Immunoblotting was employed to study the impact of desmosomal cadherin loss on desmosomal protein levels. α -tubulin (α Tub) was used as a loading control. (C) TER values were assessed in DLD1 WT and the corresponding knockout cells ($n \geq 10$), ** $p < 0,001$, *** $p < 0,001$ compared to control.

2.4 Glial cell-line derived neurotrophic factor (GDNF) regulates intestinal barrier function in inflammatory bowel diseases by stabilization of desmoglein 2

Glial cell-line derived neurotrophic factor (GDNF) regulates intestinal barrier function in inflammatory bowel diseases by stabilization of desmoglein2

Short title: GDNF regulates intestinal barrier in inflammation

Michael Meir¹, Natalie Burkard¹, Hanna Ungewiß², Markus Diefenbacher³, Sven Flemming¹, Felix Kanapin¹, Christoph-Thomas Germer¹, Matthias Schweinlin⁴, Marco Metzger⁴, Jens Waschke², Nicolas Schlegel¹

¹ Department of General, Visceral, Vascular and Pediatric Surgery University Hospital Würzburg, Oberduerrbacherstrasse 6, 97080 Würzburg, Germany

² Institute of Anatomy and Cell Biology, Department I, Ludwig-Maximilians-Universität München, Pettenkoferstrasse 11, 80336 Munich, Germany

³ Department of Biochemistry and Molecular Biochemistry, University of Würzburg, Am Hubland, 97074 Würzburg

⁴ Department for Tissue Engineering and Regenerative Medicine, University Hospital Würzburg, Roentgenring 11, 97070 Würzburg, Germany

Grant: These studies were supported by the Deutsche Forschungsgemeinschaft (DFG) Priority Program SPP 1782 to N. Schlegel and J. Waschke and by the Interdisziplinäre Zentrum für Klinische Forschung (IZKF) Z-2/63

Correspondence:

Priv.-Doz. Dr. Nicolas Schlegel

Department of General, Visceral, Vascular and Pediatric Surgery

University Hospital Würzburg,

Oberduerrbacherstrasse 6,

97080 Würzburg, Germany

Phone: +49 931 201 38217

e-mail: Schlegel_N@ukw.de

Authors' contributions:

MM: study concept, experiments, drafting figures and manuscript

NB: study concept, experiments, drafting figures and manuscript

HU: experiments, drafting figures and manuscript

MD: experiments and drafting manuscript

SF: study concept, experiments, drafting manuscript

FK: experiments

CTG: study concept, drafting manuscript

MS: experiments, drafting manuscript

MaM: experiments, drafting manuscript

JW: study concept, drafting figures and manuscript

NS: study concept, experiments, drafting figures and manuscript

Abbreviations used in this paper:

IEB intestinal epithelial barrier

GDNF Glial cell-line derived neurotrophic factor

IBD inflammatory bowel disease

CD Crohn's disease

UC ulcerative colitis

IF intermediate filaments

Dsg2 desmoglein2

Dsc2 desmocollin2

MAPK mitogen-activated protein kinase

TNF α Tumor necrosis factor α

AFM atomic force microscopy

DSS Dextran Sulfate Sodium

Abstract

Background / Aim

Breakdown of the intestinal epithelial barrier (IEB) is a hallmark in the pathogenesis of inflammatory bowel diseases (IBD). Glial cell line derived neurotrophic factor (GDNF) secreted by enteric glial cell promotes IEB function by undefined mechanisms. We hypothesized a critical contribution of GDNF on loss of IEB in IBD and investigated the underlying mechanism.

Methods

Gut specimen of patients suffering from IBD were analyzed. *In vitro*, conventional cell biology methods in Caco2 cells and human intestinal enteroids were applied. *In vivo*, Dextran Sodium Sulfate (DSS) was used to induce colitis in C57Bl6 mice.

Results

In intestinal specimen from IBD patients GDNF was significantly reduced in inflamed parts of the tissues. This reduction was paralleled by a loss of desmosomal junctional protein desmoglein2 (Dsg2), changes of the intermediate filament (IF) system, increased phosphorylation of p38 mitogen-activated protein kinase (MAPK) and cytokeratins. In Caco2 cells GDNF recruited Dsg2 to the cell borders and augmented Dsg2-mediated intercellular adhesion. The specificity of these effects on Dsg2 was proven in Dsg2-deficient cells that did not respond to GDNF. Incubation of Caco2 cells and enteroids with $\text{TNF}\alpha$ led to impaired IEB function with reduced Dsg2, which was mediated by p38MAPK-dependent phosphorylation of cytokeratins. $\text{TNF}\alpha$ -induced changes were blocked by GDNF. Similarly, in mice with DSS-colitis loss of Dsg2, breakdown of IEB, phosphorylation of p38MAPK and cytokeratins were all attenuated by treatment with GDNF.

Conclusion

GDNF attenuated inflammation-induced breakdown of IEB caused by p38MAPK-dependent cytokeratin phosphorylation leading to loss of Dsg2. Reduced GDNF in IBD patients indicates a disease-relevant contribution to breakdown of IEB.

Keywords: GDNF, inflammatory bowel disease, intestinal barrier, inflammation, desmosomes, desmoglein2, intermediate filaments, cytokeratins, keratin phosphorylation, p38MAPK enterocyte

Introduction

Inflammatory bowel diseases (IBD) i.e. Crohn's disease (CD) and ulcerative colitis (UC) are caused by a complex interplay between environmental factors, the composition of gut microbiota and an inappropriate immune response in genetically predisposed individuals (Geremia et al., 2014; Uhlig, 2013). In addition, recent evidence suggests that dysregulation of the intestinal epithelial barrier (IEB) plays a major role in the development and perpetuation of IBD (Martini et al., 2017).

Under normal conditions, the IEB is built by a monolayer of polarized enterocytes, which are sealed and held together by different junctional proteins such as tight junctions, adherens junctions and desmosomes (Farquhar and Palade, 1963b; Luissint et al., 2016). Previously it was shown that besides profound changes in tight junction integrity, loss of the desmosomal cadherin desmoglein2 (Dsg2) in intestinal epithelium plays a critical role in the pathogenesis of barrier dysfunction in patients with CD (Vielmuth et al., 2015). Desmosomes in intestinal epithelium consist of the cadherin-type adhesion molecules desmoglein 2 (Dsg2) and desmocollin 2 (Dsc2), which are tethered to the intermediate filament cytoskeleton through specific desmosomal plaque proteins. Therefore, desmosomal function is dependent from dynamics in the intermediate filament system which is known to be regulated by p38 mitogen-activated protein kinase (p38MAPK) (Berkowitz et al., 2005; Kitajima, 2014). The pro-inflammatory cytokine tumor necrosis factor α (TNF α) which is regarded as the critical link between increased intestinal permeability and immune reaction in IBD (Sanders, 2005) was shown to increase intestinal epithelial permeability by p38MAPK-dependent loss of Dsg2-mediated adhesion (Vielmuth et al., 2015).

It is known that the enteric nervous system (ENS) and factors secreted by enteric glial cells are critically involved in the regulation of IEB and therefore may be an unappreciated pathogenicity factor in the development of IBD (Neunlist et al., 2003). In support of this idea, it was reported that enteric glial cells in specimen of patients

suffering from IBD were reduced and experimental studies showed that toxic or autoimmune ablation of enteric glial cells lead to loss of the IEB (Bush et al., 1998; Cornet et al., 2001). A potential key player that is secreted by enteric glial cells is Glial cell-line derived neurotrophic factor (GDNF). Loss of GDNF in experimental models leads to morphological and functional abnormalities of IEB similar to those seen in IBD patients (Brun et al., 2013; Steinkamp et al., 2003). Furthermore, GDNF shows anti-inflammatory effects in a murine model of colitis (Zhang et al., 2010a) and was previously shown to exert direct effects on enterocytes *in vitro* which lead to the maturation of tight junctions in the IEB by largely unknown mechanisms (Meir et al., 2015a; Meir et al., 2016).

Based on this, we tested the hypothesis that GDNF critically regulates Dsg2-dependent integrity of the intestinal barrier and is thereby involved in the pathogenesis of barrier dysfunction in IBD.

Materials and Methods

Test reagents

Caco2 cells and human enteroids were treated with 100ng/ml recombinant human GDNF (PeproTech, Hamburg, Germany)(Meir et al., 2015a). TNF α (Biomol, Hamburg, Germany) was used at 100ng/ml (Vielmuth et al., 2015). The p38MAPK inhibitor SB202190 was used at 30 μ M (Callbiochem, Darmstadt, Germany) and anisomycin (Sigma-Aldrich, Munich, Germany) was used at 60 μ mol/l to activate p38MAPK (Meir et al., 2015a).

Human tissue samples

Human tissue samples derived from patients suffering from IBD with an indication for surgical resection. Tissue samples from patients with Crohn's disease (n= 9) derived from the terminal ileum. They were taken from the center of the inflamed parts of the resection specimen and from the periphery where no inflammation was seen. During the surgical procedure the extent of inflammation in the resection specimen was estimated by the surgeon using a semi-quantitative score according to the macroscopic impression (+ major inflammation, - minor inflammation). In patients with ulcerative colitis (n= 9) a sample of the affected colon was taken. Control tissue samples (colon or terminal ileum) from patients not suffering from IBD derived from patients that required right or left hemi-colectomy due to colon carcinoma in which the surgical resection routinely involves a part of the healthy small intestine or colon, respectively. All patients had given their informed consent before surgery, and ethical approval was given by the Ethical Board of the University of Würzburg (proposal numbers 113/13, 46/11, 42/16).

For Western blot analyses, samples of the mucosa and whole gut wall were taken immediately after resection from each specimen and then snap frozen in liquid nitrogen and processed for Western Blot analyses. A second part of the tissue samples was fixed in 4% paraformaldehyde embedded in paraffin, sectioned (1 μ m) and immunostaining was performed as described previously(Vielmuth et al., 2015) and in *supplementary methods*.

Cell Culture

Caco2 cells were acquired from ATCC (Wesel, Germany) and were cultured in Eagle's Minimum Essential Medium (EMEM, ATCC, Wesel, Germany) supplemented with 50 U/ml Penicillin-G, 50µg Streptomycin and 10% fetal calf serum (FCS, Biochrom, Berlin, Germany). Cultures were used for experiments when grown to confluent monolayers. For experiments, cells were serum-starved for 24h.

Generation of CRISPR/Cas9-mediated gene knockout for Dsg2 in Caco2 cells

Caco2 cells deficient for Dsg2 were generated using the CRISPR/Cas9 technique as described in the *supplementary methods*.

Enteroids

IECs were isolated from human whole gut wall resections, 1cm² in size as described in the *supplementary methods* and as described previously (Schweinlin et al., 2016).

Animal experiments

After animal care committee approval (Laboratory Animal Care and Use Committee of the district of Unterfranken; AZ 2-272), experiments were performed on male C57BL/6J mice. Animals were kept under conditions that conformed to the National Institutes of Health "Guide for the Care and Use of Laboratory Animals" approved by the Government of Unterfranken and Germany as well as for those of the US National Institutes of Health. Animals were kept on a standard diet at 12h day-and-night cycles.

Experimental setup

We used Dextran Sulfate Sodium (DSS) as a murine model for induction of colitis. 8 weeks old male mice received 2.5% DSS in autoclaved drinking water *ad libitum*. Mice were monitored daily to document a disease activity index (DAI) for body weight, changes of stool consistency and presence of blood in the stool using *Haemocult* (Care diagnostica, Voerde, Germany) as suggested previously using following scoring system(Chassaing et al., 2014): Normal stool consistency with negative haemoccult (0); soft stools with positive haemoccult (1); very soft stools with traces of blood (2); watery stools with visible rectal bleeding (3). Animals were randomized in two groups. GDNF

treated animals (n=9) received 5µg/kg bodyweight of GDNF in 100µl 0.9% NaCl intraperitoneally, while DSS-alone animals (n = 9) received 100µl 0.9 % NaCl every 24 hours.

Measurement of intestinal permeability and tissue harvesting

After 6 days, the mice were anaesthetized using isoflurane (Forene, Abbott, Wiesbaden, Germany). In deep anesthesia, a median laparotomy was performed and the colon was mobilized and opened at the ileocaecal valve and at the upper rectum.

After a flush with warm PBS to remove blood and stool the colon was ligated and 200µl of 4kDa FITC dextran (1mg/ml) was injected in the ligated colon to determine intestinal permeability by measuring the translocation of 4 kDa FITC dextran in the blood. For this, blood from the inferior vena cava was taken after 1h and centrifuged at 13.400 rpm for 10 minutes at 4°C. Afterwards the luminescence of the serum was quantified using Genios Pro Reader (Tecan, Maennedorf, Switzerland).

Thereafter mice were sacrificed by exsanguination. The complete colon was harvested and Colon length was measured. The ligations of the colon were loosened and afterwards the Colon was cut into two pieces. One part was fixed in 4% paraformaldehyde embedded in paraffin and sectioned. Two blinded investigators quantified the inflammation of the tissue in H.E.-stained sections of the colon using the following inflammation score(Erben et al., 2014): Extent of inflammatory cell infiltration (none =1, mucosal infiltration =2, submucosal infiltration =3 transmural infiltration =4) and severity of epithelial damage (no epithelial damage =1, focal lesions =2, multiple lesions =3, extended ulcerations =4), resulting in a total scoring range of 2 –8 per mouse. The other half of the colon was lysed and homogenized with a Tissue Lyzer (Quiagen, Hilden, Germany) in a SDS lysis buffer and used for Western Blot analysis and quantification of GDNF concentrations using GDNF ELISA (Promega, Mannheim, Germany). The GDNF ELISA is described in the *supplementary methods*.

Immunocytochemistry

Immunocytochemistry is described in the *supplementary methods* in detail.

Western Blotting

Cells, human and animal tissue lysates were prepared and processed for Western Blots as described in the *supplementary methods*.

Membrane Protein Extraction Assay

Protein fractionation was carried out using Mem-Per Plus Kit (Thermo Fischer, Waltham, MA, USA). Cells were harvested in growth media by scraping them from the bottom with a cell scraper. After centrifugation at 300rpm for 5 minutes and washing three times, the cells were permeabilized with a permeabilisation buffer to release the cytosolic fraction. The cytosolic fraction was separated by centrifugation at 16000rpm for 15 minutes. The pellet containing the membrane-associated proteins was then re-suspended in a solubilisation buffer. The suspension was centrifuged another time at 16000rpm for 15 minutes to remove particulate material. Then the cytosolic and membrane-associated supernatants were used for Western Blot analysis.

Atomic Force Microscopy (AFM)

Cells were grown on glass coverslips and treated with GDNF (100ng/ml) 1 day before getting confluent or with 4mM EGTA for 30 min after finished control measurements. For analysis of Dsg2 interactions on the surface of living cells, a Nanowizard III AFM (JPK Instruments, Berlin, Germany) mounted on an optical microscopy (Carl Zeiss, Jena, Germany) was used. The approach of AFM force spectroscopy on living cells was described in detail before (Vielmuth et al., 2015) and was carried out as described in the *supplementary methods*.

Dispase-based enterocyte dissociation assays

As described previously (Vielmuth et al., 2015), confluent cells in 24-well plates were exposed to the test reagents as indicated below, washed with Hank's buffered saline solution (HBSS, Sigma-Aldrich, Munich, Germany) and incubated with Dispase-II (Sigma-Aldrich, Munich, Germany) for 30 minutes to release the monolayer from the well bottom. Afterwards, the cell sheet was exposed to shear stress by pipetting 5 times. Four fields of view were photographed with BZ-9000 (BIOREVO, Keyence, Osaka, Japan) and numbers were quantified.

Measurements of Transepithelial Electrical Resistance (TER)

To measure transepithelial electrical resistance (TER) we used ECIS trans-Filter Adapter for ECIS 1600R across cell monolayers (Applied Biophysics, Ibidi GmbH, Martinsried, Germany). Cells were seeded on 24-well transwell chambers and measurement started immediately. At confluency of monolayers cells were treated with or without mediators as indicated below.

Statistics

Statistical analysis was performed using Prism (GraphPad Software, La Jolla, CA, USA). Data are presented as means \pm SE. Statistical significance was assumed for $p < 0.05$. Paired Student's t-test was performed for two-sample group analysis after checking for a Gaussian distribution. Analysis of variance (ANOVA) followed by Tukey's multiple comparisons test and Bonferroni correction was used for multiple sample groups.

Results

Reduced GDNF in the terminal ileum and colon of IBD patients is associated with loss of barrier function

Western Blot analyses of specimen from patients suffering from CD or UC showed a significant loss of GDNF in full wall lysates when compared to control lysates. This was not observed in uninflamed parts of the tissues of CD patients (Figure 1A). Loss of GDNF in CD and UC was paralleled by loss of the desmosomal adhesion protein Dsg2 at the cell borders in immunostaining of inflamed terminal ileum of CD patients (Figure 1Bc, d) or inflamed colon of UC patients (Figure 1Bk, l) compared to healthy controls of the terminal ileum (Figure 1Ba, b) and colon (Figure 1Bi, j) where Dsg2 was regularly distributed along the cell borders. The intermediate filament system as revealed by cytokeratin 18 staining was profoundly deranged in both CD and UC samples (Figure 1Bg, h, o, p) when compared to healthy controls (Figure 1Bm, n). Western blot analyses showed a significant reduction of Dsg2 in CD and UC samples (Figure 1C). Because Dsg2 is known to be regulated by p38MAPK (Ungewiss et al., 2017) and we observed alterations of cytokeratins in immunostaining we tested whether phosphorylation of these proteins was altered in IBD. In CD and in CU samples phosphorylation of p38MAPK as well as phosphorylation of cytokeratins 18 and 8 were significantly increased in Western Blot analyses (Figure 1C). The activation of p38MAPK and the phosphorylation of cytokeratin appeared to be dependent on the extent of inflammation (Suppl. Fig. 1 and 2).

GDNF effects on IEB are mediated via Dsg2

These observations in patients led to the hypothesis that GDNF might be critically involved in the regulation of Dsg2 and thereby contribute to loss of barrier function in IBD. In a first step, the effects of GDNF on Dsg2 were evaluated in Caco2 monolayers. Immunostaining showed that application of 100 ng/ml recombinant GDNF in confluent monolayers resulted in augmented staining patterns of Dsg2 at the cell borders (Figure 2A). While GDNF application did not increase total protein levels of Dsg2 (Figure 2B), triton extraction assays showed Dsg2 to be significantly increased in the

insoluble fraction which is considered to contain cytoskeleton-bound proteins following GDNF treatment (Figure 2C).

To explore the functional effect of GDNF on Dsg2 binding properties and distribution on the cell surface atomic force microscopy (AFM) was applied on living enterocytes similar to recent studies (Schinner et al., 2017; Ungewiss et al., 2017; Vielmuth et al., 2015). Imaging of the cell surface topography revealed a microvillus covered surface typical for polarized Caco2 cells and elevated cell-cell borders which allowed specific measurements at these areas (Fig. 2D). To examine Dsg2 binding properties, adhesion measurements with a Dsg2-coated tip of a flexible AFM cantilever on living cells were performed. For this purpose, 2 cell-cell border containing areas were selected for each condition with 1000 recorded force-distance curves for each area. To ensure comparability between different conditions, measurements under control conditions and on cells incubated with GDNF or EGTA were always performed with the same AFM cantilever. Under control conditions, binding events were detected with an unbinding force of around 29 pN as revealed by peakfit analysis (Fig. 2E) which resembles the values of previously measured Dsg2 specific unbinding forces on the surface of living enterocytes (Ungewiss et al., 2017). Application of GDNF significantly increased the amount of measured binding events by around 50 % (Fig. 2F, G). Additionally, EGTA was applied to demonstrate specificity of measured binding events as Ca^{2+} depletion disrupts Ca^{2+} -dependent cadherin binding. After 30 min of EGTA-mediated Ca^{2+} depletion, binding frequency was significantly reduced by around 40 % compared to control conditions (Fig. 2G). Since measured binding events after incubation with GDNF appeared to be more prominent at cell-cell borders (Fig. 2F), it was examined next whether the localization of Dsg2 specific binding events was altered compared to control conditions. Therefore, a distribution ratio defined as the percentage of measured binding events along the cell borders (cb) versus measured binding events on the cell surface was calculated (cs) (Fig. 2H). Indeed, the distribution ratio was significantly increased after incubation with GDNF. Together, these data indicate that application of GDNF either results in a redistribution of existing Dsg2-specific interactions or promotes the emergence of new Dsg2-specific interactions along the cell borders.

To verify that effects of GDNF on the IEB were primarily mediated by its effects on Dsg2 a Dsg2-deficient Caco2 (Dsg2 (-/-)) cell line was generated using the CRISPR/CAS9 technique (Figure 2I). In Caco2 cells transfected with nonsense vectors application of 100 ng/ml recombinant GDNF led to increased TER values of 1.5-fold compared to untreated controls (Figure 2J). In Dsg2 (-/-) Caco2 cells application GDNF did not show any effect on TER (Figure 2K) which confirmed that GDNF effects were dependent on Dsg2.

TNF α -induced cyokeratin retraction and loss of Dsg2 are blocked by GDNF

TNF α was used to mimic inflammation-induced alterations in differentiated Caco2 monolayers. Application of TNF α induced a significant reduction of TER to 0.73 ± 0.05 -fold of baseline values after 8h (Figure 3A). Combined treatment of monolayers with TNF α and GDNF completely blocked TNF α -induced loss of TER. Following application of GDNF Dsg2 was significantly reduced in triton extraction assays in the insoluble fraction i.e. in the cytoskeleton-bound fraction compared to controls. Combined treatment of cells with TNF α and GDNF inhibited loss of Dsg2 in the triton-insoluble fraction (Figure 3B; Suppl. Figure 3A). This observation was confirmed in immunostaining when Dsg2 which was regularly distributed at the cell borders in differentiated Caco2 cells (Figure 3Ca, arrows) and in enteroids (Figure 3Da, arrows) under control conditions was reduced after application of TNF α (Figure 3Cc and 3Dc). The loss of Dsg2 from the cell borders was attenuated by simultaneous application of TNF α and GDNF in Caco2 monolayers (Figure 3Ce, arrows) and in enteroids (Figure 3De, arrows).

Intermediate filaments visualized by cytokeratin18 immunostaining were present as a keratinring in the cell periphery under control conditions (Figure 3Cd, arrows). Application of TNF α led to a significant retraction of the intermediate filament ring (Figure 3Cd, arrows) which was diminished after combined treatment of cells with TNF α and GDNF (Figure 3Cf). The visual impression of changes within the intermediate filament system were quantified und thereby confirmed by measurements

of fluorescence intensity at the cell borders and distance of retraction of the keratinring from the cell borders (Suppl. Figure 3B, C).

In human intestinal enteroids, comparable observations were made for cytokeratin18: The keratinring was present in the cell periphery under control conditions (Figure 3Dd) and was profoundly deranged after TNF α application (Figure 3Dd). Following application of TNF α and GDNF attenuated TNF α -induced changes of intermediate filaments (Figure 3Df).

In disperse-based enterocyte dissociation assays incubation of differentiated Caco2 (Caco2 Dsg2 (+/+)) cells with TNF α led to a significantly increased number of cell fragments which was completely blocked by simultaneous application of TNF α and GDNF (Figure 3E). In Caco2 Dsg2 (-/-) we found increased cell dissociation compared to Caco2 Dsg2 (+/+) under basal conditions which was significantly augmented after application of TNF α . However, in the absence of Dsg2 increased cell dissociation was not blocked by application of GDNF (Figure 3F). Application of GDNF alone had no effect on basal cell dissociation in both cell lines.

Inflammation-induced effects on Dsg2 are mediated by activation of p38MAPK and phosphorylation of cytokeratin18

Given the alternating activation or inactivation of p38MAPK by TNF α and GDNF, we hypothesized that epithelial barrier protection by GDNF is mediated by affecting p38MAPK followed by modulation of the intermediate filament system. Accordingly, phosphorylation of p38MAPK was significantly increased following incubation with TNF α in Caco2 cells and in enteroids (Figure 4A, B). Simultaneous application of TNF α and GDNF significantly attenuated phosphorylation of p38MAPK while GDNF alone did not alter phosphorylation of p38MAPK significantly below baseline levels (Figure 4A, B, suppl. Figure 4A, B).

Because a correlation of phosphorylated cytokeratins with intestinal barrier function was suggested previously (Majumdar et al., 2012) phosphorylation of cytokeratins 18 and 8 were analyzed following treatment with TNF α or TNF α and GDNF, respectively. In

both, Caco2 cells and in enteroids application of TNF α resulted in significantly augmented phosphorylation of cytokeratin 18 at serin52 and cytokeratin 8 at serin74 in Caco2 cells and in enteroids (Figure 4A, B, suppl. Figure 4B, C, D). In contrast, no changes of phosphorylation patterns were detected for cytokeratin 18 at serin33 (suppl. Figure 5C, D). Application of TNF α together with GDNF blocked phosphorylation of both cytokeratin 18 and cytokeratin 8 (Figure 4A, B, suppl. Figure 4B, C, D).

Further experiments showed that increased phosphorylation of cytokeratin 18 and 8 by TNF α was inhibited by simultaneous treatment of cells with p38MAPK inhibitor SB202190. Application of SB202190 alone resulted in reduced phosphorylation of cytokeratin 18 and 8 below control levels (Figure 4C; suppl. Figure 5A, B). Vice versa, activation of p38MAPK by incubating Caco2 cells with anisomycin (Vielmuth et al., 2015) resulted in significantly increased phosphorylation of cytokeratin 18 and 8. These experiments demonstrated that cytokeratin phosphorylation in intestinal epithelial cells is mediated by activation of p38MAPK.

In immunostaining of Caco2 monolayers application of TNF α and SB202190 blocked TNF α -induced loss of Dsg2 at the cell borders (Figure 4Dc, e) and cytokeratin retraction as revealed by cytokeratin 18 immunostaining was not detectable any more (Figure 4Dd, f). While treatment of cells with SB2021090 alone did not induce visible alterations of Dsg2 and cytokeratin staining (Figure 4Dg, h), application of anisomycin to activate p38MAPK showed a strong increase in phosphorylation of both cytokeratins 18 and 8 which resulted in loss of Dsg2 at the cell borders in immunostaining and cytokeratin retraction, comparable to the effects observed after TNF α treatment (Figure 4Di, j).

GDNF attenuates loss of IEB and inflammation in DSS-colitis

To determine the effects of GDNF on IEB in an *in vivo* model of intestinal inflammation we induced acute colonic injury with 2.5% DSS in mice. C57Bl6 mice (n=18) received 2.5% DSS in autoclaved drinking water ad libitum, while control mice received normal drinking water. The DSS mice were divided into two groups. One group (n=9) was treated daily with 5 μ g/kg bodyweight of GDNF in 100 μ l 0.9% NaCl intraperitoneally (DSS + GDNF) whereas the other group received 100 μ l of 0.9% NaCl (DSS). The

effective administration of GDNF had been verified in preliminary experiments in ELISA-based measurements of GDNF serum concentrations and in tissue lysates of the colon (suppl. Figure 6A, B).

Following DSS application, a significant increase to 2.11 ± 0.26 of the DAI was obvious after 5 days (Figure 5A). This was attenuated in the DSS+GDNF group where DAI was significantly lower at 1.22 ± 0.15 . Measurements of colon length was 70.05 ± 1.48 mm in the control group. Due to DSS-induced inflammation the colon length was significantly reduced to 49.11 ± 0.84 mm (suppl. Figure 6D). GDNF application in the DSS+GDNF group led to a significantly less reduction of colon length to 55.1 ± 1.7 mm. Intestinal permeability as revealed by measurements of 4 kDa FITC-dextran flux across the IEB was significantly increased to 9.9 ± 1.3 -fold of controls (Figure 5B). Treatment of animals with GDNF (DSS+GDNF) significantly attenuated inflammation-induced loss of the intestinal barrier.

Histological analyses of H.E.-staining revealed an acute inflammation of the colon following DSS administration with an inflammation score of 6.7 ± 0.8 (Figure 5Ca-c, D). Treatment of animals with GDNF resulted in a visible reduction of inflammation in H.E.-staining (Figure 5Cc) which was reflected by a significant reduction of the inflammation score (Figure 5D). Comparable to observation made in patients with IEB, in Caco2 monolayers and in enteroids immunostaining of animals with DSS-colitis showed significant loss of Dsg2 at the cell borders which was attenuated by treatment of DSS animals with GDNF (Figure 5Cd-f suppl. Figure 6 E). Similarly, deranged organization patterns of cytokeratin 18, which was observed in DSS animals were blunted by treatment of animals with GDNF (Figure 5Cg-i). In Western Blot analyses phosphorylation of p38MAPK and cytokeratin18 was significantly increased in DSS-colitis, which was both attenuated by treatment with GDNF (Figure 5E, suppl. Figure 6 F).

Discussion

In the present study, we show a novel mechanism which contributes to the loss of IEB in patients with IBD: The neurotrophic factor GDNF was reduced in samples from IBD patients, which correlated with loss of Dsg2 and alterations of the intermediate filament system. *In vitro* experiments in Caco2 cells showed that GDNF acts via stabilization of desmosomal protein Dsg2, which was proven by the fact that Caco2 cells deficient for Dsg2 showed no response when stimulated by GDNF. In Caco2 cells and in human enteroids GDNF was effective to protect against inflammation-induced loss of Dsg2 and breakdown of intestinal barrier function as revealed by measurements of TER, immunostaining and dispase-based enterocyte dissociation assays. Inflammation-induced loss of IEB by application of TNF α was mediated by activation i.e. phosphorylation of p38MAPK which then augmented phosphorylation of cytokeratins 8 and 18 and consecutively reduced Dsg2 at the cell borders, which is a newly characterized mechanism in this context. Protective effects of GDNF on IEB were mediated by inhibiting TNF α -induced phosphorylation of p38MAPK and cytokeratins. The relevance of this mechanism *in vivo* was confirmed in a murine model of DSS-induced colitis where we observed increased phosphorylation of p38MAPK and cytokeratins followed by loss of Dsg2. Breakdown of IEB in DSS-colitis was demonstrated by increased flux of 4 kDa FITC dextran across the intestinal barrier. All inflammation-induced effects were attenuated by therapeutic administration of recombinant GDNF. Finally, the strong correlation of all these findings i.e. loss of GDNF and Dsg2, increased phosphorylation of p38MAPK and cytokeratins in samples from patients with CD and UC point to a disease-relevant role and mechanism of GDNF-dependent effects in IBD.

Loss of GDNF in IBD contributes to inflammation-induced breakdown of the IEB

Our present data clearly show that GDNF was significantly reduced in Western blot analyses in samples from patients with CD and UC. In a previous study, which investigated endoscopically collected colon samples from patients with IBD, GDNF was found to be significantly increased in immunostaining (von Boyen et al., 2011). Given

that patients in the latter study and in our study both displayed severe inflammation this difference of GDNF levels can hardly be explained by different stages of the diseases in the two studies. Rather, the fact that in the latter study endoscopic samples which usually comprise very small sections including only parts of the gut wall were analyzed whereas in our study larger samples of the whole gut wall that derived from surgical resection were analyzed it can be assumed that specimen in our study led to more representative results.

Since uninflamed parts of the terminal ileum of patients with CD showed no reduction of GDNF compared to healthy controls argues against a primary loss of GDNF in the context of IBD at a first glance. However, it can be speculated that there may be increased susceptibility of enteric glial cells leading to alterations of GDNF secretion. This is supported by previous data from biopsies of patients with IBD and animal models of IBD consistently suggested a role of inflammatory effects on the ENS in the generation of symptoms associated with IBD (Lakhan and Kirchgessner, 2010). The significant role for enteric glial cells and especially GDNF in the context of inflammatory response was pointed out by a study in which TLR2-deficient mice displayed disturbed architecture of the ENS, which resulted in reduced GDNF expression and caused breakdown of the IEB (Brun et al., 2013). In the latter study, application of GDNF led to reconstitution of the ENS but potentially direct effects of GDNF on enterocytes remained unexplored (Brun et al., 2013). In contrast to these observations recent studies demonstrated that enteric glial cells are not required for maintenance of the epithelium in mice (Rao et al., 2017) and do not acutely effect gut permeability (Grubisic and Gulbransen, 2017). While this is still under discussion, it must be considered that in addition to alterations of enteric glial cells in IBD smooth muscle cells in the gut wall and even enterocytes represent an additional source of GDNF which both may be critically involved in the regulation of intestinal GDNF levels in health and disease (Brun et al., 2015; Meir et al., 2015a). This idea conforms to the observation of Steinkamp et al., which observed an increase of solely epithelial GDNF in immunostaining in specimen of patients with IBD and proposed that increased epithelial GDNF may be a rescue mechanism following inflammation (Steinkamp et al., 2003).

GDNF attenuated all inflammation-induced effects in intestinal epithelial cells

Previous studies suggested that IEB is stabilized by GDNF indirectly by inducing anti-apoptotic effects on colonic enterocytes and immunomodulation (Langness et al., 2017; Reinshagen et al., 2000; Steinkamp et al., 2003; Zhang et al., 2010a). According to our *in vitro* data in Caco2 cells and in human enteroids application of GDNF resulted in direct effects on enterocytes, which prevented inflammation-induced loss of IEB. In previous studies, we and other groups confirmed the presence of GDNF receptors and responsiveness to GDNF in enterocytes (Meir et al., 2015a; Steinkamp et al., 2003). For the first time, we provide evidence that GDNF effects are primarily mediated by strengthening Dsg2 function, which was shown by the fact that Dsg2-deficient cells showed no response to GDNF. The effects on Dsg2 by GDNF were substantiated by immunostaining, triton-extraction and AFM where application of GDNF resulted in increased Dsg2 at cell borders and augmented Dsg2-mediated adhesion. Furthermore inflammation-induced loss of Dsg2 at the cell borders was restored by GDNF *in vivo* and *in vitro* while increased cell-cell adhesion was observed in dispase-based enterocyte dissociation assays. Again, in Dsg2-deficient Caco2 cells GDNF was not effective to restore TNF α -induced loss of cell-cell adhesion underlining the importance of Dsg2 in this context. In summary, all these data not only show a novel target of GDNF-induced effects in enterocytes but also support the growing evidence for the importance of desmosomal integrity to maintain the IEB in health and disease (Jiang et al., 2014; Kamekura et al., 2014; Kamekura et al., 2015; Schlegel et al., 2010; Vielmuth et al., 2015).

p38MAPK-dependent phosphorylation of intermediate filaments induces loss of IEB in inflammation

Regulation of desmosomal adhesion has been extensively investigated in the context of the skin blistering disease pemphigus in keratinocytes where autoantibody-induced loss of desmoglein3 (Dsg3)-mediated adhesion results in activation of p38MAPK and keratin filament reorganization (Berkowitz et al., 2005; Kitajima, 2014). Additionally, it was recently shown that adhesive forces of Dsg3 in keratinocytes are mediated by keratin-dependent regulation of p38MAPK (Vielmuth et al., 2017). Our present data demonstrate that p38MAPK was phosphorylated in both CU and in CD, which

correlated with loss of Dsg2. While our own study detected loss of Dsg2 in CD in our previous study (Vielmuth et al., 2015) this was not described for patients with CU before. The barrier destabilizing effect of phosphorylated p38MAPK by TNF α in intestinal epithelium is also supported by our previous study in which inflammatory stimuli induced strong activation of p38MAPK followed by loss of Dsg2-mediated adhesion (Vielmuth et al., 2015), so that p38MAPK activation appears to be detrimental for intestinal barrier integrity. On the other hand, it was reported that a proper balance of p38MAPK activation is important since activation of p38MAPK was also required for barrier recovery following Ca²⁺-depletion in a cell culture model of enterocytes (Ungewiss et al., 2017). It must be considered however that in the latter study Dsg2-mediated adhesion was directly targeted by Ca²⁺ depletion or antibodies directed against the extracellular domain of Dsg2 (Ungewiss et al., 2017). In contrast, in the present study a cytokine stimulus i.e. TNF α via its receptor led to activation of p38MAPK, which obviously resulted in barrier-compromising effects. Therefore, the role of p38MAPK in intestinal barrier regulation may differ depending on the type of activation.

Following p38MAPK activation we observed the phenomenon of keratin retraction as has amply been described in keratinocytes after stimulation with pemphigus autoantibodies directed against Dsg3 which then led to internalization of Dsg3 (Calkins et al., 2006). In the context of inflammatory bowel diseases, it was recognized earlier that patients with CD or UC have missense mutations in keratin 8 (Owens et al., 2004) which led to the assumption that this may lead to augmented susceptibility in intestinal epithelium. In support of this it was shown that interleukin6-dependent expression of keratin 8 protected the intestinal barrier from inflammatory stimuli (Wang et al., 2007). Cytokeratin8 phosphorylation at Ser74 has previously been identified as a substrate for phosphorylation by p38MAPK and it was observed that under certain conditions of inflammation increased keratin 8 phosphorylation occurs which was linked to increased susceptibility of the IEB by unknown mechanisms (Majumdar et al., 2012). This hypothesis is now substantiated by our present data where cytokeatin 8 and 18 phosphorylation is indeed critically involved in the process IEB regulation most likely by affecting desmosomal integrity. In general, it is known that phosphorylation of keratins changes the distribution of keratins in the cell, alters its polymerization behavior,

and is associated with keratin granule formation (Fois et al., 2013; Magin et al., 2007). Moreover, it was shown in keratinocytes that keratins control intercellular desmosomal adhesion since desmosomes that lack the tethering to intermediate filaments by adapter proteins undergo a more rapid endocytosis with consecutive loss of intercellular adhesion (Kroger et al., 2013). A comparable mechanism can be assumed in our present data in enterocytes since phosphorylation of keratins led to retraction of the peripheral keratinring. This may reduce tethering of Dsg2 to the intermediate filaments with consecutive loss of desmosomal adhesion and intestinal barrier function.

In summary, inflammation-induced cytokeratin phosphorylation by activation of p38MAPK which led to loss of Dsg2 as shown here *in vitro*, *in vivo* and in patients' samples suffering from IBD points to a novel and important pathomechanism for barrier dysregulation in CD and UC. GDNF-induced inhibition of this pathway as outlined above rises not only a novel view for its role in the pathogenesis of barrier dysregulation in IBD but also implies an interesting potential for novel therapeutic options.

References

1. Geremia A, Biancheri P, Allan P, et al. Innate and adaptive immunity in inflammatory bowel disease. *Autoimmun Rev* 2014;13:3-10.
2. Uhlig HH. Monogenic diseases associated with intestinal inflammation: implications for the understanding of inflammatory bowel disease. *Gut* 2013;62:1795-805.
3. Martini E, Krug SM, Siegmund B, et al. Mend Your Fences: The Epithelial Barrier and its Relationship With Mucosal Immunity in Inflammatory Bowel Disease. *Cell Mol Gastroenterol Hepatol* 2017;4:33-46.
4. Farquhar MG, Palade GE. Junctional complexes in various epithelia. *J Cell Biol* 1963;17:375-412.
5. Luissint AC, Parkos CA, Nusrat A. Inflammation and the Intestinal Barrier: Leukocyte-Epithelial Cell Interactions, Cell Junction Remodeling, and Mucosal Repair. *Gastroenterology* 2016;151:616-32.
6. Spindler V, Meir M, Vigh B, et al. Loss of Desmoglein 2 Contributes to the Pathogenesis of Crohn's Disease. *Inflamm Bowel Dis* 2015;21:2349-59.
7. Berkowitz P, Hu P, Liu Z, et al. Desmosome signaling. Inhibition of p38MAPK prevents pemphigus vulgaris IgG-induced cytoskeleton reorganization. *J Biol Chem* 2005;280:23778-84.
8. Kitajima Y. 150(th) anniversary series: Desmosomes and autoimmune disease, perspective of dynamic desmosome remodeling and its impairments in pemphigus. *Cell Commun Adhes* 2014;21:269-80.
9. Sanders DS. Mucosal integrity and barrier function in the pathogenesis of early lesions in Crohn's disease. *J Clin Pathol* 2005;58:568-72.
10. Neunlist M, Toumi F, Oreschkova T, et al. Human ENS regulates the intestinal epithelial barrier permeability and a tight junction-associated protein ZO-1 via VIPergic pathways. *Am J Physiol Gastrointest Liver Physiol* 2003;285:G1028-36.
11. Bush TG, Savidge TC, Freeman TC, et al. Fulminant jejuno-ileitis following ablation of enteric glia in adult transgenic mice. *Cell* 1998;93:189-201.
12. Cornet A, Savidge TC, Cabarrocas J, et al. Enterocolitis induced by autoimmune targeting of enteric glial cells: a possible mechanism in Crohn's disease? *Proc Natl Acad Sci U S A* 2001;98:13306-11.
13. Brun P, Giron MC, Qesari M, et al. Toll-like receptor 2 regulates intestinal inflammation by controlling integrity of the enteric nervous system. *Gastroenterology* 2013;145:1323-33.
14. Steinkamp M, Geerling I, Seufferlein T, et al. Glial-derived neurotrophic factor regulates apoptosis in colonic epithelial cells. *Gastroenterology* 2003;124:1748-57.
15. Zhang DK, He FQ, Li TK, et al. Glial-derived neurotrophic factor regulates intestinal epithelial barrier function and inflammation and is therapeutic for murine colitis. *J Pathol* 2010;222:213-22.
16. Meir M, Flemming S, Burkard N, et al. The glial cell-line derived neurotrophic factor: a novel regulator of intestinal barrier function in health and disease. *Am J Physiol Gastrointest Liver Physiol* 2016;310:G1118-23.
17. Meir M, Flemming S, Burkard N, et al. Glial cell line-derived neurotrophic factor (GDNF) promotes barrier maturation and wound healing in intestinal epithelial cells in vitro. *Am J Physiol Gastrointest Liver Physiol* 2015:ajpgi 00357 2014.
18. Schweinlin M, Wilhelm S, Schwedhelm I, et al. Development of an Advanced Primary Human In Vitro Model of the Small Intestine. *Tissue Eng Part C Methods* 2016;22:873-83.
19. Chassaing B, Aitken JD, Malleshappa M, et al. Dextran sulfate sodium (DSS)-induced colitis in mice. *Curr Protoc Immunol* 2014;104:Unit 15 25.
20. Erben U, Loddenkemper C, Doerfel K, et al. A guide to histomorphological evaluation of intestinal inflammation in mouse models. *Int J Clin Exp Pathol* 2014;7:4557-76.

21. Vielmuth F, Hartlieb E, Kugelmann D, et al. Atomic force microscopy identifies regions of distinct desmoglein 3 adhesive properties on living keratinocytes. *Nanomedicine* 2015;11:511-20.
22. Ungewiss H, Vielmuth F, Suzuki ST, et al. Desmoglein 2 regulates the intestinal epithelial barrier via p38 mitogen-activated protein kinase. *Sci Rep* 2017;7:6329.
23. Schinner C, Vielmuth F, Rotzer V, et al. Adrenergic Signaling Strengthens Cardiac Myocyte Cohesion. *Circ Res* 2017;120:1305-1317.
24. Majumdar D, Tiernan JP, Lobo AJ, et al. Keratins in colorectal epithelial function and disease. *Int J Exp Pathol* 2012;93:305-18.
25. von Boyen GB, Schulte N, Pfluger C, et al. Distribution of enteric glia and GDNF during gut inflammation. *BMC Gastroenterol* 2011;11:3.
26. Lakhan SE, Kirchgessner A. Neuroinflammation in inflammatory bowel disease. *J Neuroinflammation* 2010;7:37.
27. Rao M, Rastelli D, Dong L, et al. Enteric Glia Regulate Gastrointestinal Motility but Are Not Required for Maintenance of the Epithelium in Mice. *Gastroenterology* 2017.
28. Grubisic V, Gulbransen BD. Enteric glial activity regulates secretomotor function in the mouse colon but does not acutely affect gut permeability. *J Physiol* 2017.
29. Brun P, Gobbo S, Caputi V, et al. Toll like receptor-2 regulates production of glial-derived neurotrophic factors in murine intestinal smooth muscle cells. *Mol Cell Neurosci* 2015;68:24-35.
30. Reinshagen M, Rohm H, Steinkamp M, et al. Protective role of neurotrophins in experimental inflammation of the rat gut. *Gastroenterology* 2000;119:368-76.
31. Langness S, Kojima M, Coimbra R, et al. Enteric glia cells are critical to limiting the intestinal inflammatory response after injury. *Am J Physiol Gastrointest Liver Physiol* 2017;312:G274-G282.
32. Schlegel N, Meir M, Heupel WM, et al. Desmoglein 2-mediated adhesion is required for intestinal epithelial barrier integrity. *Am J Physiol Gastrointest Liver Physiol* 2010;298:G774-83.
33. Jiang K, Rankin CR, Nava P, et al. Galectin-3 regulates desmoglein-2 and intestinal epithelial intercellular adhesion. *J Biol Chem* 2014;289:10510-7.
34. Kamekura R, Kolegraff KN, Nava P, et al. Loss of the desmosomal cadherin desmoglein-2 suppresses colon cancer cell proliferation through EGFR signaling. *Oncogene* 2014;33:4531-6.
35. Kamekura R, Nava P, Feng M, et al. Inflammation-induced desmoglein-2 ectodomain shedding compromises the mucosal barrier. *Mol Biol Cell* 2015;26:3165-77.
36. Vielmuth F, Wanuske MT, Radeva MY, et al. Keratins Regulate the Adhesive Properties of Desmosomal Cadherins Through Signaling. *J Invest Dermatol* 2017.
37. Calkins CC, Setzer SV, Jennings JM, et al. Desmoglein endocytosis and desmosome disassembly are coordinated responses to pemphigus autoantibodies. *J Biol Chem* 2006;281:7623-34.
38. Owens DW, Wilson NJ, Hill AJ, et al. Human keratin 8 mutations that disturb filament assembly observed in inflammatory bowel disease patients. *J Cell Sci* 2004;117:1989-99.
39. Wang L, Srinivasan S, Theiss AL, et al. Interleukin-6 induces keratin expression in intestinal epithelial cells: potential role of keratin-8 in interleukin-6-induced barrier function alterations. *J Biol Chem* 2007;282:8219-27.
40. Magin TM, Vijayaraj P, Leube RE. Structural and regulatory functions of keratins. *Exp Cell Res* 2007;313:2021-32.
41. Fois G, Weimer M, Busch T, et al. Effects of keratin phosphorylation on the mechanical properties of keratin filaments in living cells. *FASEB J* 2013;27:1322-9.
42. Kroger C, Loschke F, Schwarz N, et al. Keratins control intercellular adhesion involving PKC- α -mediated desmoplakin phosphorylation. *J Cell Biol* 2013;201:681-92.
43. Labun K, Montague TG, Gagnon JA, et al. CHOPCHOP v2: a web tool for the next generation of CRISPR genome engineering. *Nucleic Acids Res* 2016;44:W272-6.
44. Schlegel N, Leweke R, Meir M, et al. Role of NF- κ B activation in LPS-induced endothelial barrier breakdown. *Histochem Cell Biol* 2012;138:627-41.

45. Schlegel N, Meir M, Spindler V, et al. Differential role of Rho GTPases in intestinal epithelial barrier regulation in vitro. *J Cell Physiol* 2011;226:1196-203.
46. Andreas E, Linda W, M. KAS, et al. A new simple method for linking of antibodies to atomic force microscopy tips. *Bioconjugate Chem.* 2007;18:1176

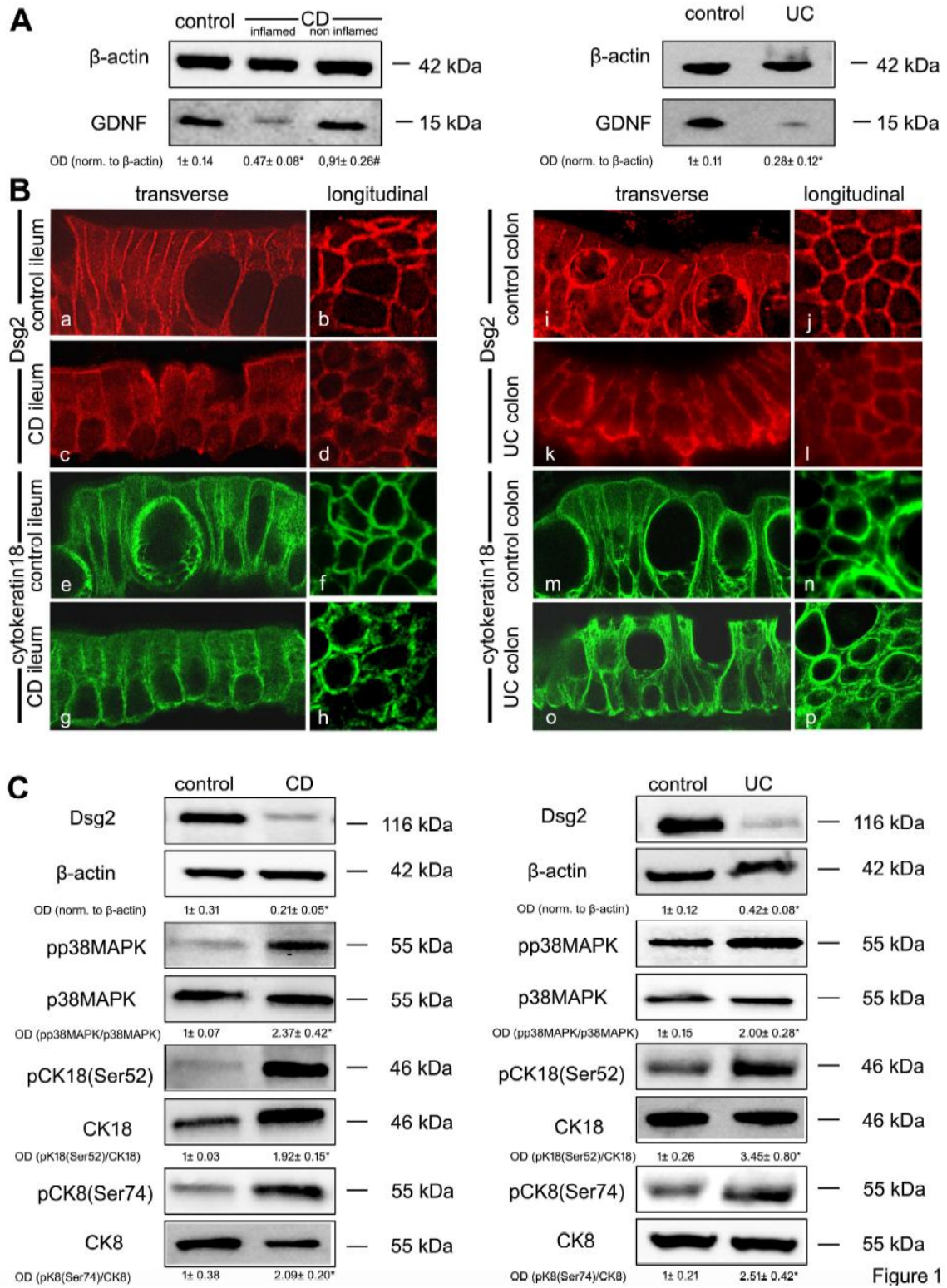


Figure 1

Figure 1: Reduction of GDNF correlated with loss of Dsg2, activation of p38MAPK and alteration of intermediate filaments in patients with IBD

A In Western Blot analyses resection specimen from patients with Crohn's Disease (CD) (n= 9) and ulcerative colitis (n= 9) were analyzed for GDNF levels. In inflamed parts of the terminal ileum of CD patients (left) and colon from CU patients, (right) GDNF was significantly reduced. **B** Immunostaining was performed for Dsg2 (a-d, i-l) or cytokeratin 18 (e-h, m-p) from resection specimen of patients with CD from the terminal ileum (a-h) or patients with CU (from the colon (i-p)). In controls of the terminal ileum (a, b) or the colon (i,j) Dsg2 is regularly distributed along the cell borders and cytokeratin18 staining shows a regular peripheral intermediate filament ring under control conditions (e,f, m,n). Patients with CD (c,d) and CU (k, l) showed loss of Dsg2 at the cell borders which was paralleled by a profoundly deranged cytokeratin18 staining pattern (g,h, o, p). Scale bar is 20 μ m. **C** In Western Blot analyses of CD and UC samples significant loss of Dsg2, augmented phosphorylation of p38MAPK, cytokeratin18 and cytokeratin8 were found. Western Blots are representative for n= 9 patients for each group. OD= optical density values normalized to β -actin or to total p38MAPK, cytokeratin18 or 8 are indicated below the Western Blots, * p<0.05 compared to control, # p<0.05 compared to uninfamed tissue.

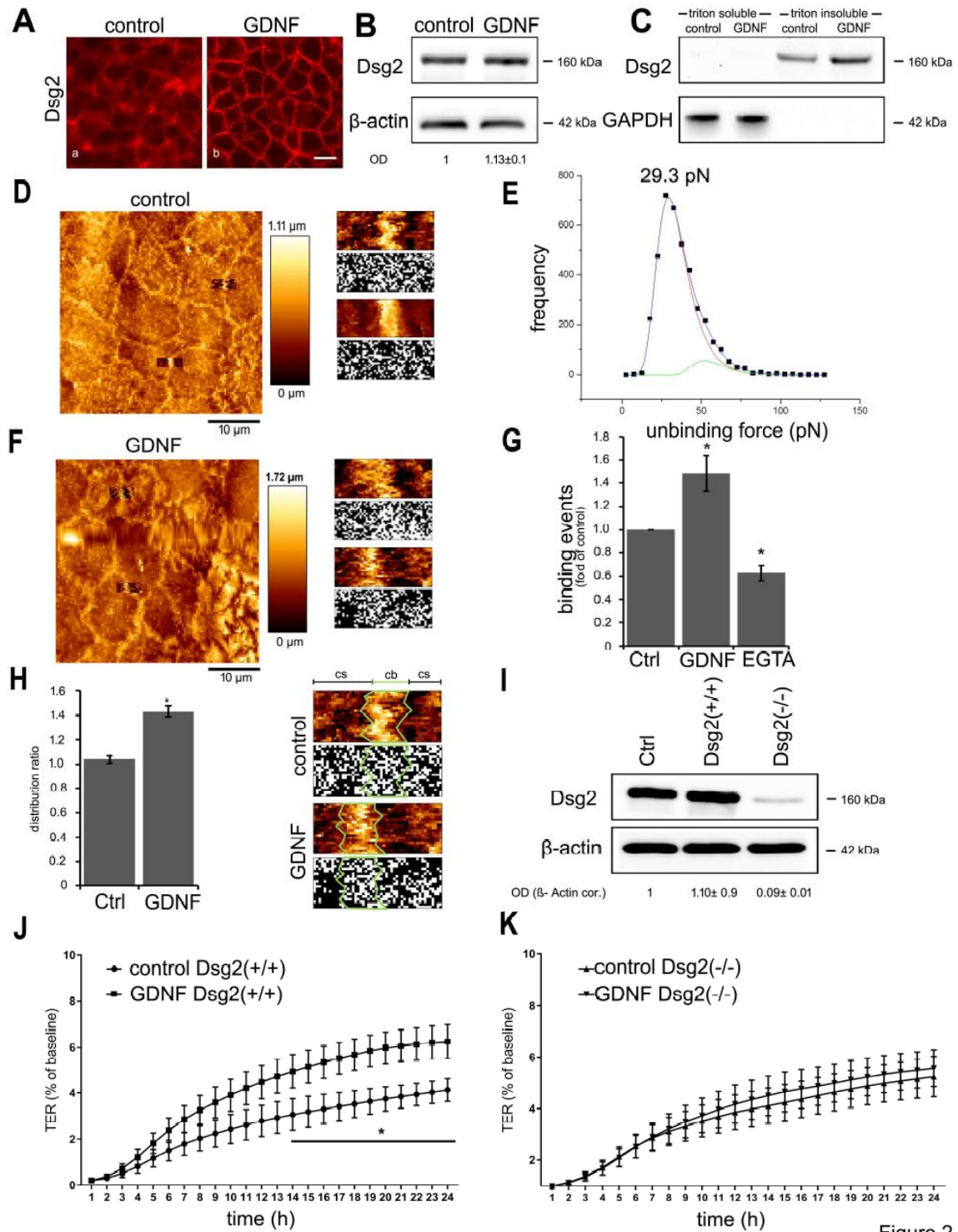
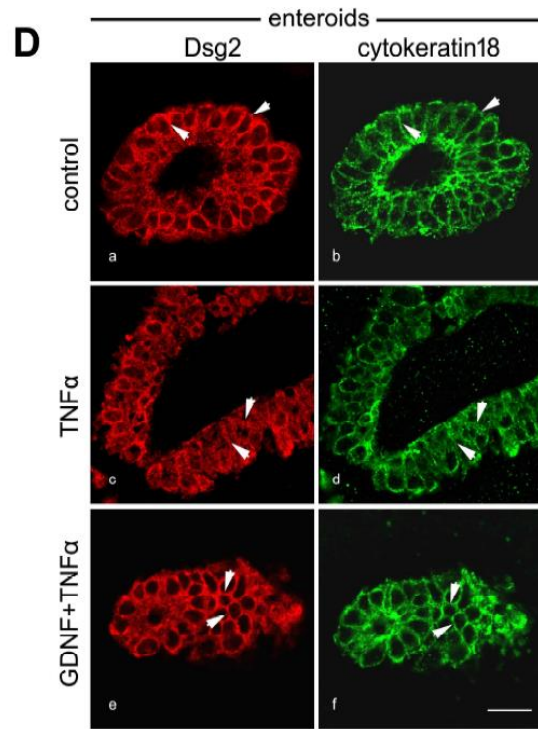
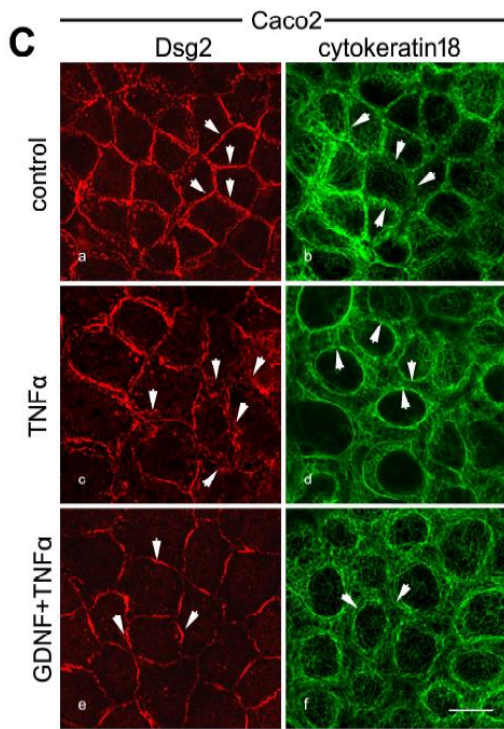
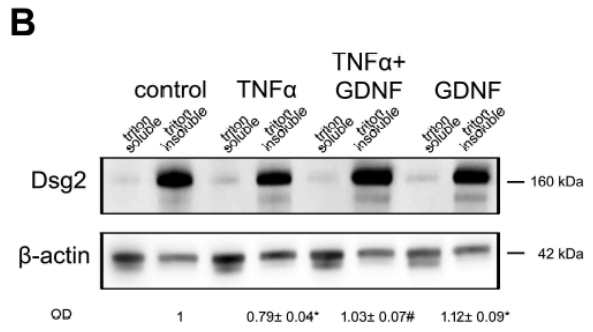
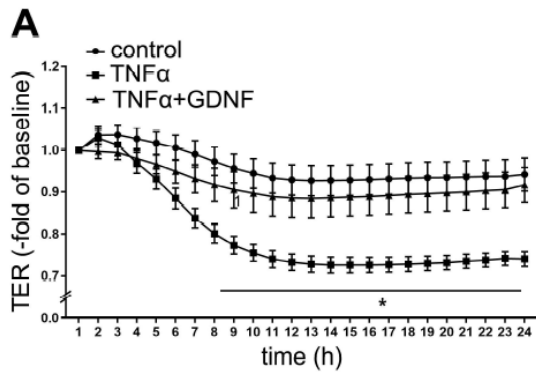


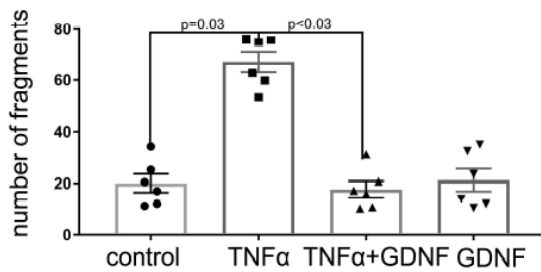
Figure 2

Figure 2: GDNF stabilizes the intestinal barrier via Dsg2

A Immunostaining of Caco2 monolayers at confluence showed faint Dsg2 staining patterns (a) at the cell borders which was augmented by application of 100 ng/ml GDNF for 24h (b). Images shown are representative for $n > 5$ experiments. **B** In Western Blot analyses application of GDNF did not result in significantly increased protein amounts; OD= optical density values normalized to β -actin; representative for $n > 5$ experiments. **C** In triton extraction experiments GDNF led to augmented Dsg2 in the triton-insoluble fraction; representative for $n > 5$ experiments. **D** AFM measurements were performed on living Caco2 cells at 37°C. Cell topography images were created for selection of specific areas at cell borders (left panel). Force measurements with a Dsg2 coated AFM cantilever revealed binding events on the surface of Caco2 cells with each white dot representing one binding event (right panel). **E** Analysis of measured Dsg2-specific unbinding forces resulted in a distribution-peak of 29,3 pN. **F** Cell topography of Caco2 cells was imaged after incubation with GDNF (left panel). Force maps of Dsg2 adhesion measurements display more binding events along the cell border (right panel) after application of GDNF. **G** Quantification of measured binding events points out a significantly increased binding frequency after application of GDNF and a significantly decreased binding frequency after EGTA mediated Ca^{2+} depletion (means \pm SEM, $n = 6$ for GDNF, $n = 3$ for EGTA; * $p < 0.05$). **H** Distribution ratio of Dsg2-specific binding events was calculated as the quotient of measured binding events along the cell border (cb) and measured binding events on the surrounding cell surface (cs) (shown are means \pm SE, $n = 6$, * $p < 0.05$). **I** Western Blot analyses for Dsg2 is shown to demonstrate the effective knock-out of Dsg2 in the Caco2 Dsg2 (-/-) cell line in comparison to Caco2wt (control) and Caco2 cells transfected with nonsense plasmids; OD= optical density values normalized to β -actin; representative for $n > 5$ experiments. **J, K** TER measurements of Caco2 Dsg2 (+/+) cells transfected with nonsense plasmids (J) and Caco2 Dsg2 (-/-) following application of 100 ng/ml GDNF are shown. While in of Caco2 Dsg2 (+/+) GDNF application resulted in a significant increase of TER values no effect on TER was observed in Caco2 Dsg2 (-/-); $n=6$ experiments for each condition; * $p < 0.05$.



E dispase-based enterocyte dissociation assay Caco2 Dsg2(+/+)



F dispase-based enterocyte dissociation assay Caco2 Dsg2(-/-)

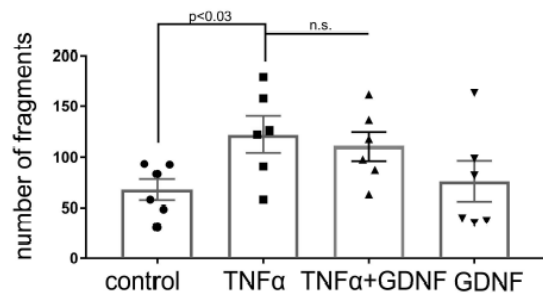


Figure3: GDNF attenuated all inflammation-induced effects in Caco2 cells and in human enteroids

A In TER measurements application of $\text{TNF}\alpha$ resulted in significant reduction of TER which was attenuated by simultaneous application of GDNF; $n=6$ experiments for each condition; $*p<0.05$ compared to control. **B** In triton extraction experiments $\text{TNF}\alpha$ led to a reduction of Dsg2 in the triton-insoluble fraction. Simultaneous application of GDNF blocked $\text{TNF}\alpha$ -induced loss of Dsg2 and application of GDNF alone augmented Dsg2 in the triton-insoluble fraction; representative for $n>5$ experiments; OD= optical density values normalized to β -actin; representative for $n>5$ experiments, $p<0.05$ compared to control. **C, D** Immunostaining was performed in Caco2 cells (C) and in human enteroids for Dsg2 (Ca,c,e, Da, c, e) and for cytokeratin18 (Cb, f, h, Db, f, h). Under control conditions Dsg2 and cytokeratin 18 were both found regularly at the cell borders (arrowheads) in Caco2 (C) and in enteroids (D). $\text{TNF}\alpha$ induced loss of Dsg2 at the cell borders (arrowheads) in Caco2 (Cc) and in enteroids (Dc) which was blocked by simultaneous application of GDNF (arrowhead in Ce, De). $\text{TNF}\alpha$ led to retraction of the cytokeratin ring from the cell borders in Caco2 cells (arrowheads Cd) which was attenuated by GDNF (Cf). In enteroids, cytokeratin18 architecture was profoundly deranged following $\text{TNF}\alpha$ (arrowhead Dd) which was blocked by simultaneous application of GDNF (arrowhead Df). Images are representatives; for $n>6$ experiments; scale bar is 20 μm . **E, F** Dispase-based enterocyte dissociation assays were performed in Caco2 Dsg2 (+/+) (E) transfected with nonsense plasmids or Caco2 Dsg2 (-/-) (F), respectively. Application of $\text{TNF}\alpha$ to Caco2 Dsg2 (+/+) cells (E) resulted in a significantly increased number of fragments which was blocked when cells were treated with GDNF. No effect was observed when cells were treated with GDNF alone. In Caco2 Dsg2 (-/-) (E) an increased number of fragments compared to Dsg2 (+/+) was observed under baseline conditions which was further increased following incubation with $\text{TNF}\alpha$. Co-incubation with GDNF and GDNF had no influence on the number of fragments. $n>6$ individual experiments.

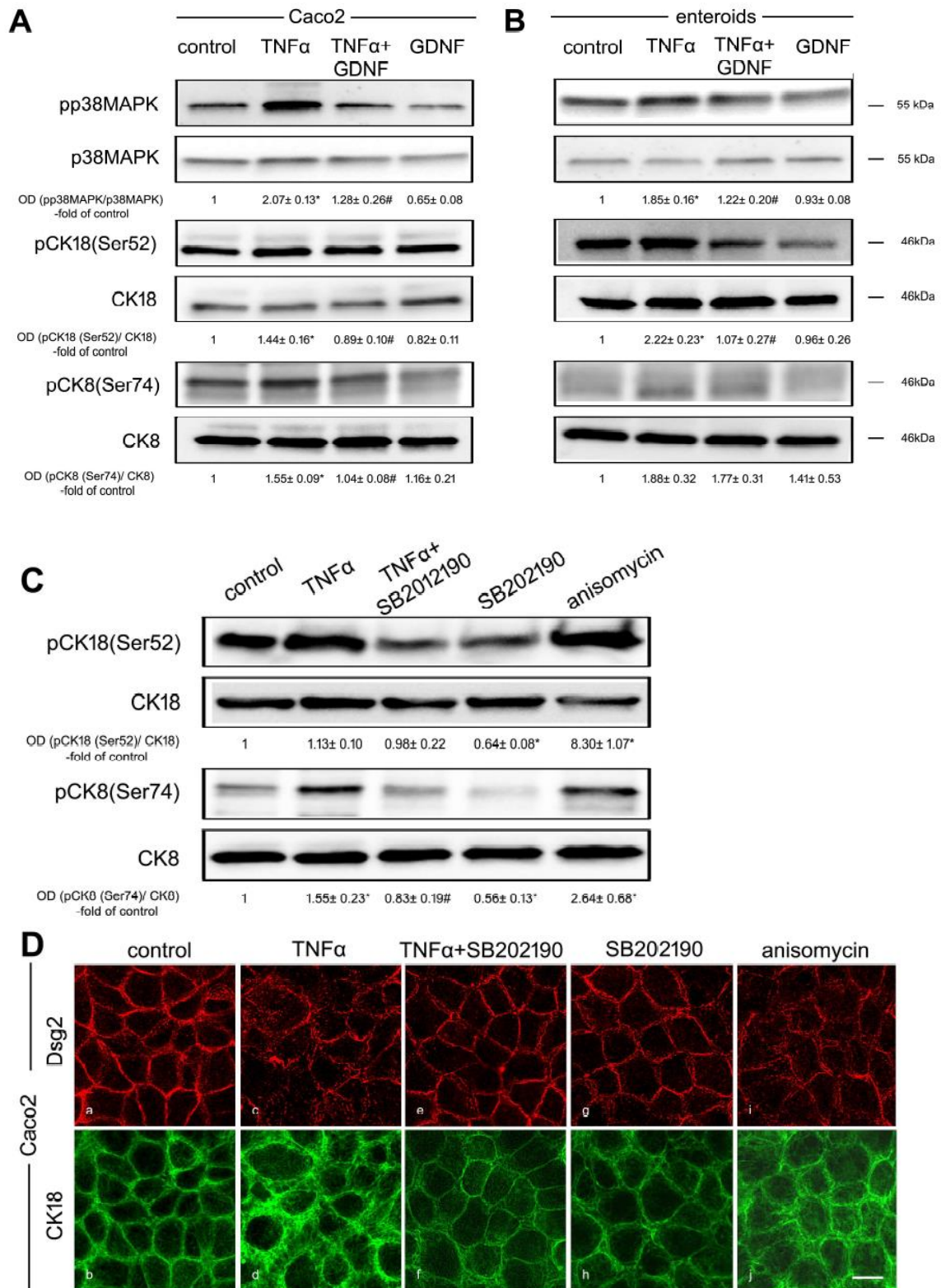


Figure 4: TNF α -induced cyokeratin phosphorylation is p38MAPK-dependent

A, B, C Western Blot analyses were performed in Caco2 cells (A, C) and in enteroids (B). Following application of TNF α phosphorylation of p38MAPK, cyokeratin18 and 8 were significantly increased. Co-incubation of GDNF blocked TNF α -induced phosphorylation in Caco2 and in enterocytes while application of GDNF alone did not change phosphorylation compared to controls. Inhibition of p38MAPK using SB202190 attenuated TNF α -induced phosphorylation of cyokeratin 18 and 8 whereas activation of p38MAPK using anisomycin augmented phosphorylation of both cyokeratin above control levels. OD= optical density values normalized to loading controls; representative for n>5 experiments, *p<0.05 compared to control; # p<0.05 compared to TNF α .

D Immunostaining of Dsg2 (a,c,e,g,i) and cyokeratin 18 (b, d, f, h, i) were performed in Caco2 monolayers. Application of TNF α resulted in loss of Dsg2 at the cell borders (c) and induced cyokeratin retraction (d). This was blocked by co-incubation of TNF α with SB202190 when Dsg2 (e) was regularly distributed at cell borders and cyokeratin retraction was blunted (f). SB202190 (g,h) alone did not show changes when compared to controls (a, b) whereas anisomycin induced loss of Dsg2 at the cell borders (i) and cyokeratin retraction (j). Experiments shown are representative for n>6; scale bar is 20 μ m.

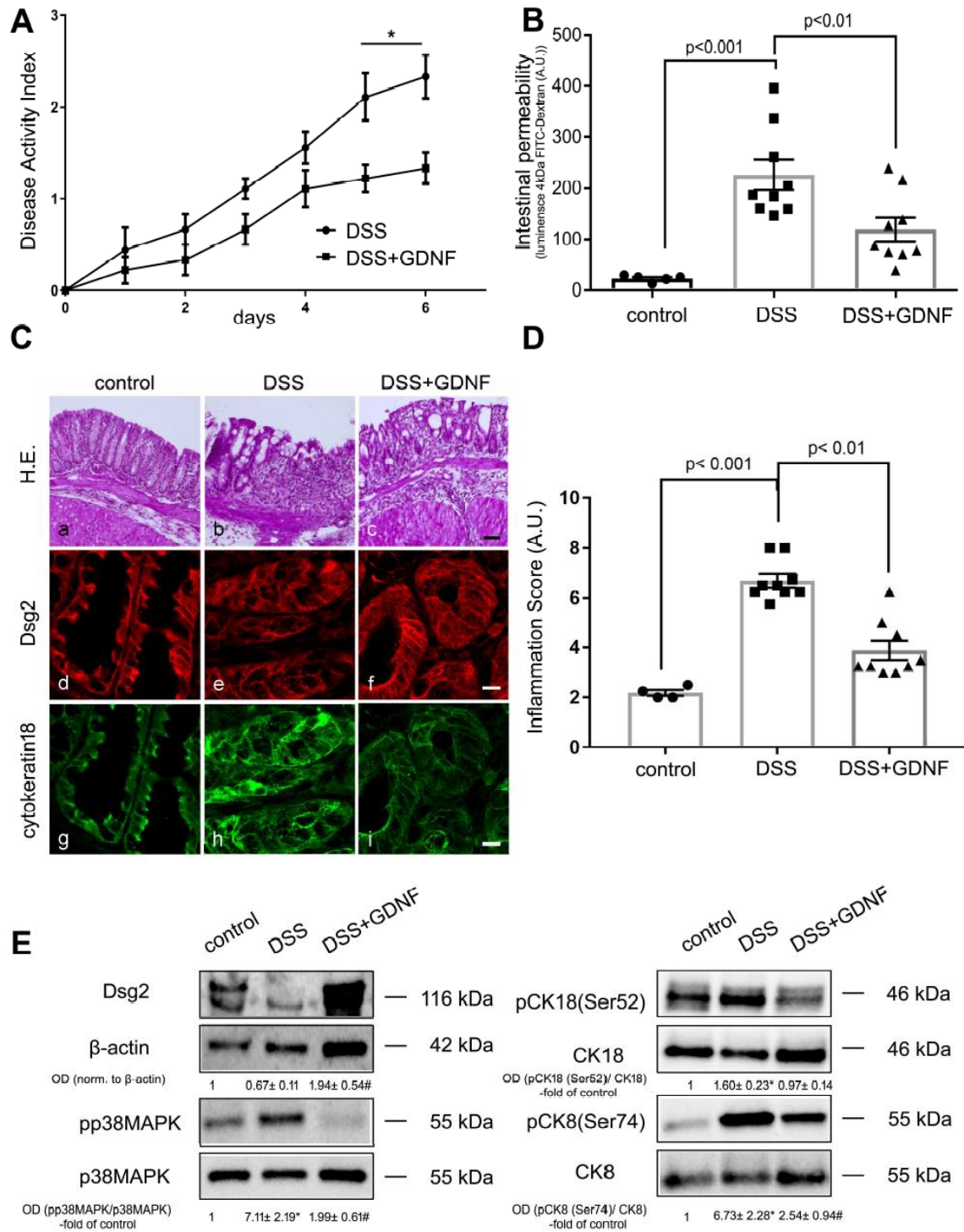
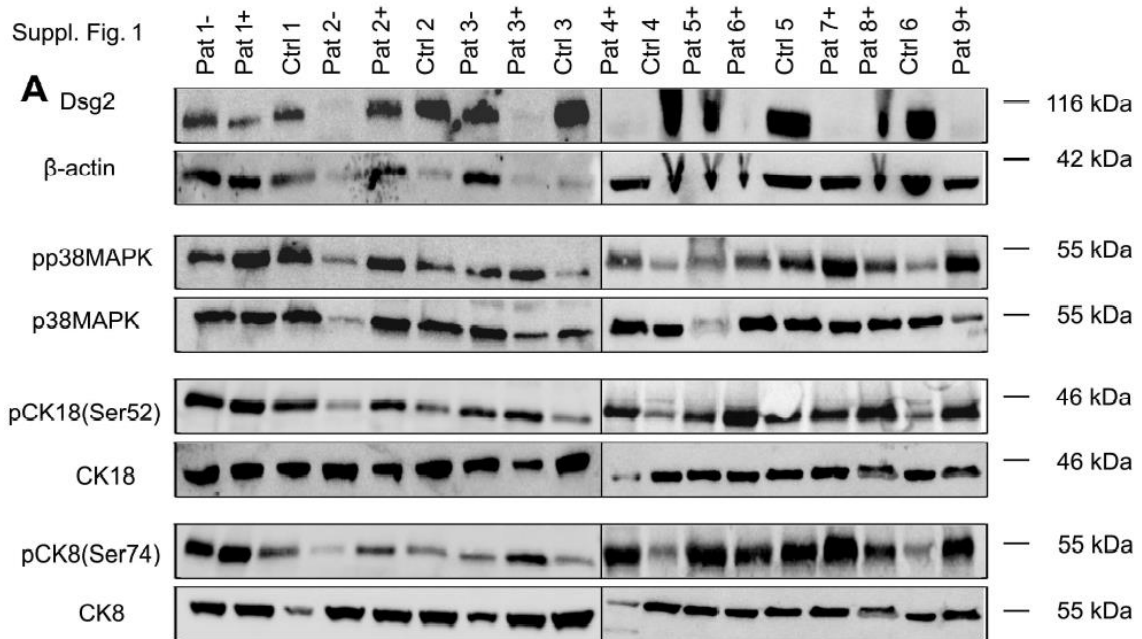
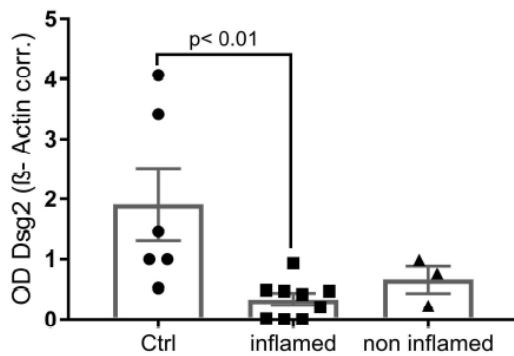
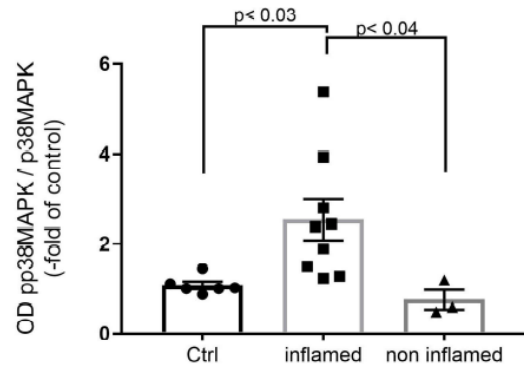
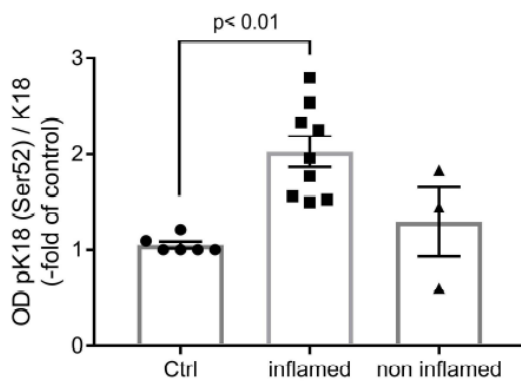
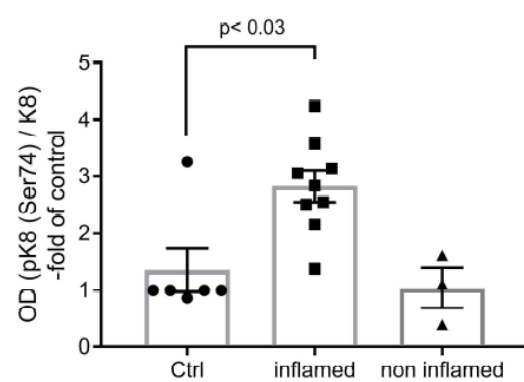


Figure 5 GDNF stabilizes intestinal barrier function in DSS-colitis

A Disease activity index (DAI) for DSS animals is shown. Application of GDNF led to significant reduction of DAI; * $p < 0.05$ compared to DSS alone **B** Intestinal permeability was measured by translocation of 4kDa FITC-dextran from the intestinal lumen into the blood. In DSS-colitis intestinal permeability was significantly increased which was attenuated by treatment with GDNF. **C** H.E. staining of representative images of colon sections from mice are shown for controls (a), DSS-colitis (b) and DSS colitis with GDNF treatment (c). Inflammation was reduced by GDNF treatment. Immunostaining of Dsg2 (d-f) showed reduced Dsg2 at the cell borders in DSS-colitis (e) which was restored following application of GDNF (f). Immunostaining for cytokeratin18 (g-i) was deranged in DSS-colitis which was not observed after treatment of GDNF (i). Scale bar is 20 μm . **D** Inflammation score was evaluated in H.E. staining. In DSS-colitis inflammation score was significantly increased above control values. Treatment with GDNF resulted in significantly reduced inflammation scores. **E** Western Blots from colon tissue lysates of animals are shown. Dsg2 reduction in DSS-colitis was blocked by application of GDNF. Augmented phosphorylation of p38MAPK, cytokeratin18 and cytokeratin8 in DSS-colitis was attenuated by treatment with GDNF. OD= optical density values normalized to loading controls; representative for $n > 5$ experiments, * $p < 0.05$ compared to control; # $p < 0.05$ compared to DSS.

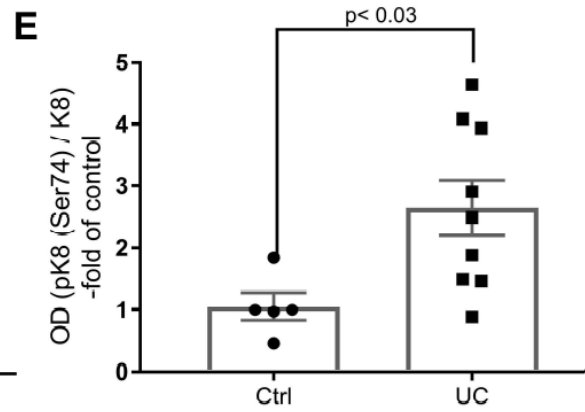
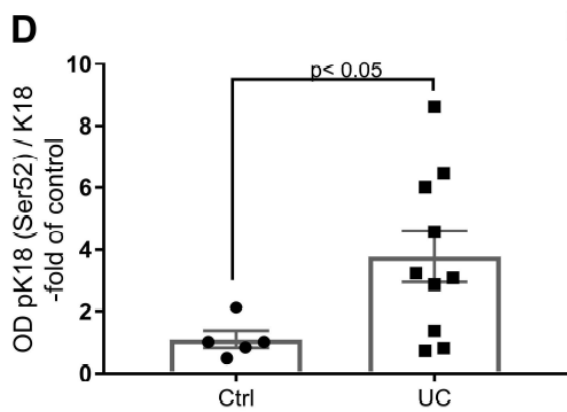
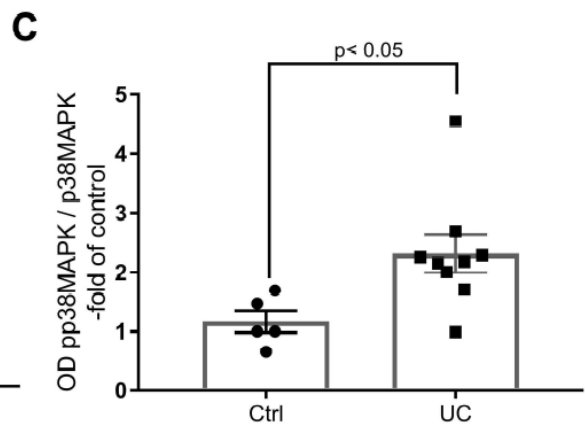
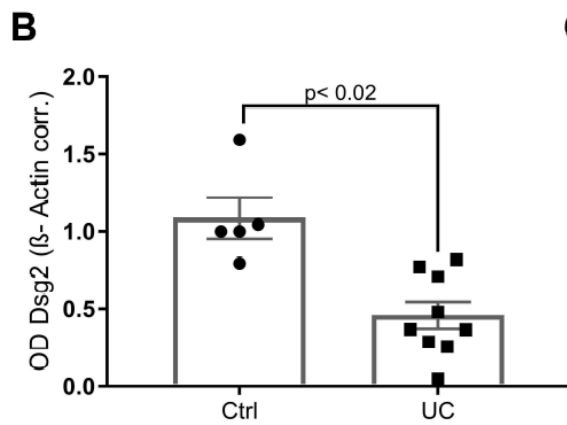
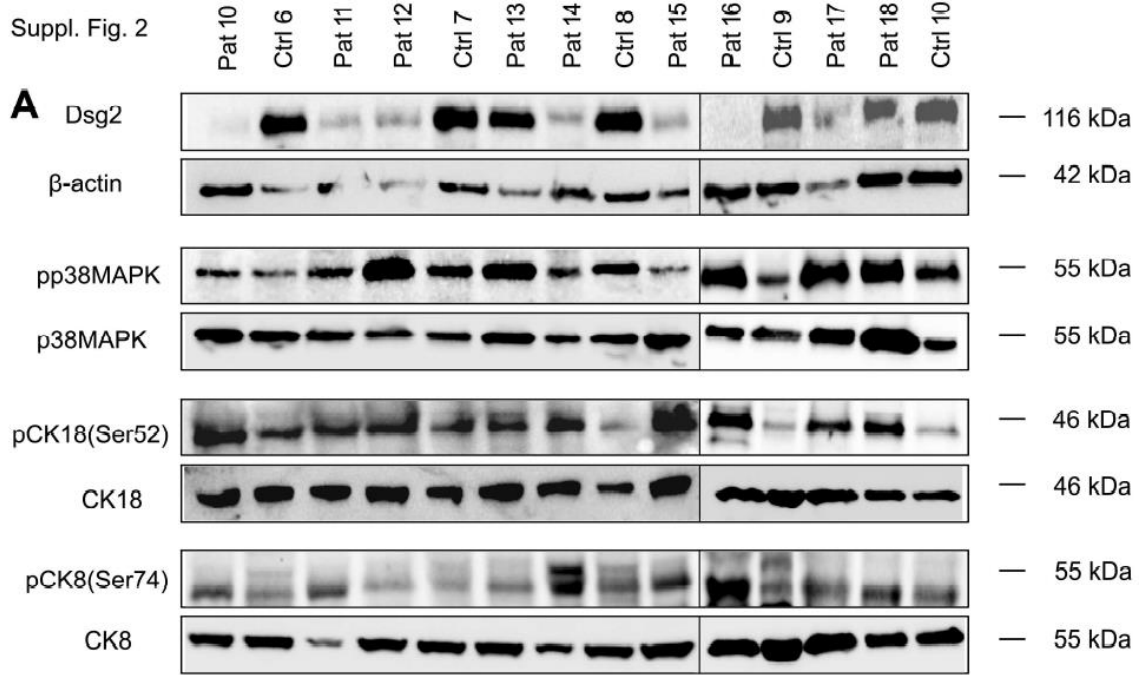
Supplementary information

Suppl. Fig. 1

**B****C****D****E**

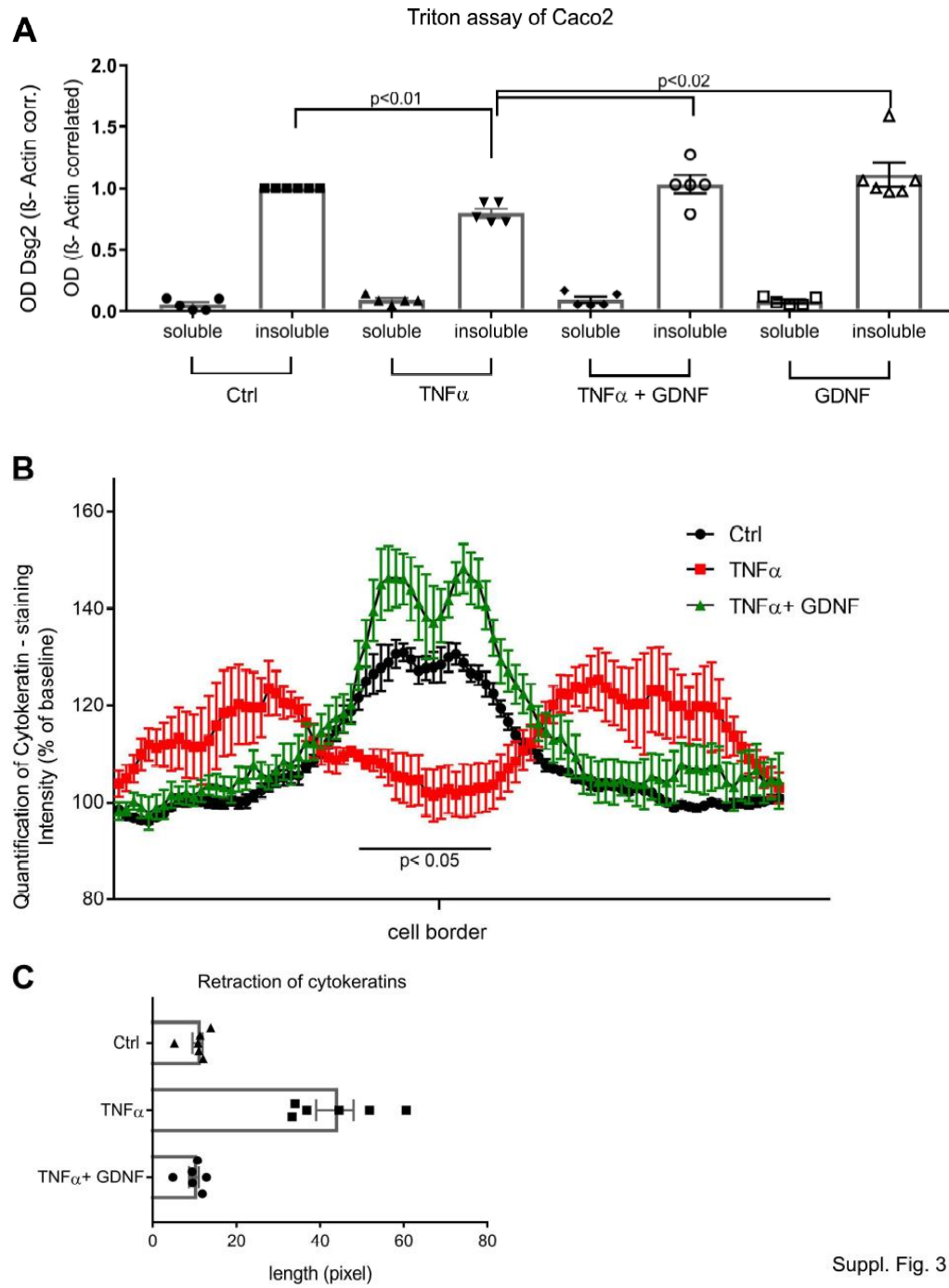
Supplemental Figure 1

A Western blot analyses of resection specimen of patients suffering from Crohn's disease showed a significant loss of Dsg2, an augmented phosphorylation of p38 MAPK, cytokeratin 18 at Serin 52 and cytokeratin 8 at Serin 74 in the inflamed parts of the tissue. These changes were not seen in the uninflamed resection margins. (- uninflamed; + inflamed). **B** Analysis of Dsg2 protein levels, through measurements of the optical density of western blots, demonstrated a reduction of Dsg2 in the inflamed parts of the specimen to 0.33 ± 0.10 (equates 0.21 ± 0.05 of controls) compared to 1.91 ± 0.56 in control specimen. In the uninflamed resection, margins of the specimen no changes compared to controls were observed when OD was 0.66 ± 0.22 . (OD = optical density, n=9) **C** Quantification of the optical density resulted in a significant increase of phosphorylation of p38 MAPK to 2.37 ± 0.42 (-fold of controls) in the inflamed areas of the tissue that was not seen in the non-inflamed specimen when OD was 0.76 ± 0.22 (OD = optical density, n=9). **D** In inflamed tissue phosphorylation of cytokeratin 18 at Serin 52 was increased to 1.92 ± 0.15 compared to 1.29 ± 0.36 in the non-inflamed tissue (OD = optical density, n=9). **E** Increased phosphorylation of cytokeratin 8 at Serin 74 was observed dependent in inflamed tissue specimen (OD = optical density, n=9).



Supplemental Figure 2

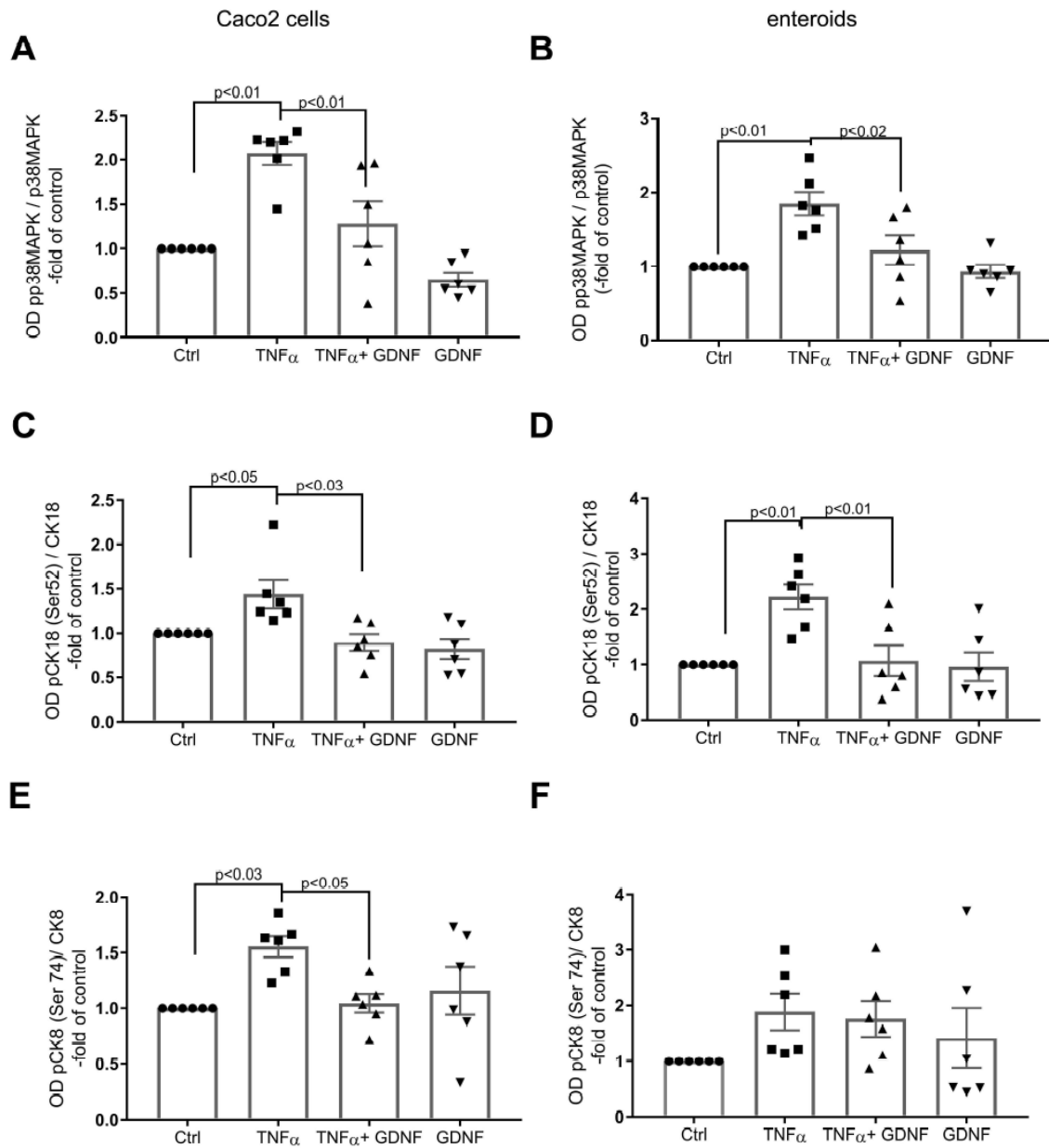
A Western blot analyses of resection specimen of patients suffering from ulcerative colitis revealed a significant loss of Dsg2, an increased phosphorylation of p38 MAPK, cytokeratin 18 at Serin 52 and cytokeratin 8 at Serin 74 compared to non-inflamed colon of control specimen. **B** Statistic analysis of optical density of Dsg2 demonstrated a significant reduction of Dsg2 in inflamed colon specimen of patients suffering from ulcerative colitis (OD = optical density, n=9) **C- E** The loss of desmoglein2 in specimen of ulcerative colitis was paralleled by an increase in phosphorylation of p38MAPK, cytokeratin18 at Serin52 and cytokeratin 8 at Serin74 as shown by an augmented optical density of western blots (OD = optical density, n=9).



Suppl. Fig. 3

Supplemental Figure 3

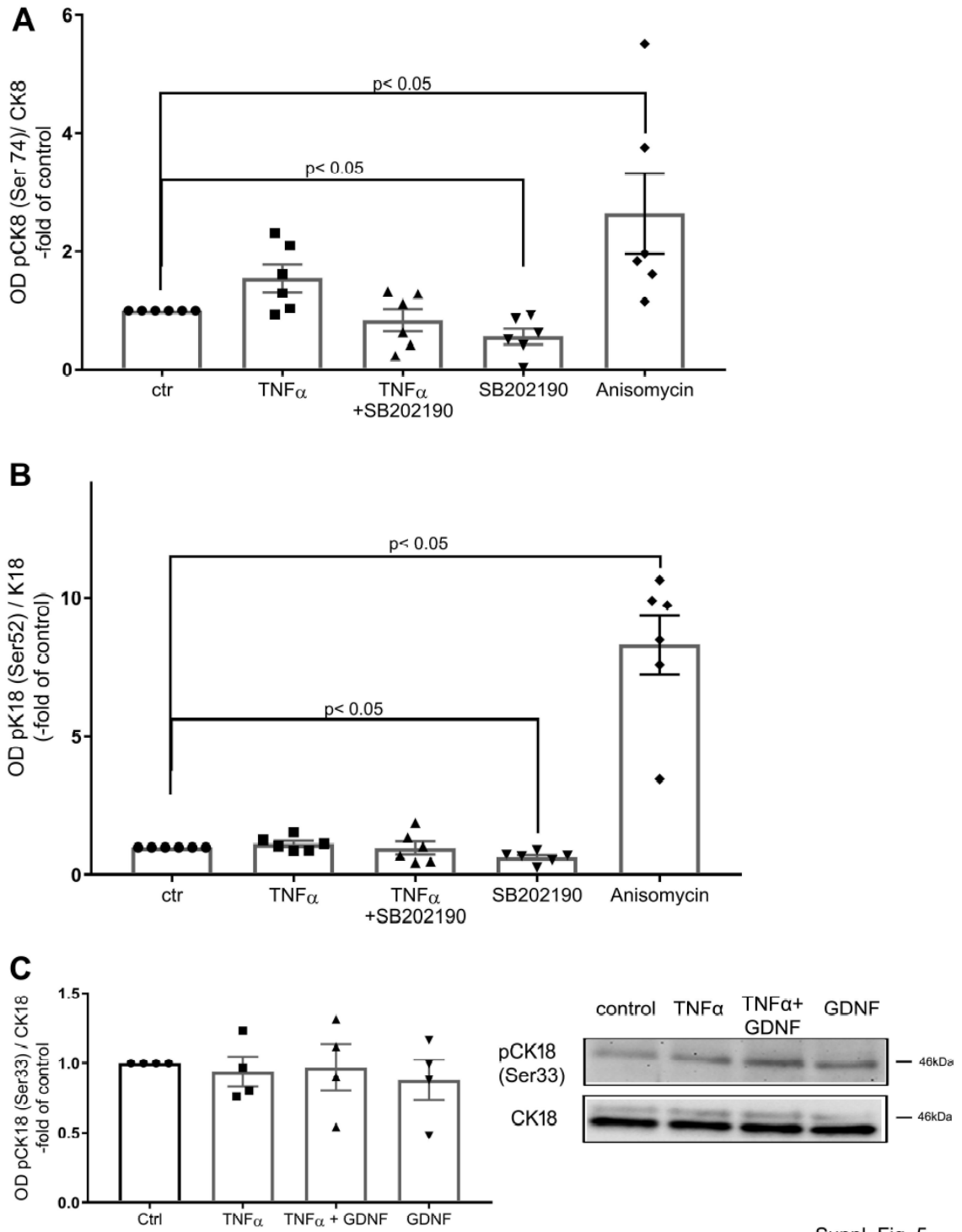
A Quantification of the optical densities of Dsg2 western blot signaling in Caco2 cells after Triton assay are shown. $\text{TNF}\alpha$ led to a reduced signal in the triton-insoluble fraction. In contrast incubation with GDNF increased the intensity of Dsg2 in the triton-insoluble fraction and blocked the effects of $\text{TNF}\alpha$ (OD = optical density, n=5). **B** Analyses of the cytokeratin immunostaining revealed a shift of the intensity peak away from the cell border after incubation with $\text{TNF}\alpha$. Co-incubation with GDNF attenuated the effect of $\text{TNF}\alpha$ (n = 6). **C** The distance of keratin retraction is shown. The distance between the highest intensities and the cell borders was determined. $\text{TNF}\alpha$ increased the keratin retraction to 43.52 ± 4.48 pixel compared to 9.84 ± 1.14 after co-incubation of $\text{TNF}\alpha$ with GDNF (n=6)



Suppl. Fig. 4

Supplemental Figure 4

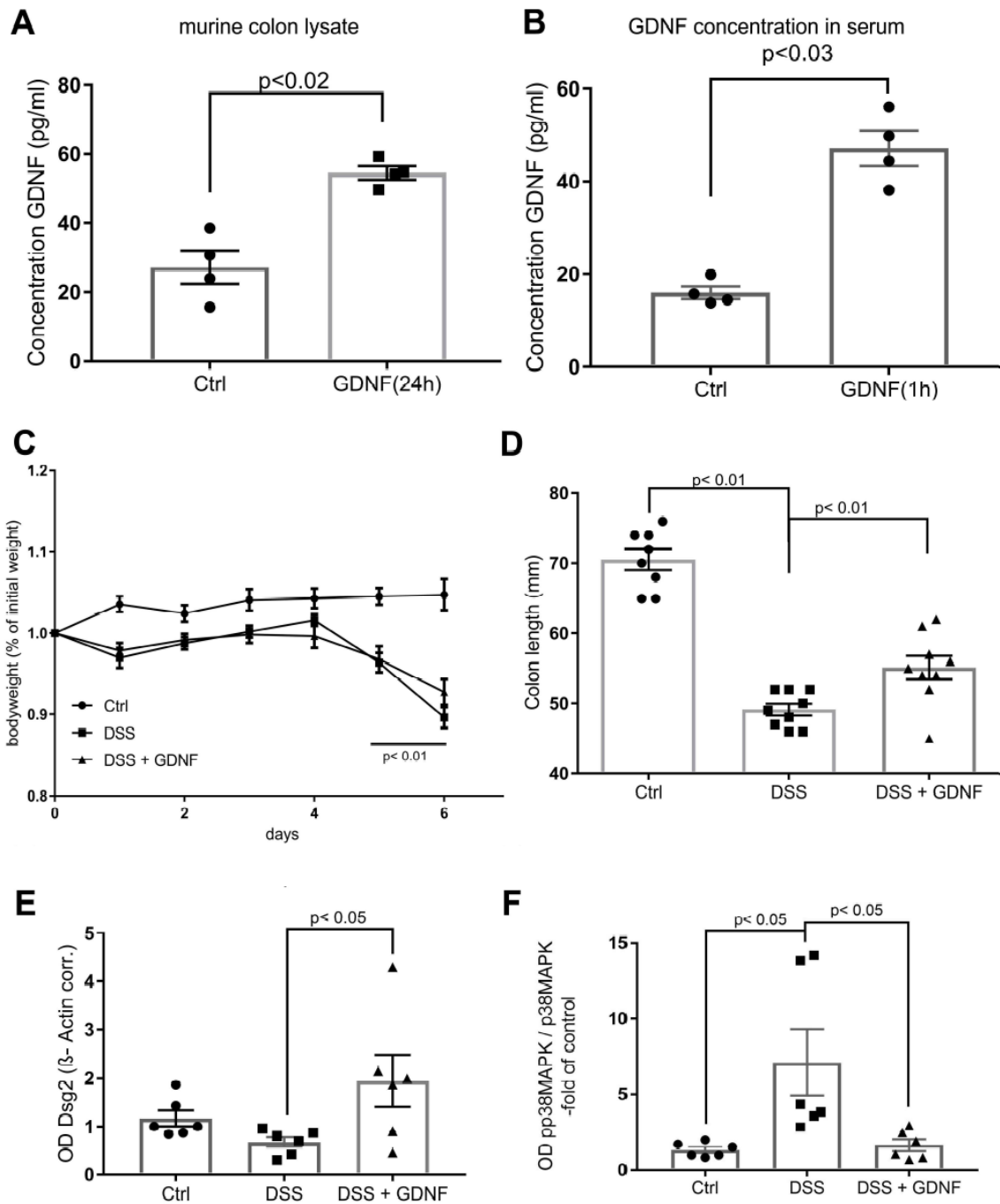
A, C, E Measurements of the western blot intensity after application of TNF α and GDNF in Caco2 cells demonstrate that TNF α showed increased phosphorylation of p38MAPK, cytokeratin18 at Serin 52 and cytokeratin 8 at Serin 74. This was attenuated following co-incubation of TNF α with GDNF, where phosphorylation patterns were comparable to control levels (OD = optical density, n=6). **B, D, F** TNF α enhanced phosphorylation of p38MAPK and cytokeratin 18 at Serin 52 in human enteroids, which was not that strong for cytokeratin 8 at serin 74. Application of GDNF reduced this effect of TNF α -induced phosphorylation (OD = optical density, n=6).



Suppl. Fig. 5

Supplemental Figure 5

A Phosphorylation of cytokeratin 18 at Serin 52 was altered following modulation with p38MAPK inhibitor SB202190 and p38MAPK activator anisomycin. Anisomycin led to a significant increase in phosphorylation, while Sb202190 attenuated phosphorylation of cytokeratin 18 at Serin 52 (OD = optical density, n=6). **B** Anisomycin increased phosphorylation of cytokeratin 8 at Serin 74 and vice versa Sb202190 reduced this phosphorylation (OD = optical density, n=6). **C** In contrast, TNF α and GDNF did not influence the phosphorylation of cytokeratin 18 at Serin 33 (OD = optical density, n=4).



Suppl. Fig. 6

Supplemental Figure 6

A The concentration of GDNF in murine lysates of the colon was determined with a GDNF ELISA. The application of 100µg GDNF intraperitoneally led to a significant increase of GDNF after 24h (n=4). **B** In murine serum concentration of GDNF increased after 1h following the intraperitoneal injection of 100µg GDNF (n=4). **C** Dextran Sodium Sulfate in the drinking water of the mice led to a significant reduction of their bodyweight compared to controls. Intraperitoneal application of 100µg GDNF did not block this effect of Dextran Sodium Sulfate (n=9). **D** The colon of the mice was significantly shortened following the application of Dextran Sodium Sulfate in mice. Intraperitoneal injection of GDNF for 6 days attenuated this effect on the colon length (n=9). **E** Western blots of murine colon lysates showed a significant increase of the signal of Dsg2 in the Dextran Sodium Sulfate mice that were treated with GDNF compared to the Dextran Sodium Sulfate alone group (n=6). **F** Quantification of the phosphorylation of p38MAPK is shown. In SDD animals phosphorylation of p38MAPK was significantly increased which was blocked by treatment with GDNF (OD = optical density, n=6).

Supplementary Methods

Generation of CRISPR/Cas9-mediated gene knockout for Dsg2 in Caco2 cells

sgRNA for SpCas9-mediated genome editing were designed using the Chopchop-web based sgRNA design tool (Labun et al., 2016). Two oligos targeting exon 3 and exon 13 of human Dsg2 were designed and subcloned into two lentiviral vectors; sgRNA targeting exon 3 into pLentiCRISPR v2 (was a gift from Feng Zhang, Addgene plasmid # 52961) and sgRNA targeting exon 13 in pLKO5.sgRNA.EFS.GFP (was a gift from Benjamin Ebert, Addgene plasmid # 57822). Lentiviral particles were produced using HEk293T cells utilising second generation lentiviral packaging system comprising pPAX and pMD2 packaging plasmids. Caco-2 cells were seeded in 6 well plates and 24h later infected in the presence of polybrene, with viral supernatant comprising both viral particles, LKO-sgRNA-EFS GFP and CrisprV2.

3 days post infection infected cells were selection with Puromycin (15ug/ml) for 1 week with medium changes every two days. Puromycin-positive clones were FACS sorted for GFP-expression and reseeded as single cells in a 24 well plate. Single clones were propagated and loss of Dsg2 was assessed in single clones by western blot and qPCR.

<i>Primer name</i>	<i>Sequence</i>
hDSG2-1 f	caccgCTTTGGCGCCCTTTCCGCAA
hDSG2-1 r	aaacTTGCGGAAAGGGCGCCAAAGc
hDSG2-2 f	caccgCTAAACATCCTCATTAGTG
hDSG2-2 r	aaacCACTAAATGAGGATGTTTAGc
<i>qPCR primer</i>	<i>Sequence</i>
DSG2 f	Aattgcgctcatgatttgg
DSG2 r	Gcaatggcacatcagcagta

Enteroids

IECs were isolated from human full-wall gut resections, 1cm² in size as described previously (Schweinlin et al., 2016). Briefly, villi were scraped off the muscle-free mucosa using a sterile glass slide. The remaining tissue was transferred into a 50mL falcon tube with 20mL 4°C cold HBSS (Sigma-Aldrich, St. Louis, MO, USA), vortexed for 5s and the supernatant discarded. This washing step was repeated until the supernatant was completely cleared of cell debris. Afterward, the tissue was incubated in 4°C cold 2 mM EDTA/HBSS solution (Sigma- Aldrich, St. Louis, MO, USA) for 30min at 4°C under gentle rotation on a shaker. Subsequently, the tissue was washed once in 20 mL HBSS by manually inverting the tube five times. The mucosa was transferred in a new tube with 10mL HBSS and manually shaken five times. This shaking procedure was repeated four times always using a new tube. Each cell fraction was checked for the amount and size of crypts within small drops under the microscope. The supernatants containing the most vital appearing crypts were pooled and centrifuged at 350g for 3 min at room temperature (RT). Pellet was resuspended in 10mL basal medium, DMEM-F12 Advanced (Invitrogen, Carlsbad, CA, USA) supplemented with N2, B27, Anti-Anti, 10mM HEPES, 2 mM GlutaMAX-I (all from Invitrogen, Carlsbad, CA, USA), 1 mM N-acetylcysteine (Sigma-Aldrich, St. Louis, MO, USA), and the crypt number was estimated in a 10µL drop by microscopy. Crypts were centrifuged in a nonstick 1.5 mL tube at 350g for 3 min at RT and the supernatant was removed. The tube with the cell pellet was placed on ice until further use. The pellet was resuspended in an appropriate amount of cold Matrigel (Corning, Hickory, NC, USA) that is, 5000 crypts/mL Drops of 50µl per well were seeded in a 24- well plate and incubated for 10–20 min until the Matrigel was well solidified. The culture medium contained a mixture of 50% fresh basal medium and 50% Wnt3A-conditioned medium.

Furthermore, the following growth factors were added: 500 ng/mL hR-Spondin 1 (PeproTech, Rocky Hill, NY, USA), 100 ng/mL IECs were isolated from human small intestinal tissue and expanded as organoid culture for 3–4 weeks.

GDNF-ELISA

GDNF ELISA was performed according to manufacturer's protocol (Promega, Mannheim, Germany). The assay is an antibody sandwich ELISA in which 96-well plates are coated with anti-GDNF monoclonal antibody, which binds soluble GDNF. Nonspecific bindings were blocked with block & sample buffer. 100µl GDNF standard or test samples were added to the 96-well plate and incubated with shaking for 6h. As test samples either mouse serum or tissue lysates of mouse gut were used. Mouse serum was collected during the animal surgery as described above. 10µl serum was diluted in 40µl PBS. Tissue lysates were obtained from the mouse gut by homogenization using tissue lyzer in 500µl buffer. After centrifugation (30min, 4°C, 13.000g), the supernatant was used for the ELISA measurements. After several wash steps, an anti-human GDNF primary antibody was added to the 96-well plate followed by incubation at 4°C overnight and by several washing steps. Next, anti-Chicken IgY HRP conjugate was incubated for 2 hours. As a final step, TMB One solution was added, reaction was stopped with 1N hydrochloric acid and color change was detected with an ELISA reader at 450nm.

Immuncytochemistry

Cultured cell monolayers were prepared for immunostaining as described previously (Schlegel et al., 2012). In brief, epithelial cells were grown to confluence on coverslips or transwell chambers (0.4 µm pore size, Falcon, Heidelberg, Germany). After incubation with or without different mediators, cells were fixated with 2% formaldehyde for 10 minutes and treated with 0.1% Triton-X for 15 minutes afterwards, at room temperature. The human and animal tissue samples and enteroids embedded in paraffin were sectioned in 1µm slices. Immunostaining was performed after removal of paraffin as described for epithelial monolayers (Schlegel et al., 2010). Then monolayers and tissue slides were incubated at 4° C overnight using following primary antibodies at 1:100 in phosphate-buffered saline (PBS): rabbit anti-Desmoglein2 (Merck Milipore, Darmstadt, Germany); mouse anti-Cytokeratin 18 and 8 (both Santa Cruz Biotechnology, Heidelberg, Germany). As secondary antibodies, we used Cy3- or 488- labeled goat anti-mouse, goat anti-rabbit, or mouse anti-goat (all diluted 1:600, Dianova, Hamburg, Germany). Coverslips and filters were mounted on glass slides with Vector Shield

Mounting Medium as anti-fading compound, which included DAPI to stain cell nuclei additionally (Vector Laboratories, Burlingame, CA). Representative experiments were photographed with a fluorescence microscope BZ-9000 (BIOREVO, Keyence, Osaka Japan) and a confocal microscope (Leica TCS SP2, Wetzlar, Germany).

Western blot

For Western blot analysis cells were grown on 6-well plates and homogenized in SDS lysis buffer containing 25mmol/l HEPES, 2mmol/l EDTA, 25mmol/l NaF and 1% sodium dodecyl sulfate. To analyze human enterocytes, the mucosa was mechanically dissected from the underlying tissue immediately after the resection. Full wall specimen were used for analyses of the animal experiments.

Then the specimens were lysed in a SDS lysis buffer using TissueLyzer (Quiagen, Hilden Germany). In similar fashion, a part of the distal murine colon was lysed in SDS lysis buffer with TissueLyzer.

SDS gel electrophoresis and blotting were carried out after normalization of the protein amount using BCA assay (Thermo Fisher, Waltham, MA), as described previously (Schlegel et al., 2011). Antibodies against pp38MAPK and p38MPAK (Cell Signaling Technology, Cambridge, UK), Phospho-Cytokeratin18 Serin52 (abcam, Cambridge, UK), Phospho-Cytokeratin18 Serin33 (abcam, Cambridge, UK), Cytokeratin 18 (Santa Cruz biotechnology, Heidelberg, Germany), Phospho-Cytokeratin 8 Serin74 (Thermo Fisher, Waltham, MA), Desmoglein2 goat anti-mouse (Life technologies, Carlsbad, CA) and GDNF (R+D Systems, Abingdon, UK) were used at a dilution of 1:1000 in 5% bovine serum albumin (BSA) and 0.1% Tween. As secondary antibodies horseradish peroxidase-labeled goat anti-rabbit IgG, goat anti-mouse IgG (all Santa Cruz Biotechnology, Heidelberg, Germany) were used (1:3000 in 5% BSA, 0.1% Tween). To validate normalization Peroxidase-labeled β -Actin and GAPDH (both Sigma-Aldrich, Munich, Germany) antibodies were applied. Chemiluminescence signal detection and quantification were performed by densitometry (ChemicDoc Touch Bio-Rad Laboratories GmbH, Munich, Germany). Optical densities (OD) were quantified in each Western Blot using Image Lab ChemicDoc Touch Bio-Rad Laboratories GmbH, Munich, Germany) for statistical evaluation.

Atomic force microscopy

Cells were grown on glass coverslips and treated with GDNF (100ng/ml) 1 day before getting confluent or with 4mM EGTA for 30 min after finished control measurements. For analysis of Dsg2 interactions on the surface of living cells, a Nanowizard III AFM (JPK Instruments, Berlin, Germany) mounted on an optical microscopy (Carl Zeiss, Jena, Germany) was used. The approach of AFM force spectroscopy on living cells was described in detail before (Vielmuth et al., 2015). Imaging and force measurements were performed in cell culture medium using flexible Si₃N₄ AFM cantilevers (MLCT probes, Bruker, Calle Tecate, CA, USA) coated with a flexible bifunctional polyethylene glycol linker (Gruber Lab, Institute of Biophysics, Linz, Austria) and recombinant Dsg2-Fc containing the complete extracellular domain (ED) of Dsg2, as outlined elsewhere (Andreas et al., 2007). At first, AFM topography images of 50 x 50 μm and 128 x 128 pixels were created using a force curve-based imaging mode (QI-mode) with a setpoint adjusted to 0,5 nN, a z-length of 1500 nm and a pulling speed of 50 μm/s. For adhesion measurements, a small area of 2 x 5 μm was selected and 1000 force-distance curves were recorded for each area using the force mapping mode with a relative setpoint of 0,5 nN, a z-length of 3 μm and a pulling speed 5 μm/s. JPK data processing software (JPK instruments) was applied for processing AFM images and analysis of force distance curves and Origin 9.1 (Originlab, Northampton, MA, USA) was used for peakfit analysis of measured unbinding force curves.

3 Discussion

3.1 Cultured enterocytes as suitable model for the human intestinal epithelium

Aim of this study was to analyze the adhesive and signaling function of Dsg2 in the intestinal epithelium. The usage of *in vitro* cell culture represents a convenient and low cost approach that is suitable for genetic manipulation and allows easy stimulation with activators, inhibitors, cytokines or growth factors (Fig. 8). In contrast, *in vivo* studies are cost-expensive, difficult to manipulate without inducing physiological complications and can raise ethical concerns. In addition, some techniques are not applicable in an *in vivo* or *ex vivo* model of the intestine, such as the AFM to measure binding properties of desmosomal cadherins. Here, two human colon carcinoma cell lines were used, DLD1 and Caco2 cells, which were derived from different patients (Caro et al., 1995; Chen et al., 1995; Dexter et al., 1981). A thorough characterization revealed that both cell lines were polarized after growing for four (DLD1) or six (Caco2) days post confluence, with mature cell junctions at the apical side, characteristic microvilli on the cell surface and fully developed desmosomes similar as seen in human tissue samples. Moreover, they form a cell monolayer that physically and functionally resemble an intestinal epithelial barrier, with a steady transepithelial resistance that was maintained over days. This is in line with previous studies that also reported the development of a mature epithelial barrier (Artursson et al., 1993; Matsumoto et al., 1990; Schlegel et al., 2010; Wang et al., 2008; Wilson et al., 1990; Zweibaum A., 1991). Furthermore, several results obtained in cell culture, were also reproducible in an *in vivo* mouse model, organoid cultures and human tissue samples, which suggests that cultured enterocytes represent a suitable model to investigate the biological functions of Dsg2. However, one has to consider that the human intestinal epithelium is composed of several different cell types and differences in gene expression profiles are present along the crypt-villus axis as well as along the diverse sections of the gastrointestinal tract (Anderle et al., 2005). Although enterocytes make up the largest portion in the intestinal epithelium, the specific functions of other cell types shape the environment of the intestinal epithelium, which

is missing in the enterocyte cell culture. For instance, Caco2 as well as DLD1 cells produce no or only moderate amounts of mucus (Dexter et al., 1981; Engle et al., 1998), which might affect the binding properties of Dsg2 on the cell surface. Hence, a co-culture system of enterocytes and goblet cells could provide further insights into the real physiological situation and should be tested in future studies. However, complex interactions with the immune system highly influences the barrier properties *in vivo* (Luissint et al., 2016), which cannot or only partly be simulated in a cell culture system. Furthermore, some considerations must be taken into account when choosing a cell line for studies. Since the various available cell lines derived from different carcinomas, they differ in their genetic profiles (Ahmed et al., 2013), which might influence the outcome of a study and could explain contradictory results of the same investigation in different labs. For instance, in this study using Caco2 and DLD1 cells, loss of Dsg2 had a proproliferative effect, while another study conducted in SW480 cells reported the opposite (Kamekura et al., 2014). A constitutive active β -catenin signaling and deregulated expression of pro-proliferative genes that are present in SW480 but not in DLD1 cells (Rowan et al., 2000; Yang et al., 2006) might be an explanation. Hence, it is reasonable to conduct a study in different cell lines to assure that the outcome is universal, as it has been done in this thesis. All in all, cultured enterocytes represent a suitable model to study functions of proteins in the intestinal epithelium.

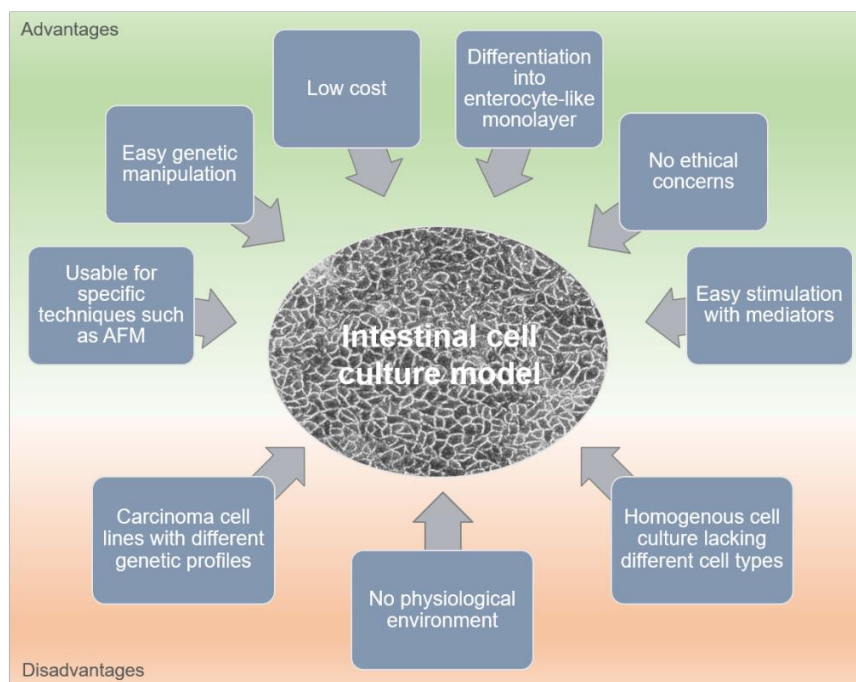


Figure 8. Advantages and disadvantages of intestinal cell culture model.

Several advantages argue in favor of using cultured enterocytes (confluent Caco2 cells are shown) as model system to study functions of proteins in the intestinal epithelium. Disadvantages such as diverging genetic profiles should be considered when choosing a cell line and co-culture systems with multiple cell types might provide more insights.

3.2 Dsg2 as cell surface receptor for signal transduction of environmental stimuli

Dsg2 constitutes the adhesive core of desmosomes (Owen and Stokes, 2010), which until recently have been considered to provide first and foremost the mechanical strength to intercellular cohesion (Green and Simpson, 2007). In the mature intestinal epithelium, desmosomes are located beneath the TJ and AJ, thereby sealing the paracellular space, which is also referred to as the “terminal bar “ (Capaldo et al., 2014; Farquhar and Palade, 1963a). A previous study reported that a specific antibody targeting the ED of Dsg2 impaired barrier function and led to rupture of TJ (Schlegel et al., 2010). However, the underlying mechanism was not investigated. The authors speculated that the antibody might bind to Dsg2 present outside of desmosomes, thus inducing signaling events, rather than passing the AJC and interfering with desmosomal Dsg2. From studies on pemphigus, it is already known that binding of desmoglein-specific autoantibodies to extradesmosomal desmoglein molecules on the cell surface of keratinocytes, activates intracellular signaling cascades, leading to impaired desmoglein-mediated cell adhesion (Berkowitz et al., 2008a; Kawasaki et al., 2006; Saito et al., 2012; Spindler et al., 2013; Tsunoda et al., 2011; Waschke et al., 2005). However, nothing was known about extradesmosomal Dsg2 on the surface of intestinal epithelial cells. This study demonstrates for the first time that extradesmosomal Dsg2 is present on the surface of cultured polarized enterocytes. Moreover, immunostaining of human tissue samples and enteroids revealed extradesmosomal Dsg2 on the cell surface, as well. Binding of an antibody directed against the ED of Dsg2 led to impaired cell adhesion, which was preceded by p38MAPK activation, indicating that Dsg2 transmits the extracellular stimuli thereby activating signaling events that control intercellular adhesion. Along this line, Dsg2 has been reported as a receptor utilized by adenoviruses to infect intestinal epithelial cells. Adenovirus interaction with Dsg2 activated intracellular signaling cascades such as PI3K and Erk1/2, resulting in the opening of intercellular junctions (Wang et al., 2011). Since desmosomal Dsg2 in polarized epithelial cells is inaccessible for adenoviruses, this underlines the appearance of extradesmosomal Dsg2 on the cell surface. In accordance to the present study, in which binding of the Dsg2-specific antibody to the ED 3 activates p38MAPK signaling, Dsg2 ED 3 is also critical for

adenovirus binding thereby inducing activation of the MAPK pathway (Vassal-Stermann et al., 2018; Wang et al., 2011). Similarly, in keratinocytes an antibody targeting the Dsg3 ED 3 and 4 caused p38MAPK-mediated endocytosis of Dsg3 (Saito et al., 2012). Hence, beside its adhesive function, Dsg2 can transmit extracellular signals through ED 3. At present, it is unclear how this function is achieved. Given that no enzymatic activity of the cytoplasmic Dsg2 tail is known to date, interaction with enzymatic active proteins might be involved. A possible candidate is the RTK EGFR.

3.2.1 Direct interaction of Dsg2 and EGFR via their extracellular domains regulates cell adhesion and proliferation

In this study, a direct interaction between the extracellular part of Dsg2 and EGFR has been shown for the first time. Dsg2 is required for localization of EGFR to the cell borders where it is phosphorylated at Y845, which is catalyzed by the kinase Src. In Dsg2-deficient cells, phosphorylation at Y845 is reduced and EGFR is retracted from cell borders. Moreover, proliferation is drastically increased upon loss of Dsg2 and can be restored by inhibition of EGFR activity as well as by reintroduction of Dsg2. These findings led us to propose a new mechanism that Dsg2 interacts directly with its extracellular domain with EGFR, shapes EGFR function towards adhesion, and suppresses proliferation (Fig. 9). In concordance, reduced phosphorylation of EGFR Y845 upon loss of Dsg2 was also reported in other studies (Kamekura et al., 2014; Overmiller et al., 2016). EGFR phosphorylation at Y845 activates a series of downstream events, thus regulating various cellular functions (Biscardi et al., 1999; Maa et al., 1995; Sato et al., 1995). Enhanced cell transformation, motility and invasion have been linked to Y845 phosphorylation-mediated signaling and increased levels of EGFR and Src are observed in several cancer cells (Chung et al., 2009; Jung et al., 2011; Jung et al., 2013; Kannangai et al., 2006; Maa et al., 1995). Furthermore, Src-mediated phosphorylation at Y845 has been shown to inhibit apoptosis and to promote proliferation (Ray et al., 2007; Tice et al., 1999). Along this line, recent studies reported that reduced levels of EGFR Y845 phosphorylation upon loss of Dsg2 result in decreased cell proliferation (Kamekura et al., 2014; Overmiller et al., 2016). This is contradictory to our data, showing that reduced phosphorylation at EGFR Y845 upon loss of Dsg2 enhances cell

proliferation. However, and in support of our data, Y845 phosphorylation is also known to induce cell-cycle arrest and to inhibit growth (Godek et al., 2011; Sato et al., 2003). Several reasons are conceivable for the diverging outcomes that are triggered by the same phosphorylation site. First of all, EGFR signaling is spatially compartmentalized (Bakker et al., 2017). EGFR is activated upon ligand binding at the cell surface, which is followed by its internalization and passage of different routes of the endosome network, whereby signaling continues (Francavilla et al., 2016; Haugh et al., 1999; Vieira et al., 1996; Wu et al., 2012). Thus, different mechanisms leading to the observed EGFR Y845 phosphorylation might explain diverging outcomes. Consistently, the study reporting a decreased proliferation after loss of Dsg2, suggests EGFR activation through Dsg2-mediated displacement of EGFR from lipid rafts (Overmiller et al., 2016), while our data propose direct interaction of Dsg2 and EGFR that suppress proliferation. In addition, we demonstrate that antibodies targeting the ED of Dsg2 or of EGFR inhibit the interaction. In line with this, another study shows that Dsg2 ED fragments capable of binding to the same region as the inhibitory antibody, disrupt intercellular adhesion and enhance proliferation of IECs (Kamekura et al., 2015), thus underpinning our hypothesis that Dsg2-EGFR interaction fosters adhesion and suppresses proliferation. In addition, Dsg2 has been shown to support differentiation and thus acts as tumor suppressor gene in gastric cancer (Yashiro et al., 2006), which also points to an anti-proliferative function of Dsg2. Moreover, beside our results from experiments with cultured cells, we observed a close co-localization of Dsg2 and EGFR also in human tissue samples and enteroids, which supports the physiological relevance of this newly discovered complex. Furthermore, our collaboration-study on intestine-specific Dsg2 knockout mice revealed increased proliferation under inflammatory conditions in the Dsg2-KO. This further indicates that Dsg2 might inhibit EGFR-mediated proliferation under normal conditions and that loss of Dsg2-EGFR interaction enables proliferation for instance to induce wound healing during inflammation. Although EGFR is generally thought to be located in the basolateral membrane of polarized epithelial cells (Bishop and Wen, 1994; Scheving et al., 1989), several studies report its presence also in the apical membrane in IECs (Gonnella et al., 1987; Kelly et al., 1992; Yoo et al., 2011). Hence, a receptor complex consisting of Dsg2 and EGFR at the apical cell surface is plausible. Recently, a similar complex consisting of EGFR and the AJ component Ecad was reported, which

likewise suppresses EGFR activity and stabilizes cell adhesion (Rubsam et al., 2017b). Furthermore, apical and basolateral located EGFR has been demonstrated to exert differential functions (Kuwada et al., 1998), which might also explain diverging outcomes of EGFR phosphorylation at Y845.

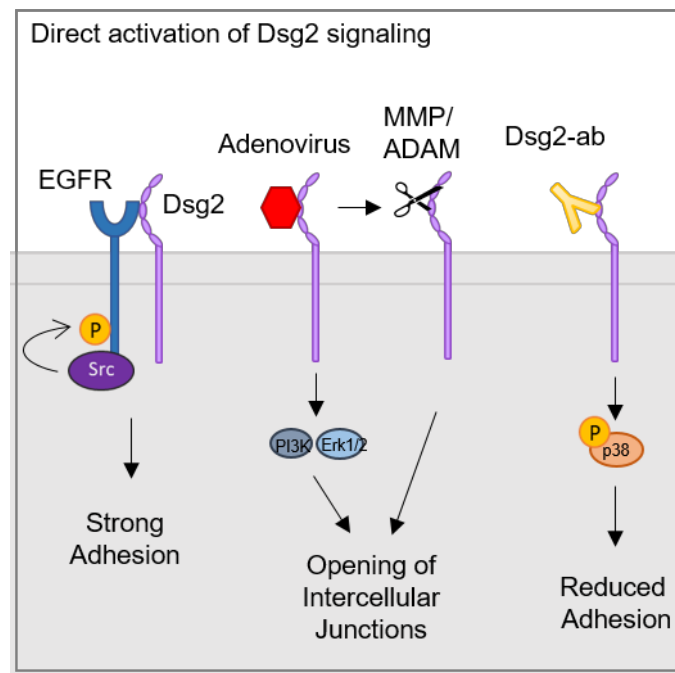


Figure 9. Schematic model of Dsg2-mediated signaling functions through direct binding to Dsg2. Direct interaction with RTK and binding of adenoviruses or Dsg2-specific antibodies (ab) to Dsg2 molecules can induce signaling cascades that modulate intercellular adhesion. Mechanisms include Dsg2-mediated inhibition of the canonical EGFR-triggered proliferation pathway. Adenovirus-binding leads to activation of downstream signaling molecules such as PI3K and Erk1/2, resulting in opening of other junctions (Wang et al., 2011) and activation of MMPs and ADAM proteins that cleave Dsg2 ED (Wang et al., 2015). Dsg2-specific antibody binding results in activation of p38MAPK.

3.2.2 Indirect activation of Dsg2 signaling function through environmental stimuli

Here, we suggest that Dsg2 functions as receptor on the cell surface and that direct binding to Dsg2, such as binding of other receptors, autoantibodies or adenoviruses, activates intracellular signaling pathways. However, there is evidence that Dsg2 signaling is activated through environmental stimuli, such as cytokines or growth factors, in an indirect manner, as well (Fig 10).

3.2.2.1 Activation of Dsg2 signaling function through inflammatory cytokines

Inflammatory cytokines such as $\text{TNF}\alpha$, $\text{INF}\gamma$ or $\text{IL-1}\beta$ are known to alter epithelial barrier function and to be increased in IBD (Koch and Nusrat, 2012; Nava et al., 2010; Rogler and Andus, 1998; Sanders, 2005), which also display deregulated Dsg2 function (Spindler et al., 2015). Cytokines influence Dsg2 function by activation of MMPs and ADAM proteins, whose activities are known to be enhanced in IBD (Baugh et al., 1999; Rogler and Andus, 1998). Activated proteinases cleave the ED of Dsg2, which on the one hand reduces intercellular adhesion through disruption of the adhesive core of desmosomes, on the other hand the fragments can serve as ligands for other receptors. For instance, soluble Dsg2 fragments have been demonstrated to bind to HER2 and HER3 receptors, resulting in activation of the Akt/mTOR and MAPK pathway and subsequently enhanced proliferation (Kamekura et al., 2015). Although, in this case proliferation was induced through Dsg2 fragment-mediated activation of HER2 and HER3, Dsg2 ED fragments can likewise bind homophilic to Dsg2 and thus might possibly lead to disruption of Dsg2-EGFR binding that induces EGFR-mediated proliferation. In addition, it is not clear whether desmosomal or extradesmosomal Dsg2 is cleaved. In this study, we observed ultrastructural changes of desmosomes in samples from CD patients, or found them to be completely missing, indicating that desmosomal Dsg2 molecules might be cleaved under inflammatory conditions, which results in loss of functional desmosomes. In this line, endocytosis of desmosomal Dsg2 has been reported to be regulated by ADAM proteins (Klessner et al., 2009). However, direct binding of adenoviruses to Dsg2 has been reported to induce Dsg2 ED shedding, as well (Wang et al., 2015). Since desmosomal Dsg2 is not accessible to the virus, it is likely

that the virus binds to extradesmosomal Dsg2. One could speculate that cleavage of desmosomal and extradesmosomal Dsg2 induces different signaling events. In addition, it is not clarified whether the cleaved Dsg2 fragments induce autocrine signaling, or act on neighboring cells. A recently published study propose that cleaved Dsg2 fragments, resulting from apoptotic stimuli, induce proliferation of neighboring cells to promote wound closure (Yulis et al., 2018). In case of adenovirus-mediated Dsg2 shedding, it is more likely that shedding-mediated signaling occurs in the same cell, as the goal of adenovirus binding to Dsg2 is to increase access to receptors trapped in intercellular junctions (Wang et al., 2015; Wang et al., 2011).

3.2.2.2 Activation of Dsg2 signaling function through growth factors

We demonstrated a direct interaction of Dsg2 and EGFR in this study, hence activation of Dsg2 signaling via growth factor binding to EGFR, is expectable. In line with the above findings, we observed that EGF inhibits the interaction and induces internalization of both, EGFR as well as Dsg2. Thus, it is likely that interaction with EGFR stabilizes Dsg2 at the cell surface. A possible mechanism for stabilizing Dsg2 might involve tyrosine phosphorylation of Dsg2 that has been shown to be blocked by EGFR tyrosine kinase inhibitors (Lorch et al., 2004). Furthermore, EGFR mediated phosphorylation of Dsg2 associated plaque proteins such as PG, upon stimulation with growth factors, has been assumed critical in modulating the association of the cadherin-catenin complex with the cytoskeleton (Gaudry et al., 2001; Kanai et al., 1995; Shibamoto et al., 1994; Valles et al., 1990), which supports stability of desmogleins at cell borders. Moreover, EGF stimulation is known to activate p38MAPK (Frey et al., 2004; Vergarajauregui et al., 2006) that is a well-known modulator of Dsg2 signaling. Finally, EGFR activity has also been shown to induce MMPs (Lochter et al., 1997; McCawley et al., 1998), which cleave Dsg2 molecules as described above.

Recently, another growth factor was identified to regulate intestinal barrier functions, namely the GDNF that enhances barrier properties of IECs (Meir et al., 2015b). A further objective of this thesis was, to address the impact of GDNF on Dsg2 function, which was part of a study investigating how GDNF regulates intestinal barrier function in IBD. Here, AFM analyses revealed that GDNF increases Dsg2 binding at cell-cell

borders, either through redistribution of existing Dsg2 molecules or through formation of new Dsg2 interactions at cell borders. In line with this, decreased levels of GDNF have been associated with a barrier breakdown of the intestinal epithelial barrier in mice, underlining its beneficial function for barrier properties (Brun et al., 2013). Moreover, analyses of immunostainings for cytokeratin18 after stimulation with the cytokine TNF α and GDNF revealed a significant retraction of the keratin cytoskeleton after TNF α -stimulation, which was prevented by simultaneous application of GDNF. Furthermore, the data suggest that this protective effect is mediated via reduced p38MAPK and cytokeratin phosphorylation. This is in line with a previous study, showing that stimulation with TNF α induced p38MAPK phosphorylation and subsequent loss of Dsg2-mediated adhesion (Spindler et al., 2015). However, the role of p38MAPK activity in barrier regulation seems to differ depending on the type of activation, since Dsg2-deficient enterocytes show impaired barrier properties despite reduced p38MAPK activity and activation of p38MAPK enhanced barrier formation. Thus, p38MAPK has a central role in regulating intercellular adhesion and a proper balance of its activity is required. Furthermore, stimulation with GDNF alone did not alter phosphorylation of p38MAPK, but enhanced Dsg2 binding frequency as well as its distribution at cell borders in AFM experiments. In conclusion, this data indicates that GDNF prevents p38MAPK-mediated keratin retraction and subsequent loss of cell adhesion but also directly enhances Dsg2-mediated cell adhesion at cell borders. Since GDNF is clearly reduced in samples from patients suffering from CD or UC, our data points to a new pathomechanism for barrier dysregulation in IBD and offers new possibilities for therapeutic approaches. Accordingly, GDNF has already been proposed to serve as rescue mechanism during inflammation (Steinkamp et al., 2003).

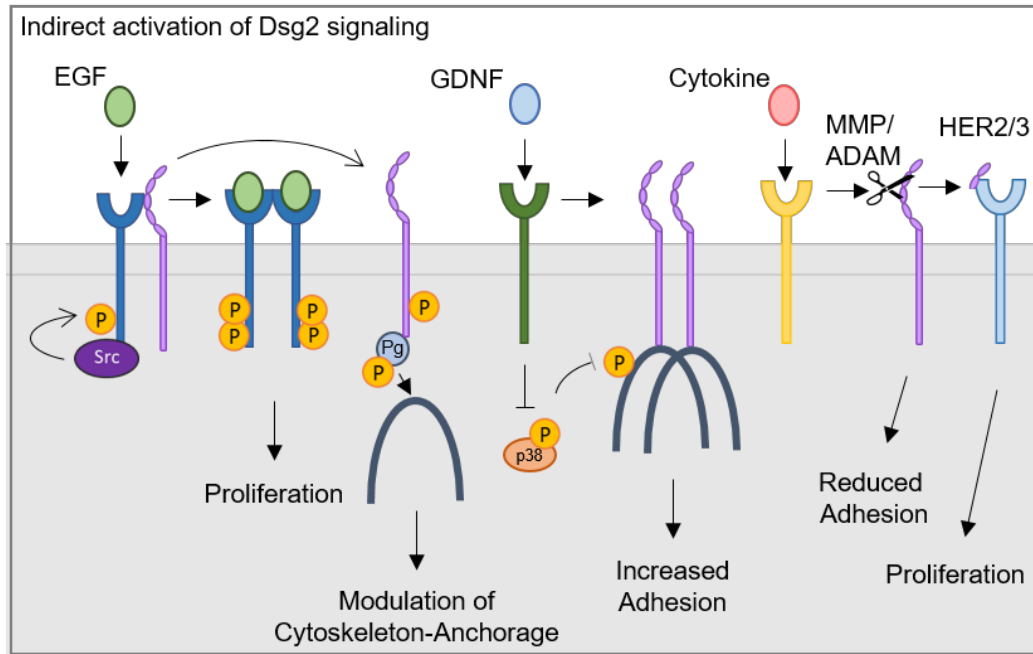


Figure 10. Schematic model of indirect activation of Dsg2-mediated signaling functions. Dsg2 mediated signaling function is induced indirectly via extracellular stimuli such as growth factors and cytokines. EGF binding to EGFR blocks its interaction with Dsg2 and induces the canonical signaling cascade resulting in cell proliferation. In addition, activated EGFR results in phosphorylation of the Dsg2 cytoplasmic tail (Lorch et al., 2004) or plaque proteins such as PG (Gaudry et al., 2001; Shibamoto et al., 1994), thus modulating anchorage to the cytoskeleton. GDNF has protective function by inhibiting phosphorylation of p38MAPK and keratins but also influences Dsg2 distribution at cell borders. Cytokines induce Dsg2 ED shedding, resulting in reduced adhesion and increased proliferation (Kamekura et al., 2015).

3.3 Tissue dependent function of desmogleins

In previous studies, our group has characterized what mechanisms regulate desmosomal adhesion in keratinocytes. In this context, several key players were identified that play also a role in regulating cell adhesion in IECs. However, the functional mechanism in keratinocytes differs from that in IECs. For instance, in keratinocytes Dsg2 has been found to be less important for cell cohesion than Dsg3 and does not influence p38MAPK activity. Moreover, activated p38MAPK was shown to reduce intercellular cohesion and was found in a complex with Dsg3 but not Dsg2 (Hartlieb et al., 2013; Hartlieb et al., 2014; Spindler et al., 2013). In contrast, this study demonstrates that IECs require p38MAPK activity for barrier formation and maintenance. Furthermore, Dsg2 is indispensable for cell cohesion and regulates the activity of p38MAPK. Collectively, these results point towards a tissue-specific function of desmosomal cadherins.

Although p38MAPK activity is known to be dependent on the cell type and stimulus, as its signaling has been shown to promote cell death in some cell lines, while enhancing survival, cell growth and differentiation in different cell lines (Cuenda and Rousseau, 2007), the diverging mechanisms that regulate cell adhesion pathways might also come from tissue-specific expression pattern of desmogleins. Simple epithelia, like the intestinal epithelium, comprises only two desmosomal cadherin isoforms, Dsg2 and Dsc2. In contrast, seven desmosomal cadherin isoforms can be found in multilayered stratified epithelia like the human epidermis, with a differential distribution between the specific layers and very low levels of Dsg2 and Dsc2 (Dusek et al., 2007; Garrod and Chidgey, 2008; Mahoney et al., 2006) (Fig. 11). In one individual cell, several isoforms are expressed and various isoforms can be found in one single desmosome (North et al., 1996; Nuber et al., 1996; Shimizu et al., 1995). Thus, functions associated with desmosomal cadherins can be distributed on several isoforms in keratinocytes, whereas in IECs they have to be combined in Dsg2 and Dsc2. In keratinocytes, desmosomal cadherin isoforms have specific functions in epithelial differentiation. For instance, Dsg2 is concentrated in basal layers where proliferation takes place and is absent in suprabasal layers, whereas Dsg1 gets expressed on initiation of differentiation that is paralleled by cell movement into the first suprabasal layer and shows highest expression rates in suprabasal layers (Johnson et al., 2014).

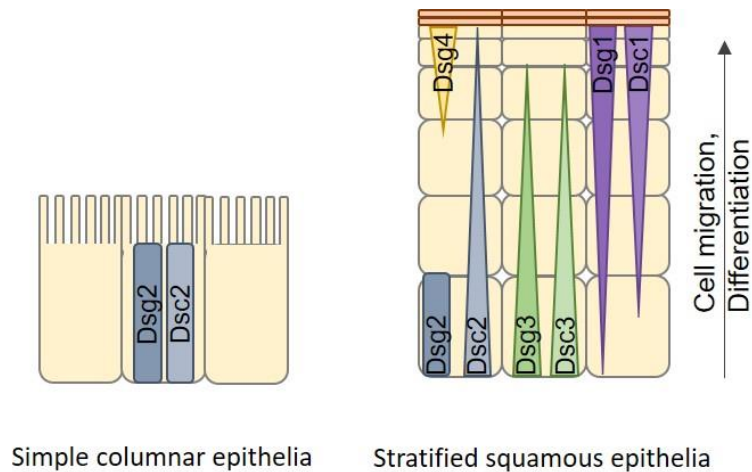


Figure 11. Schematic outline of tissue-dependent expression of desmosomal cadherins in simple and stratified epithelial tissue. While simple columnar epithelial cells express only two desmosomal cadherin isoforms, seven isoforms are expressed in stratified epithelia in a differentiation dependent pattern. Dsg2, which is the only desmoglein in simple epithelia, is concentrated in basal proliferative layers in stratified epithelia and is absent in suprabasal layers where Dsg1 levels are at their highest.

Their distinct functions become clear when expression of a desmosomal cadherin is forced in the wrong layer. Hence, it has been shown that ectopic expression of Dsg2 in the suprabasal skin layer acts contrarily to Dsg1 and induces enhanced proliferation as well as activation of growth and survival pathways (Brennan et al., 2007). Therefore, it is not surprising that loss of Dsg2 has diverging effects on signaling pathways, depending on tissue type. In keratinocytes, loss of Dsg2 has been reported to reduce the phosphorylation level of EGFR resulting in decreased cell proliferation (Overmiller et al., 2016), while our data from IECs revealed an enhanced proliferation. Furthermore, Dsg2-deficient pancreatic cells display increased levels of EGFR phosphorylation at Y845 (Hutz et al., 2017), which is also in contrast to IECs, showing decreased levels of Y845 phosphorylation. The manifold functions of Dsg2 become even more apparent when it comes to its role in human cancer. Several studies report Dsg2 expression to be downregulated in diffuse-type gastric cancer, prostate cancer and pancreatic cancer (Barber et al., 2014; Ramani et al., 2008; Yashiro et al., 2006). In human breast cancer cells, Dsg2 is believed to be a putative tumor suppressor and to reduce cell aggregation, invasion and motility (Davies et al., 1997). In contrast, other studies suggest an oncogenic function of Dsg2, as it has been shown to be overexpressed in non-small cell lung cancer, skin squamous cell carcinoma as well as basal cell carcinoma and its loss suppressed colon cancer proliferation (Brennan and Mahoney, 2009; Fukuoka et al.,

2007; Kamekura et al., 2014). Hence, it is likely that desmosomal cadherin functions in a spatiotemporal fashion, which implies the involvement of specific interaction partners or protein modifications that modulate their function.

3.4 Differential biological functions of Dsg2 and Dsc2

In this study, we investigated the adhesive and signaling functions of Dsg2 in IECs. However, beside Dsg2, a second desmosomal cadherin is expressed in the intestinal epithelium, namely Dsc2, which raises the question whether and, if so, how their functions differ. Although, both homo- and heterophilic interactions between Dsg2 and Dsc2 ED can be found in desmosomes, heterophilic interactions have been reported to be preferred and that both protein types are required for cell cohesion (Harrison et al., 2016; Nekrasova and Green, 2013). Moreover, it is assumed that a specific ratio of desmogleins and desmocollins is essential to maintain intercellular adhesion (Getsios et al., 2004). In contrast, another study reported that Dsc2 alone is sufficient to form functional desmosomes in IECs (Fujiwara et al., 2015), while a study on pancreatic cells revealed that silencing of Dsg2 but not Dsc2 results in loss of cell cohesion (Hutz et al., 2017).

Our data demonstrate that both proteins have unique properties. We observed that Dsg2, but not Dsc2, regulates activity of p38MAPK. Furthermore, we detected co-localization between Dsg2 and EGFR, which did not appear between Dsc2 and EGFR. In line with this, loss of Dsc2 had no effect on localization as well as protein levels of EGFR, while loss of Dsg2 led to decreased EGFR levels, decreased EGFR phosphorylation at Y845 and EGFR redistribution away from cell borders. Moreover, loss of Dsg2 increased cell proliferation of IECs via EGFR signaling, whereas loss of Dsc2 resulted in similar proliferation as seen in WT cells. In addition, we participated in a study that explored the properties of Dsg2 and Dsc2 in the intestinal epithelium with regard to their importance under inflammatory conditions. Comparison of TER values from different KO cell lines revealed a lower resistance for cells deficient for both desmosomal cadherins, which was not restored by reintroduction of Dsc2. Along this line, that study shows that mice deficient for Dsg2 in the intestinal epithelium, display

increased intestinal permeability, which was not noted in Dsc2 deficient mice. However, we observed that loss of Dsc2 in cultured IECs resulted in reduced TER values, as well, albeit the values were not as much reduced as upon loss of Dsg2. In addition, unpublished data from our lab shows a significantly reduced intercellular cohesion in DLD1 cells lacking Dsc2 compared to cells lacking Dsg2. Collectively, these data indicates that Dsc2 is required to provide strong cohesion, while Dsg2 might exert rather regulatory functions. This hypothesis is supported by a study, reporting that a global Dsg2 knockout in mice is not viable, while Dsc2 knockout mice do not display any defects (Eshkind et al., 2002). Hence, this points to a crucial signaling function of Dsg2, whereas the adhesive function of Dsc2 might be compensated more easily. However, a compensatory up-regulation has been observed for Dsc2 upon loss of Dsg2, but not for Dsg2 upon loss of Dsc2 (Kolegraff et al., 2011). In addition, another study reports a signaling function for Dsc2, as well, and proposes Dsg2 and Dsc2 to act in an opposing way (Kamekura et al., 2014). Hence, this issue is still an open question and awaits further investigation. A possible starting point could be the analysis of putative interaction partners that might specifically shape the Dsg2 and Dsc2 function. In this study, we identified EGFR as interaction partner for Dsg2 and that its function is influenced by loss of Dsg2 but not Dsc2. Data from our cooperation study, investigating the properties of Dsg2 and Dsc2 in knockout mice, show an interaction of the chaperone heat shock protein 70 (Hsp70) with Dsg2 but not with Dsc2. Furthermore, comparison of so far known interaction partners for Dsg2 and Dsc2 using the BioGRID Database (Stark et al., 2006) revealed 52 physical interactors for Dsg2 and 26 physical interactors for Dsc2, of which only 10 interaction partners overlap, pointing towards different interactomes that might regulate specifically the functions of Dsg2 and Dsc2 (Fig. 12).

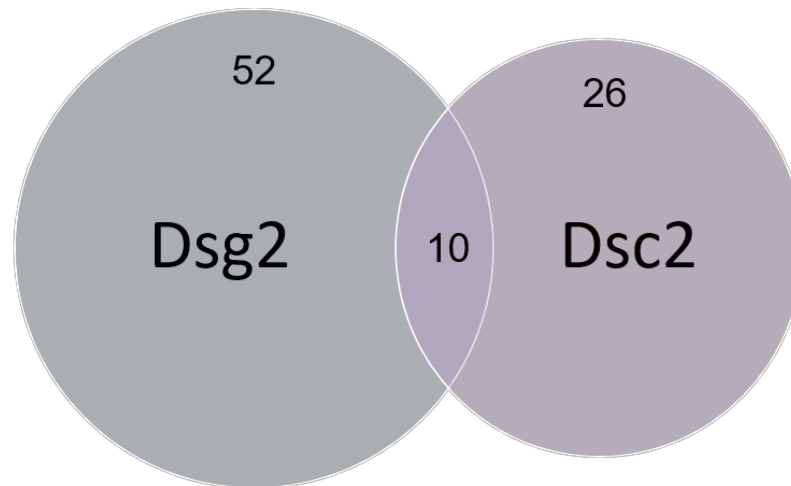


Figure 12. Overview of up to date known interactomes of Dsg2 and Dsc2. Comparison of physical interaction partners of Dsg2 and Dsc2, published on the BioGRID Database (Stark et al., 2006) reveals different interactomes for Dsg2 and Dsc2, with 52 interaction partners for Dsg2, 26 interaction partner for Dsc2 and only 10 interaction partners found in both datasets.

In conclusion, this study reveals new functional properties for Dsg2, beside its adhesive function and suggests a receptor like mechanism to transmit extracellular stimuli. In the rapidly renewing intestinal epithelium, Dsg2 might act as a sensor to regulate the switch between adhesive and proliferative or apoptotic state for instance to enable cell shedding of senescent cells at the villus tip or to promote wound healing in response to inflammatory stimuli. Furthermore, this study demonstrates that Dsg2 and Dsc2 have unique properties and are likely to be regulated differentially. Thus, identification of interactomes specific for Dsg2 or Dsc2 might unveil new targets for protein regulation that could be useful for the development of therapeutic approaches for diseases such as IBD that evince dysregulated Dsg2 function.

4 Annex

4.1 References

Abdo, H., Derkinderen, P., Gomes, P., Chevalier, J., Aubert, P., Masson, D., Galmiche, J.P., Vanden Berghe, P., Neunlist, M., and Lardeux, B. (2010). Enteric glial cells protect neurons from oxidative stress in part via reduced glutathione. *FASEB J* 24, 1082-1094.

Adams, C.L., Chen, Y.T., Smith, S.J., and Nelson, W.J. (1998). Mechanisms of epithelial cell-cell adhesion and cell compaction revealed by high-resolution tracking of E-cadherin-green fluorescent protein. *J Cell Biol* 142, 1105-1119.

Ahmed, D., Eide, P.W., Eilertsen, I.A., Danielsen, S.A., Eknæs, M., Hektoen, M., Lind, G.E., and Lothe, R.A. (2013). Epigenetic and genetic features of 24 colon cancer cell lines. *Oncogenesis* 2, e71.

Al-Ghadban, S., Kaissi, S., Homaidan, F.R., Naim, H.Y., and El-Sabban, M.E. (2016). Cross-talk between intestinal epithelial cells and immune cells in inflammatory bowel disease. *Sci Rep* 6, 29783.

Allen, S.J., Watson, J.J., Shoemark, D.K., Barua, N.U., and Patel, N.K. (2013). GDNF, NGF and BDNF as therapeutic options for neurodegeneration. *Pharmacol Ther* 138, 155-175.

Amagai, M., Matsuyoshi, N., Wang, Z.H., Andl, C., and Stanley, J.R. (2000). Toxin in bullous impetigo and staphylococcal scalded-skin syndrome targets desmoglein 1. *Nat Med* 6, 1275-1277.

Amagai, M., and Stanley, J.R. (2012). Desmoglein as a target in skin disease and beyond. *J Invest Dermatol* 132, 776-784.

Amasheh, S., Meiri, N., Gitter, A.H., Schoneberg, T., Mankertz, J., Schulzke, J.D., and Fromm, M. (2002). Claudin-2 expression induces cation-selective channels in tight junctions of epithelial cells. *J Cell Sci* 115, 4969-4976.

Anderle, P., Sengstag, T., Mutch, D.M., Rumbo, M., Praz, V., Mansourian, R., Delorenzi, M., Williamson, G., and Roberts, M.A. (2005). Changes in the transcriptional profile of transporters in the intestine along the anterior-posterior and crypt-villus axes. *BMC Genomics* 6, 69.

Andl, C.D., Mizushima, T., Oyama, K., Bowser, M., Nakagawa, H., and Rustgi, A.K. (2004). EGFR-induced cell migration is mediated predominantly by the JAK-STAT pathway in primary esophageal keratinocytes. *Am J Physiol Gastrointest Liver Physiol* 287, G1227-1237.

Andreas, E., Linda, W., M., K.A.S., Christian, R., Jürgen, W., D., H.C., Martin, H., Rong, Z., Ferry, K., Dieter, B., *et al.* (2007). A new simple method for linking of antibodies to atomic force microscopy tips. *Bioconjugate Chem* 18, 1176-1184.

Arimoto, K., Burkart, C., Yan, M., Ran, D., Weng, S., and Zhang, D.E. (2014). Plakophilin-2 promotes tumor development by enhancing ligand-dependent and -independent epidermal growth factor receptor dimerization and activation. *Mol Cell Biol* **34**, 3843-3854.

Artursson, P., Ungell, A.L., and Lofroth, J.E. (1993). Selective paracellular permeability in two models of intestinal absorption: cultured monolayers of human intestinal epithelial cells and rat intestinal segments. *Pharm Res* **10**, 1123-1129.

Bagrodia, S., Derijard, B., Davis, R.J., and Cerione, R.A. (1995). Cdc42 and PAK-mediated signaling leads to Jun kinase and p38 mitogen-activated protein kinase activation. *J Biol Chem* **270**, 27995-27998.

Bakker, J., Spits, M., Neefjes, J., and Berlin, I. (2017). The EGFR odyssey - from activation to destruction in space and time. *J Cell Sci*.

Barber, A.G., Castillo-Martin, M., Bonal, D.M., Rybicki, B.A., Christiano, A.M., and Cordon-Cardo, C. (2014). Characterization of desmoglein expression in the normal prostatic gland. Desmoglein 2 is an independent prognostic factor for aggressive prostate cancer. *PLoS One* **9**, e98786.

Baselga, J., and Hammond, L.A. (2002). HER-targeted tyrosine-kinase inhibitors. *Oncology* **63 Suppl 1**, 6-16.

Baugh, M.D., Perry, M.J., Hollander, A.P., Davies, D.R., Cross, S.S., Lobo, A.J., Taylor, C.J., and Evans, G.S. (1999). Matrix metalloproteinase levels are elevated in inflammatory bowel disease. *Gastroenterology* **117**, 814-822.

Bech-Serra, J.J., Santiago-Josefat, B., Esselens, C., Saftig, P., Baselga, J., Arribas, J., and Canals, F. (2006). Proteomic identification of desmoglein 2 and activated leukocyte cell adhesion molecule as substrates of ADAM17 and ADAM10 by difference gel electrophoresis. *Mol Cell Biol* **26**, 5086-5095.

Bektas, M., Jolly, P.S., Berkowitz, P., Amagai, M., and Rubenstein, D.S. (2013). A pathophysiologic role for epidermal growth factor receptor in pemphigus acantholysis. *J Biol Chem* **288**, 9447-9456.

Ben-Ze'ev, A., Shtutman, M., and Zhurinsky, J. (2000). The integration of cell adhesion with gene expression: the role of beta-catenin. *Exp Cell Res* **261**, 75-82.

Berkowitz, P., Chua, M., Liu, Z., Diaz, L.A., and Rubenstein, D.S. (2008a). Autoantibodies in the autoimmune disease pemphigus foliaceus induce blistering via p38 mitogen-activated protein kinase-dependent signaling in the skin. *Am J Pathol* **173**, 1628-1636.

Berkowitz, P., Diaz, L.A., Hall, R.P., and Rubenstein, D.S. (2008b). Induction of p38MAPK and HSP27 phosphorylation in pemphigus patient skin. *J Invest Dermatol* **128**, 738-740.

Berkowitz, P., Hu, P., Liu, Z., Diaz, L.A., Enghild, J.J., Chua, M.P., and Rubenstein, D.S. (2005). Desmosome signaling. Inhibition of p38MAPK prevents pemphigus vulgaris IgG-induced cytoskeleton reorganization. *J Biol Chem* **280**, 23778-23784.

Bertocchi, C., Vaman Rao, M., and Zaidel-Bar, R. (2012). Regulation of adherens junction dynamics by phosphorylation switches. *J Signal Transduct* 2012, 125295.

Bevins, C.L., and Salzman, N.H. (2011). Paneth cells, antimicrobial peptides and maintenance of intestinal homeostasis. *Nat Rev Microbiol* 9, 356-368.

Biscardi, J.S., Maa, M.C., Tice, D.A., Cox, M.E., Leu, T.H., and Parsons, S.J. (1999). c-Src-mediated phosphorylation of the epidermal growth factor receptor on Tyr845 and Tyr1101 is associated with modulation of receptor function. *J Biol Chem* 274, 8335-8343.

Bishop, W.P., and Wen, J.T. (1994). Regulation of Caco-2 cell proliferation by basolateral membrane epidermal growth factor receptors. *Am J Physiol* 267, G892-900.

Blair, S.A., Kane, S.V., Clayburgh, D.R., and Turner, J.R. (2006). Epithelial myosin light chain kinase expression and activity are upregulated in inflammatory bowel disease. *Lab Invest* 86, 191-201.

Blay, J., and Brown, K.D. (1985). Epidermal growth factor promotes the chemotactic migration of cultured rat intestinal epithelial cells. *J Cell Physiol* 124, 107-112.

Bouyain, S., Longo, P.A., Li, S., Ferguson, K.M., and Leahy, D.J. (2005). The extracellular region of ErbB4 adopts a tethered conformation in the absence of ligand. *Proc Natl Acad Sci U S A* 102, 15024-15029.

Brand, T.M., Iida, M., Luthar, N., Starr, M.M., Huppert, E.J., and Wheeler, D.L. (2013). Nuclear EGFR as a molecular target in cancer. *Radiother Oncol* 108, 370-377.

Brennan, D., Hu, Y., Joubert, S., Choi, Y.W., Whitaker-Menezes, D., O'Brien, T., Uitto, J., Rodeck, U., and Mahoney, M.G. (2007). Suprabasal Dsg2 expression in transgenic mouse skin confers a hyperproliferative and apoptosis-resistant phenotype to keratinocytes. *J Cell Sci* 120, 758-771.

Brennan, D., and Mahoney, M.G. (2009). Increased expression of Dsg2 in malignant skin carcinomas: A tissue-microarray based study. *Cell Adh Migr* 3, 148-154.

Brun, P., Giron, M.C., Qesari, M., Porzionato, A., Caputi, V., Zoppellaro, C., Banzato, S., Grillo, A.R., Spagnol, L., De Caro, R., *et al.* (2013). Toll-like receptor 2 regulates intestinal inflammation by controlling integrity of the enteric nervous system. *Gastroenterology* 145, 1323-1333.

Brun, P., Gobbo, S., Caputi, V., Spagnol, L., Schirato, G., Pasqualin, M., Levorato, E., Palu, G., Giron, M.C., and Castagliuolo, I. (2015). Toll like receptor-2 regulates production of glial-derived neurotrophic factors in murine intestinal smooth muscle cells. *Mol Cell Neurosci* 68, 24-35.

Buck, V.U., Hodecker, M., Eisner, S., Leube, R.E., Krusche, C.A., and Classen-Linke, I. (2018). Ultrastructural changes in endometrial desmosomes of desmoglein 2 mutant mice. *Cell Tissue Res*.

Burgess, A.W., Cho, H.S., Eigenbrot, C., Ferguson, K.M., Garrett, T.P., Leahy, D.J., Lemmon, M.A., Sliwkowski, M.X., Ward, C.W., and Yokoyama, S. (2003). An open-and-shut case? Recent insights into the activation of EGF/ErbB receptors. *Mol Cell* **12**, 541-552.

Bush, T.G., Savidge, T.C., Freeman, T.C., Cox, H.J., Campbell, E.A., Mucke, L., Johnson, M.H., and Sofroniew, M.V. (1998). Fulminant jejuno-ileitis following ablation of enteric glia in adult transgenic mice. *Cell* **93**, 189-201.

Cadwell, C.M., Su, W., and Kowalczyk, A.P. (2016). Cadherin tales: Regulation of cadherin function by endocytic membrane trafficking. *Traffic* **17**, 1262-1271.

Calkins, C.C., Setzer, S.V., Jennings, J.M., Summers, S., Tsunoda, K., Amagai, M., and Kowalczyk, A.P. (2006). Desmoglein endocytosis and desmosome disassembly are coordinated responses to pemphigus autoantibodies. *J Biol Chem* **281**, 7623-7634.

Capaldo, C.T., Farkas, A.E., and Nusrat, A. (2014). Epithelial adhesive junctions. *F1000Prime Rep* **6**, 1.

Caro, I., Boulenc, X., Rousset, M., Meunier, V., Bourrié, M., Julian, B., Joyeux, H., Roques, C., Berger, Y., Zweibaum, A., *et al.* (1995). Characterisation of a newly isolated Caco-2 clone (TC-7), as a model of transport processes and biotransformation of drugs. *International Journal of Pharmaceutics* **116**, 147-158.

Cerejido, M., Valdes, J., Shoshani, L., and Contreras, R.G. (1998). Role of tight junctions in establishing and maintaining cell polarity. *Annu Rev Physiol* **60**, 161-177.

Ceresa, B.P., and Peterson, J.L. (2014). Cell and molecular biology of epidermal growth factor receptor. *International review of cell and molecular biology* **313**, 145-178.

Cerf-Bensussan, N., and Gaboriau-Routhiau, V. (2010). The immune system and the gut microbiota: friends or foes? *Nat Rev Immunol* **10**, 735-744.

Chassaing, B., Aitken, J.D., Malleshappa, M., and Vijay-Kumar, M. (2014). Dextran sulfate sodium (DSS)-induced colitis in mice. *Current protocols in immunology / edited by John E Coligan [et al]* **104**, Unit 15 25.

Chen, J., Nekrasova, O.E., Patel, D.M., Klessner, J.L., Godsel, L.M., Koetsier, J.L., Amargo, E.V., Desai, B.V., and Green, K.J. (2012). The C-terminal unique region of desmoglein 2 inhibits its internalization via tail-tail interactions. *J Cell Biol* **199**, 699-711.

Chen, T.R., Dorotinsky, C.S., McGuire, L.J., Macy, M.L., and Hay, R.J. (1995). DLD-1 and HCT-15 cell lines derived separately from colorectal carcinomas have totally different chromosome changes but the same genetic origin. *Cancer Genet Cytogenet* **81**, 103-108.

Chiasson-MacKenzie, C., and McClatchey, A.I. (2018). Cell-Cell Contact and Receptor Tyrosine Kinase Signaling. *Cold Spring Harb Perspect Biol* **10**.

Cho, H.S., and Leahy, D.J. (2002). Structure of the extracellular region of HER3 reveals an interdomain tether. *Science* **297**, 1330-1333.

Chung, B.M., Dimri, M., George, M., Reddi, A.L., Chen, G., Band, V., and Band, H. (2009). The role of cooperativity with Src in oncogenic transformation mediated by non-small cell lung cancer-associated EGF receptor mutants. *Oncogene* 28, 1821-1832.

Chung, Y., Law, S., Kwong, D.L., and Luk, J.M. (2011). Serum soluble E-cadherin is a potential prognostic marker in esophageal squamous cell carcinoma. *Dis Esophagus* 24, 49-55.

Citalan-Madrid, A.F., Garcia-Ponce, A., Vargas-Robles, H., Betanzos, A., and Schnoor, M. (2013). Small GTPases of the Ras superfamily regulate intestinal epithelial homeostasis and barrier function via common and unique mechanisms. *Tissue Barriers* 1, e26938.

Clevers, H. (2013). The intestinal crypt, a prototype stem cell compartment. *Cell* 154, 274-284.

Clevers, H.C., and Bevins, C.L. (2013). Paneth cells: maestros of the small intestinal crypts. *Annu Rev Physiol* 75, 289-311.

Cliffe, L.J., Humphreys, N.E., Lane, T.E., Potten, C.S., Booth, C., and Grecis, R.K. (2005). Accelerated intestinal epithelial cell turnover: a new mechanism of parasite expulsion. *Science* 308, 1463-1465.

Cohen, B.L., Torres, J., and Colombel, J.F. (2012). Immunosuppression in inflammatory bowel disease: how much is too much? *Curr Opin Gastroenterol* 28, 341-348.

Collins, J.T., and Bhimji, S.S. (2018). Anatomy, Abdomen, Small Intestine. In *StatPearls* (Treasure Island (FL)).

Conte, A., and Sigismund, S. (2016). Chapter Six - The Ubiquitin Network in the Control of EGFR Endocytosis and Signaling. *Prog Mol Biol Transl Sci* 141, 225-276.

Cornet, A., Savidge, T.C., Cabarrocas, J., Deng, W.L., Colombel, J.F., Lassmann, H., Desreumaux, P., and Liblau, R.S. (2001). Enterocolitis induced by autoimmune targeting of enteric glial cells: a possible mechanism in Crohn's disease? *Proc Natl Acad Sci U S A* 98, 13306-13311.

Cox, H.M. (2016). Neuroendocrine peptide mechanisms controlling intestinal epithelial function. *Curr Opin Pharmacol* 31, 50-56.

Cuenda, A., and Rousseau, S. (2007). p38 MAP-kinases pathway regulation, function and role in human diseases. *Biochim Biophys Acta* 1773, 1358-1375.

Daly, J.M., Olayioye, M.A., Wong, A.M., Neve, R., Lane, H.A., Maurer, F.G., and Hynes, N.E. (1999). NDF/herregulin-induced cell cycle changes and apoptosis in breast tumour cells: role of PI3 kinase and p38 MAP kinase pathways. *Oncogene* 18, 3440-3451.

Davies, E., Cochrane, R., Hiscox, S., Jiang, W., Sweetland, H., and Mansel, R. (1997). The role of desmoglein 2 and E-cadherin in the invasion and motility of human breast cancer cells. *Int J Oncol* 11, 415-419.

De Maio, A., Vega, V.L., and Contreras, J.E. (2002). Gap junctions, homeostasis, and injury. *J Cell Physiol* *191*, 269-282.

Delva, E., Jennings, J.M., Calkins, C.C., Kottke, M.D., Faundez, V., and Kowalczyk, A.P. (2008). Pemphigus vulgaris IgG-induced desmoglein-3 endocytosis and desmosomal disassembly are mediated by a clathrin- and dynamin-independent mechanism. *J Biol Chem* *283*, 18303-18313.

Den, Z., Cheng, X., Merched-Sauvage, M., and Koch, P.J. (2006). Desmocollin 3 is required for pre-implantation development of the mouse embryo. *J Cell Sci* *119*, 482-489.

Derycke, L., De Wever, O., Stove, V., Vanhoecke, B., Delanghe, J., Depypere, H., and Bracke, M. (2006). Soluble N-cadherin in human biological fluids. *Int J Cancer* *119*, 2895-2900.

Dexter, D.L., Spremulli, E.N., Fligel, Z., Barbosa, J.A., Vogel, R., VanVoorhees, A., and Calabresi, P. (1981). Heterogeneity of cancer cells from a single human colon carcinoma. *Am J Med* *71*, 949-956.

Dieckgraefe, B.K., Weems, D.M., Santoro, S.A., and Alpers, D.H. (1997). ERK and p38 MAP kinase pathways are mediators of intestinal epithelial wound-induced signal transduction. *Biochem Biophys Res Commun* *233*, 389-394.

Dieding, M., Debus, J.D., Kerkhoff, R., Gaertner-Rommel, A., Walhorn, V., Milting, H., and Anselmetti, D. (2017). Arrhythmogenic cardiomyopathy related DSG2 mutations affect desmosomal cadherin binding kinetics. *Sci Rep* *7*, 13791.

Dusek, R.L., Getsios, S., Chen, F., Park, J.K., Amargo, E.V., Cryns, V.L., and Green, K.J. (2006). The differentiation-dependent desmosomal cadherin desmoglein 1 is a novel caspase-3 target that regulates apoptosis in keratinocytes. *J Biol Chem* *281*, 3614-3624.

Dusek, R.L., Godsel, L.M., and Green, K.J. (2007). Discriminating roles of desmosomal cadherins: beyond desmosomal adhesion. *J Dermatol Sci* *45*, 7-21.

Engle, M.J., Goetz, G.S., and Alpers, D.H. (1998). Caco-2 cells express a combination of colonocyte and enterocyte phenotypes. *J Cell Physiol* *174*, 362-369.

Enslin, H., Raingeaud, J., and Davis, R.J. (1998). Selective activation of p38 mitogen-activated protein (MAP) kinase isoforms by the MAP kinase kinases MKK3 and MKK6. *J Biol Chem* *273*, 1741-1748.

Erben, U., Loddenkemper, C., Doerfel, K., Spieckermann, S., Haller, D., Heimesaat, M.M., Zeitz, M., Siegmund, B., and Kuhl, A.A. (2014). A guide to histomorphological evaluation of intestinal inflammation in mouse models. *Int J Clin Exp Pathol* *7*, 4557-4576.

Esaki, C., Seishima, M., Yamada, T., Osada, K., and Kitajima, Y. (1995). Pharmacologic evidence for involvement of phospholipase C in pemphigus IgG-induced inositol 1,4,5-trisphosphate generation, intracellular calcium increase, and plasminogen activator secretion in DJM-1 cells, a squamous cell carcinoma line. *J Invest Dermatol* *105*, 329-333.

Escobar, D.J., Desai, R., Ishiyama, N., Folmsbee, S.S., Novak, M.N., Flozak, A.S., Daugherty, R.L., Mo, R., Nanavati, D., Sarpal, R., *et al.* (2015). alpha-Catenin phosphorylation promotes intercellular adhesion through a dual-kinase mechanism. *J Cell Sci* **128**, 1150-1165.

Eshkind, L., Tian, Q., Schmidt, A., Franke, W.W., Windoffer, R., and Leube, R.E. (2002). Loss of desmoglein 2 suggests essential functions for early embryonic development and proliferation of embryonal stem cells. *Eur J Cell Biol* **81**, 592-598.

Fabre-Lafay, S., Garrido-Urbani, S., Reymond, N., Goncalves, A., Dubreuil, P., and Lopez, M. (2005). Nectin-4, a new serological breast cancer marker, is a substrate for tumor necrosis factor-alpha-converting enzyme (TACE)/ADAM-17. *J Biol Chem* **280**, 19543-19550.

Farquhar, M.G., and Palade, G.E. (1963a). JUNCTIONAL COMPLEXES IN VARIOUS EPITHELIA. *The Journal of Cell Biology* **17**, 375.

Farquhar, M.G., and Palade, G.E. (1963b). Junctional complexes in various epithelia. *The Journal of cell biology* **17**, 375-412.

Feakins, R.M. (2014). Ulcerative colitis or Crohn's disease? Pitfalls and problems. *Histopathology* **64**, 317-335.

Ferguson, K.M., Berger, M.B., Mendrola, J.M., Cho, H.S., Leahy, D.J., and Lemmon, M.A. (2003). EGF activates its receptor by removing interactions that autoinhibit ectodomain dimerization. *Mol Cell* **11**, 507-517.

Fois, G., Weimer, M., Busch, T., Felder, E.T., Oswald, F., von Wichert, G., Seufferlein, T., Dietl, P., and Felder, E. (2013). Effects of keratin phosphorylation on the mechanical properties of keratin filaments in living cells. *FASEB J* **27**, 1322-1329.

Foltz, I.N., Lee, J.C., Young, P.R., and Schrader, J.W. (1997). Hemopoietic growth factors with the exception of interleukin-4 activate the p38 mitogen-activated protein kinase pathway. *J Biol Chem* **272**, 3296-3301.

Francavilla, C., Papetti, M., Rigbolt, K.T., Pedersen, A.K., Sigurdsson, J.O., Cazzamali, G., Karemire, G., Blagoev, B., and Olsen, J.V. (2016). Multilayered proteomics reveals molecular switches dictating ligand-dependent EGFR trafficking. *Nat Struct Mol Biol* **23**, 608-618.

Frey, M.R., Dise, R.S., Edelblum, K.L., and Polk, D.B. (2006). p38 kinase regulates epidermal growth factor receptor downregulation and cellular migration. *EMBO J* **25**, 5683-5692.

Frey, M.R., Golovin, A., and Polk, D.B. (2004). Epidermal growth factor-stimulated intestinal epithelial cell migration requires Src family kinase-dependent p38 MAPK signaling. *J Biol Chem* **279**, 44513-44521.

Fujiwara, M., Nagatomo, A., Tsuda, M., Obata, S., Sakuma, T., Yamamoto, T., and Suzuki, S.T. (2015). Desmocollin-2 alone forms functional desmosomal plaques, with the plaque formation requiring the juxtamembrane region and plakophilins. *J Biochem* *158*, 339-353.

Fukuoka, J., Dracheva, T., Shih, J.H., Hewitt, S.M., Fujii, T., Kishor, A., Mann, F., Shilo, K., Franks, T.J., Travis, W.D., *et al.* (2007). Desmoglein 3 as a prognostic factor in lung cancer. *Hum Pathol* *38*, 276-283.

Funderburg, N., Lederman, M.M., Feng, Z., Drage, M.G., Jadowsky, J., Harding, C.V., Weinberg, A., and Sieg, S.F. (2007). Human α -defensin-3 activates professional antigen-presenting cells via Toll-like receptors 1 and 2. *Proc Natl Acad Sci U S A* *104*, 18631-18635.

Furness, J.B. (2012). The enteric nervous system and neurogastroenterology. *Nat Rev Gastroenterol Hepatol* *9*, 286-294.

Furuse, M., Fujimoto, K., Sato, N., Hirase, T., Tsukita, S., and Tsukita, S. (1996). Overexpression of occludin, a tight junction-associated integral membrane protein, induces the formation of intracellular multilamellar bodies bearing tight junction-like structures. *J Cell Sci* *109* (Pt 2), 429-435.

Gallicano, G.I., Kouklis, P., Bauer, C., Yin, M., Vasioukhin, V., Degenstein, L., and Fuchs, E. (1998). Desmoplakin is required early in development for assembly of desmosomes and cytoskeletal linkage. *J Cell Biol* *143*, 2009-2022.

Garcia-Gras, E., Lombardi, R., Giocondo, M.J., Willerson, J.T., Schneider, M.D., Khoury, D.S., and Marian, A.J. (2006). Suppression of canonical Wnt/beta-catenin signaling by nuclear plakoglobin recapitulates phenotype of arrhythmogenic right ventricular cardiomyopathy. *J Clin Invest* *116*, 2012-2021.

Garrod, D., and Chidgey, M. (2008). Desmosome structure, composition and function. *Biochim Biophys Acta* *1778*, 572-587.

Garrod, D.R., Berika, M.Y., Bardsley, W.F., Holmes, D., and Taberner, L. (2005). Hyperadhesion in desmosomes: its regulation in wound healing and possible relationship to cadherin crystal structure. *J Cell Sci* *118*, 5743-5754.

Gaudry, C.A., Palka, H.L., Dusek, R.L., Huen, A.C., Khandekar, M.J., Hudson, L.G., and Green, K.J. (2001). Tyrosine-phosphorylated plakoglobin is associated with desmogleins but not desmoplakin after epidermal growth factor receptor activation. *J Biol Chem* *276*, 24871-24880.

Ge, B., Gram, H., Di Padova, F., Huang, B., New, L., Ulevitch, R.J., Luo, Y., and Han, J. (2002). MAPKK-independent activation of p38alpha mediated by TAB1-dependent autophosphorylation of p38alpha. *Science* *295*, 1291-1294.

Geremia, A., Biancheri, P., Allan, P., Corazza, G.R., and Di Sabatino, A. (2014). Innate and adaptive immunity in inflammatory bowel disease. *Autoimmun Rev* *13*, 3-10.

Getsios, S., Amargo, E.V., Dusek, R.L., Ishii, K., Sheu, L., Godsel, L.M., and Green, K.J. (2004). Coordinated expression of desmoglein 1 and desmocollin 1 regulates intercellular adhesion. *Differentiation* 72, 419-433.

Getsios, S., Simpson, C.L., Kojima, S., Harmon, R., Sheu, L.J., Dusek, R.L., Cornwell, M., and Green, K.J. (2009). Desmoglein 1-dependent suppression of EGFR signaling promotes epidermal differentiation and morphogenesis. *J Cell Biol* 185, 1243-1258.

Gialeli, C., Theocharis, A.D., and Karamanos, N.K. (2011). Roles of matrix metalloproteinases in cancer progression and their pharmacological targeting. *FEBS J* 278, 16-27.

Giepmans, B.N. (2004). Gap junctions and connexin-interacting proteins. *Cardiovasc Res* 62, 233-245.

Godek, J., Sargiannidou, I., Patel, S., Hurd, L., Rothman, V.L., and Tuszynski, G.P. (2011). Angioidin inhibits breast cancer proliferation through activation of epidermal growth factor receptor and nuclear factor kappa (NF- κ B). *Exp Mol Pathol* 90, 244-251.

Godsel, L.M., Dubash, A.D., Bass-Zubek, A.E., Amargo, E.V., Klessner, J.L., Hobbs, R.P., Chen, X., and Green, K.J. (2010). Plakophilin 2 couples actomyosin remodeling to desmosomal plaque assembly via RhoA. *Mol Biol Cell* 21, 2844-2859.

Gonnella, P.A., Siminoski, K., Murphy, R.A., and Neutra, M.R. (1987). Transepithelial transport of epidermal growth factor by absorptive cells of suckling rat ileum. *J Clin Invest* 80, 22-32.

Grace, M.P., Kim, K.H., True, L.D., and Fuchs, E. (1985). Keratin expression in normal esophageal epithelium and squamous cell carcinoma of the esophagus. *Cancer Res* 45, 841-846.

Granholt, A.C., Reyland, M., Albeck, D., Sanders, L., Gerhardt, G., Hoernig, G., Shen, L., Westphal, H., and Hoffer, B. (2000). Glial cell line-derived neurotrophic factor is essential for postnatal survival of midbrain dopamine neurons. *J Neurosci* 20, 3182-3190.

Green, K.J., and Simpson, C.L. (2007). Desmosomes: new perspectives on a classic. *J Invest Dermatol* 127, 2499-2515.

Grubisic, V., and Gulbransen, B.D. (2017). Enteric glial activity regulates secretomotor function in the mouse colon but does not acutely affect gut permeability. *The Journal of physiology*.

Gunzel, D., and Yu, A.S. (2013). Claudins and the modulation of tight junction permeability. *Physiol Rev* 93, 525-569.

Han, J., Lee, J.D., Bibbs, L., and Ulevitch, R.J. (1994). A MAP kinase targeted by endotoxin and hyperosmolarity in mammalian cells. *Science* 265, 808-811.

Hanakawa, Y., Schechter, N.M., Lin, C., Garza, L., Li, H., Yamaguchi, T., Fudaba, Y., Nishifuji, K., Sugai, M., Amagai, M., *et al.* (2002). Molecular mechanisms of blister formation in bullous impetigo and staphylococcal scalded skin syndrome. *J Clin Invest* 110, 53-60.

Hanks, S.K., and Hunter, T. (1995). Protein kinases 6. The eukaryotic protein kinase superfamily: kinase (catalytic) domain structure and classification. *FASEB J* 9, 576-596.

Harris, R.C., Chung, E., and Coffey, R.J. (2003). EGF receptor ligands. *Exp Cell Res* 284, 2-13.

Harrison, O.J., Brasch, J., Lasso, G., Katsamba, P.S., Ahlsen, G., Honig, B., and Shapiro, L. (2016). Structural basis of adhesive binding by desmocollins and desmogleins. *Proc Natl Acad Sci U S A* 113, 7160-7165.

Hartlieb, E., Kempf, B., Partilla, M., Vigh, B., Spindler, V., and Waschke, J. (2013). Desmoglein 2 is less important than desmoglein 3 for keratinocyte cohesion. *PLoS One* 8, e53739.

Hartlieb, E., Rotzer, V., Radeva, M., Spindler, V., and Waschke, J. (2014). Desmoglein 2 compensates for desmoglein 3 but does not control cell adhesion via regulation of p38 mitogen-activated protein kinase in keratinocytes. *J Biol Chem* 289, 17043-17053.

Hattrup, C.L., and Gendler, S.J. (2008). Structure and function of the cell surface (tethered) mucins. *Annu Rev Physiol* 70, 431-457.

Haugh, J.M., Huang, A.C., Wiley, H.S., Wells, A., and Lauffenburger, D.A. (1999). Internalized epidermal growth factor receptors participate in the activation of p21(ras) in fibroblasts. *J Biol Chem* 274, 34350-34360.

Heidenreich, K.A., and Kummer, J.L. (1996). Inhibition of p38 mitogen-activated protein kinase by insulin in cultured fetal neurons. *J Biol Chem* 271, 9891-9894.

Helander, H.F., and Fandriks, L. (2014). Surface area of the digestive tract - revisited. *Scand J Gastroenterol* 49, 681-689.

Heller, F., Florian, P., Bojarski, C., Richter, J., Christ, M., Hillenbrand, B., Mankertz, J., Gitter, A.H., Burgel, N., Fromm, M., *et al.* (2005). Interleukin-13 is the key effector Th2 cytokine in ulcerative colitis that affects epithelial tight junctions, apoptosis, and cell restitution. *Gastroenterology* 129, 550-564.

Hofmann, I., Casella, M., Schnolzer, M., Schlechter, T., Spring, H., and Franke, W.W. (2006). Identification of the junctional plaque protein plakophilin 3 in cytoplasmic particles containing RNA-binding proteins and the recruitment of plakophilins 1 and 3 to stress granules. *Mol Biol Cell* 17, 1388-1398.

Hollander, D. (1999). Intestinal permeability, leaky gut, and intestinal disorders. *Curr Gastroenterol Rep* 1, 410-416.

Hollander, D., Vadheim, C.M., Brettholz, E., Petersen, G.M., Delahunty, T., and Rotter, J.I. (1986). Increased intestinal permeability in patients with Crohn's disease and their relatives. A possible etiologic factor. *Ann Intern Med* 105, 883-885.

Holthofer, B., Windoffer, R., Troyanovsky, S., and Leube, R.E. (2007). Structure and function of desmosomes. *International review of cytology* 264, 65-163.

Honegger, A.M., Kris, R.M., Ullrich, A., and Schlessinger, J. (1989). Evidence that autophosphorylation of solubilized receptors for epidermal growth factor is mediated by intermolecular cross-phosphorylation. *Proc Natl Acad Sci U S A* 86, 925-929.

Hoschuetzky, H., Aberle, H., and Kemler, R. (1994). Beta-catenin mediates the interaction of the cadherin-catenin complex with epidermal growth factor receptor. *J Cell Biol* 127, 1375-1380.

Hoy, B., Geppert, T., Boehm, M., Reisen, F., Plattner, P., Gadermaier, G., Sewald, N., Ferreira, F., Briza, P., Schneider, G., *et al.* (2012). Distinct roles of secreted HtrA proteases from gram-negative pathogens in cleaving the junctional protein and tumor suppressor E-cadherin. *J Biol Chem* 287, 10115-10120.

Hughes, R.C. (2001). Galectins as modulators of cell adhesion. *Biochimie* 83, 667-676.

Huguenin, M., Muller, E.J., Trachsel-Rosmann, S., Oneda, B., Ambort, D., Sterchi, E.E., and Lottaz, D. (2008). The metalloprotease mepribeta processes E-cadherin and weakens intercellular adhesion. *PLoS One* 3, e2153.

Hulpiau, P., and van Roy, F. (2009). Molecular evolution of the cadherin superfamily. *Int J Biochem Cell Biol* 41, 349-369.

Hutz, K., Zeiler, J., Sachs, L., Ormanns, S., and Spindler, V. (2017). Loss of desmoglein 2 promotes tumorigenic behavior in pancreatic cancer cells. *Mol Carcinog* 56, 1884-1895.

Hynes, N.E., and Lane, H.A. (2005). ERBB receptors and cancer: the complexity of targeted inhibitors. *Nat Rev Cancer* 5, 341-354.

Itoh, M., Tsukita, S., Yamazaki, Y., and Sugimoto, H. (2012). Rho GTP exchange factor ARHGEF11 regulates the integrity of epithelial junctions by connecting ZO-1 and RhoA-myosin II signaling. *Proc Natl Acad Sci U S A* 109, 9905-9910.

Jager, S., Stange, E.F., and Wehkamp, J. (2013). Inflammatory bowel disease: an impaired barrier disease. *Langenbecks Arch Surg* 398, 1-12.

Ji, H., Wang, J., Nika, H., Hawke, D., Keezer, S., Ge, Q., Fang, B., Fang, X., Fang, D., Litchfield, D.W., *et al.* (2009). EGF-induced ERK activation promotes CK2-mediated disassociation of alpha-Catenin from beta-Catenin and transactivation of beta-Catenin. *Mol Cell* 36, 547-559.

Jiang, K., Rankin, C.R., Nava, P., Sumagin, R., Kamekura, R., Stowell, S.R., Feng, M., Parkos, C.A., and Nusrat, A. (2014). Galectin-3 regulates desmoglein-2 and intestinal epithelial intercellular adhesion. *J Biol Chem* 289, 10510-10517.

Johansson, M.E., Sjovall, H., and Hansson, G.C. (2013). The gastrointestinal mucus system in health and disease. *Nat Rev Gastroenterol Hepatol* 10, 352-361.

Johnson, G.L., Dohman, H.G., and Graves, L.M. (2005). MAPK kinase kinases (MKKKs) as a target class for small-molecule inhibition to modulate signaling networks and gene expression. *Curr Opin Chem Biol* 9, 325-331.

Johnson, J.L., Najor, N.A., and Green, K.J. (2014). Desmosomes: regulators of cellular signaling and adhesion in epidermal health and disease. *Cold Spring Harb Perspect Med* 4, a015297.

Jung, J., Kim, H.Y., Kim, M., Sohn, K., Kim, M., and Lee, K. (2011). Translationally controlled tumor protein induces human breast epithelial cell transformation through the activation of Src. *Oncogene* 30, 2264-2274.

Jung, O., Choi, Y.J., Kwak, T.K., Kang, M., Lee, M.S., Ryu, J., Kim, H.J., and Lee, J.W. (2013). The COOH-terminus of TM4SF5 in hepatoma cell lines regulates c-Src to form invasive protrusions via EGFR Tyr845 phosphorylation. *Biochim Biophys Acta* 1833, 629-642.

Kamekura, R., Kolegraff, K.N., Nava, P., Hilgarth, R.S., Feng, M., Parkos, C.A., and Nusrat, A. (2014). Loss of the desmosomal cadherin desmoglein-2 suppresses colon cancer cell proliferation through EGFR signaling. *Oncogene* 33, 4531-4536.

Kamekura, R., Nava, P., Feng, M., Quiros, M., Nishio, H., Weber, D.A., Parkos, C.A., and Nusrat, A. (2015). Inflammation-induced desmoglein-2 ectodomain shedding compromises the mucosal barrier. *Mol Biol Cell* 26, 3165-3177.

Kamio, T., Shigematsu, K., Sou, H., Kawai, K., and Tsuchiyama, H. (1990). Immunohistochemical expression of epidermal growth factor receptors in human adrenocortical carcinoma. *Hum Pathol* 21, 277-282.

Kanai, Y., Ochiai, A., Shibata, T., Oyama, T., Ushijima, S., Akimoto, S., and Hirohashi, S. (1995). c-erbB-2 gene product directly associates with beta-catenin and plakoglobin. *Biochem Biophys Res Commun* 208, 1067-1072.

Kannangai, R., Sahin, F., and Torbenson, M.S. (2006). EGFR is phosphorylated at Ty845 in hepatocellular carcinoma. *Mod Pathol* 19, 1456-1461.

Kaplan, M., Narasimhan, S., de Heus, C., Mance, D., van Doorn, S., Houben, K., Popov-Celeketic, D., Damman, R., Katrukha, E.A., Jain, P., *et al.* (2016). EGFR Dynamics Change during Activation in Native Membranes as Revealed by NMR. *Cell* 167, 1241-1251 e1211.

Katayama, M., Hirai, S., Kamihagi, K., Nakagawa, K., Yasumoto, M., and Kato, I. (1994). Soluble E-cadherin fragments increased in circulation of cancer patients. *Br J Cancer* 69, 580-585.

Kawasaki, Y., Aoyama, Y., Tsunoda, K., Amagai, M., and Kitajima, Y. (2006). Pathogenic monoclonal antibody against desmoglein 3 augments desmoglein 3 and p38 MAPK phosphorylation in human squamous carcinoma cell line. *Autoimmunity* 39, 587-590.

Keil, R., Rietscher, K., and Hatzfeld, M. (2016). Antagonistic Regulation of Intercellular Cohesion by Plakophilins 1 and 3. *J Invest Dermatol* 136, 2022-2029.

Kelly, D., McFadyen, M., King, T.P., and Morgan, P.J. (1992). Characterization and autoradiographic localization of the epidermal growth factor receptor in the jejunum of neonatal and weaned pigs. *Reprod Fertil Dev* 4, 183-191.

Kim, Y.S., and Ho, S.B. (2010). Intestinal goblet cells and mucins in health and disease: recent insights and progress. *Curr Gastroenterol Rep* 12, 319-330.

Kitajima, Y. (2014). 150(th) anniversary series: Desmosomes and autoimmune disease, perspective of dynamic desmosome remodeling and its impairments in pemphigus. *Cell Commun Adhes* 21, 269-280.

Klessner, J.L., Desai, B.V., Amargo, E.V., Getsios, S., and Green, K.J. (2009). EGFR and ADAMs cooperate to regulate shedding and endocytic trafficking of the desmosomal cadherin desmoglein 2. *Mol Biol Cell* 20, 328-337.

Kloth, M.T., Catling, A.D., and Silva, C.M. (2002). Novel activation of STAT5b in response to epidermal growth factor. *J Biol Chem* 277, 8693-8701.

Koch, P.J., Goldschmidt, M.D., Zimbelmann, R., Troyanovsky, R., and Franke, W.W. (1992). Complexity and expression patterns of the desmosomal cadherins. *Proc Natl Acad Sci U S A* 89, 353-357.

Koch, P.J., Walsh, M.J., Schmelz, M., Goldschmidt, M.D., Zimbelmann, R., and Franke, W.W. (1990). Identification of desmoglein, a constitutive desmosomal glycoprotein, as a member of the cadherin family of cell adhesion molecules. *Eur J Cell Biol* 53, 1-12.

Koch, S., and Nusrat, A. (2012). The life and death of epithelia during inflammation: lessons learned from the gut. *Annu Rev Pathol* 7, 35-60.

Kolegraff, K., Nava, P., Helms, M.N., Parkos, C.A., and Nusrat, A. (2011). Loss of desmocollin-2 confers a tumorigenic phenotype to colonic epithelial cells through activation of Akt/beta-catenin signaling. *Mol Biol Cell* 22, 1121-1134.

Koval, M. (2013). Differential pathways of claudin oligomerization and integration into tight junctions. *Tissue Barriers* 1, e24518.

Kowalczyk, A.P., and Nanes, B.A. (2012). Adherens junction turnover: regulating adhesion through cadherin endocytosis, degradation, and recycling. *Subcell Biochem* 60, 197-222.

Kroger, C., Loschke, F., Schwarz, N., Windoffer, R., Leube, R.E., and Magin, T.M. (2013). Keratins control intercellular adhesion involving PKC-alpha-mediated desmoplakin phosphorylation. *The Journal of cell biology* 201, 681-692.

- Krug, S.M., Schulzke, J.D., and Fromm, M. (2014). Tight junction, selective permeability, and related diseases. *Semin Cell Dev Biol* 36, 166-176.
- Kubota, K., Furuse, M., Sasaki, H., Sonoda, N., Fujita, K., Nagafuchi, A., and Tsukita, S. (1999). Ca(2+)-independent cell-adhesion activity of claudins, a family of integral membrane proteins localized at tight junctions. *Curr Biol* 9, 1035-1038.
- Kuwada, S.K., Lund, K.A., Li, X.F., Cliften, P., Amsler, K., Opresko, L.K., and Wiley, H.S. (1998). Differential signaling and regulation of apical vs. basolateral EGFR in polarized epithelial cells. *Am J Physiol* 275, C1419-1428.
- Kyriakis, J.M., and Avruch, J. (2001). Mammalian mitogen-activated protein kinase signal transduction pathways activated by stress and inflammation. *Physiol Rev* 81, 807-869.
- Labun, K., Montague, T.G., Gagnon, J.A., Thyme, S.B., and Valen, E. (2016). CHOPCHOP v2: a web tool for the next generation of CRISPR genome engineering. *Nucleic Acids Res* 44, W272-276.
- Lakhan, S.E., and Kirchgessner, A. (2010). Neuroinflammation in inflammatory bowel disease. *J Neuroinflammation* 7, 37.
- Langness, S., Kojima, M., Coimbra, R., Eliceiri, B.P., and Costantini, T.W. (2017). Enteric glia cells are critical to limiting the intestinal inflammatory response after injury. *American journal of physiology Gastrointestinal and liver physiology* 312, G274-G282.
- Laskin, J.J., and Sandler, A.B. (2004). Epidermal growth factor receptor: a promising target in solid tumours. *Cancer Treat Rev* 30, 1-17.
- Lee, J.C., Laydon, J.T., McDonnell, P.C., Gallagher, T.F., Kumar, S., Green, D., McNulty, D., Blumenthal, M.J., Heys, J.R., Landvatter, S.W., *et al.* (1994). A protein kinase involved in the regulation of inflammatory cytokine biosynthesis. *Nature* 372, 739-746.
- Lemmon, M.A., and Schlessinger, J. (2010). Cell signaling by receptor tyrosine kinases. *Cell* 141, 1117-1134.
- Lochter, A., Galosy, S., Muschler, J., Freedman, N., Werb, Z., and Bissell, M.J. (1997). Matrix metalloproteinase stromelysin-1 triggers a cascade of molecular alterations that leads to stable epithelial-to-mesenchymal conversion and a premalignant phenotype in mammary epithelial cells. *J Cell Biol* 139, 1861-1872.
- Lopez-Posadas, R., Becker, C., Gunther, C., Tenzer, S., Amann, K., Billmeier, U., Atreya, R., Fiorino, G., Vetrano, S., Danese, S., *et al.* (2016). Rho-A prenylation and signaling link epithelial homeostasis to intestinal inflammation. *J Clin Invest* 126, 611-626.
- Lorch, J.H., Klessner, J., Park, J.K., Getsios, S., Wu, Y.L., Stack, M.S., and Green, K.J. (2004). Epidermal growth factor receptor inhibition promotes desmosome assembly and strengthens intercellular adhesion in squamous cell carcinoma cells. *J Biol Chem* 279, 37191-37200.

Luissint, A.C., Parkos, C.A., and Nusrat, A. (2016). Inflammation and the Intestinal Barrier: Leukocyte-Epithelial Cell Interactions, Cell Junction Remodeling, and Mucosal Repair. *Gastroenterology* 151, 616-632.

Maa, M.C., Leu, T.H., McCarley, D.J., Schatzman, R.C., and Parsons, S.J. (1995). Potentiation of epidermal growth factor receptor-mediated oncogenesis by c-Src: implications for the etiology of multiple human cancers. *Proc Natl Acad Sci U S A* 92, 6981-6985.

MacDonald, T.T., Biancheri, P., Sarra, M., and Monteleone, G. (2012). What's the next best cytokine target in IBD? *Inflamm Bowel Dis* 18, 2180-2189.

Magin, T.M., Vijayaraj, P., and Leube, R.E. (2007). Structural and regulatory functions of keratins. *Experimental cell research* 313, 2021-2032.

Mahoney, M.G., Hu, Y., Brennan, D., Bazzi, H., Christiano, A.M., and Wahl, J.K., 3rd (2006). Delineation of diversified desmoglein distribution in stratified squamous epithelia: implications in diseases. *Exp Dermatol* 15, 101-109.

Majumdar, D., Tiernan, J.P., Lobo, A.J., Evans, C.A., and Corfe, B.M. (2012). Keratins in colorectal epithelial function and disease. *Int J Exp Pathol* 93, 305-318.

Mankertz, J., and Schulzke, J.D. (2007). Altered permeability in inflammatory bowel disease: pathophysiology and clinical implications. *Curr Opin Gastroenterol* 23, 379-383.

Mao, X., Choi, E.J., and Payne, A.S. (2009). Disruption of desmosome assembly by monovalent human pemphigus vulgaris monoclonal antibodies. *J Invest Dermatol* 129, 908-918.

Maretzky, T., Reiss, K., Ludwig, A., Buchholz, J., Scholz, F., Proksch, E., de Strooper, B., Hartmann, D., and Saftig, P. (2005). ADAM10 mediates E-cadherin shedding and regulates epithelial cell-cell adhesion, migration, and beta-catenin translocation. *Proc Natl Acad Sci U S A* 102, 9182-9187.

Martin-Padura, I., Lostaglio, S., Schneemann, M., Williams, L., Romano, M., Fruscella, P., Panzeri, C., Stoppacciaro, A., Ruco, L., Villa, A., *et al.* (1998). Junctional adhesion molecule, a novel member of the immunoglobulin superfamily that distributes at intercellular junctions and modulates monocyte transmigration. *J Cell Biol* 142, 117-127.

Martini, E., Krug, S.M., Siegmund, B., Neurath, M.F., and Becker, C. (2017). Mend Your Fences: The Epithelial Barrier and its Relationship With Mucosal Immunity in Inflammatory Bowel Disease. *Cell Mol Gastroenterol Hepatol* 4, 33-46.

Matsumoto, H., Erickson, R.H., Gum, J.R., Yoshioka, M., Gum, E., and Kim, Y.S. (1990). Biosynthesis of alkaline phosphatase during differentiation of the human colon cancer cell line Caco-2. *Gastroenterology* 98, 1199-1207.

Mayhew, T.M., Myklebust, R., Whybrow, A., and Jenkins, R. (1999). Epithelial integrity, cell death and cell loss in mammalian small intestine. *Histol Histopathol* 14, 257-267.

McCawley, L.J., and Matrisian, L.M. (2001). Matrix metalloproteinases: they're not just for matrix anymore! *Curr Opin Cell Biol* 13, 534-540.

McCawley, L.J., O'Brien, P., and Hudson, L.G. (1998). Epidermal growth factor (EGF)- and scatter factor/hepatocyte growth factor (SF/HGF)- mediated keratinocyte migration is coincident with induction of matrix metalloproteinase (MMP)-9. *J Cell Physiol* 176, 255-265.

McClatchey, A.I., and Yap, A.S. (2012). Contact inhibition (of proliferation) redux. *Curr Opin Cell Biol* 24, 685-694.

McCrea, P.D., and Gumbiner, B.M. (1991). Purification of a 92-kDa cytoplasmic protein tightly associated with the cell-cell adhesion molecule E-cadherin (uvomorulin). Characterization and extractability of the protein complex from the cell cytostructure. *J Biol Chem* 266, 4514-4520.

McCrea, P.D., Maher, M.T., and Gottardi, C.J. (2015). Nuclear signaling from cadherin adhesion complexes. *Curr Top Dev Biol* 112, 129-196.

McLachlan, R.W., and Yap, A.S. (2007). Not so simple: the complexity of phosphotyrosine signaling at cadherin adhesive contacts. *J Mol Med (Berl)* 85, 545-554.

Meir, M., Flemming, S., Burkard, N., Bergauer, L., Metzger, M., Germer, C.T., and Schlegel, N. (2015a). Glial cell line-derived neurotrophic factor (GDNF) promotes barrier maturation and wound healing in intestinal epithelial cells in vitro. *American journal of physiology Gastrointestinal and liver physiology*, *ajpgi* 00357 02014.

Meir, M., Flemming, S., Burkard, N., Bergauer, L., Metzger, M., Germer, C.T., and Schlegel, N. (2015b). Glial cell line-derived neurotrophic factor promotes barrier maturation and wound healing in intestinal epithelial cells in vitro. *Am J Physiol Gastrointest Liver Physiol* 309, G613-624.

Meir, M., Flemming, S., Burkard, N., Wagner, J., Germer, C.T., and Schlegel, N. (2016). The glial cell-line derived neurotrophic factor: a novel regulator of intestinal barrier function in health and disease. *American journal of physiology Gastrointestinal and liver physiology* 310, G1118-1123.

Menzel, K., Hausmann, M., Obermeier, F., Schreiter, K., Dunger, N., Bataille, F., Falk, W., Scholmerich, J., Herfarth, H., and Rogler, G. (2006). Cathepsins B, L and D in inflammatory bowel disease macrophages and potential therapeutic effects of cathepsin inhibition in vivo. *Clin Exp Immunol* 146, 169-180.

Mertens, C., Kuhn, C., and Franke, W.W. (1996). Plakophilins 2a and 2b: constitutive proteins of dual location in the karyoplasm and the desmosomal plaque. *J Cell Biol* 135, 1009-1025.

Michels, C., Buchta, T., Bloch, W., Krieg, T., and Niessen, C.M. (2009). Classical cadherins regulate desmosome formation. *J Invest Dermatol* 129, 2072-2075.

Miguel, J.C., Maxwell, A.A., Hsieh, J.J., Harnisch, L.C., Al Alam, D., Polk, D.B., Lien, C.L., Watson, A.J., and Frey, M.R. (2017). Epidermal growth factor suppresses intestinal epithelial cell shedding through a MAPK-dependent pathway. *J Cell Sci* 130, 90-96.

Mineta, K., Yamamoto, Y., Yamazaki, Y., Tanaka, H., Tada, Y., Saito, K., Tamura, A., Igarashi, M., Endo, T., Takeuchi, K., *et al.* (2011). Predicted expansion of the claudin multigene family. *FEBS Lett* 585, 606-612.

Moog, F. (1981). The lining of the small intestine. *Sci Am* 245, 154-158, 160, 162 *et passim*.

Morandell, S., Stasyk, T., Skvortsov, S., Ascher, S., and Huber, L.A. (2008). Quantitative proteomics and phosphoproteomics reveal novel insights into complexity and dynamics of the EGFR signaling network. *Proteomics* 8, 4383-4401.

Moro, L., Dolce, L., Cabodi, S., Bergatto, E., Boeri Erba, E., Smeriglio, M., Turco, E., Retta, S.F., Giuffrida, M.G., Venturino, M., *et al.* (2002). Integrin-induced epidermal growth factor (EGF) receptor activation requires c-Src and p130Cas and leads to phosphorylation of specific EGF receptor tyrosines. *J Biol Chem* 277, 9405-9414.

Mowat, A.M. (2003). Anatomical basis of tolerance and immunity to intestinal antigens. *Nat Rev Immunol* 3, 331-341.

Muise, A.M., Walters, T.D., Glowacka, W.K., Griffiths, A.M., Ngan, B.Y., Lan, H., Xu, W., Silverberg, M.S., and Rotin, D. (2009). Polymorphisms in E-cadherin (CDH1) result in a mis-localised cytoplasmic protein that is associated with Crohn's disease. *Gut* 58, 1121-1127.

Muller, E.J., Williamson, L., Kolly, C., and Suter, M.M. (2008). Outside-in signaling through integrins and cadherins: a central mechanism to control epidermal growth and differentiation? *J Invest Dermatol* 128, 501-516.

Muniz, L.R., Knosp, C., and Yeretssian, G. (2012). Intestinal antimicrobial peptides during homeostasis, infection, and disease. *Front Immunol* 3, 310.

Munoz, W.A., Lee, M., Miller, R.K., Ahmed, Z., Ji, H., Link, T.M., Lee, G.R., Kloc, M., Ladbury, J.E., and McCrea, P.D. (2014). Plakophilin-3 catenin associates with the ETV1/ER81 transcription factor to positively modulate gene activity. *PLoS One* 9, e86784.

Nagar, B., Overduin, M., Ikura, M., and Rini, J.M. (1996). Structural basis of calcium-induced E-cadherin rigidification and dimerization. *Nature* 380, 360-364.

Nava, P., Kamekura, R., and Nusrat, A. (2013). Cleavage of transmembrane junction proteins and their role in regulating epithelial homeostasis. *Tissue Barriers* 1, e24783.

Nava, P., Koch, S., Laukoetter, M.G., Lee, W.Y., Kolegraff, K., Capaldo, C.T., Beeman, N., Addis, C., Gerner-Smidt, K., Neumaier, I., *et al.* (2010). Interferon-gamma regulates intestinal epithelial homeostasis through converging beta-catenin signaling pathways. *Immunity* 32, 392-402.

Navid, F., Boniotto, M., Walker, C., Ahrens, K., Proksch, E., Sparwasser, T., Muller, W., Schwarz, T., and Schwarz, A. (2012). Induction of regulatory T cells by a murine beta-defensin. *J Immunol* *188*, 735-743.

Nekrasova, O., and Green, K.J. (2013). Desmosome assembly and dynamics. *Trends Cell Biol* *23*, 537-546.

Neunlist, M., Rolli-Derkinderen, M., Latorre, R., Van Landeghem, L., Coron, E., Derkinderen, P., and De Giorgio, R. (2014). Enteric glial cells: recent developments and future directions. *Gastroenterology* *147*, 1230-1237.

Neunlist, M., Toumi, F., Oreschkova, T., Denis, M., Leborgne, J., Laboisse, C.L., Galmiche, J.P., and Jarry, A. (2003). Human ENS regulates the intestinal epithelial barrier permeability and a tight junction-associated protein ZO-1 via VIPergic pathways. *American journal of physiology Gastrointestinal and liver physiology* *285*, G1028-1036.

Niessen, C.M., Leckband, D., and Yap, A.S. (2011). Tissue organization by cadherin adhesion molecules: dynamic molecular and cellular mechanisms of morphogenetic regulation. *Physiol Rev* *91*, 691-731.

Noah, T.K., Donahue, B., and Shroyer, N.F. (2011). Intestinal development and differentiation. *Exp Cell Res* *317*, 2702-2710.

Noe, V., Fingleton, B., Jacobs, K., Crawford, H.C., Vermeulen, S., Steelant, W., Bruyneel, E., Matrisian, L.M., and Mareel, M. (2001). Release of an invasion promoter E-cadherin fragment by matrilysin and stromelysin-1. *J Cell Sci* *114*, 111-118.

North, A.J., Chidgey, M.A., Clarke, J.P., Bardsley, W.G., and Garrod, D.R. (1996). Distinct desmocollin isoforms occur in the same desmosomes and show reciprocally graded distributions in bovine nasal epidermis. *Proc Natl Acad Sci U S A* *93*, 7701-7705.

Nuber, U.A., Schafer, S., Stehr, S., Rackwitz, H.R., and Franke, W.W. (1996). Patterns of desmocollin synthesis in human epithelia: immunolocalization of desmocollins 1 and 3 in special epithelia and in cultured cells. *Eur J Cell Biol* *71*, 1-13.

Ogiso, H., Ishitani, R., Nureki, O., Fukai, S., Yamanaka, M., Kim, J.H., Saito, K., Sakamoto, A., Inoue, M., Shirouzu, M., *et al.* (2002). Crystal structure of the complex of human epidermal growth factor and receptor extracellular domains. *Cell* *110*, 775-787.

Olayioye, M.A., Neve, R.M., Lane, H.A., and Hynes, N.E. (2000). The ErbB signaling network: receptor heterodimerization in development and cancer. *EMBO J* *19*, 3159-3167.

Oshima, T., and Miwa, H. (2016). Gastrointestinal mucosal barrier function and diseases. *J Gastroenterol* *51*, 768-778.

Overmiller, A.M., McGuinn, K.P., Roberts, B.J., Cooper, F., Brennan-Crispi, D.M., Deguchi, T., Peltonen, S., Wahl, J.K., 3rd, and Mahoney, M.G. (2016). c-Src/Cav1-dependent activation of the EGFR by Dsg2. *Oncotarget* *7*, 37536-37555.

Overmiller, A.M., Pierluissi, J.A., Wermuth, P.J., Sauma, S., Martinez-Outschoorn, U., Tuluc, M., Luginbuhl, A., Curry, J., Harshyne, L.A., Wahl, J.K., 3rd, *et al.* (2017). Desmoglein 2 modulates extracellular vesicle release from squamous cell carcinoma keratinocytes. *FASEB J* **31**, 3412-3424.

Owen, G.R., and Stokes, D.L. (2010). Exploring the Nature of Desmosomal Cadherin Associations in 3D. *Dermatology research and practice* **2010**, 930401.

Owens, D.W., Wilson, N.J., Hill, A.J., Rugg, E.L., Porter, R.M., Hutcheson, A.M., Quinlan, R.A., van Heel, D., Parkes, M., Jewell, D.P., *et al.* (2004). Human keratin 8 mutations that disturb filament assembly observed in inflammatory bowel disease patients. *J Cell Sci* **117**, 1989-1999.

Padmanabhan, A., Rao, M.V., Wu, Y., and Zaidel-Bar, R. (2015). Jack of all trades: functional modularity in the adherens junction. *Curr Opin Cell Biol* **36**, 32-40.

Pal, M., Bhattacharya, S., Kalyan, G., and Hazra, S. (2018). Cadherin profiling for therapeutic interventions in Epithelial Mesenchymal Transition (EMT) and tumorigenesis. *Exp Cell Res* **368**, 137-146.

Peeters, M., Geypens, B., Claus, D., Nevens, H., Ghoois, Y., Verbeke, G., Baert, F., Vermeire, S., Vlietinck, R., and Rutgeerts, P. (1997). Clustering of increased small intestinal permeability in families with Crohn's disease. *Gastroenterology* **113**, 802-807.

Perez-Moreno, M., and Fuchs, E. (2006). Catenins: keeping cells from getting their signals crossed. *Dev Cell* **11**, 601-612.

Pokutta, S., Herrenknecht, K., Kemler, R., and Engel, J. (1994). Conformational changes of the recombinant extracellular domain of E-cadherin upon calcium binding. *Eur J Biochem* **223**, 1019-1026.

Polk, D.B. (1998). Epidermal growth factor receptor-stimulated intestinal epithelial cell migration requires phospholipase C activity. *Gastroenterology* **114**, 493-502.

Prasad, A., and Pedigo, S. (2005). Calcium-dependent stability studies of domains 1 and 2 of epithelial cadherin. *Biochemistry* **44**, 13692-13701.

Raingaud, J., Gupta, S., Rogers, J.S., Dickens, M., Han, J., Ulevitch, R.J., and Davis, R.J. (1995). Pro-inflammatory cytokines and environmental stress cause p38 mitogen-activated protein kinase activation by dual phosphorylation on tyrosine and threonine. *J Biol Chem* **270**, 7420-7426.

Ramani, V.C., Hennings, L., and Haun, R.S. (2008). Desmoglein 2 is a substrate of kallikrein 7 in pancreatic cancer. *BMC Cancer* **8**, 373.

Rao, M., Rastelli, D., Dong, L., Chiu, S., Setlik, W., Gershon, M.D., and Corfas, G. (2017). Enteric Glia Regulate Gastrointestinal Motility but Are Not Required for Maintenance of the Epithelium in Mice. *Gastroenterology*.

Ravi, A., Garg, P., and Sitaraman, S.V. (2007). Matrix metalloproteinases in inflammatory bowel disease: boon or a bane? *Inflamm Bowel Dis* 13, 97-107.

Ray, R.M., Bhattacharya, S., and Johnson, L.R. (2007). EGFR plays a pivotal role in the regulation of polyamine-dependent apoptosis in intestinal epithelial cells. *Cell Signal* 19, 2519-2527.

Reinshagen, M., Rohm, H., Steinkamp, M., Lieb, K., Geerling, I., Von Herbay, A., Flamig, G., Eysselein, V.E., and Adler, G. (2000). Protective role of neurotrophins in experimental inflammation of the rat gut. *Gastroenterology* 119, 368-376.

Reiss, K., Maretzky, T., Ludwig, A., Tousseyn, T., de Strooper, B., Hartmann, D., and Saftig, P. (2005). ADAM10 cleavage of N-cadherin and regulation of cell-cell adhesion and beta-catenin nuclear signalling. *EMBO J* 24, 742-752.

Rietscher, K., Keil, R., Jordan, A., and Hatzfeld, M. (2018). 14-3-3 proteins regulate desmosomal adhesion via plakophilins. *J Cell Sci* 131.

Rocks, N., Paulissen, G., El Hour, M., Quesada, F., Crahay, C., Gueders, M., Foidart, J.M., Noel, A., and Cataldo, D. (2008). Emerging roles of ADAM and ADAMTS metalloproteinases in cancer. *Biochimie* 90, 369-379.

Rodriguez-Garcia, M., Oliva, H., Climent, N., Escribese, M.M., Garcia, F., Moran, T.M., Gatell, J.M., and Gallart, T. (2009). Impact of alpha-defensins1-3 on the maturation and differentiation of human monocyte-derived DCs. Concentration-dependent opposite dual effects. *Clin Immunol* 131, 374-384.

Rodriguez, J.M., Murphy, K., Stanton, C., Ross, R.P., Kober, O.I., Juge, N., Avershina, E., Rudi, K., Narbad, A., Jenmalm, M.C., *et al.* (2015). The composition of the gut microbiota throughout life, with an emphasis on early life. *Microb Ecol Health Dis* 26, 26050.

Rogler, G., and Andus, T. (1998). Cytokines in inflammatory bowel disease. *World J Surg* 22, 382-389.

Rosenblatt, J., Raff, M.C., and Cramer, L.P. (2001). An epithelial cell destined for apoptosis signals its neighbors to extrude it by an actin- and myosin-dependent mechanism. *Curr Biol* 11, 1847-1857.

Roskoski, R., Jr. (2014). The ErbB/HER family of protein-tyrosine kinases and cancer. *Pharmacol Res* 79, 34-74.

Rotzer, V., Hartlieb, E., Vielmuth, F., Gliem, M., Spindler, V., and Waschke, J. (2015). E-cadherin and Src associate with extradesmosomal Dsg3 and modulate desmosome assembly and adhesion. *Cell Mol Life Sci* 72, 4885-4897.

Rouse, J., Cohen, P., Trigon, S., Morange, M., Alonso-Llamazares, A., Zamanillo, D., Hunt, T., and Nebreda, A.R. (1994). A novel kinase cascade triggered by stress and heat shock that stimulates MAPKAP kinase-2 and phosphorylation of the small heat shock proteins. *Cell* 78, 1027-1037.

Rowan, A.J., Lamlum, H., Ilyas, M., Wheeler, J., Straub, J., Papadopoulou, A., Bicknell, D., Bodmer, W.F., and Tomlinson, I.P. (2000). APC mutations in sporadic colorectal tumors: A mutational "hotspot" and interdependence of the "two hits". *Proc Natl Acad Sci U S A* 97, 3352-3357.

Rubsam, M., Broussard, J.A., Wickstrom, S.A., Nekrasova, O., Green, K.J., and Niessen, C.M. (2017a). Adherens Junctions and Desmosomes Coordinate Mechanics and Signaling to Orchestrate Tissue Morphogenesis and Function: An Evolutionary Perspective. *Cold Spring Harb Perspect Biol*.

Rubsam, M., Mertz, A.F., Kubo, A., Marg, S., Jungst, C., Goranci-Buzhala, G., Schauss, A.C., Horsley, V., Dufresne, E.R., Moser, M., *et al.* (2017b). E-cadherin integrates mechanotransduction and EGFR signaling to control junctional tissue polarization and tight junction positioning. *Nat Commun* 8, 1250.

Rutgeerts, P., Vermeire, S., and Van Assche, G. (2009). Biological therapies for inflammatory bowel diseases. *Gastroenterology* 136, 1182-1197.

Saito, M., Stahley, S.N., Caughman, C.Y., Mao, X., Tucker, D.K., Payne, A.S., Amagai, M., and Kowalczyk, A.P. (2012). Signaling dependent and independent mechanisms in pemphigus vulgaris blister formation. *PLoS One* 7, e50696.

Samuelov, L., and Sprecher, E. (2015). Inherited desmosomal disorders. *Cell Tissue Res* 360, 457-475.

Sanders, D.S. (2005). Mucosal integrity and barrier function in the pathogenesis of early lesions in Crohn's disease. *J Clin Pathol* 58, 568-572.

Sato, K., Nagao, T., Iwasaki, T., Nishihira, Y., and Fukami, Y. (2003). Src-dependent phosphorylation of the EGF receptor Tyr-845 mediates Stat-p21waf1 pathway in A431 cells. *Genes Cells* 8, 995-1003.

Sato, K., Sato, A., Aoto, M., and Fukami, Y. (1995). c-Src phosphorylates epidermal growth factor receptor on tyrosine 845. *Biochem Biophys Res Commun* 215, 1078-1087.

Scheving, L.A., Shiurba, R.A., Nguyen, T.D., and Gray, G.M. (1989). Epidermal growth factor receptor of the intestinal enterocyte. Localization to laterobasal but not brush border membrane. *J Biol Chem* 264, 1735-1741.

Schinner, C., Vielmuth, F., Rotzer, V., Hiermaier, M., Radeva, M.Y., Co, T.K., Hartlieb, E., Schmidt, A., Imhof, A., Messoudi, A., *et al.* (2017). Adrenergic Signaling Strengthens Cardiac Myocyte Cohesion. *Circulation research* 120, 1305-1317.

Schlegel, N., Leweke, R., Meir, M., Germer, C.T., and Waschke, J. (2012). Role of NF-kappaB activation in LPS-induced endothelial barrier breakdown. *Histochemistry and cell biology* 138, 627-641.

Schlegel, N., Meir, M., Heupel, W.M., Holthofer, B., Leube, R.E., and Waschke, J. (2010). Desmoglein 2-mediated adhesion is required for intestinal epithelial barrier integrity. *Am J Physiol Gastrointest Liver Physiol* 298, G774-783.

Schlegel, N., Meir, M., Spindler, V., Germer, C.T., and Waschke, J. (2011). Differential role of Rho GTPases in intestinal epithelial barrier regulation in vitro. *Journal of cellular physiology* 226, 1196-1203.

Schulze, K., Galichet, A., Sayar, B.S., Scothern, A., Howald, D., Zymann, H., Siffert, M., Zenhausem, D., Bolli, R., Koch, P.J., *et al.* (2012). An adult passive transfer mouse model to study desmoglein 3 signaling in pemphigus vulgaris. *J Invest Dermatol* 132, 346-355.

Schweinlin, M., Wilhelm, S., Schwedhelm, I., Hansmann, J., Rietscher, R., Jurowich, C., Walles, H., and Metzger, M. (2016). Development of an Advanced Primary Human In Vitro Model of the Small Intestine. *Tissue Eng Part C Methods* 22, 873-883.

Segretain, D., and Falk, M.M. (2004). Regulation of connexin biosynthesis, assembly, gap junction formation, and removal. *Biochim Biophys Acta* 1662, 3-21.

Seishima, M., Esaki, C., Osada, K., Mori, S., Hashimoto, T., and Kitajima, Y. (1995). Pemphigus IgG, but not bullous pemphigoid IgG, causes a transient increase in intracellular calcium and inositol 1,4,5-triphosphate in DJM-1 cells, a squamous cell carcinoma line. *J Invest Dermatol* 104, 33-37.

Shapiro, L., Fannon, A.M., Kwong, P.D., Thompson, A., Lehmann, M.S., Grubel, G., Legrand, J.F., Als-Nielsen, J., Colman, D.R., and Hendrickson, W.A. (1995). Structural basis of cell-cell adhesion by cadherins. *Nature* 374, 327-337.

Sharma, G.D., He, J., and Bazan, H.E. (2003). p38 and ERK1/2 coordinate cellular migration and proliferation in epithelial wound healing: evidence of cross-talk activation between MAP kinase cascades. *J Biol Chem* 278, 21989-21997.

Shibamoto, S., Hayakawa, M., Takeuchi, K., Hori, T., Oku, N., Miyazawa, K., Kitamura, N., Takeichi, M., and Ito, F. (1994). Tyrosine phosphorylation of beta-catenin and plakoglobin enhanced by hepatocyte growth factor and epidermal growth factor in human carcinoma cells. *Cell Adhes Commun* 1, 295-305.

Shimizu, F., Sano, Y., Saito, K., Abe, M.A., Maeda, T., Haruki, H., and Kanda, T. (2012). Pericyte-derived glial cell line-derived neurotrophic factor increase the expression of claudin-5 in the blood-brain barrier and the blood-nerve barrier. *Neurochem Res* 37, 401-409.

Shimizu, H., Masunaga, T., Ishiko, A., Kikuchi, A., Hashimoto, T., and Nishikawa, T. (1995). Pemphigus vulgaris and pemphigus foliaceus sera show an inversely graded binding pattern to extracellular regions of desmosomes in different layers of human epidermis. *J Invest Dermatol* 105, 153-159.

Shinoda, T., Shinya, N., Ito, K., Ohsawa, N., Terada, T., Hirata, K., Kawano, Y., Yamamoto, M., Kimura-Someya, T., Yokoyama, S., *et al.* (2016). Structural basis for disruption of claudin assembly in tight junctions by an enterotoxin. *Sci Rep* 6, 33632.

Shoelson, S.E. (1997). SH2 and PTB domain interactions in tyrosine kinase signal transduction. *Curr Opin Chem Biol* 1, 227-234.

Shore, E.M., and Nelson, W.J. (1991). Biosynthesis of the cell adhesion molecule uvomorulin (E-cadherin) in Madin-Darby canine kidney epithelial cells. *J Biol Chem* **266**, 19672-19680.

Singh, A.B., and Harris, R.C. (2005). Autocrine, paracrine and juxtacrine signaling by EGFR ligands. *Cell Signal* **17**, 1183-1193.

Singh, P.K., and Hollingsworth, M.A. (2006). Cell surface-associated mucins in signal transduction. *Trends Cell Biol* **16**, 467-476.

Spindler, V., Eming, R., Schmidt, E., Amagai, M., Grando, S., Jonkman, M.F., Kowalczyk, A.P., Muller, E.J., Payne, A.S., Pincelli, C., *et al.* (2018). Mechanisms Causing Loss of Keratinocyte Cohesion in Pemphigus. *J Invest Dermatol* **138**, 32-37.

Spindler, V., Meir, M., Vigh, B., Flemming, S., Hutz, K., Germer, C.T., Waschke, J., and Schlegel, N. (2015). Loss of Desmoglein 2 Contributes to the Pathogenesis of Crohn's Disease. *Inflamm Bowel Dis* **21**, 2349-2359.

Spindler, V., Rotzer, V., Dehner, C., Kempf, B., Gliem, M., Radeva, M., Hartlieb, E., Harms, G.S., Schmidt, E., and Waschke, J. (2013). Peptide-mediated desmoglein 3 crosslinking prevents pemphigus vulgaris autoantibody-induced skin blistering. *J Clin Invest* **123**, 800-811.

Spindler, V., and Waschke, J. (2014). Desmosomal cadherins and signaling: lessons from autoimmune disease. *Cell Commun Adhes* **21**, 77-84.

Staehelin, L.A. (1972). Three types of gap junctions interconnecting intestinal epithelial cells visualized by freeze-etching. *Proc Natl Acad Sci U S A* **69**, 1318-1321.

Stark, C., Breitkreutz, B.-J., Reguly, T., Boucher, L., Breitkreutz, A., and Tyers, M. (2006). BioGRID: a general repository for interaction datasets. *Nucleic Acids Research* **34**, D535-D539.

Steinkamp, M., Geerling, I., Seufferlein, T., von Boyen, G., Egger, B., Grossmann, J., Ludwig, L., Adler, G., and Reinshagen, M. (2003). Glial-derived neurotrophic factor regulates apoptosis in colonic epithelial cells. *Gastroenterology* **124**, 1748-1757.

Stevenson, B.R., Siliciano, J.D., Mooseker, M.S., and Goodenough, D.A. (1986). Identification of ZO-1: a high molecular weight polypeptide associated with the tight junction (zonula occludens) in a variety of epithelia. *J Cell Biol* **103**, 755-766.

Sudol, M. (1998). From Src Homology domains to other signaling modules: proposal of the 'protein recognition code'. *Oncogene* **17**, 1469-1474.

Sumigray, K., Zhou, K., and Lechler, T. (2014). Cell-cell adhesions and cell contractility are upregulated upon desmosome disruption. *PLoS One* **9**, e101824.

Sun, H., Charles, C.H., Lau, L.F., and Tonks, N.K. (1993). MKP-1 (3CH134), an immediate early gene product, is a dual specificity phosphatase that dephosphorylates MAP kinase in vivo. *Cell* 75, 487-493.

Sweeney, G., Somwar, R., Ramlal, T., Volchuk, A., Ueyama, A., and Klip, A. (1999). An inhibitor of p38 mitogen-activated protein kinase prevents insulin-stimulated glucose transport but not glucose transporter translocation in 3T3-L1 adipocytes and L6 myotubes. *J Biol Chem* 274, 10071-10078.

Takahashi, M. (2001). The GDNF/RET signaling pathway and human diseases. *Cytokine Growth Factor Rev* 12, 361-373.

Takekawa, M., Maeda, T., and Saito, H. (1998). Protein phosphatase 2C α inhibits the human stress-responsive p38 and JNK MAPK pathways. *EMBO J* 17, 4744-4752.

Terry, S.J., Zihni, C., Elbediwy, A., Vitiello, E., Leefa Chong San, I.V., Balda, M.S., and Matter, K. (2011). Spatially restricted activation of RhoA signalling at epithelial junctions by p114RhoGEF drives junction formation and morphogenesis. *Nat Cell Biol* 13, 159-166.

Tice, D.A., Biscardi, J.S., Nickles, A.L., and Parsons, S.J. (1999). Mechanism of biological synergy between cellular Src and epidermal growth factor receptor. *Proc Natl Acad Sci U S A* 96, 1415-1420.

Tinkle, C.L., Pasolli, H.A., Stokes, N., and Fuchs, E. (2008). New insights into cadherin function in epidermal sheet formation and maintenance of tissue integrity. *Proc Natl Acad Sci U S A* 105, 15405-15410.

Tong, J., Taylor, P., and Moran, M.F. (2014). Proteomic analysis of the epidermal growth factor receptor (EGFR) interactome and post-translational modifications associated with receptor endocytosis in response to EGF and stress. *Mol Cell Proteomics* 13, 1644-1658.

Tsang, S.M., Brown, L., Gadmor, H., Gammon, L., Fortune, F., Wheeler, A., and Wan, H. (2012). Desmoglein 3 acting as an upstream regulator of Rho GTPases, Rac-1/Cdc42 in the regulation of actin organisation and dynamics. *Exp Cell Res* 318, 2269-2283.

Tsukita, S., and Furuse, M. (2000). Pores in the wall: claudins constitute tight junction strands containing aqueous pores. *J Cell Biol* 149, 13-16.

Tsukita, S., Furuse, M., and Itoh, M. (2001). Multifunctional strands in tight junctions. *Nat Rev Mol Cell Biol* 2, 285-293.

Tsunoda, K., Ota, T., Saito, M., Hata, T., Shimizu, A., Ishiko, A., Yamada, T., Nakagawa, T., Kowalczyk, A.P., and Amagai, M. (2011). Pathogenic relevance of IgG and IgM antibodies against desmoglein 3 in blister formation in pemphigus vulgaris. *Am J Pathol* 179, 795-806.

Tucker, D.K., Stahley, S.N., and Kowalczyk, A.P. (2014). Plakophilin-1 protects keratinocytes from pemphigus vulgaris IgG by forming calcium-independent desmosomes. *J Invest Dermatol* 134, 1033-1043.

Turner, J.R. (2006). Molecular basis of epithelial barrier regulation: from basic mechanisms to clinical application. *Am J Pathol* 169, 1901-1909.

Uhlig, H.H. (2013). Monogenic diseases associated with intestinal inflammation: implications for the understanding of inflammatory bowel disease. *Gut* 62, 1795-1805.

Ullrich, A., and Schlessinger, J. (1990). Signal transduction by receptors with tyrosine kinase activity. *Cell* 61, 203-212.

Ungewiss, H., Vielmuth, F., Suzuki, S.T., Maiser, A., Harz, H., Leonhardt, H., Kugelmann, D., Schlegel, N., and Waschke, J. (2017). Desmoglein 2 regulates the intestinal epithelial barrier via p38 mitogen-activated protein kinase. *Scientific reports* 7, 6329.

Valles, A.M., Tucker, G.C., Thiery, J.P., and Boyer, B. (1990). Alternative patterns of mitogenesis and cell scattering induced by acidic FGF as a function of cell density in a rat bladder carcinoma cell line. *Cell Regul* 1, 975-988.

van der Flier, L.G., and Clevers, H. (2009). Stem cells, self-renewal, and differentiation in the intestinal epithelium. *Annu Rev Physiol* 71, 241-260.

Van Itallie, C.M., and Anderson, J.M. (2014). Architecture of tight junctions and principles of molecular composition. *Semin Cell Dev Biol* 36, 157-165.

Van Itallie, C.M., Colegio, O.R., and Anderson, J.M. (2004). The cytoplasmic tails of claudins can influence tight junction barrier properties through effects on protein stability. *J Membr Biol* 199, 29-38.

Vasioukhin, V., Bauer, C., Degenstein, L., Wise, B., and Fuchs, E. (2001a). Hyperproliferation and defects in epithelial polarity upon conditional ablation of alpha-catenin in skin. *Cell* 104, 605-617.

Vasioukhin, V., Bowers, E., Bauer, C., Degenstein, L., and Fuchs, E. (2001b). Desmoplakin is essential in epidermal sheet formation. *Nat Cell Biol* 3, 1076-1085.

Vassal-Stermann, E., Mottet, M., Ducournau, C., Iseni, F., Vragliau, C., Wang, H., Zubieta, C., Lieber, A., and Fender, P. (2018). Mapping of Adenovirus of serotype 3 fibre interaction to desmoglein 2 revealed a novel 'non-classical' mechanism of viral receptor engagement. *Sci Rep* 8, 8381.

Vergarajauregui, S., San Miguel, A., and Puertollano, R. (2006). Activation of p38 mitogen-activated protein kinase promotes epidermal growth factor receptor internalization. *Traffic* 7, 686-698.

Vieira, A.V., Lamaze, C., and Schmid, S.L. (1996). Control of EGF receptor signaling by clathrin-mediated endocytosis. *Science* 274, 2086-2089.

Vielmuth, F., Hartlieb, E., Kugelmann, D., Waschke, J., and Spindler, V. (2015). Atomic force microscopy identifies regions of distinct desmoglein 3 adhesive properties on living keratinocytes. *Nanomedicine* 11, 511-520.

Vielmuth, F., Wanuske, M.T., Radeva, M.Y., Hiermaier, M., Kugelmann, D., Walter, E., Buechau, F., Magin, T.M., Waschke, J., and Spindler, V. (2017). Keratins Regulate the Adhesive Properties of Desmosomal Cadherins Through Signaling. *J Invest Dermatol*.

Vielmuth, F., Wanuske, M.T., Radeva, M.Y., Hiermaier, M., Kugelmann, D., Walter, E., Buechau, F., Magin, T.M., Waschke, J., and Spindler, V. (2018). Keratins Regulate the Adhesive Properties of Desmosomal Cadherins through Signaling. *J Invest Dermatol* **138**, 121-131.

Vinken, M., Vanhaecke, T., Papeleu, P., Snykers, S., Henkens, T., and Rogiers, V. (2006). Connexins and their channels in cell growth and cell death. *Cell Signal* **18**, 592-600.

von Boyen, G.B., Schulte, N., Pfluger, C., Spaniol, U., Hartmann, C., and Steinkamp, M. (2011). Distribution of enteric glia and GDNF during gut inflammation. *BMC gastroenterology* **11**, 3.

von Boyen, G.B., Steinkamp, M., Reinshagen, M., Schafer, K.H., Adler, G., and Kirsch, J. (2004). Proinflammatory cytokines increase glial fibrillary acidic protein expression in enteric glia. *Gut* **53**, 222-228.

Walsh, D., McCarthy, J., O'Driscoll, C., and Melgar, S. (2013). Pattern recognition receptors--molecular orchestrators of inflammation in inflammatory bowel disease. *Cytokine Growth Factor Rev* **24**, 91-104.

Walter, E., Vielmuth, F., Rotkopf, L., Sardy, M., Horvath, O.N., Goebeler, M., Schmidt, E., Eming, R., Hertl, M., Spindler, V., *et al.* (2017). Different signaling patterns contribute to loss of keratinocyte cohesion dependent on autoantibody profile in pemphigus. *Sci Rep* **7**, 3579.

Wang, H., Ducournau, C., Saydaminova, K., Richter, M., Yumul, R., Ho, M., Carter, D., Zubieta, C., Fender, P., and Lieber, A. (2015). Intracellular Signaling and Desmoglein 2 Shedding Triggered by Human Adenoviruses Ad3, Ad14, and Ad14P1. *J Virol* **89**, 10841-10859.

Wang, H., Hughes, I., Planer, W., Parsadonian, A., Grider, J.R., Vohra, B.P., Keller-Peck, C., and Heuckeroth, R.O. (2010). The timing and location of glial cell line-derived neurotrophic factor expression determine enteric nervous system structure and function. *J Neurosci* **30**, 1523-1538.

Wang, H., Li, Z.Y., Liu, Y., Persson, J., Beyer, I., Moller, T., Koyuncu, D., Drescher, M.R., Strauss, R., Zhang, X.B., *et al.* (2011). Desmoglein 2 is a receptor for adenovirus serotypes 3, 7, 11 and 14. *Nat Med* **17**, 96-104.

Wang, L., Srinivasan, S., Theiss, A.L., Merlin, D., and Sitaraman, S.V. (2007). Interleukin-6 induces keratin expression in intestinal epithelial cells: potential role of keratin-8 in interleukin-6-induced barrier function alterations. *J Biol Chem* **282**, 8219-8227.

Wang, Q., Guo, X.L., Wells-Byrum, D., Noel, G., Pritts, T.A., and Ogle, C.K. (2008). Cytokine-induced epithelial permeability changes are regulated by the activation of the p38 mitogen-activated protein kinase pathway in cultured Caco-2 cells. *Shock* **29**, 531-537.

- Waschke, J. (2008). The desmosome and pemphigus. *Histochem Cell Biol* 130, 21-54.
- Waschke, J., Bruggeman, P., Baumgartner, W., Zillikens, D., and Drenckhahn, D. (2005). Pemphigus foliaceus IgG causes dissociation of desmoglein 1-containing junctions without blocking desmoglein 1 transinteraction. *J Clin Invest* 115, 3157-3165.
- Waschke, J., and Spindler, V. (2014). Desmosomes and extradesmosomal adhesive signaling contacts in pemphigus. *Med Res Rev* 34, 1127-1145.
- Waschke, J., Spindler, V., Bruggeman, P., Zillikens, D., Schmidt, G., and Drenckhahn, D. (2006). Inhibition of Rho A activity causes pemphigus skin blistering. *J Cell Biol* 175, 721-727.
- Weiske, J., Schoneberg, T., Schroder, W., Hatzfeld, M., Tauber, R., and Huber, O. (2001). The fate of desmosomal proteins in apoptotic cells. *J Biol Chem* 276, 41175-41181.
- Wilson, G., Hassan, I.F., Dix, C.J., Williamson, I., Shah, R., Mackay, M., and Artursson, P. (1990). Transport and permeability properties of human Caco-2 cells: An in vitro model of the intestinal epithelial cell barrier. *Journal of Controlled Release* 11, 25-40.
- Wilson, K.J., Gilmore, J.L., Foley, J., Lemmon, M.A., and Riese, D.J., 2nd (2009). Functional selectivity of EGF family peptide growth factors: implications for cancer. *Pharmacol Ther* 122, 1-8.
- Windoffer, R., Borchert-Stuhltrager, M., and Leube, R.E. (2002). Desmosomes: interconnected calcium-dependent structures of remarkable stability with significant integral membrane protein turnover. *J Cell Sci* 115, 1717-1732.
- Wong, V., and Gumbiner, B.M. (1997). A synthetic peptide corresponding to the extracellular domain of occludin perturbs the tight junction permeability barrier. *J Cell Biol* 136, 399-409.
- Wu, P., Wee, P., Jiang, J., Chen, X., and Wang, Z. (2012). Differential regulation of transcription factors by location-specific EGF receptor signaling via a spatio-temporal interplay of ERK activation. *PLoS One* 7, e41354.
- Wu, Z., Nybom, P., and Magnusson, K.E. (2000). Distinct effects of *Vibrio cholerae* haemagglutinin/protease on the structure and localization of the tight junction-associated proteins occludin and ZO-1. *Cell Microbiol* 2, 11-17.
- Xia, Z., Dickens, M., Raingeaud, J., Davis, R.J., and Greenberg, M.E. (1995). Opposing effects of ERK and JNK-p38 MAP kinases on apoptosis. *Science* 270, 1326-1331.
- Yamada, S., and Nelson, W.J. (2007). Localized zones of Rho and Rac activities drive initiation and expansion of epithelial cell-cell adhesion. *J Cell Biol* 178, 517-527.
- Yang, J., Zhang, W., Evans, P.M., Chen, X., He, X., and Liu, C. (2006). Adenomatous polyposis coli (APC) differentially regulates beta-catenin phosphorylation and ubiquitination in colon cancer cells. *J Biol Chem* 281, 17751-17757.

Yarden, Y., and Sliwkowski, M.X. (2001). Untangling the ErbB signalling network. *Nat Rev Mol Cell Biol* 2, 127-137.

Yashiro, M., Nishioka, N., and Hirakawa, K. (2006). Decreased expression of the adhesion molecule desmoglein-2 is associated with diffuse-type gastric carcinoma. *Eur J Cancer* 42, 2397-2403.

Yoo, B.K., He, P., Lee, S.J., and Yun, C.C. (2011). Lysophosphatidic acid 5 receptor induces activation of Na(+)/H(+) exchanger 3 via apical epidermal growth factor receptor in intestinal epithelial cells. *Am J Physiol Cell Physiol* 301, C1008-1016.

Yu, Y.B., and Li, Y.Q. (2014). Enteric glial cells and their role in the intestinal epithelial barrier. *World J Gastroenterol* 20, 11273-11280.

Yulis, M., Quiros, M., Hilgarth, R., Parkos, C.A., and Nusrat, A. (2018). Intracellular Desmoglein-2 cleavage sensitizes epithelial cells to apoptosis in response to pro-inflammatory cytokines. *Cell Death Dis* 9, 389.

Zarubin, T., and Han, J. (2005). Activation and signaling of the p38 MAP kinase pathway. *Cell Res* 15, 11-18.

Zeissig, S., Burgel, N., Gunzel, D., Richter, J., Mankertz, J., Wahnschaffe, U., Kroesen, A.J., Zeitz, M., Fromm, M., and Schulzke, J.D. (2007). Changes in expression and distribution of claudin 2, 5 and 8 lead to discontinuous tight junctions and barrier dysfunction in active Crohn's disease. *Gut* 56, 61-72.

Zhang, D.K., He, F.Q., Li, T.K., Pang, X.H., Cui de, J., Xie, Q., Huang, X.L., and Gan, H.T. (2010a). Glial-derived neurotrophic factor regulates intestinal epithelial barrier function and inflammation and is therapeutic for murine colitis. *The Journal of pathology* 222, 213-222.

Zhang, D.K., He, F.Q., Li, T.K., Pang, X.H., Cui, D.J., Xie, Q., Huang, X.L., and Gan, H.T. (2010b). Glial-derived neurotrophic factor regulates intestinal epithelial barrier function and inflammation and is therapeutic for murine colitis. *J Pathol* 222, 213-222.

Zhang, S., Han, J., Sells, M.A., Chernoff, J., Knaus, U.G., Ulevitch, R.J., and Bokoch, G.M. (1995). Rho family GTPases regulate p38 mitogen-activated protein kinase through the downstream mediator Pak1. *J Biol Chem* 270, 23934-23936.

Zweibaum A., L.M., Grasset E., Louvard D. (1991). Use of cultured cell lines in studies of intestinal cell differentiation and function. In *Handbook of physiology: the gastrointestinal system, intestinal absorption and secretion* (American Physiological Society), pp. 223-255.

4.2 Abbreviations

%	per cent
(Co-) IP	(Co-) Immunoprecipitation
°C	degree Celsius
μl	microliter, 10 ⁻⁶ l
μM	micromolar, 10 ⁻⁶ M
ADAM	A disintegrin and metalloproteinase domain-containing protein
AFM	Atomic force microscopy
AJ	Adherens junctions
AJC	Apical junctional complex
AMP	Antimicrobial peptides
APC	Adematous polyposis coli
Ca ²⁺	Calcium
CaCl ₂	Calcium chloride
CD	Crohn's disease
Cld4	Claudin 4
Cld2	Claudin 2
CNS	Central nervous sytem
C.rod	<i>Citrobacter rodentium</i>
Cxs	Connexins
DP	Desmoplakin
Dsc2	Descmocollin 2
Dsg2	Desmoglein 2
DSS	Dextran sodium sulphate
DTD	Desmoglein terminal domain
DUR	Desmoglein unique region
EA	Extracellular anchoring domain
EC	Extracellular cadherin repeat
Ecad	E-cadherin
ED	Extracellular domain
EGC	Enteric glial cell

EGF	Epidermal growth factor
EGFR	Epidermal growth factor receptor
EGTA	Ethylene glycol tetraacetic acid
ENS	Enteric nervous system
Fc	Constant effector-determining region
Fig.	Figure
FL	Full-length
GAPDH	Glycerinaldehyd-3-phosphat-Dehydrogenase
GDNF	Glial-derived neurotrophic factor
GFP	Green Fluorescent Protein
GJ	Gap junctions
h	Hour
HER2	Human epidermal growth factor receptor 2
HER3	Human epidermal growth factor receptor 3
Hsp70	Heat shock protein 70
Hz	Hertz
IA	Intracellular anchoring domain
IBD	Inflammatory bowel disease
ICS	Intracellular cadherin-like sequence
IEC	Intestinal epithelial cells
IF	Immunofluorescence
IgG	Immunoglobulin G
IL-1 β	Interleukin 1 beta
INF γ	Interferon gamma
IPL	Proline rich linker region
JAMs	Junctional adhesion molecules
kD	kilo dalton
KO	Knockout
MAPK	Mitogen-activated protein kinase
min	Minute
MLCK	Myosin light chain kinase

MMP	Matrix metallo protease
Ncad	N-cadherin
nm	nanometer
n.s.	not significant
PG	Plakoglobin
Pkp	Plakophilin
pN	pico newton
RTK	Receptor tyrosine kinase
RUD	Repeat unit domain
SE	Standard error
SIM	Structured illumination microscopy
siRNA	small interfering ribonucleic acid
Src	Rous sarcoma kinase
STAT3	Signal transducer and activator of transcription 3
STED	Stimulated emission depletion microscopy
Suppl.	Supplementary
TER	Transepithelial resistance
TGF	Transforming growth factor
TJ	Tight junctions
TM	Transmembrane domain
TNF α	Tumor necrosis factor alpha
UC	Ulcerative colitis
WT	Wildtype
ZO1	Zonula occludens 1

4.3 Contributions

Declaration of contributions to “Desmoglein 2 regulates the intestinal epithelial barrier via p38 mitogen-activated protein kinase”

This study was planned and designed by Jens Waschke and me. I performed all experiments, prepared the figures and wrote the manuscript. SIM and STED experiments were performed together with Andreas Maiser under the supervision of Hartmann Harz. DLD1 knockout cell lines were provided by Shintaro T. Suzuki. Human tissue samples were provided by Nicolas Schlegel.

Declaration of contributions to “Dsg2 via Src-mediated transactivation shapes EGFR signaling towards cell adhesion”

This study was planned and designed by Jens Waschke and me. I performed all experiments except of the hanging drop bead aggregation assay that was performed by Vera Rötzer. The Caco2 knockout cell line was provided by Markus Diefenbacher. Michael Meir obtained and prepared the human tissue samples. Christina Fey generated the enteroids. I wrote the manuscript and prepared all figures.

Declaration of contributions to “Desmoglein 2, but not desmocollin 2, protects intestinal epithelia from injury”

This study was planned and designed by Annika Gross, Rudolf E. Leube and Pavel Strnad. I performed ultrastructural analyses of human tissue samples from CD patients and did TER measurements, immunostainings and western blot analyses of DLD1 KO cell lines. I prepared the figures S1 A and S17 A-D, wrote the corresponding figure legends as well as the method parts and proofread the manuscript.

Declaration of contributions to “Glial cell-line derived neurotrophic factor (GDNF) regulates intestinal barrier function in inflammatory bowel diseases by stabilization of desmoglein 2”

This study was planned and designed by Nicolas Schlegel, Michael Meir, Natalie Burkhard, Sven Flemming, Christoph-Thomas Germer and Jens Waschke. I performed the AFM experiments and quantified the keratin retraction. I prepared the figures 2D-H and S3 B and C, wrote the corresponding figure legends, the respective result and method parts and proofread the manuscript.

Hanna Ungewiß

Prof. Dr. Jens Waschke

4.4 Statutory declaration and statement

Declaration according to the

“Promotionsordnung der LMU München für die Fakultät Biologie”

Betreuung: Hiermit erkläre ich, dass die vorgelegte Arbeit an der LMU von Herrn Prof. Dr. Leonhardt betreut wurde.

Anfertigung: Hiermit versichere ich an Eides statt, dass die vorgelegte Dissertation selbstständig und ohne unerlaubte Hilfsmittel angefertigt wurde. Über Beiträge, die im Rahmen der kumulativen Dissertation in Form von Manuskripten in der Dissertation enthalten sind, wurde im Kapitel 4.3 Rechenschaft abgelegt und die eigenen Leistungen wurden aufgelistet.

Prüfung: Hiermit erkläre ich, dass die Dissertation weder als Ganzes noch in Teilen an einem anderen Ort einer Prüfungskommission vorgelegt wurde. Weiterhin habe ich weder an einem anderen Ort eine Promotion angestrebt oder angemeldet oder versucht eine Doktorprüfung abzulegen.

München, den 31.07.2018

Hanna Ungewiß

(Hanna Ungewiß)

